Best Available Copy

AD-773 177

TECHNOLOGY DEVELOPMENT FOR TRANSITION
METAL-RARE EARTH HIGH-PERFORMANCE
MAGNETIC MATERIALS

J. J. Becker, et al

General Electric Corporate Research and
Development

Prepared for:

Air Force Materials Laboratory

30 June 1973

AFML-TR-73-238

TECHNOLOGY DEVELOPMENT FOR TRANSITION METAL-RARE EARTH HIGH-PERFORMANCE MAGNETIC MATERIALS

AD773177

Submitted to:

Air Force Materials Laboratory, AFSC, USAF
Project Engineer: J.C. Olson, LPE, Tel. (513)255-4474

By:

J.J. Becker, Principal Investigator, Tel. (518) 346-8771, Ext. 6114
GENERAL ELECTRIC COMPANY
CORPORATE RESEARCH AND DEVELOPMENT
P.O. Box 8
SCHENECTADY, NEW YORK 12301

SRD-73-149

NOTICE

When Government drawings, specifications, or other data are used for any purpose other than in connection with a definitely related Government procurement operation, the United States Government thereby incurs no responsibility nor any obligation whatsoever; and the fact that the government may have formulated, furnished, or in any way supplied the said drawings, specifications, or other data, is not to be regarded by implication or otherwise as in any manner licensing the holder or any other person or corporation, or conveying any rights or permission to manufacture, use, or sell any patented invention that may in any way be related thereto.

Copies of this report should not be returned unless return is required by security considerations, contractual obligations, or notice on a specific document.

i

AFML-TR-73-238

AD773177

TECHNOLOGY DEVELOPMENT FOR TRANSITION METAL-RARE
EARTH HIGH-PERFORMANCE MAGNETIC MATERIALS

J.J. Becker et al.

Approved for public release;
distribution is unlimited.

FOREWORD

This report describes work carried out in the Metallurgy and Ceramics Laboratory of the General Electric Research and Development Center, Schenectady, New York, under USAF Contract No. F33615-70-C-1626, entitled "Technology Development for Transition Metal-Rare Earth High-Performance Magnetic Materials." This work was administered by the Air Force Materials Laboratory, under Project 7371, "Electronic and Magnetic Materials"; Task 737103 at Wright-Patterson Air Force Base, Ohio, J. C. Olson (AFML/LPE), Project Engineer.

This Final Technical Report covers work conducted under the above program during the period 30 June 1970 - 30 June 1973. The principal participants in the research are J. J. Becker, M. G. Benz, R. E. Cech, R. J. Charles, M. Doser, S. Foner, E. F. Koch, R. P. Laforce, J. D. Livingston, D. L. Martin, M. C. McConnell, E. J. McNiff, Jr., P. Rao, A. C. Rockwood, J. G. Smeggil, and L. Valentine. The report was submitted by the author in August 1973.

The contractor's report number is SRD-73-149.

This technical report has been reviewed and is approved.

CHARLES H. ROBISON
Major, USAF
Chief, Solid State Materials Branch
Materials Physics Division
Air Force Materials Laboratory

ii

ABSTRACT

The development of the technology for transition metal-rare earth high-performance magnetic materials that has taken place over the three year contract period is described in this report. This work has covered three general areas: the origin of the coercive force in high-anisotropy materials, phase equilibrium and chemistry, and studies of new materials and processing variables. The coercive force of single particles has been shown to be controlled by defects whose nature determines the behavior of magnetization discontinuities. Magnetic domain observations have been used to measure domain wall energies in several cobalt-rare-earths. The domain behavior of sintered magnets has been observed and correlated with their magnetic properties. A comparative study of chemical analytical techniques has been made and the use of x-ray fluorescence spectroscopy developed as a fast and accurate instrumental technique. Optical and electron microscopy of surfaces and transmission sections of materials that have been exposed to temperatures of 700° to 800°C indicate that Co_5Sm decomposes into $Co_{17}Sm_2$ and Co_7Sm_2, the latter by a form of lattice shear transformation. Diffusion couple studies show 17-2 precipitating readily and striated 7-2 forming more slowly. A number of sintered magnets have been made in a study of the effect of careful control of processing variables. A magnet has been made of Co and Sm alone with $(BH)_{max} = 24$ mGOe. A Co-Pr-Sm magnet was made with a B-coercive force of 10.1 kOe and $(BH)_{max}$ of 26 mGOe. The work under this contract is summarized in the first portion of the report and then presented in detail.

TABLE OF CONTENTS

TECHNOLOGY DEVELOPMENT FOR TRANSITION METAL - RARE EARTH HIGH-PERFORMANCE MAGNETIC MATERIALS

J.J. Becker

I. INTRODUCTION

This is the final technical report for Contract No. F33615-70-C-1626, sponsored by the Defense Advanced Research Projects Agency and monitored by the Air Force Materials Laboratory. It covers the period 30 June 1970 through 30 June 1973.

The objective of this work is set forth in the Statement of Work appearing as Exhibit A of the contract. This objective is to develop the technology of high-performance transition metal - rare earth magnets for critical applications. High-performance permanent magnets are defined in this context as those having remanences greater than ten thousand gauss and permeabilities of very nearly unit throughout the second and well into the third quadrants of their hysteresis loops. Three general approaches to the development of such technology are defined in the work statement. In outline, they are 1) studies of the intrinsic coercive force in high anisotropy materials, 2) development of information on phase equilibria in these materials, and 3) identification and investigation of new materials. This report describes the progress that has been made during the contract period toward the achievement of this objective.

II. ORGANIZATION OF THIS REPORT

During the three-year period of this contract, no less than nineteen
publications acknowledging its support have already appeared in the scientific
and technical literature. Several more have been submitted or are in the
process of preparation. Many of these publications have also been presented
orally at various technical conferences. Most of the work performed under
this contract has been described in these publications. In many cases, work
that was first described in a quarterly or semi-annual report subsequently
appeared as a publication in the literature. Since they are finished accounts
that have undergone the scrutiny of the scientific and technical community,
these publications will comprise the main body of this report.

The progress that has been made in this work, as indicated most directly
by its fruitfulness, attests to the value of the far-sighted support it has re-
ceived. Its interaction with and stimulation of other work both here and
elsewhere cannot be estimated but is surely great.

Section III contains a summary of the major technical accomplishments
of this program along the lines of investigation defined in the Work Statement.
This is followed by more detailed accounts in Section IV. The first portion
of this section consists of an account of work not reported in the literature,
including some performed during the last quarter. This is followed by the
various technical publications referred to above.

III. SUMMARY OF TECHNICAL ACCOMPLISHMENTS

As stated in the Introduction, the objective of the work under this contract is to develop the technology of transition metal - rare earth magnets with energy products greater than 25 mGOe by following three general approaches: fundamental studies of the origin of the coercive force, phase equilibrium studies, and identification and investigation of new materials. This section gives the highlights of the progress that has been made during the contract period along these lines. Section IV gives the full details of this work, primarily in the form of technical publications.

Origin of the coercive force

Magnetization reversal discontinuities have been studied in samples consisting of a few particles or a single particle. Experiments with successive polishing treatments indicate that individual defects are responsible for the observed magnetization behavior. A particle of Co_5Y showed a perfectly rectangular hysteresis loop and a maximum energy product of 27.6 mGOe, illustrating the potential of this material, even though such properties have never been achieved in bulk. It has become very clear during this study that the properties of these materials are dominated by imperfections, and the underlying objective of the fundamental studies has been to elucidate their nature. The angular dependence and temperature dependence of nucleation fields in single particles were investigated. In a Co_5Gd particle, a $1/\cos\theta$ angular dependence centering about an angle 28° from the alignment axis was observed for the nucleation field of one magnetization discontinuity. Analysis of the data indicated that the reversal was triggered by a bit of misoriented material pinning a wall fragment, and that the nucleus was very small and caused the jump to occur in the main body of the sample. It has been found that powders of Co_5Sm show great differences in their dependence of coercive force on magnetizing field at different temperatures. For example, the H_c of a 50μ Co_5Sm powder in H_m of 44 kOe was more than three times as large at 77°K as at room T. This is in complete contrast to reported data on the variation of K and M with T and indicates that the T dependence must be determined by the T variation of the relevant properties of the nucleation site, not those of the matrix. In a single particle, two magnetization discontinuities were followed as a function of temperature and it was found that their jumping fields H_n had different T dependences, strongly suggesting that they were of different natures. On the theoretical side, a phenomenological model has been developed involving only two magnetically different types of nuclei, without regard to the details of their structure, which describes a large variety of phenomena related to the field dependence of coercive force and nucleating fields in high-anisotropy materials, including not only experimental results to date on cobalt-rare-earths, but such things as the field dependence of H_c in MnBi and the details of the hysteresis loops reported in orthoferrites. During this period the critical problems in understanding H_c have been much more sharply defined, with the concept of defect-controlled

3

coercive force gaining wide acceptance, and substantial progress has been made toward their solution.

Direct observation of magnetic domain structure utilizing the magnetic Kerr effect has been done both in bulk materials and in sintered permanent magnets. From measurements of equilibrium domain widths in thin crystals, the domain wall energy in Co_5Sm, Co_5Y, Co_5Ce, and Co_5Pr was estimated to be 85, 35, 25, and 40 ergs/cm^2, respectively. Rough estimates of wall energy have also been made for Co_5Nd, Co_5La, and Co_5Gd from surface domain observations on bulk crystals. From these wall energies and published anisotropy constants, calculations were made of exchange constants, domain wall thicknesses, and critical single-domain particle sizes. The critical size is larger for Co_5Sm and Co_5Gd than for the other compounds, and this factor may be related to the greater ease of obtaining high coercive forces in these two materials. A number of 17-2 and 7-2 phases have also been examined. Characteristic easy-axis domain patterns were seen in $Co_{17}Sm_2$, $Co_{17}Gd_2$, and $(Co, Fe)_{17}R_2$ and Co_7R_2 phases. Domains were not seen in $Co_{17}Pr_2$, $Co_{17}Ce_2$, $Co_{17}Y_2$, and $Co_{17}Nd_2$, all of which are believed to have easy-plane rather than easy-axis magnetic symmetry. Magnetic domains in high-coercivity sintered Co_5Sm magnets have also been studied. Grain boundaries block the propagation of magnetic reversal from grain to grain. General domain-wall pinning is low, and oversized grains show low-coercivity, multidomain behavior. In most grains, however, once domain walls are removed, large reverse fields are required to nucleate magnetization reversal. The relative independence of the grains in their magnetic behavior even at near 100% density is remarkable.

Chemistry and phase structure

The chemical analysis of the cobalt-rare-earths poses difficult problems. It is the phase structure of the material that is important in establishing its magnetic behavior, but this cannot be deduced from a chemical analysis in the absence of knowledge of the oxidation state of the rare earth present. That is, some of it may be present in the form of oxide rather than in combination with the cobalt. A technique was developed for analyzing the rare earth present in a compound in the reduced state by selectively oxidizing the rare earth while maintaining the cobalt in the reduced state. Indications have been that the rare earth present in the reduced state is substantially less than the total rare earth, in keeping with other observations. A continuing study of analytical techniques has shown that different analytical laboratories show systematic discrepancies in their analyses of Co-Sm alloys. An objective of the analytical work in this study has been to establish a fast, accurate instrumental technique that could establish all major constituents to ±0.10 wt % within an hour. The technique of x-ray fluorescence analysis has been thoroughly studied and appears to be entirely suitable for this purpose.

The details of the phase structure of these materials are of crucial importance in determining their magnetic properties. There is now considerable

controversy over the exact nature of the 5-1 phase and the transformations that take place in it at moderately elevated temperatures. Two approaches to this problem have been taken in this work. One is the examination by optical and electron microscopy techniques of surfaces and transmission sections of materials that have been exposed to treatments at temperatures at which decomposition appears to take place, that is, in the 700°-800°C range. These observations indicate that Co_5Sm decomposes into $Co_{17}Sm_2$ and Co_7Sm_2, the latter by a form of lattice shear transformation. Another approach has been to prepare diffusion couples between cobalt and a samarium-rich alloy, resulting in adjacent layers of all the equilibrium phases, and to heat treat these and observe the resulting structural changes. In these samples, 17-2 appears to precipitate readily, both in grain boundaries and within grains, and 7-2 more slowly. The latter shows a striated structure consistent with a shear transformation. Mechanisms that have been suggested elsewhere do not appear to be confirmed by these experiments. The process is not a eutectoid decomposition, at least as usually defined.

New materials and processing studies

In addition to studies of materials with potential energy products greater than 25 mGOe, a number of sintered magnets have been made in a study of the effect of careful control of processing variable on final properties. A magnet has been made of cobalt and samarium alone with an energy product of 24 mGOe, the largest ever reported in this material and close to the maximum possible. Its properties have been measured in fields up to 140 kOe and at temperatures down to 4.2°K utilizing the facilities of the MIT Francis Bitter National Magnet Laboratory. A Co-Pr-Sm magnet was made with a B-coercive force of 10.1 kOe and a $(BH)_{max}$ of 26 mGOe. A study was made of two approaches to the precise composition control necessary to develop high properties. These are 1) direct control of composition at the melting stage and 2) control of composition by blending together of powders of different compositions at a stage prior to alignment and classification. Although high-performance magnets can be produced by either approach, the blending approach is favored because of the ability to optimize properties by making small shifts in composition at the powder stage. The importance of the role of alignment in influencing magnetic properties is indicated by measurements of B_r and of magnetization at various fields in Co-Pr-Sm magnets. The temperature variation of coercive force and anisotropy in sintered Co-Sm magnets has been measured. The temperature dependence of coercive force is very strong, in agreement with the results on powders. However, the anisotropy seems to increase linearly with decreasing temperature, in sharp contrast to the single crystal results reported in the literature. It has also been established that the best permanent magnet properties occur when the overall composition is close to the Co_5Sm - Co_7Sm_2 phase boundary. A final factor that strongly influences the properties of sintered magnets is the cooling rate from the post-sintering heat treatment at 900°C.

During the time of the present report, the principal investigator organized and chaired a session on the origin of the coercive force in high-anisotropy materials, the Symposium-Workshop on Cobalt-Rare-Earths, held at the 18th Annual Conference on Magnetism and Magnetic Materials in November 1972. The session consisted of a paper reviewing the present status of the problem, given by J. D. Livingston, and a discussion by an international panel of experts. The purpose of the session was to pinpoint as precisely as possible where the understanding of the problem stands, what discrepancies exist, and what exactly should be done next to advance the understanding of this subject most effectively, thereby establishing the strongest possible base for continued development of this class of materials. The size of the audience and the degree of its participation throughout the session were most gratifying and amply testified to the widespread interest in this important subject.

The above summary outlines the main directions of work under this contract both in exploring the behavior of potentially high-performance materials and developing high-performance properties in actual magnets. The details of the work indicated above, as well as some additional investigations, are given in the next section.

IV. DETAILED TECHNICAL WORK

In the listing below, each publication and each section of this portion of the report is identified by a number-letter code, for example 2B. In view of the breadth of the approaches defined in the work statement, and the resulting diversity of the work reported here, it was thought that a useful classification could be made in terms of the type of investigation, as follows:

A = Bulk material or particles

B = Sintered magnets

1 = Observations of magnetic behavior

2 = Phase structure and chemistry

3 = Effects of processing on properties

Thus a paper on the lattice parameters of sintered magnets would be denoted 2B. It is hoped that this classification will enhance the usefulness of this report.

a. Work not reported in technical journals

13A J.J. Becker: Effect of Chemical Treatment of $Co_{17}Sm_2$

1A J.J. Becker: Magnetic Behavior of Co_7R_2 Compounds

123AB J.J. Becker: Session on the Origin of the Coercive Force

123AB J.D. Livingston: Present Understanding of Coercivity

2AB R.E. Cech: Analysis for Rare Earth Present in the Reduced State by Selective Oxidation

12A J.D. Livingston: Preparation and Examination of Co_5Tm, Co_5Yb, Co_5Sc, Co_5Eu, and Co_5Lu

3B D.L. Martin: The Alignment Factor

2A D.L. Martin: Diffusion Couple Studies

2AB J.G. Smeggil: Summary of Analytical Results by Wet Chemistry and X-ray Fluorescence Spectroscopy

3B J.G. Smeggil: Effect of Processing Techniques on Composition

3B J.G. Smeggil: Mechanical Hardness and Coercive Force of Heat-treated Magnets

7

b.   Publications in the scientific and technical literature

1A   J. J. Becker, "Magnetization Discontinuities in Cobalt-Rare-Earth Particles," J. Appl. Phys. 42, 1537 (1971)

1A   J. J. Becker, "Interpretation of Hysteresis Loops of Cobalt-Rare Earth Single Particles," IEEE Trans. on Magnetics MAG-7, 644 (1971)

1A   J. J. Becker, "Angular Dependence of Nucleating Fields in Co-Rare Earth Particles," AIP Conference Proc. 5, 1067 (1972)

1A   J. J. Becker, "Temperature Dependence of Coercive Force and Nucleating Fields in Co_5Sm," IEEE Trans. on Magnetics MAG-8, 520 (1972)

1A   J. J. Becker, "A Model for the Field Dependence of Magnetization Discontinuities in High-Anisotropy Materials," IEEE Trans. on Magnetics MAG-9, September 1973

3B   M. G. Benz and D. L. Martin, "Sintering of Cobalt-Rare Earth Permanent Magnets," AIP Conference Proc. 5, 1082 (1972)

1B   M. G. Benz and D. L. Martin, "Anisotropy Parameters and Coercivity for Sintered Co_5Sm Permanent Magnet Alloys," J. Appl. Phys. 43, 4733 (1972)

3B   R. J. Charles, D. L. Martin, L. Valentine, and R. E. Cech, "A 10,000 Oe B-Coercive Force Magnet," AIP Conference Proc. 5, 1072 (1972)

3B   M. Doser and J. G. Smeggil, "Some Observations of the Magnetic Properties of Fluid-Quenched Co_5Sm Magnets," IEEE Trans. on Magnetics MAG-9, September 1973

1B   S. Foner, E. J. McNiff, Jr., D. L. Martin, and M. G. Benz, "Magnetic Properties of Cobalt-Samarium with a 24-MG Oe Energy Product," Appl. Phys. Lett. 20, 447 (1972)

1A   J. D. Livingston, "Magnetic Domains in $Co_{17}R_2$, $(Co, Fe)_{17}R_2$, and Co_7R_2 Compounds," J. Mat. Sci. 7, 1472 (1972)

1A   J. D. Livingston and M. D. McConnell, "Domain-Wall Energy in Cobalt-Rare Earth Compounds," J. Appl. Phys. 43, 4756 (1972)

123AB   J. D. Livingston, "Present Understanding of Coercivity in Cobalt-Rare Earths," AIP Conference Proc. 10, 643 (1973)

1B   J. D. Livingston, "Domains in Sintered Co_5Sm Magnets," Phys. stat. solidi (a) 18 (1973)

1B   D. L. Martin and M. G. Benz, "Temperature Dependence of Coercivity for Co-Sm Permanent Magnet Alloys," IEEE Trans. on Magnetics MAG-8, 562 (1972)

2B   D. L. Martin, M. G. Benz, and A. C. Rockwood, "Cobalt-Samarium Permanent Magnet Alloys: Variation of Lattice Parameters with Composition and Temperature," AIP Conference Proc. 10, 583 (1973)

3B   D. L. Martin, R. P. Laforce, and M. G. Benz, "Post-Sintering Heat Treatment of Cobalt-Samarium Magnet Alloys," IEEE Trans. on Magnetics MAG-9, September 1973

2A   P. Rao, J. G. Smeggil, and E. F. Koch, "Phase Transformations in Co_5Sm," Proc. Electron Mic. Soc. Am.

2B   J. G. Smeggil, "Phase Analysis of Liquid Phase Sintered Co_5Sm Magnet Compacts," IEEE Trans. on Magnetics MAG-9, September 1973

2A   J. G. Smeggil, P. Rao, J. D. Livingston, and E. F. Koch, "Microstructural Implications Concerning the Magnetic Behavior of Co_5Sm," Conference on Magnetism and Magnetic Materials 1973

Effect of Chemical Treatment on $Co_{17}Sm_2$ (J. J. Becker)

The compound $Co_{17}Sm_2$ is a potentially high-performance material as defined in the work statement. Its saturation magnetization $4\pi M_s$ is 12030 gauss, so the energy product could be greater than 36 mGOe. It has a high easy-axis anisotropy but has shown only low coercive forces when ground into particles in the usual way. It has previously been shown that chemical smoothing of the particle surface, or alternatively attack by a dilute acid, could greatly raise the coercive force of Co_5Y and Co_5Sm. The coercive force of $Co_{17}Sm_2$ can also be increased by treatment in either a chemical polishing solution or a dilute acid solution. This has been demonstrated in two samples. While both of them are nominally $Co_{17}Sm_2$, chemical analysis showed that one, sample MH577, contained 75.7 wt % Co, and the other, MH506, 77.0 wt % Co. Both showed the effect, and since they straddle the stoichiometric composition of $Co_{17}Sm_2$, which is 76.9 wt % Co, it appears that the effect is truly a property of that phase.

The results are summarized below; the numbers are intrinsic coercive forces:

	MH577	MH506
As ground to -325 mesh	240	310
5 sec in chemical polishing solution*	620	540
10 sec in chemical polishing solution*	870	580
20 sec in chemical polishing solution*	800	495
10 sec in 2% HNO_3	320	325
30 sec in 2% HNO_3	550	550
60 sec in 2% HNO_3	605	390

*3 parts HNO_3, 1 part H_2SO_4, 1 part H_3PO_4, and
5 parts CH_3COOH by volume.

These values of coercive force are not yet as high as they need to be, but the fact that H_c can be increased by a factor of nearly 4 in this potentially high-performance material appears to be significant.

Magnetic Behavior of Co_7R_2 Compounds (J. J. Becker)

The successful preparation of high-performance cobalt-rare earth permanent magnets seems to require that the final overall composition be on the rare earth-rich side of the Co_5R composition, presumably because of the requirements for successful liquid-phase sintering. Thus it seemed appropriate to examine the magnetic properties of some Co_7R_2 compounds in more detail. Several alloys were prepared with the following nominal compositions:

Co 57.84% Sm 42.16%
Co 69.88% Y 30.12%
Co 59.55% Ce 40.45%
Co 58.85% Nd 41.15%
Co 59.76% La 40.24%
Co 59.41% Pr 40.59%

These correspond to Co_7R_2 in each instance. This compound may not necessarily exist in every case. These materials were simply ground to -325 mesh powder and their coercive force measured. The results were as follows.

Rare Earth	Intrinsic Coercive Force
Sm	4300 Oe (H_m=21 kOe), 5200 Oe (H_m=30 kOe)
Y	360 Oe (H_m=21 kOe)
Pr	810 Oe (H_m=21 kOe)
Ce	1210 Oe (H_m=21 kOe)
Nd	475 Oe (H_m=21 kOe)
La	320 Oe (H_m=21 kOe)

The pronounced difference between the Sm compound and all the others is entirely analogous to the behavior of the 5 - 1 series and raises the same question: Why is the Sm compound so different?

Session on Origin of Coercive Force (J. J. Becker)

During the time of the present report, the author organized and chaired a session on the origin of the coercive force in high-anisotropy materials, the Symposium-Workshop on Cobalt-Rare-Earths, held at the 18th Annual Conference on Magnetism and Magnetic Materials in November 1972. The session consisted of a paper reviewing the present status of the problem, given by J. D. Livingston, followed by a panel discussion. The panel members included K. J. Strnat, University of Dayton; R. A. McCurrie, University of Bradford, England; K. Bachmann, Brown-Boveri, Switzerland; and G. Y. Chin, Bell Laboratories. The purpose of the session was to pinpoint as precisely as possible where the understanding of the problem stands, what discrepancies exist, and what exactly should be done next to advance the understanding of this subject most effectively, thereby establishing the strongest possible base for continued development of this class of materials. The size of the audience and the degree of its participation throughout the session were most gratifying and amply testified to the widespread interest in this important subject.

A precis of the oral presentation of the review paper is given next, to supplement the published paper. This is done because for the oral version several additional slides were prepared to present the material in somewhat simpler form. These figures and the comments on them are included here for the pedagogical value they may have.

Present Understanding of Coercivity (J. D. Livingston)

Figure 1 shows the various coercivity models so far suggested for high-anisotropy uniaxial materials such as Co_5Sm. Coherent rotation and curling can be eliminated because the experimentally observed coercivities are much lower than the theoretical values for these reversal processes. Thus we conclude that reversal occurs by the nucleation and growth of reverse domains.

MODEL	COERCIVITY
COHERENT ROTATION	$\frac{2K}{M_S} + (N_\perp - N_\parallel)M_S$
CURLING	$\frac{2K}{M_S} - N_\parallel M_S$
DOMAIN NUCLEATION AT DEFECTS	H_{nucl}
GENERAL DOMAIN-WALL PINNING	H_{unpin}
LOCAL DOMAIN-WALL PINNING	H_{unpin}

Figure 1 Coercivity models and corresponding coercivities.

Coercivity is controlled either by the nucleation event, by general wall pinning, or, according to models developed by Zijlstra, Westendorp, and Strnat and co-workers, by a localized wall-pinning.

Figure 2 shows schematically the different magnetic behavior predicted by general pinning and nucleation models. The behavior at the top, characteristic of general pinning, is observed by copper-bearing precipitation alloys. The behavior at the bottom, on the other hand, is characteristic of predominantly single-phase Co_5R materials. This observation rules out general pinning in these cases, and is consistent with nucleation-controlled reversal. However, certain local pinning models can also explain such behavior.

Study of the magnetization curves of individual Co_5R particles shows that both nucleation and local pinning can play a role in controlling coercivity. Considered in detail, the models in fact can be difficult to distinguish in some respects. However, as shown schematically in Fig. 3, the two models involve opposite dependences on defect density. The curve shows that a few defects can lower coercivity by nucleation of reverse domains, but a sufficiently high density of defects can raise coercivity through wall pinning. Therefore, in principle, to establish whether nucleation or local pinning is dominating coercivity in powder assemblies or sintered magnets, we need only determine

GENERAL PINNING

NUCLEATION
(and local pinning ?)
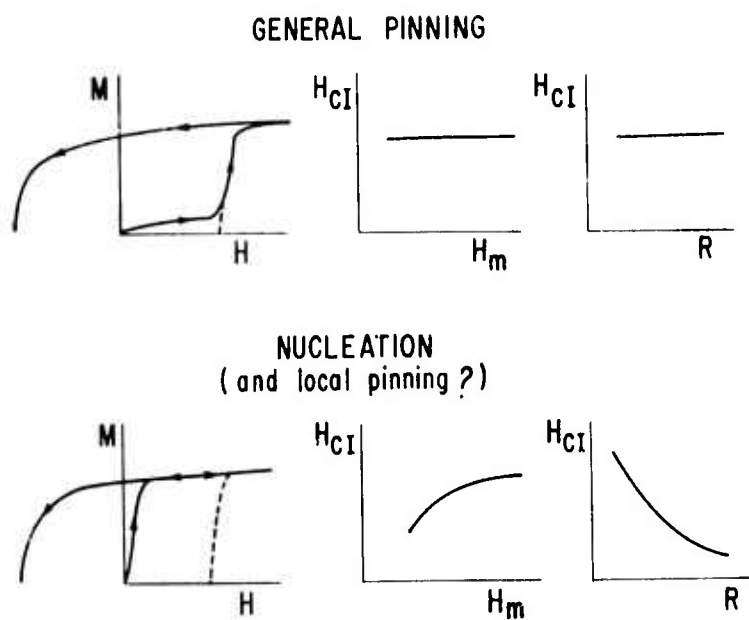

Figure 2   Magnetic behavior predicted by general pinning and nucleation
models.

NUCLEATION   PINNING

Defects   Defects
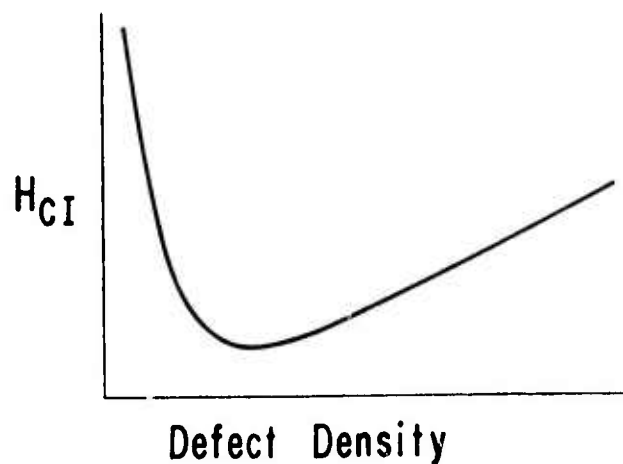
lower H_{CI} raise H_{CI}

Figure 3   Dependence on defect density of nucleation and pinning models.

whether coercivity is increasing or decreasing with increasing defect density. In practice, interpretation is somewhat ambiguous because the nature of the important defects, and their connection with various processing steps, are generally unestablished.

Figure 4 shows schematically the effect on coercivity of various processes such as grinding, low-temperature aging, etc., and a possible explanation for a nucleation-controlled model. In some cases, other workers have explained these results by a pinning-controlled model. For example, the increase of coercivity on etching has been attributed to an introduction of pinning centers, perhaps due to hydrogen, by the etching process. The explanation based on nucleation seems more plausible in view of our general knowledge of defects, but more metallographic studies are needed to establish definitively the significant defects and their density after various processing steps.

Finally, Fig. 5 summarizes the conclusions reached in the above discussion.

PROCESS	EFFECT ON H_{cI}	POSSIBLE CAUSE
GRINDING		PARTICLE SIZE, DISLOCATIONS
AGING (OXIDATION)		COBALT-RICH REGIONS
ETCHING		REMOVAL OF SURFACE DEFECTS
ANNEALING NEAR 1000°C		REMOVAL OF DEFECTS
ANNEALING NEAR 700°C		PRECIPITATES

Figure 4 Effect on coercivity of various processes, and possible cause on nucleation model.

MECHANISMS DETERMINING COERCIVITY

Precipitation Alloys ($Co-Cu-Fe-R$)	GENERAL WALL PINNING
Co_5R Single Particles	NUCLEATION & LOCAL PINNING
Powders Sintered Magnets	} NUCLEATION (& LOCAL PINNING ?)
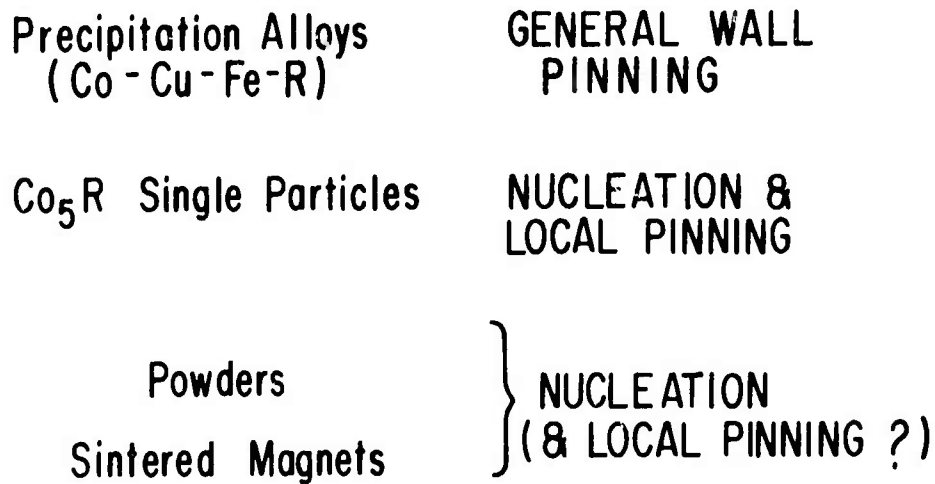
Figure 5 Mechanisms determining coercivity.

Analysis for Rare Earth Present in the Reduced State by Selective Oxidation (R. E. Cech)

The Co_5-rare earth compounds may be viewed as combinations of a relatively noble or difficult-to-oxidize metal (cobalt) and highly reactive rare earth metals. It should, therefore, be possible to selectively oxidize the rare earth while maintaining the cobalt in a reduced state. If one carries out this selective oxidation of rare earth, the weight gain due to oxygen pickup can be used as a measure of only that portion of the rare earth element in the sample which exists in the reduced state. For example, for samarium (Sm°, At wt = 150.35) oxidized to Sm^{+3} the Sm:0 factor would be:

$$\frac{2 \times \text{At wt Sm}}{3 \times \text{At wt Oxygen}} = 6.2646.$$

From this one could determine percent reduced samarium:

$$\% \text{ Sm} = \frac{\Delta W(\text{from oxygen pickup}) \times 6.2646 \times 100}{\text{Sample wt}}$$

For the elements praseodymium and cerium that have both +3 and +4 oxidation states, it would be necessary to determine empirically the oxidation state of the selectively oxidized rare earth element under a standard set of furnacing conditions.

The atmosphere for carrying out this process could be varied over a wide range of operating conditions.

If one considers the reaction:

$$CoO + H_2 \rightarrow Co + H_2O \quad \Delta F°_{1000°K} = -6,050 \text{ cal.}$$

$$K = \frac{pH_2O}{pH_2} = 21$$

For 1 atm of 750 torr:

$$pH_2O = 716 \text{ torr}$$

$$pH_2 = 34 \text{ torr.}$$

One could obtain wet hydrogen by passing H_2 through water at any temperature up to 98.4°C and still maintain cobalt in the reduced state while oxidizing the rare earth element.

As an alternative to this procedure one could oxidize the sample completely and then selectively reduce the cobalt using hydrogen of any desired dew point. If one considers that a hydrogen dew point of -90°C is about the dryest gas that one would normally encounter without taking elaborate steps to dry the gas:

$$\frac{pH_2O}{pH_2} = 10^{-7} \text{ for } -90°C \text{ dew point } H_2$$

For the reaction:

$$1/3 \, Sm_2O_3 + H_2 \rightarrow 2/3 \, Sm + H_2O \quad \Delta F°_{1000°K} = +76,200 \text{ cal.}$$
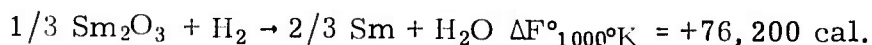
$$\log_{10}K = -16.66$$

$$K = \frac{pH_2O}{pH_2} = 10^{-16.66} .$$

Thus, dry hydrogen cannot reduced Sm_2O_3.

A simple procedure may be carried out to selectively oxidize the rare earth element with wet hydrogen if one includes a small rubber stoppered "U" tube at the gas inlet point of the reaction tube. The system containing the Co_5-rare earth powder specimen can be flushed with N_2, then raised to temperature under dry H_2. A small amount of water can then be injected into the "U" tube using a hypodermic syringe. After all the water has been evaporated into the flowing H_2 stream, the system then reverts to dry H_2 needed for cooling the system to room temperature.

16

A series of oxidation and reduction experiments were performed using mixed sample 3943B13-16 (2.6943 grams). All heat treatments were for 1 hour in designated atmospheres:

1. Dry hydrogen, nominally -60°C dew point.
2. Wet hydrogen, +25°C dew point.
3. Air.

Specimens treated in wet hydrogen were given an additional 10 minutes at temperature in dry hydrogen before cooling.

It was noted that selectively oxidized Co_5Sm or reduced CoO would pick up weight on exposure to the atmosphere, presumably because of adsorption of oxygen from the atmosphere. This would cause a variation in ΔW leading to an apparent change in $Sm°$ (reduced samarium) content. The following results illustrate the point:

	Wt % $Sm°$
Specimen after 2 hours in wet H_2, promply weighed in air --	32.99
Specimen stirred in air using clean S.S. spatula-----------	33.18
Specimen aged in room air at room temperature 1 hour ----	33.43

In order to minimize errors due to this effect, and recognizing that the initial powder is coated with adsorbed oxygen, all samples were stirred in air and weighed promptly.

The following results were obtained on sample 3943B13-16:

	Wt % $Sm°$
1 hour 800°C, wet H_2--	32.95
+1 hour 800°C, wet H_2--	33.18
+1 hour 800°C, wet H_2--	33.11
+1 hour 800°C, air (complete oxidation)	
+1 hour 800°C, dry H_2--	33.97
+1 hour 800°C, dry H_2--	33.69

The true $Sm°$ content must lie somewhere between 33.18% and 33.69%. One can simply presume that it lies midway between the selective oxidation and selective reduction figure. The true $Sm°$ content would then be 33.44 wt %. Note that the same figure is obtained by averaging the results of the first hour of oxidation and reduction as is found by averaging the second hour of each.

The following procedure is suggested for determination of Sm°:

1. Selective oxidation in wet H_2 1 hour at 800°C.
2. Determine wt of stirred sample.
3. Oxidize completely in air.
4. Reduce for 1 hour at 800°C in dry H_2.
5. Determine wt of stirred sample.
6. Average ΔW and calculate the percent of Sm° from the stoichiometry factor.

Also, the "aged one hour at R. T. " should be checked to see if the agreement here is fortuitous.

Preparation and examination of Co_5Tm, Co_5Yb, Co_5Sc, Co_5Eu, and Co_5Lu (J. D. Livingston)

Attempts were made to case alloys of nominal compositions corresponding to Co_5Tm, Co_5Yb, Co_5Sc, Co_5Eu, and Co_5Lu. The Co-Tm casting exhibited a lamellar microstructure (Fig. 6) which showed an intricate pattern of magnetic domains when viewed under polarized light (Fig. 7). X-ray powder patterns indicate the presence of Co_5Tm and Co_7Tm_2. The Co-Yb and Co-Sc castings consisted of Co-rich dendrites and an interdentritic eutectic (Figs. 8 and 9). X-ray powder patterns indicate Co, $Co_{17}Yb_2$, and possibly Co_5Yb in the former casting and Co_2Sc in the latter. The Co-Eu casting was very inhomogeneous and a portion was very reactive. No

Figure 6 Co-Tm as-cast.   250X

18
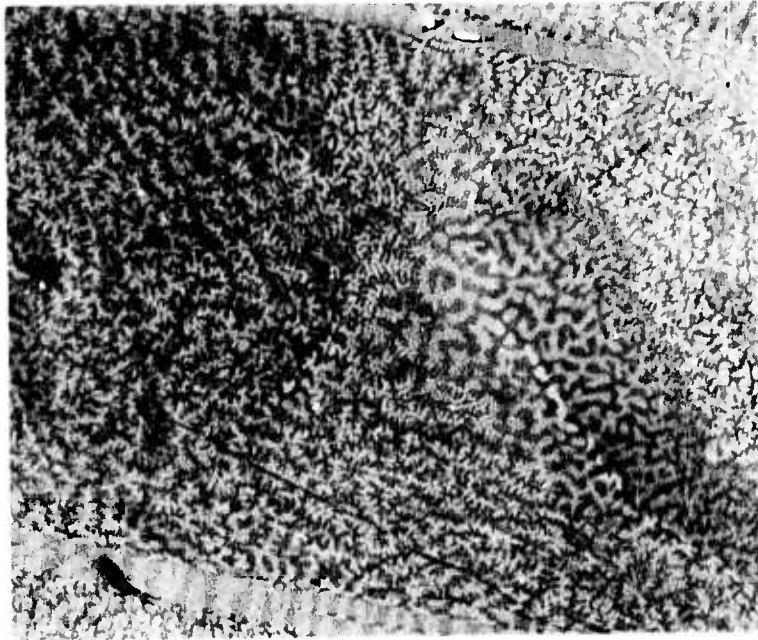
Figure 7 Co-Tm as-cast (domains).   250X
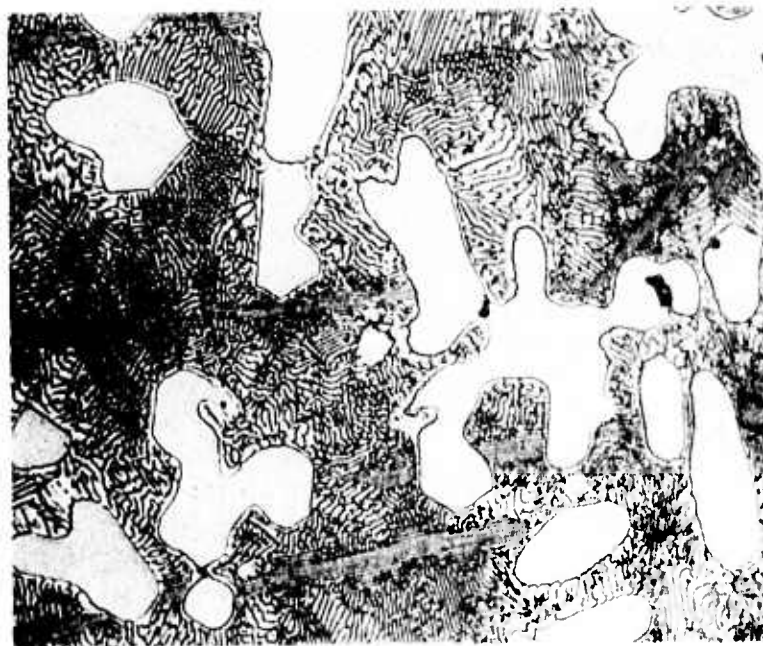
Figure 8 Co-Sc as-cast.   1500X
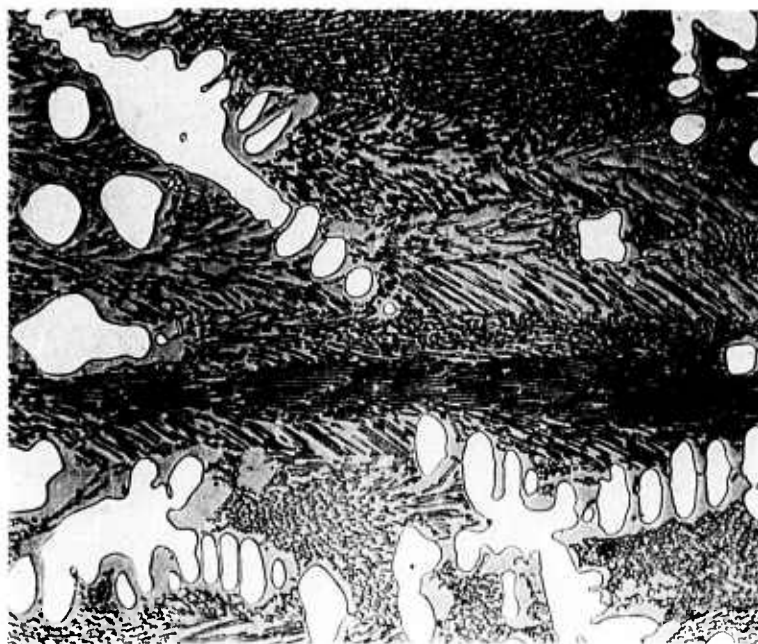
Figure 9 Co-Yb as -cast.   500X

intermetallic compounds were detected, but $Eu(OH)_3$ was prominent in the x-ray patterns. The Co-Lu melt reacted violently and rapidly with the alumina crucible, and no casting could be prepared.

The Alignment Factor (D. L. Martin)

The role of alignment factor and its effect on magnetic properties has been studied in detail. A series of Co-Sm specimens with different degrees of alignment were prepared by varying the prealignment packing of the powder and the magnitude of the alignment field. The first quadrant magnetization curves and the second quadrant demagnetization curves were measured.

Each sample was exposed to a series of increasing magnetizing fields and the magnetization then measured. After each measurement, the sample was taken out of the field and the open circuit magnetization was measured. For a long bar, the $4\pi J$ value so measured is a close approximation of the B_r value. Thus, data was obtained on the variation of $4\pi J_s$ and B_r with peak magnetizing field. The results are plotted in Figs. 10 and 11.

The alignment factors listed were obtained by the following relation:

$$A' = \frac{B_{r\,(100)}}{pB_s}$$

20

where $B_{r(100)}$ is the residual induction value obtained after magnetizing at 100 kOe, p is the packing fraction, and B_S is the saturation value of the alloy used in the study. The saturation was calculated from the B_r measured for a random unaligned sample with a known packing fraction as follows:

$$B_S = \frac{2 \times B_{r(random)}}{P_{(random)}} \quad \text{or } 10,000 \text{ gauss}$$

The results in Fig. 10 show the change in B_r with alignment factor and magnetizing field. Above a field of 60 kOe, the B_r value for each sample does not change noticeably. In contrast, the magnetization, $4\pi J$, for the samples with a poor degree of alignment is still increasing at 100 kOe (Fig. 11). It is quite clear from these two figures that alignment is an important factor to control if optimum properties are to be realized. The demagnetization results listed in Table I give additional emphasis to the importance of alignment in alloy development studies. Thus, the energy product varied from 5 to 15 mGOe as the alignment increased from a random condition to over 0.9.

A surprising result of this study is the strong dependence of the magnetization measured at 100 kOe on the alignment. This is shown in Fig. 12 as well as in Fig. 11.
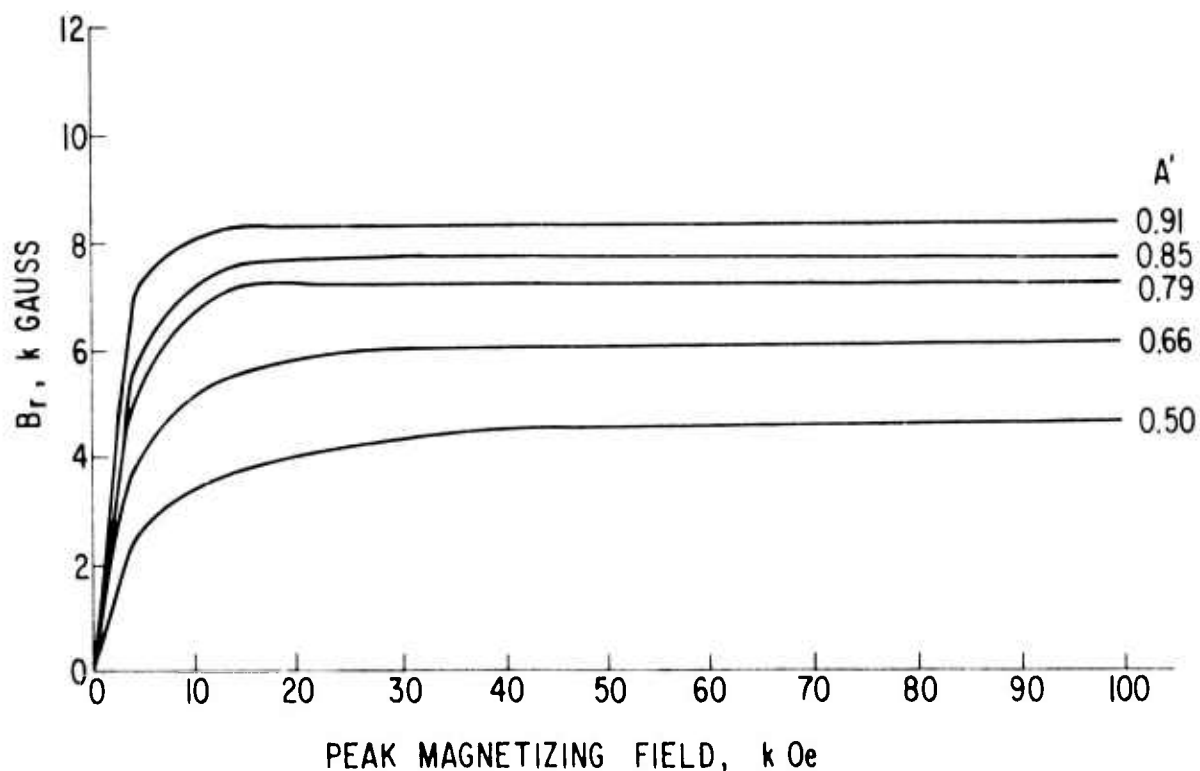
Figure 10 Variation of B_r with magnetizing field for a series of Co-Sm samples with different degrees of alignment.
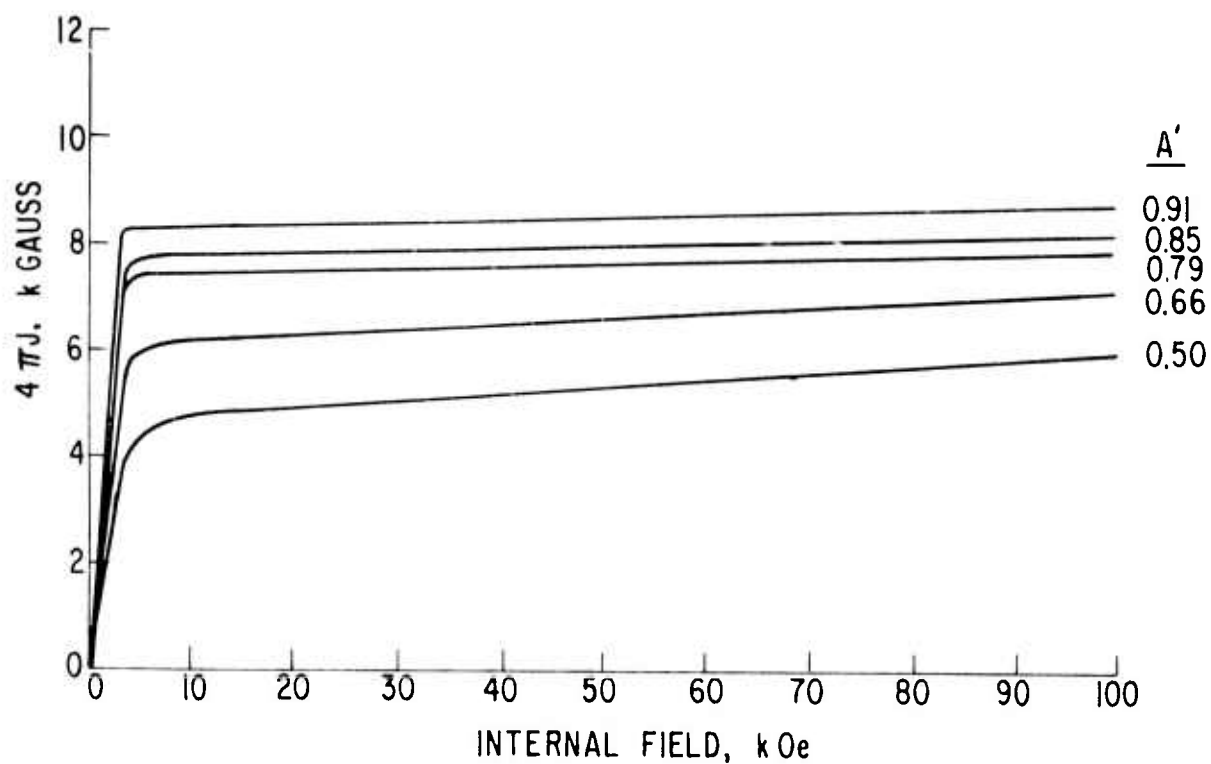
Figure 11 Variation of $4\pi J$ with magnetizing field for a series of samples with different degrees of alignment.

TABLE I

Demagetization Results on a Series of Cobalt-Samarium Magnets with Varying Alignment Factors. The Samples were Magnetized at 100 kOe Prior to Testing

No.	Nominal w/o Cobalt	Treatment (°C)	$4\pi J_s$ (kG)	B_r (kG)	H_c (kOe)	H_k (kOe)	$_jH_c$ (kOe)	$(BH)_{max}$ (mGOe)	Density (g/cc)	P	A'
A	37	1 hr 1120	6.07	4.56	-4.2	-4.8	-25.1	5.1	7.82	0.909	0.50
B	37	1 hr 1120	7.42	6.08	-5.2	-4.6	-22.2	8.7	7.83	0.911	0.67
C	37	1 hr 1125	8.61	7.31	-5.4	-3.4	-15.0	11.3	7.74	0.90	0.81
D	37	1 hr 1125	8.93	7.76	-5.7	-4.2	-16.9	13.3	7.79	0.906	0.86
E	37	1 hr 1125	9.42	8.28	-5.9	-4.7	-13.4	15.3	7.80	0.907	0.91
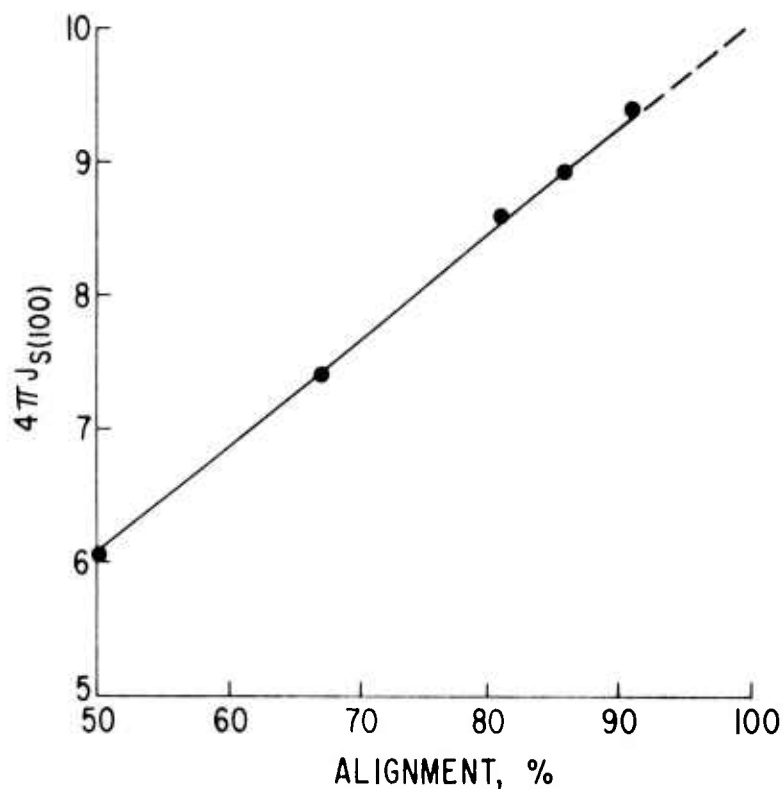
Figure 12 Variation of magnetization, $4\pi J_{100}$, with degree
of alignment, A'.

Diffusion couple studies (D. L. Martin)

Diffusion couples have been made between cobalt and a 60 wt % Sm alloy.
The alloy powder was placed in a hole in a cobalt block and a cobalt rod then
inserted into the hole. The assembly was heated, then sectioned and observed
under the microscope.

Figure 13 shows the structure resulting from 1 hour at 1120°C. The pure
cobalt is at the bottom of the picture, and all the phases corresponding to the
published phase diagrams can be seen, as marked in the figure. Figure 14
shows the same area as Fig. 13 but under polarized light, showing the magnetic
domain structures of the various phases. These structures indicate that the
c-axis of the 5-1 phase is approximately vertical in the picture, that is, in
the diffusion direction. The domain structure of the 17-2 region is consid-
erably smaller in scale, in keeping with its higher magnetization and lower
anisotropy.

The diffusion couples provide an excellent medium for the study of the
transformations that appear to take place in the 5-1 phase at moderately
elevated temperatures. Figure 15 shows the structure resulting when a 5-1
region, originally produced by a 15 hour diffusion treatment at 1120°C, is

Co_3Sm

Co_2Sm

Co_3Sm
Co_7Sm_2

$Co_{17}Sm$

$Co_{17}Sm_2$

Co

Figure 13   Cobalt + 60 wt % Sm alloy diffused 1 hour at
1120°C.   525X

Co_3Sm

Co_2Sm

Co_3Sm
Co_7Sm_2

$Co_{17}Sm$

$Co_{17}Sm_2$

Co

Figure 14   Cobalt + 60 wt % Sm alloy diffused 1 hour at 1120°C.
Polarized light.   525X

24

Co_7Sm_2

Co_5Sm

$Co_{17}Sm_2$

Co

Figure 15 Cobalt + 60 wt % Sm alloy diffused 15 hours at 1120°C and then
   heat treated for 206 hours at 700°C.   228X

Co_5Sm

$Co_{17}Sm_2$

Co

Figure 16 Cobalt + 60 wt % Sm alloy diffused 15 hours at 1120°C and then
   heat treated for 206 hours at 700°C.   570X

25

held at 700°C for 206 hours. Figure 16 shows a region of the same sample
at higher magnification. $Co_{17}Sm_2$ appears to precipitate much more readily,
both at grain boundaries and within grains, than Co_7Sm_2. The structure ap-
pearing after 48 hours at 750°C is shown in Fig. 17. Much 17-2 is visible.
After a longer time, Fig. 18, a striated structure within the grains is visible.
This structure, which can also be seen in Figs. 15 and 16, is tentatively
identified as 7-2. In Figs. 15 and 16, it can be seen to form along with 17-2
on the 17-2 side of the diffusion couple. The exact mechanism of its formation
may involve various types of cooperative lattice displacements and has not yet
been identified positively.
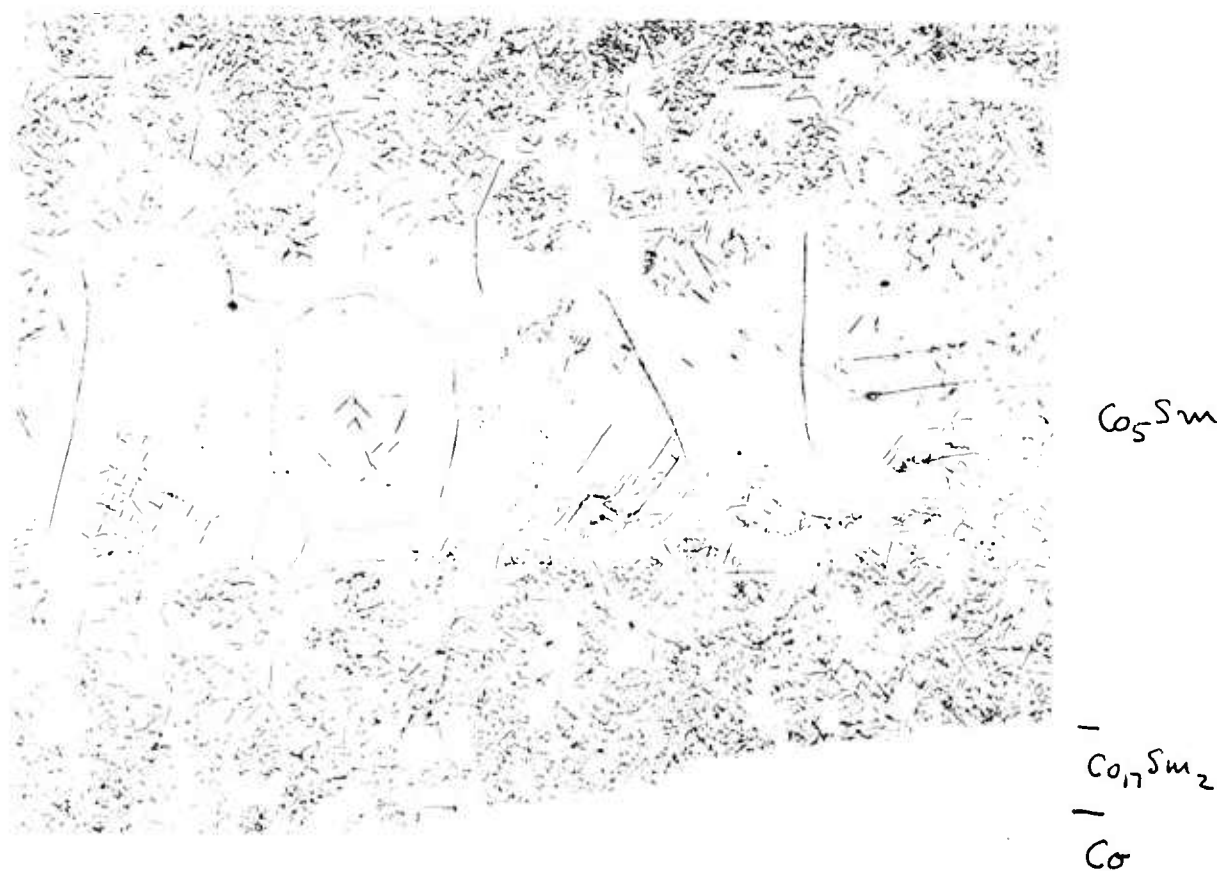

Figure 17   Cobalt + 60 wt % Sm alloy diffused 19 hours at 1130°C and then
   heat treated for 48 hours at 750°C.   279X
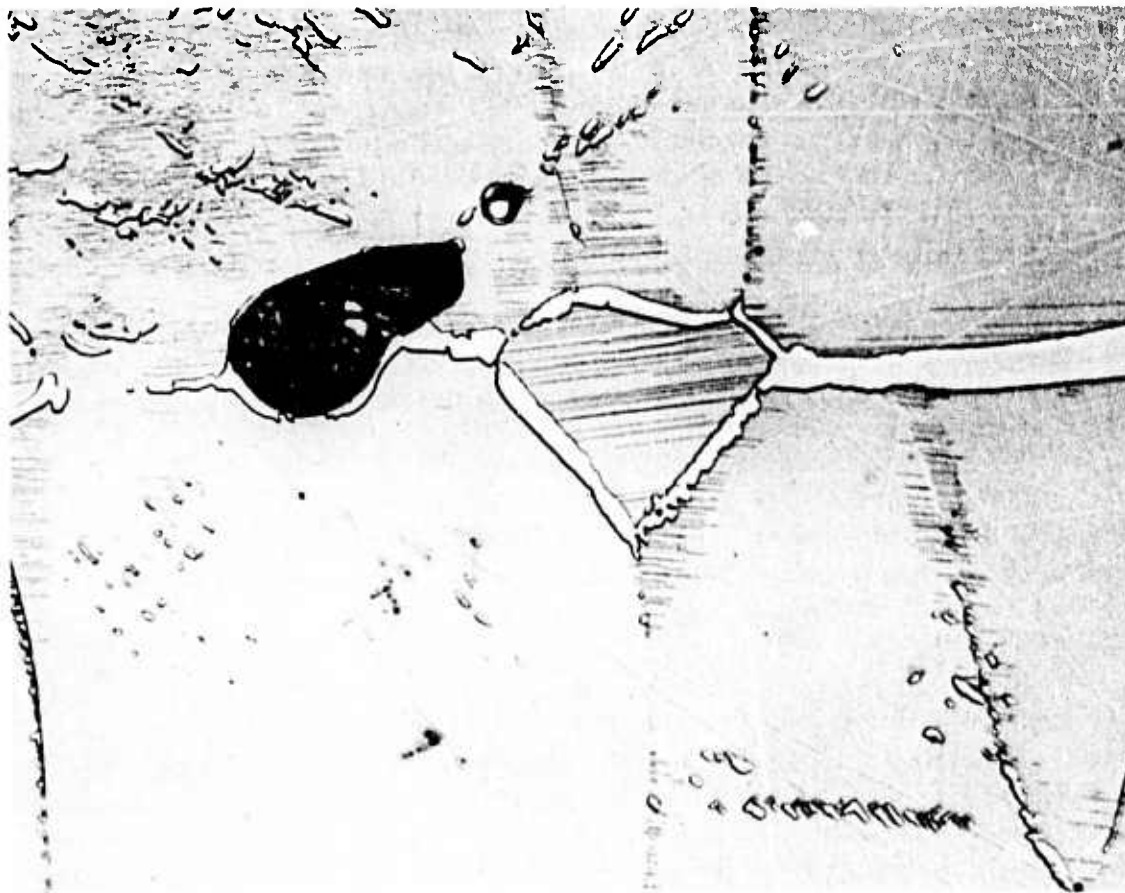
Figure 18   Cobalt + 60 wt % Sm alloy diffused 19 hours at 1130°C and then
heat treated for 237 hours at 750°C.   1500X

Summary of analytical results by wet chemistry and x-ray
fluorescence spectroscopy (J. G. Smeggil)

It is becoming increasingly evident that the magnetic properties of
cobalt-rare-earths are closely related to their chemical composition. Never-
theless, quantitative analytical chemical procedures are little used in char-
acterizing these materials.   Standard analytical practices are time-consuming
and of questionable reliability.

The objective of this work was to establish a fast, accurate instrumental
technique for these materials which could establish all major constituents to
±0.10 wt % within an hour.   The technique of x-ray fluorescence analysis was
selected for application toward this goal.

Before proceeding with the development of any instrumental technique,
it is necessary to prepare suitable samples for composition standards,
established by classical analytical methods.

Two different laboratories analyzed a series of specimens, using some-
what different techniques. The results are summarized in Fig. 19. They
indicate very good agreement in the variation from one sample to another,
but an absolute difference of approximately 0.5 wt %. While the origin of this
difference has not yet been traced to the analytical procedures, the samples
are entirely usable as self-consistent composition standards based on either
one of the sets of reported values. They have been used in this way to evaluate
x-ray fluorescence spectroscopy procedures.

A number of different instrumental techniques were considered, including
atomic absorption, solution spectrophotometry, emission spectroscopy, and
x-ray fluorescence. For various reasons only the last was considered worthy
of further evaluation.

Results from two outside laboratories gave virtually random scatter in
counting rate as a function of composition over a range of about 4 wt %. It
was then decided to optimize the procedure using the equipment available at
the General Electric Research and Development Center.

A very thorough study of counting time, sample configuration, recording
method, linearity, noise, 2θ optimization, stability, and other parameters
was made. Data taken on two different days on four samples, along with an
"unknown" sample, are summarized in Fig. 20. It is felt that the precision
of these results is limited by the particular instrument used, and that with
currently available equipment the objectives of this program would be fully
realized.
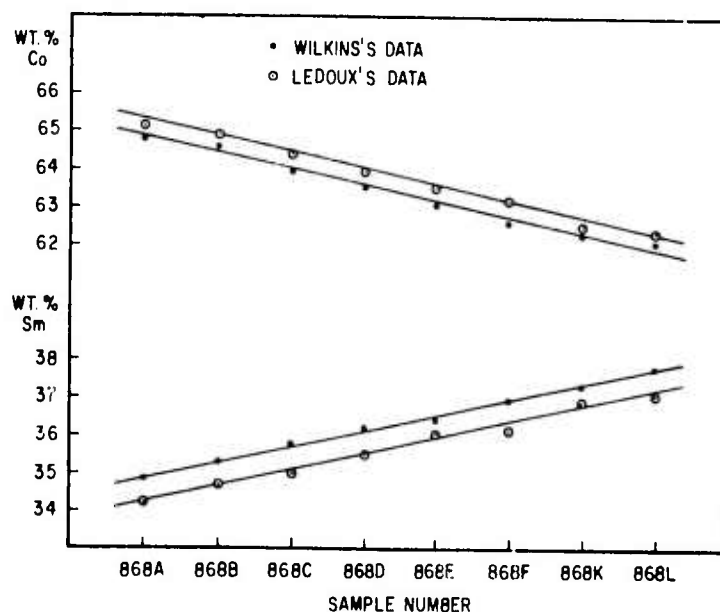
Figure 19 Comparison of analytical data from two sources on series of
Co-Sm alloys.
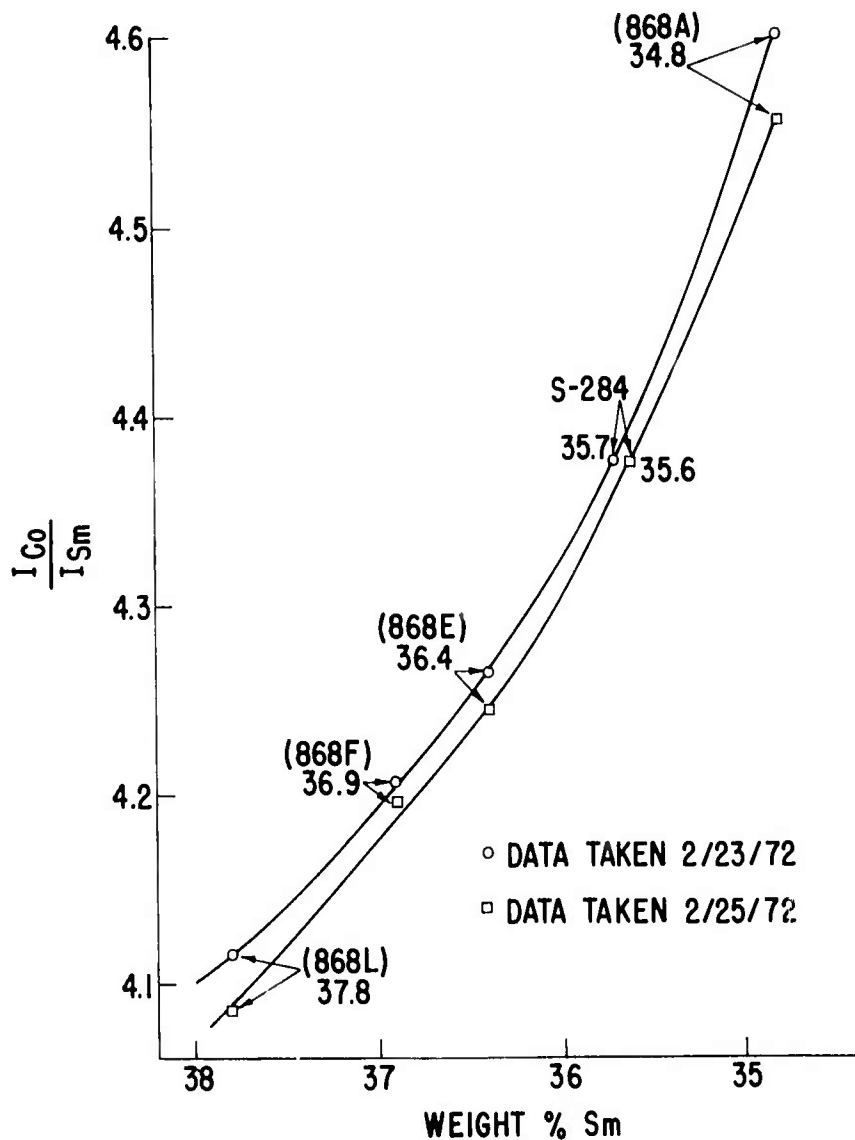
Figure 20 X-ray fluoreseence intensity ratio data taken on four samples on two different days.

Effeet of Proeessing Techniques on Composition (J. G. Smeggil)

To determine if processing teehniques for liquid-phase sintered materials are sueh that the material is depleted by preferential Sm vaporization or is degraded by substantial oxidation, a ehemieal analysis was undertaken of a bar of Co-Sm material pressed from the powder. The bar was cut into two pieces and then one of the pieees was sintered at about 1100°C for one hour. The results of this analysis are as follows.

	Pressed Powder	Sintered Rod
Wt % Co	63.54 ± 0.03	63.54 ± 0.03
Wt % Sm	35.55 ± 0.03	35.61 ± 0.03
Wt % O	0.39 ± 0.03	0.34 ± 0.03

These results indicate that the present processing techniques do not substantially alter the composition of the starting material. The initial Co contained 0.45 wt % Ni, and the sintered material probably contained about 0.26 wt % Al.

Variation of mechanical hardness and coercive force with post-sintering heat treatment (J. G. Smeggil)

Hardness measurements were made on cylindrical liquid-phase-sintered Co_5Sm magnets using a Knoop indenter. The samples were sintered at 1100°C for 1/2 hour, then annealed at either 750°, 900°, or 1100°C for 1/2 hour. A circular cross-section was polished on each specimen. A 200-gram load was applied to the indenter at a rate of 0.05 mm/sec for 10 seconds. The hardness values and coercive forces observed on these samples are as follows:

T(°C)	KHN (kg/mm^2)	H_{ci} (kOe)
750	541 (±54)	1.2
900	575 (±40)	20.3
1100	618 (±51)	2.0

The hardness data are in agreement with those reported in McCurrie, Carswell, and O'Neill, J. Mater. Sci. 6, 164 (1970). Even though the hardness values are the same within experimental error, the coercive forces vary by a factor of twenty.

GENERAL ⊛ ELECTRIC

RESEARCH
AND
DEVELOPMENT
CENTER

SCHENECTADY, NEW YORK

TECHNICAL INFORMATION SERIES

AUTHOR	SUBJECT	NO
Becker, JJ	magnetism	70-C-347

		DATE
		October 1970

TITLE	GE CLASS
Magnetization Discontinuities in Cobalt-Rare Earth Particles	1

	NO. PAGES
	2

ORIGINATING COMPONENT	
Metallurgy and Ceramics Laboratory	RESEARCH & DEVELOPMENT CENTER SCHENECTADY, N.Y.

SUMMARY

Hysteresis loops of single particles of Co_5Sm have previously shown that magnetization discontinuities (jumps) occur at fields H_n that are quite discrete and whose values depend on the previous magnetizing field H_m. Some effects of chemical polishing and air aging on the values of H_n and their H_m dependence in Co_5Sm particles are described. Jumps have now been observed in Co_5Y. A particle of Co_5Y showed a rectangular hysteresis loop with H_n = 3800 Oe for H_m of only 4100 Oe, remaining unchanged for H_m up to 30 kOe, and a maximum energy product of 27.6×10^6 gauss-Oe.

KEY WORDS

magnetism, magnetic materials, permanent magnets

INFORMATION PREPARED FOR _____

_____

MAGNETIZATION DISCONTINUITIES IN COBALT-RARE EARTH PARTICLES*

J. J. Becker

It has previously been observed[1,2] that individual particles of Co_5Sm can show sudden discontinuities in M as a function of H as the particle traverses a hysteresis loop. The values of H at which these jumps occur are quite discrete and reproducible for a given particle.[1] This behavior suggests very strongly that the magnetic properties of such particles, and of bulk permanent magnets made from this material, are determined by imperfections whose function is to act as nuclei or pinning sites for domain boundaries. Since the observed nucleating fields or coercive forces are at most a few percent of $2K/M_S$, large-scale magnetization rotation must be negligible, with magnetization rotation occurring only in the interior of a domain boundary. Imperfections thus become important by acting as nuclei for such local rotations. A study of the behavior of these magnetization discontinuities as a function of various chemical, mechanical, and thermal treatments is under way. Some novel results are described here.

In one experiment, a sample was prepared that consisted of three particles of Co_5Sm. These were each about 100μ in average dimension. They had been prepared from a magnetically sieved[1] powder prepared from a cast ingot that analyzed 66.8% Co (nominal Co_5Sm is 66.2). They had also been chemically polished[1] in a solution consisting of 3 parts HNO_3, 1 part H_2SO_4, 1 part H_3PO_4, and 5 parts CH_3COOH by volume. They were mounted in paraffin in the tip of a small glass capillary tube, so that they were in contact with each other, and aligned in a field as the paraffin solidified. Hysteresis loops at various maximum magnetizing fields H_m were measured in a vibrating-sample magnetometer. Some of these loops are shown, superimposed, in Fig. 1. A number of interesting features appear. In 5 kOe, the hysteresis loop resulting from free wall motion can be seen. Its slope is determined by the sample shape and corresponds to an effective shape demagnetizing field of about 3000 Oe. As H_m is increased, very pronounced jumps appear, along with curve segments. At large H_m, the reversal takes place almost entirely by jumps. It seems clear that the curved segments, including the entire 5 kOe loop, are due to gradual wall motion, while the sudden jumps are caused by the nucleation or unpinning and abrupt motion of a wall. The curves drawn at different H_m often have segments that appear to be continuations of each other, and frequently have jumping field values in common. Often the absolute value of the field at which a jump occurs is the same for both senses of H, strongly suggesting that the domain configuration at that point is the same except with the directions of magnetization
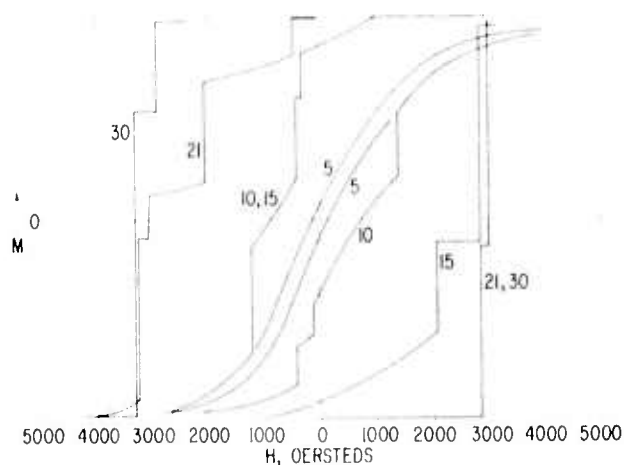

Fig. 1 Hysteresis loops of a sample consisting of three particles of Co_5Sm for various values of maximum magnetizing field H_m. Numbers next to loops are values of H_m in kOe.

reversed. Individual loops can be highly unsymmetrical, as for example the 15 kOe loop. It is interesting to note that at high H_m the magnetization reversal may be complete in two jumps, even though three particles are present.

Experiments were then performed on single particles. Figure 2 shows some results for a sample consisting of a single particle of this same material that was originally approximately 100μ in each dimension. The field at which the jump occurred, H_n, is plotted vertically and the previous magnetizing field H_m is shown horizontally. The sign of H_n is such that a positive value corresponds to the same direction as H_m and a negative value to the opposite direction. Of course, H_n, which is the applied field, always corresponds to a negative internal field. The trend that can be seen in Fig. 2 is that chemical polishing tends to produce jumps at less positive or more negative fields, that is, to remove the strongest nucleating sites. A strong site is here defined as one that produces a large local demagnetizing field and thus contributes to a low coercive force. Heating in air, in these preliminary experiments, seems to add new strong sites. Generally speaking, observed values of H_n seem to appear and disappear rather than being gradually modified by chemical treatment or aging, again suggesting that magnetization jumps are associated with discrete imperfections that are either present or entirely absent. The dependence of coercive force on H_m and on particle size is inherently discontinuous.
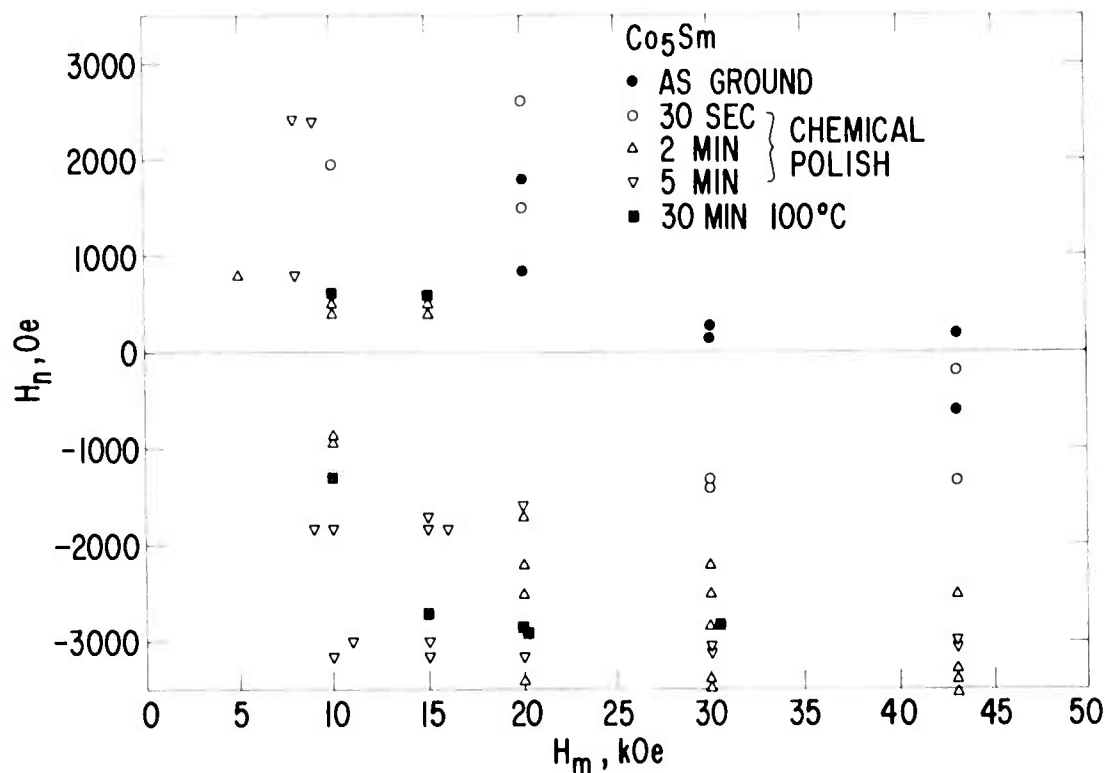
A single particle of stoichiometric Co_5Y was

Fig. 2 Behavior of a single particle of Co_5Sm after various treatments. The applied field H_n at which magnetization jumps take place is shown as a function of the previously applied magnetizing field H_m.

prepared and mounted as above. As ground, it showed mostly the wall-motion loop, with only two small jumps at +550 and -350 Oe, at all H_m from 5 to 30 kOe. This behavior persisted through successive treatments in the chemical polishing solution totaling 5 minutes. After two additional minutes, the behavior of the sample changed completely. By this time it had been reduced to about 40% of its original volume. The hysteresis loop, a photograph of which is shown in Fig. 3, became a perfect rectangle, with the magnetization reversing abruptly at 3800 Oe. Furthermore, this was true at all H_m down to 4100 Oe. It is remarkable that Co_5Y, which so far has not proven very tractable as a permanent-magnet material, shows such ideal behavior in single-particle form.

Most remarkable of all is the energy product of this particle. The perfect rectangularity of the hysteresis loop of this aligned particle means that the magnetization is equal to its saturation value. Then B_r is $4\pi M_s$, or 10,600 gauss. In a field of -3800 Oe, B would be 6800 gauss, for a maximum energy product of 25.8×10^6 gauss-Oe. If one corrects for the demagnetizing field of 800 Oe, measured from the free-wall hysteresis loop of this rather elongated particle, H_c is 4600 Oe and $(BH)_{max} = 27.6 \times 10^6$ gauss-Oe. This procedure can be justified on the basis that the reversal process does not depend inherently on the shape of the particle, in contrast to the Stoner-Wohlfarth coherent-rotation mechanism.

In either case, the energy product is believed to be the largest ever observed in any material at room temperature.
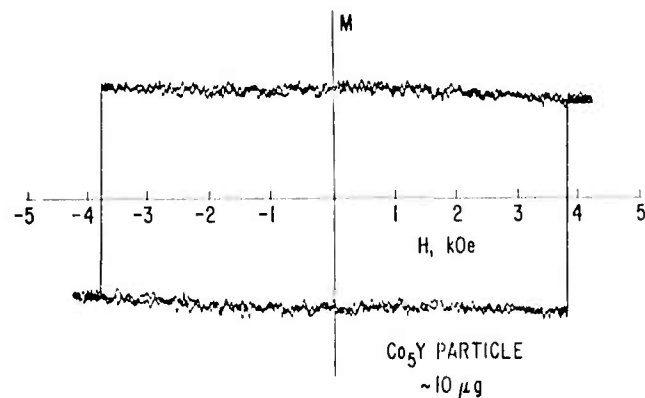

Fig. 3 Hysteresis loop of a single particle of Co_5Y: H_c = 3800 Oe, H_m = 4200 Oe. Loop traced twice in vibrating-sample magnetometer.

REFERENCES

1. J.J. Becker, IEEE Trans. on Magnetics, MAG-5, 211 (1969).

2. H. Zijlstra, IEEE Trans. on Magnetics, MAG-6, 179 (1970).

71-C-069

J.J. Becker

THE INTERPRETATION OF HYSTERESIS LOOPS OF COBALT-RARE
EARTH SINGLE PARTICLES

35<

GENERAL ⟨ge⟩ ELECTRIC

General Electric Company
Corporate Research and Development
Schenectady, New York

TECHNICAL INFORMATION
SERIES

AUTHOR Becker, JJ	SUBJECT magnetism	NO. 71-C-069
		DATE March 1971
TITLE The Interpretation of Hysteresis Loops of Cobalt-Rare Earth Single Particles		GE CLASS 1
		NO. PAGES 4
ORIGINATING COMPONENT Metallurgy and Ceramics Laboratory		CORPORATE RESEARCH AND DEVELOPMENT SCHENECTADY, N.Y.

SUMMARY
The magnetic behavior of single particles of Co_5Sm is being studied in an effort to understand the origin of the coercive force in cobalt-rare earths. It has been found that the complex hysteresis loops often observed, containing several magnetization discontinuities, can be analyzed as the linear sum of single-discontinuity hysteresis loops, implying that regions of a particle can act magnetically independently.

KEY WORDS

magnetism, magnetic materials, permanent magnet
materials

INFORMATION PREPARED FOR _____

THE INTERPRETATION OF HYSTERESIS LOOPS OF COBALT-RARE EARTH
SINGLE PARTICLES*

INTRODUCTION

In the brief period since the discovery of the extremely high magnetocrystalline anisotropy of Co_5Y (Ref. 1), the cobalt-rare earths have been successfully fabricated into permanent magnets with unique properties[2-1] and are already finding device applications. [5] So far, useful magnets have been based on Co_5Sm. It is not at present understood why Co_5Sm yields better permanent magnet properties than other closely related cobalt-rare earth compounds. What has been known for some time is that cast and ground Co_5Sm alloys show much higher intrinsic coercive forces H_c for a given particle size than similarly prepared powders of related materials. [6] This heightened coercive force somehow persists even in magnets made by sintering. Yet the coercive forces attainable even in Co_5Sm are a smaller fraction of $2K/M_s$ than those that have been achieved in $MnBi$[8] or the hard ferrites, [9] materials whose properties are similarly dominated by crystal anisotropy. In the cobalt-rare earths the coercive force gradually increases with decreasing particle size, and furthermore it can vary by orders of magnitude at a given particle size, depending on the surface treatment the particles have received. [10] It is also known that particulate Co_5Sm shows an unusually strong dependence of H_c on the previous magnetizing field H_m. [7] It seems quite clear that these materials are not to be regarded as representatives of classic fine-particle theory. [11] Rather, their magnetization reversal is controlled by domain boundary nucleation and motion. [7] Thus the understanding of the magnetic properties of these materials must be based on the study of the relationship of domain processes to material structure.

Two lines of approach suggest themselves. Ideally, of course, they should complement each other. One is the direct observation of magnetic domain structure and its correlation with other visible structural features, either in bulk material or in individual particles. Another is the measurement of hysteresis behavior and its interpretation in terms of magnetization reversal mechanisms. [12,13] This type of study should be especially fruitful with single particles. It has already been shown that a single Co_5Y particle could be made to exhibit ideal square-loop behavior and a $(BH)_{max}$ of 27.6 mG-Oe (Ref. 12). The present report describes how the hysteresis behavior of a single particle of Co_5Sm can be analyzed in a surprisingly simple manner.

MAGNETIC BEHAVIOR OF SMALL PARTICLES

The grain size of conventional cast cobalt-rare earth ingots is large enough so that individual particles on the order of 50μ in average diameter prepared by grinding are very likely to be single crystals. Aligned aggregates of such particles show the dependence of H_c on particle size, on magnetizing field, and on surface treatment mentioned above. When the hysteresis properties of individual particles are measured, striking magnetization discontinuities or jumps appear. [10,12,13] These occur at definite, quantized fields H_n whose value in each case depends on the previous H_m. For low values of H_m, the hysteresis behavior may consist entirely of the traversal of the narrow loop due to the motion of free walls. At higher H_m, jumps appear. By way of illustration, Figs. 1, 2, and 3 show hysteresis loops of a particle of Co_5Sm after magnetization in H_m of 5, 16, and 21 kOe, respectively. This particle was approximately equiaxed, with an average diameter of about 50μ. It had been chemically polished. [10] The figures are recorder traces of magnetization vs applied field, measured in a vibrating-sample magnetometer. Figure 1 shows the wall-motion loop in $H_m = 5$ kOe. Figures 2 and 3 show jumps that appear in higher H_m. The 21 kOe loop in Fig. 3 differs from the 16 kOe loop in Fig. 2 only in that the second jump in the descending branch has moved out to a more negative H.

Although the loops shown in Figs. 2 and 3 might appear disappointingly complex, they can be analyzed into simple components as shown below.
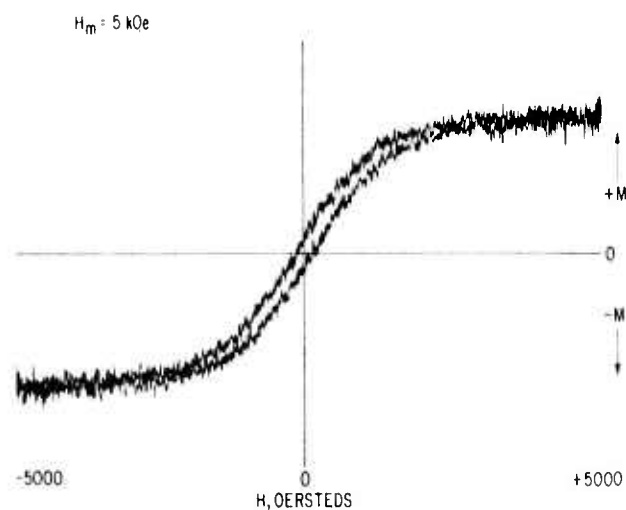

Fig. 1 Hysteresis loop of 50μ single particle of Co_5Sm. $H_m = 5$ kOe.
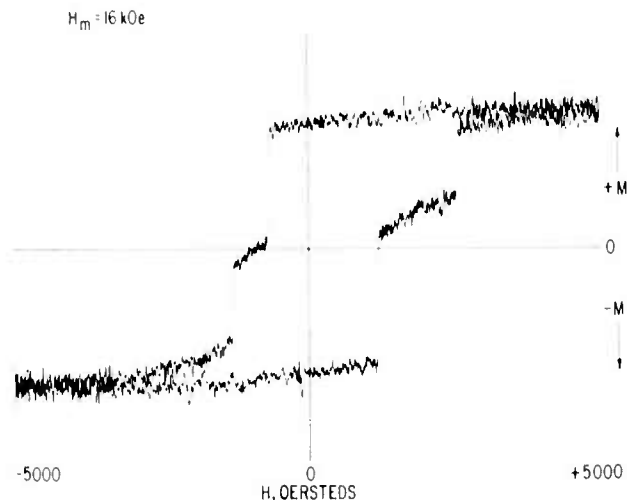
$H_m = 16 \, kOe$

+M

0

−M

−5000   0   +5000

H, OERSTEDS

Fig. 2 Hysteresis loop of 50μ single particle of Co$_5$Sm. Same particle as in Fig. 1, but H$_m$ = 16 kOe.

$H_m = 21 \, kOe$

+M

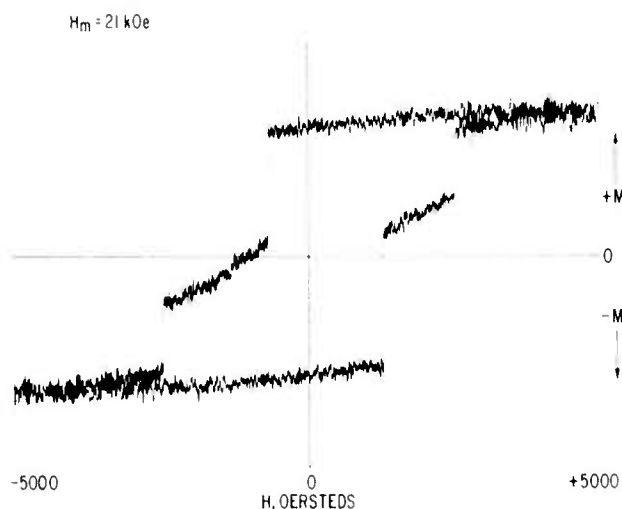0

−M

−5000   0   +5000

H, OERSTEDS

Fig. 3 Hysteresis loop of 50μ single particle of Co$_5$Sm. Same particle as in Fig. 1, but H$_m$ = 21 kOe.

ANALYSIS OF SMALL-PARTICLE HYSTERESIS LOOPS

First we define "single-particle behavior." This is the behavior exhibited by a particle that shows only one jump on each branch of the hysteresis loop. This is illustrated schematically in Fig. 4. In small H$_m$, with free walls present, the hysteresis loop has a slope 1/N, where N is a particle demagnetizing factor such that H$_d$ = NM. The loop has a width corresponding to the small coercive force for wall motion H$_w$. If H$_w$ were zero, that is, if the permeability were infinite, the loop would shrink to a line, for which

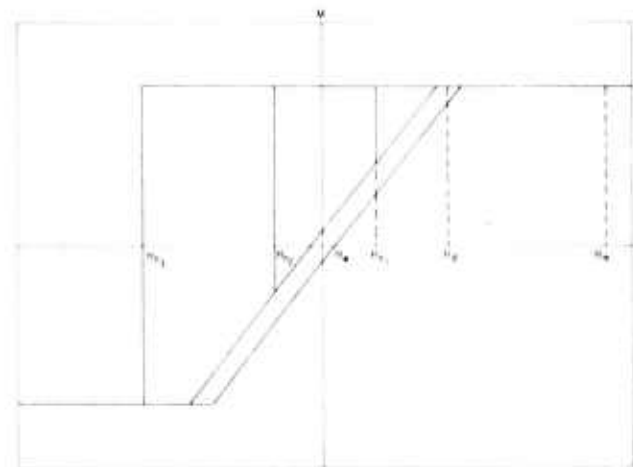$$H_{internal} = H_{applied} - NM = 0.$$

Fig. 4 Single-particle behavior, schematic.

In increasingly larger H$_m$, jumps will occur in increasingly negative fields, such as H$_{n_1}$, H$_{n_2}$, and H$_{n_3}$. After saturation in the other direction, jumps--not shown in the figure--would occur at other H$_n$, which might or might not have the same numerical values as H$_{n_1}$, H$_{n_2}$, and H$_{n_3}$. The essence of "single-particle behavior" as here defined is that only one jump per branch of the loop occurs after a given H$_m$. It is very important to note that a jump will not in general completely reverse the magnetization. Only the jump at H$_{n_3}$ in Fig. 4 does so. In general the wall will move until the field on it becomes zero, or, more precisely, H$_w$. It moves until M reaches a value corresponding to the free-wall loop. The wall stops, not because it has encountered any obstacles, but because the applied field and the demagnetizing field are equal and opposite and there is no force on the wall.

An experimental realization of this behavior is shown in Fig. 5. This particle of Co$_5$Sm was nearly 200μ in average diameter, but shows ideal single-particle behavior even though it is much larger than the particle shown in Figs. 1 through 3. The jump field is symmetrical, suggesting that the same imperfection is responsible for wall nucleation for both senses of M.

The loops shown in Figs. 1 through 3 can be synthesized by the addition of single-particle loops as defined above (in this case nonsymmetrical). The way this is done is illustrated in Fig. 6. Each of the lower loops, 6e and 6f, is a composite of the two loops above it obtained simply by adding their ordinates. Physically this is as though the particle showing the loops in 6e and 6f consisted of two magnetically independent regions. One of them shows the behavior with H$_m$ shown in 6a and 6b, the other in 6c and 6d (no change from 16 to 21 kOe). The heights of these single-particle component loops are proportional to the volume of independently acting material. The degree to which the observed behavior can be reproduced in this way is shown in Fig. 7.
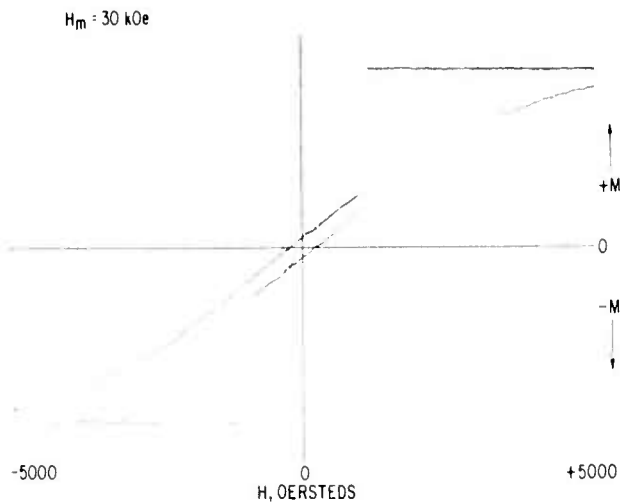
$H_m = 30$ kOe

H, OERSTEDS

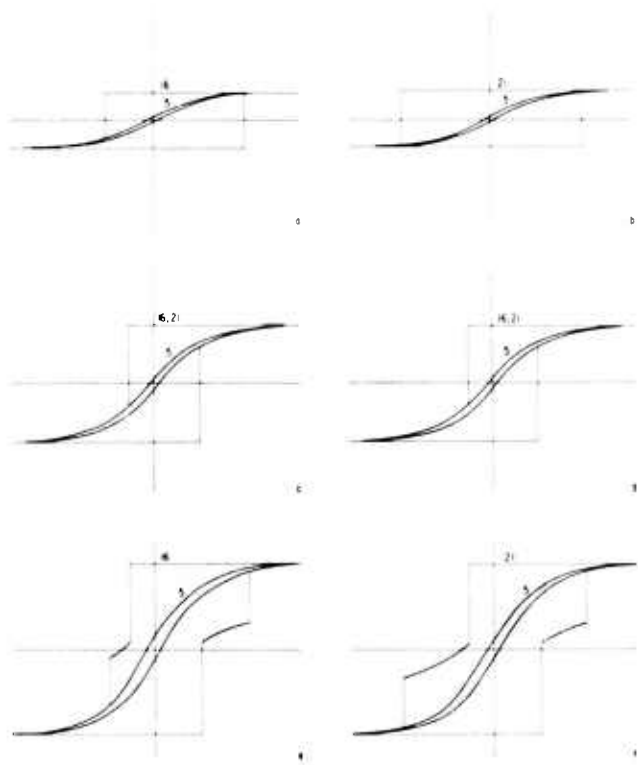Fig. 5 Observed single-particle behavior in 200μ particle of Co$_5$Sm.

Fig. 6 Synthesis of complex hysteresis loops from single-particle loops. Numbers on loops are H_m in kOe. Figure 6a + 6c, and 6f is 6b + 6d. Figures 6a and 6b are one region of the particle in different H_m; 6c and 6d are another; and 6e and 6f are the entire particle, composed of these two regions.
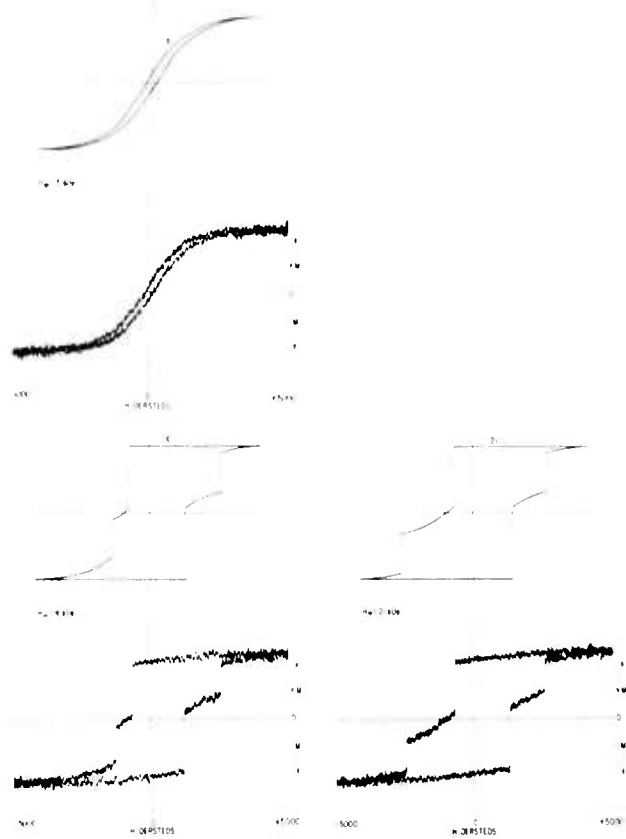
Fig. 7 Comparison of 5, 16, and 21 kOe loops from Figs. 6e and 6f with measured loops shown in Figs. 1 through 3.

DISCUSSION

This simple model has the following implications:

1. A particle can consist of regions that act magnetically independently.

2. Each jump corresponds to the nucleation and motion of a different wall, one in each region.

3. The end of the jump occurs when the wall has moved sufficiently to reduce the local field on it to zero. This has nothing to do with pinning but is a purely magnetic effect.

4. Each region has its own dependence of H_n on H_m, determined by the defects it contains.

How can two regions of a small particle be magnetically so independent? In small samples of high-anisotropy materials, the state of intermediate M is one of a complex labyrinthine domain structure which forms to keep magnetostatic energy low.[14, 15] During a jump, as such a structure propagates from a nucleus, it could be blocked by a low-angle boundary.

The presence of such a boundary might be the reason that the 50μ particle in Figs. 1 through 3 does not show single-particle behavior, while the 200μ particle in Fig. 5 does. This speculation is suggested by the simple and puzzling fact that highly oriented dense magnets prepared from Co_5Sm or barium ferrite have high coercive forces. These too contain low-angle boundaries between their grains, and even though the magnets are 95% dense or more, their properties are still remarkably like those of their constituent particles.

REFERENCES

1. G. Hoffer and K. Strnat, "Magnetocrystalline Anisotropy of YCo_5 and Y_2Co_{17}," IEEE Trans. Magnetics MAG-2, 487-489 (Sept. 1966).

2. D. K. Das, "Twenty Million Energy Product Samarium-Cobalt Magnet," IEEE Trans. Magnetics MAG-5, 214-216 (Sept. 1969).

3. M. G. Benz and D. L. Martin, "Cobalt-Samarium Permanent Magnets Prepared by Liquid Phase Sintering," Appl. Phys. Letters 17, 176-177 (Aug. 15, 1970).

4. F. F. Westendorp and K. H. J. Buschow, "Permanent Magnets with Energy Products of 20 Million Gauss-Oersteds," Solid State Commun. 7, 639-640 (Aug. 1969).

5. J. E. Grant, M. G. Benz, and D. L. Martin, "A 2 kw, Multi-Octave TWT Focused with Cobalt-Samarium Magnets," presented at IEEE Intern. Devices Meeting, Washington, D.C., Oct. 28-30, 1970; to be published in IEEE Trans.

6. K. Strnat, G. Hoffer, J. Olson, W. Ostertag, and J. Becker, "A Family of New Cobalt-Base Permanent Magnet Materials," J. Appl. Phys. 38, 1001-1002 (March 1967).

7. J. J. Becker, "A Domain Boundary Model for a High Coercive Force Material," J. Appl. Phys. 39, 1270-1271 (Feb. 1968).

8. C. Guillaud, "Ferromagnetism of Binary Alloys," PhD Dissertation, Univ. of Strasbourg, Strasbourg, France (1943).

9. K. Friess, "New Results on Strontium-Ferrite Magnets," Z. Angew. Phys. 21, 90-92 (Aug. 1966).

10. J. J. Becker, "Observations of Magnetization Reversal in Cobalt-rare-earth Particles," IEEE Trans. Magnetics MAG-5, 211-214 (Sept. 1969).

11. E. C. Stoner and E. P. Wohlfarth, "A Mechanism of Magnetic Hysteresis in Heterogeneous Alloys," Phil. Trans. Roy. Soc. (London) A240, 599-642 (May 1948).

12. J. J. Becker, "Magnetization Discontinuities in Cobalt-rare-earth Particles," presented at Conf. on Magnetism and Magnetic Materials, Miami Beach, Florida, Nov. 16-20, 1970; to be published in J. Appl. Phys.

13. H. Zijlstra, "Domain-Wall Processes in $SmCo_5$ Powders," J. Appl. Phys. 41, 4881-4885 (Nov. 1970).

14. C. Kooy and U. Enz, "Experimental and Theoretical Study of the Domain Configuration in Thin Layers of $BaFe_{12}O_{19}$," Philips Res. Repts. 15, 7-29 (Feb. 1960).

15. H. Kojima and K. Goto, "Determination of Critical Field for Magnetoplumbite Type Oxides by Domain Observation," Proc. Intern. Conf. on Magnetism, Nottingham, Sept. 1964, pp. 727-730.

71-C-296

J.J. Becker

ANGULAR DEPENDENCE OF NUCLEATING FIELDS IN Co-RARE
EARTH PARTICLES

41<

TECHNICAL INFORMATION SERIES

AUTHOR	SUBJECT	NO 71-C-296
Becker, JJ	magnetism	DATE October 1971

TITLE	GE CLASS 1
Angular Dependence of Nucleating Fields in Co-Rare Earth Particles	NO. PAGES 5

ORIGINATING COMPONENT	CORPORATE RESEARCH AND DEVELOPMENT SCHENECTADY, N.Y.
Metallurgy and Ceramics Laboratory	

SUMMARY The coercive force of cobalt-rare earth compounds is determined by the influence on domain boundary processes of imperfections. One means of distinguishing among various possible types is the angular dependence of the field at which a magnetization jump occurs in a single particle. In a Co_5Gd particle, a $1/\cos\theta$ dependence centering about an angle 28° from the alignment axis was observed. Analysis of the data indicates that the reversal was triggered by a bit of misoriented material pinning a wall fragment, and that the nucleus is very small and causes the jump to occur in the main body of the sample.

KEY WORDS   magnetism, permanent magnet materials

ANGULAR DEPENDENCE OF NUCLEATING FIELDS
IN Co-RARE EARTH PARTICLES*

J. J. Becker

INTRODUCTION

The nature of the relationship of the coercive force to relevant structural features of cobalt-rare earth materials is not yet entirely clear. Co_5Sm seems consistently to yield much higher coercive forces for any type of treatment than other Co_5 (rare earth) or related compounds. On the other hand, the coercive forces attainable are still only a small fraction of the anisotropy field $2K/M_s$.

Vibrating-sample magnetometer measurements have shown[1] that single particles in the ~50µ size region show prominent discontinuities (jumps) in magnetization and may even reverse completely in one jump.[2] A more sensitive measuring technique has shown the same general behavior for still smaller particles.[3] It has been shown that each magnetization jump corresponds to the independent reversal of a portion of the particle.[4]

It seems clear that such behavior is to be interpreted not in classical single-domain terms but as the result of domain boundary motion.[5] Boundaries can be nucleated or pinned by imperfections (Refs. 2, 3). In principle they can also be impeded by their inherent interaction with the crystal lattice,[6] but the importance of this effect at room temperature in these materials seems very doubtful.

The coercive force is then governed by imperfections, whose nature determines the fields at which domain boundary processes take place. Such imperfections could be of a number of types, somewhat as follows:

(1) <u>Purely geometrical</u>. M is uniform, but local fields are produced by the pole distributions on surface projections or indentations or internal voids or cracks. Nonmagnetic inclusions would be of this class, but there might be lattice strain associated with them as well.

(2) <u>Lattice deformation.</u> Elastic deformation, as around an inclusion, would add a local strain-magnetostriction anisotropy,

* This research was sponsored by the Advanced Research Projects Agency of the Department of Defense and was monitored by the Air Force Materials Laboratory, MAYE, under Contract F33615-70-C-1626.

1 43<

whose magnitude would be unknown in these materials, in the absence of any information on their magnetostriction coefficients. Plastic deformation, as by mechanical processing, in which the lattice is disrupted, might well drastically affect the local anisotropy and perhaps also M.

(3) Composition variations. These can be inhomogeneities resulting from preparation, as for example from a peritectic reaction. They can result from local oxidation or volatilization of a component. They can also be associated with a discrete two-phase structure. In all cases the local M and K will gradually or suddenly change.

(4) Orientation variations. The local K axis may be displaced relative to the rest of the material either because of local deformation or because of the presence of a small grain of different orientation from the matrix.

Further information about their nature can be deduced in various ways. Direct visual observation of domains shows the sudden appearance of new reversed regions. [7] Etching experiments show that the particle surface can be an important site for imperfections. [1] The coercive force can be very sensitive to small amounts of strain. [8] Another way to infer information about the imperfections is to study the way in which the jump fields H_n depend on various parameters.

The parameter studied in this investigation was the angle at which the field H_n was applied. Different types of imperfections would be expected to have different angular dependences. In particular, if a jump were nucleated by a fragment of wall requiring a definite field H_n to bring it over some energy barrier, a $1/\cos\theta$ dependence would be expected, assuming that only 180° walls are present and that magnetization rotation is negligible. This is surely justifiable, as the H_n reported here are less than 1% of the anisotropy field. Reich, Shtrikman, and Treves[9] have found a $1/\cos\theta$ angular dependence of the coercive force in orthoferrite single crystals, in which the reversal took place in a single jump, and concluded that "the coercive force is governed by the nucleation of a 180° domain wall." This can be understood if "nucleation" includes the initiation of the motion of a wall fragment already present.

EXPERIMENTAL RESULTS AND DISCUSSION

Measurements were made on a sample consisting of a roughly equiaxed particle of Co_5Gd approximately 500μ in average diameter. This particle was placed in the tip of a fine glass tube, in which it could move freely, with a small amount of paraffin. The tube was mounted in the sample holder of a vibrating-sample magnetometer.
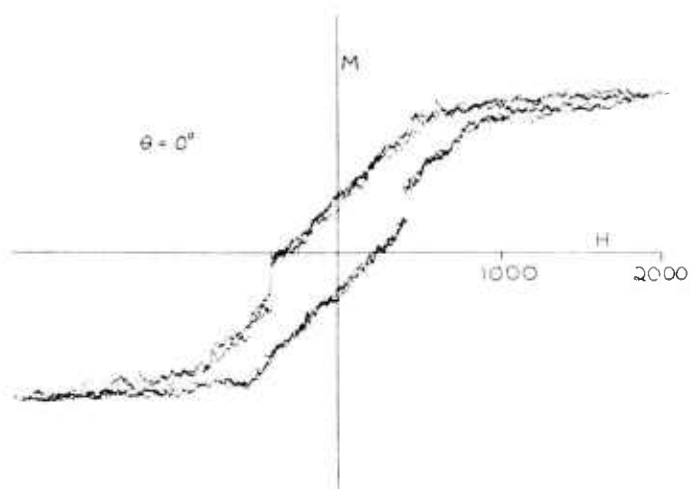
Fig. 1 Hysteresis loop of ~500μ particle of
Co$_5$Gd showing magnetization jumps.
Traced three times. H_m = 21 kOe.

This sample holder was rotatable about the axis of vibration; that is, about an axis perpendicular to the field. With the sample holder set at 0°, the paraffin was melted, and then allowed to resolidify while a field of about 15 kOe was applied. Thus the orientation of the sample corresponding to θ = 0° was that which it spontaneously took up in the field. In this orientation, it showed pronounced and reproducible magnetization jumps like those that have been previously reported in other cobalt-rare earths (Refs. 1, 2, 3). The angular dependence of the jump field was then investigated.

For each value of θ at which measurements were made, the sample was first magnetized in a field H_m of 21 kOe at θ = 0°. Then the field was reduced to zero, the sample rotated to the angle θ, and the magnetization as a function of increasing negative field recorded. Then the sample was returned to 0°, magnetized in 21 kOe in the opposite direction, and the opposite branch of the hysteresis loop similarly recorded. The hysteresis loop for θ = 0° is shown in Fig. 1. In this case, since the sample was not rotated, it was possible to record the magnetization in decreasing positive fields as well. In general this was not done.

Figure 1 shows one conspicuous magnetization jump at about 400 Oe, occurring on both sides of the hysteresis loop. The field at which this jump occurred was measured as a function of θ as described above. The jumps remained symmetrical about H = 0, and for each value of θ, both positive and negative values of the field H_n at which the jump occurred were recorded. This procedure was followed for both clockwise and counterclockwise rotations of the sample from the original magnetization direction. The results are shown in Fig. 2. Each experimental value represents from 6 to 24 observations and the error bars show ± one standard deviation.
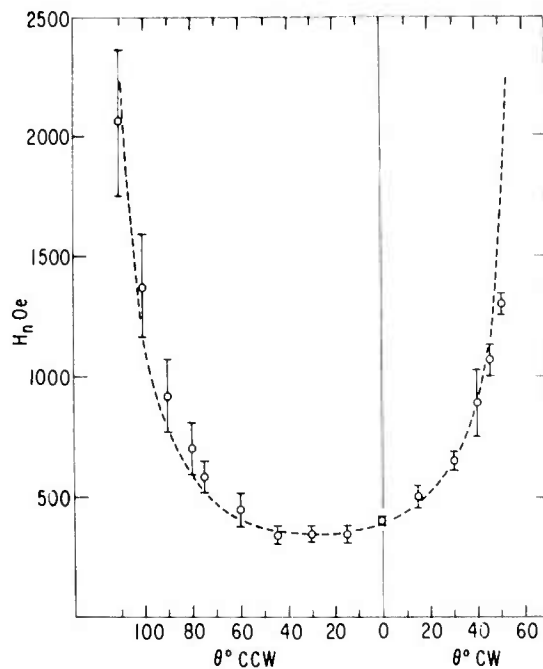
Fig. 2 Jump field H_n as a function of angle θ for Co_5Gd particle shown in Fig. 1.   Dotted line is $H_n = 350/\cos(\theta + 28°)$.

It can be seen that the jump field follows an inverse cosine dependence quite well, but with a substantial angular offset.   The dotted line in Fig. 2 is a plot of $H_n = 350/\cos(\theta + 28°)$ where θ is positive clockwise. This suggests that the nucleus for this jump is a small bit of material misoriented in such a way that the direction of its easy axis, projected on the plane of rotation, is 28° from that of the main body of the sample, and that it acts by trapping a fragment of wall within itself.   This nucleus then triggers a reversal in the main body of the sample. This reversal does not go to completion, as has often been observed before. [4]   The total magnetization change M, while not measured precisely, varied approximately as $\cos\theta$, not $\cos(\theta + 28°)$, eliminating the very unlikely possibility that the entire sample was misoriented 28° from the aligning field.

The question can then be raised: how can an off-orientation nucleus be distinguished from an off-orientation grain large enough so that its reversal would account for the entire magnetization jump? The jump gives about 12.8% of the total change in magnetization in Fig. 1.   Such a change could conceivably, in the absence of positive structural information to the contrary, be caused by a secondary grain occupying 14% of the total volume and oriented in such a way that the projection of its easy axis on the plane of rotation is 32° from that of the main axis.   This sample would align itself with the main axis 4° from the direction of the aligning field and would give the angular dependence observed.   However, these two possibilities can be distinguished by the behavior of the fractional change in magnetization due to the jump, $\Delta M/M$, with angle. For an infinitesimally small nucleus, $\Delta M/M$ will be the same for any θ, since both ΔM and M take place in the bulk of the material, and, being collinear, will have the same components at any angle. If ΔM occurs in a portion of the sample having a different
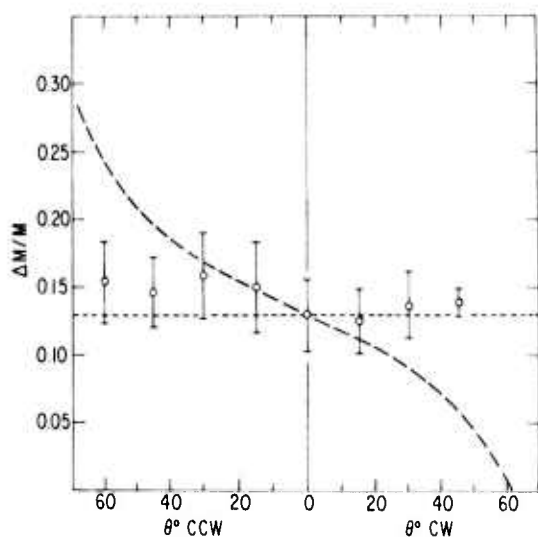
Fig. 3 Fractional change in magnetization $\Delta M/M$ as a function of angle θ for Co_5Gd particle shown in Fig. 1. Horizontal dotted line is calculated for infinitesimally small nucleus, curved dashed line for secondary grain.

orientation from the rest, the value of $\Delta M/M$ will range from zero, when the small grain is at 90° to the $\theta = 0$ axis, to infinity, when the large grain is thus oriented. Both of these cases are shown, along with the experimental results, in Fig. 3. It can be seen that the concept of a very small nucleus triggering a portion of the main body of the sample fits the data best.

A further question that might be raised is whether it should not be the total internal field H_i, consisting of the vector sum of the local internal field H_ℓ and the applied field H_n, whose angular dependence should be considered rather than that of H_n alone. However, if H_i varies as $1/\cos\theta$, so will H_n, since whatever H_ℓ may be, its orientation relative to the sample remains the same.

REFERENCES

1. J. J. Becker, IEEE Trans. Magnetics MAG-5, 211 (1969).
2. J. J. Becker, J. Appl. Phys. 42, 1537 (1971).
3. H. Zijlstra, ibid, p. 1510.
4. J. J. Becker, to be published, IEEE Trans. Magnetics (Sept. 1971).
5. J. J. Becker, J. Appl. Phys. 39, 1270 (1968).
6. J. J. van den Broek and H. Zijlstra, IEEE Trans. Magnetics MAG-7, 226 (1971).
7. K. Bachmann, to be published, IEEE Trans. Magnetics (Sept. 1971).
8. J. J. Becker, J. Appl. Phys. 41, 1055 (1970).
9. S. Reich, S. Shtrikman, and D. Treves, J. Appl. Phys. 36, 140 (1965).

72CRD070

J.J. Becker

TEMPERATURE DEPENDENCE OF COERCIVE FORCE
AND NUCLEATING FIELDS IN Co$_5$Sm

48<

GENERAL ⟨GE⟩ ELECTRIC

General Electric Company
Corporate Research and Development
Schenectady, New York

TECHNICAL INFORMATION SERIES

AUTHOR	SUBJECT	NO 72CRD070
Becker, JJ	magnetism	
		DATE February 1972

TITLE Temperature Dependence of Coercive Force and Nucleating Fields in Co_5Sm	GE CLASS 1
	NO. PAGES 3

ORIGINATING COMPONENT Metallurgy and Ceramics Laboratory	CORPORATE RESEARCH AND DEVELOPMENT SCHENECTADY, N.Y.

SUMMARY In Co_5Sm, the coercive force of aggregates of powders or sintered magnets is much greater at 77°K than at room temperature. In single particles, the field at which an individual magnetization jump occurs increases rapidly and monotonically with decreasing T. On the other hand, the K reported for Co_5Sm is the same at 77°K and room T, with a broad maximum between. It thus appears that the reversal process is not controlled by the properties of bulk Co_5Sm. The observed T dependence must be ascribable to the imperfections that govern the magnetization reversal process.

KEY WORDS

magnetism, permanent magnetic materials

INFORMATION PREPARED FOR _____

TEMPERATURE DEPENDENCE OF COERCIVE FORCE AND NUCLEATING FIELDS IN Co$_5$Sm*

J. J. Becker

INTRODUCTION

It is generally agreed that the coercive forces of the Co$_5$R cobalt-rare earth intermetallic compounds are determined by the nucleation and motion of magnetic domain boundaries. These highly structure-sensitive processes are controlled by the number and nature of the imperfections present, which cause the coercive force to be far less than the $2K/M_s$ one might expect ideally.

One way to study the nature of these imperfections is to observe the way in which H_c depends on various physical parameters. For example, in Co$_5$Sm the dependence of H_c on the previous magnetizing field H_m is very strong, even when H_m is far larger than H_c.[1] A more direct approach is to study the fields H_n at which magnetization jumps have been found to occur in single particles.[2-5] Thus, while the H_m dependence of H_c might appear to be attributable to H_c distributions present in a bulk sample, this type of dependence is in fact also a property of individual particles, in which H_n is observed to take on different quantized values as H_m is varied.[2]

Another parameter, at a given H_m, is the angle ϑ to the alignment direction of the sample at which H_c or H_n is measured. This has been studied in bulk samples[6] and single particles.[7] In the latter case a good $1/\cos^2$ dependence is sometimes observed.

A number of types of imperfections can be envisaged,[7] including purely geometrical effects, lattice deformations, composition variations, orientation variations, and combinations of these. In the attempt to deduce their nature from magnetic measurements, one of the most important parameters at one's disposal is the temperature, as the magnetic behavior of different types of imperfections should vary in quite different ways with temperature.

Some investigations of the temperature dependence of H_c of powders or sintered magnets have been reported. Velge and Buschow[8] investigated the dependence between 80° and 290°K of a series of (La, Nd)Co$_5$ powders. McCurrie and Carswell[9] found a linear variation of H_c and also of H_r, the zero-remanence coercive force, with T in the same temperature range for Co$_5$Sm powders. The data of Martin and Benz[10] on sintered Co$_5$Sm magnets, over a broader temperature range, appear to fit a $T^{1/2}$ dependence best. In the data of Velge and Buschow,[8] the H_c of NdCo$_5$
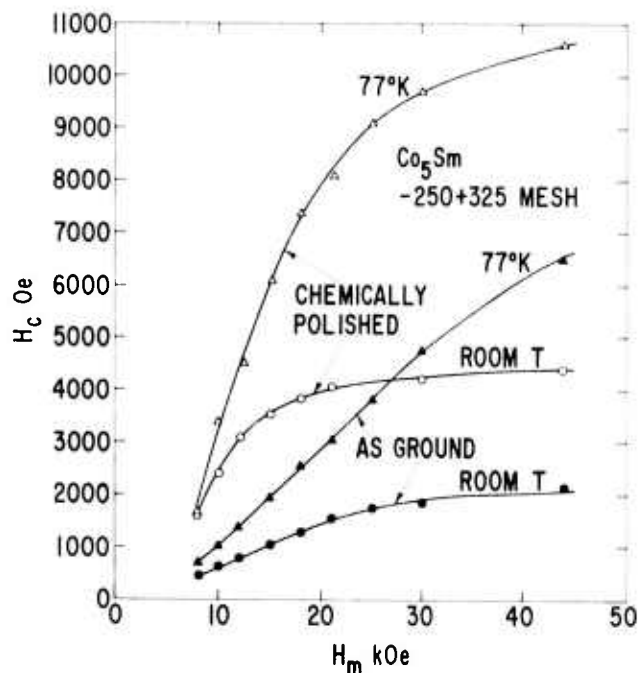

Fig. 1 Dependence of H_c on H_m for Co$_5$Sm samples at room T and 77°K.

powders varies in a way that is qualitatively consistent with the known variation of K with temperature.[11,12] However, the reported variations of H_c of Co$_5$Sm with T[9,10] are much greater than the variation of K or K/M_s with T reported by Tatsumoto et al.[12] In fact, their data show a broad peak in K_1 for Co$_5$Sm at about 180°K.

EXPERIMENTAL RESULTS

Two experiments related to this problem are described here. In the first, Co$_5$Sm particles were prepared by lightly grinding a cast ingot and sizing to -250 +325 mesh (-61μ + 43μ) by the method of magnetic sieving.[2] Aggregates of particles were aligned in paraffin and the dependence of H_c on H_m measured in a vibrating-sample magnetometer at room T and in liquid nitrogen. The strong H_m dependence of H_c is shown in Fig. 1. At room T, the H_c of the as-ground material nearly doubles as H_m goes from 20 to 44 kOe, even though H_c is only on the order of $0.05H_m$. At 77°K, the dependence is even more extreme. At H_m = 44 kOe, H_c is rising practically proportionally to H_m. Evidently the H_c values for a given H_m are several times as large as they are at room T. However, this comparison contains a conceptual difficulty. We appear to be observing that the effectiveness of

---

reversal nuclei changes rapidly with T. However, this implies that a given H_m at low T is regarded as equivalent to the same H_m at high T. But, whatever the details may be, the significance of H_m certainly depends on its magnitude relative to the material constants, including those of the imperfections, at the relevant temperature. It is not obvious what numbers should be compared at two temperatures, unless perhaps H_c is clearly approaching some limiting value with increasing H_m. This is more nearly the case for the chemically polished[2] particles shown in Fig. 1. Comparing this sample to the ground particles, the dependence of H_c on H_m is different at each T, the actual H_c levels are different, and their relative changes with T are not the same, all as a result of the surface changes brought about by chemical polishing.

The second experiment was based on the idea that a way out of the dilemma presented by measurements on multiparticle samples is to follow individual magnetization jumps in single particles. A given magnetization jump persists over a range of H_m,[2] and if the temperature is gradually changed, the H_n for a given jump can be followed, with some confidence that the same physical event is being observed as a function of temperature. The sample studied showed a room T hysteresis loop with each side consisting of two jumps, the corresponding jumps having numerically equal H_n on both sides. Presumably, then, only two nuclei were active. In Fig. 2 are shown the H_n observed as the temperature was gradually lowered, H_m having always the value of 21 kOe and applied at the temperature of measurement. At high temperature, each pair of nearly identical points corresponds to a symmetrical jump on opposite sides of the loop. As the temperature is lowered, the H_n for both jumps increase rapidly, but the one with the initially lower H_n rises more rapidly with decreasing T and overtakes the other at about -60°C. Below this temperature, the hysteresis loop is rectangular, the entire reversal being accomplished in one jump.

DISCUSSION

Several comments can be made on these results:

1. The variation of H_n with T is very large. H_n here is plotted as applied field. Whether and how much it should be modified to take account of internal demagnetizing effects is not entirely obvious. In any case, H_n varies much more rapidly with T than the reported values of K or M or plausible combinations of them.

2. This fact eliminates purely geometrical and orientation-variation imperfections, and suggests that local lattice deformations or composition variations are important.

3. Two jumps in the same sample show different T dependences of H_n. This certainly suggests that two nuclei of different nature are responsible for them.
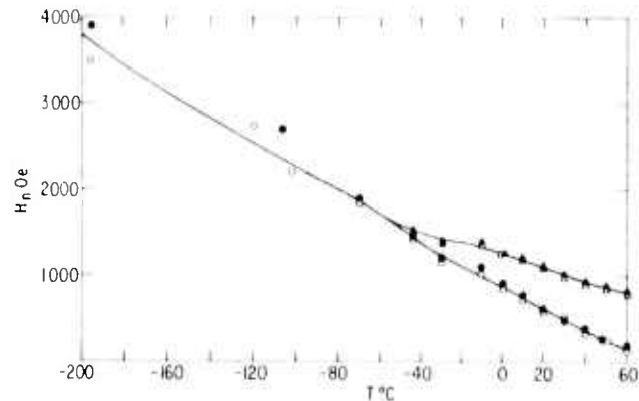

Fig. 2 Variation of jump field H_n with T for Co_5Sm single particle.

4. Since these jumps can be individually followed with slowly changing temperature, H_m is in some sense the same and we are observing the temperature dependence of the reversal process for a fixed initial condition.

5. The temperature dependence is monotonic and, like the H_c measurements on larger samples, shows nothing suggesting the peak in K at ~180°K reported by Tatsumoto et al.[12] However, it should be pointed out that there is a considerable amount of discrepancy between their values and comparable measurements given elsewhere.[13, 14] It is to be hoped that further measurements of K in these materials will be forthcoming.

6. A final possibility is that the T variation is attributable to thermal activation over an energy barrier, as suggested by McCurrie.[15] Order-of-magnitude calculations of the possible size of thermally reversible regions[16, 17] suggest that this is unlikely.

CONCLUSIONS

In conclusion, it appears that the T variation of both H_c in powders and sintered magnets and H_n in single particles is much more rapid than, and functionally different from, reported values of the T variation of K for Co_5Sm. This appears to indicate that magnetization reversal is not controlled by the properties of pure Co_5Sm, but by those of the magnetization reversal nuclei present.

REFERENCES

1. J.J. Becker, "A Domain-boundary Model for a High Coercive Force Material," J. Appl. Phys. 39, 1270-1271 (Feb. 1, 1968).

2. J.J. Becker, "Observations of Magnetization Reversal in Cobalt-rare-earth Particles," IEEE Trans. Magn. MAG-5, 211-214 (Sept. 1969).

3. J. J. Becker, "Magnetization Discontinuities in Cobalt-rare-earth Particles," J. Appl. Phys. 42, 1537-1538 (Mar. 15, 1971).

4. H. Zijlstra, "Critical Fields Determining Magnetic Coercivity in Microparticles of $SmCo_5$ and $LaCo_5$," J. Appl. Phys. 42, 1510-1515 (Mar. 15, 1971).

5. J. J. Becker, "Interpretation of Hysteresis Loops of Cobalt-rare-earth Single Particles," IEEE Trans. Magn. MAG-7, 644-647 (Sept. 1971).

6. J. J. Becker, "Angular Variation of Coercive Force in Permanent Magnet Materials," J. Appl. Phys. 38, 1015-1017 (Mar. 1, 1967).

7. J. J. Becker, "Angular Dependence of Nucleating Fields in Cobalt-rare-earth Particles," 17th Ann. Conf. on Magnetism and Magnetic Materials, Chicago (Nov. 1971).

8. W. A. J. J. Velge and K. H. J. Buschow, "Permanent Magnetic Properties of Rare Earth Cobalt Compounds (RCo_5)," IEEE Conf. on Magnetic Materials and their Applications, London, Sept. 1967.

9. R. A. McCurrie and G. P. Carswell, "Magnetic Hardness of the Intermetallic Compound $SmCo_5$ as a Function of Particle Size," Phil. Mag. 23, 333-343 (Feb. 1971).

10. D. L. Martin and M. G. Benz, "Temperature Dependence of Coercivity for Co-Sm Permanent Magnet Alloys," Intermag. Conf., Kyoto, Japan, Apr. 16-19, 1972.

11. H. Bartholin, B. van Laar, R. Lemaire, and J. Schweizer, "Etude magnetique du compose intermetallique $NdCo_5$," J. Phys. Chem. Solids 27, 1287-1293 (1966).

12. E. Tatsumoto, T. Okamoto, H. Fujii, and C. Inoue, "Saturation Magnetic Moment and Crystalline Anisotropy of Single Crystals of Light Rare Earth Cobalt Compounds RCo_5," J. Physique 32, C1-550 - C1-551 (1971).

13. K. J. Strnat, "The Recent Development of Permanent Magnet Materials Containing Rare Earth Metals," IEEE Trans. Magn. MAG-6, 182-190 (June 1970).

14. K. H. J. Buschow and W. A. J. J. Velge, "Permanent Magnetic Materials of Rare Earth Cobalt Compounds," Z. angew. Phys. 26, 157-160 (1969).

15. R. A. McCurrie, "Determination of Intrinsic Coercivity Distributions in Aligned Assemblies of Uniaxial $SmCo_5$ and $LaCo_5$ Particles," Phil. Mag. 22, 1013-1023 (1970).

16. W. F. Brown, Jr., Micromagnetics, Interscience Publishers, New York, pp. 71-72 (1963).

17. A. Aharoni, "Possibility of Domain Wall Nucleation by Thermal Agitation," J. Appl. Phys. 33, 1324-1325 (Mar. 1962).

3

73CRD093

J.J. Becker

A MODEL FOR THE FIELD DEPENDENCE OF MAGNETIZATION
DISCONTINUITIES IN HIGH-ANISOTROPY MATERIALS

GENERAL ⚡ ELECTRIC

General Electric Company
Corporate Research and Development
Schenectady, New York

TECHNICAL INFORMATION SERIES

AUTHOR Becker, JJ	SUBJECT magnetism	NO 73CRD093
		DATE March 1973
TITLE A Model for the Field Dependence of Magnetization Discontinuities in High-Anisotropy Materials		GE CLASS 1
		NO. PAGES 5

ORIGINATING COMPONENT Metallurgy and Ceramics Laboratory	CORPORATE RESEARCH AND DEVELOPMENT SCHENECTADY, N.Y.

SUMMARY A simple model involving two types of nuclei, neither with any unusual or unsymmetrical properties, can describe a large variety of phenomena related to the field dependence of coercive force in powders and nucleating fields in single particles of high-anisotropy materials, including orthoferrites and hexagonal oxides as well as cobalt-rare-earths. One type of nucleus is a domain wall trap that is activated by capturing a fragment of moving wall. The other type is any local disturbance that provides a reversal site by its interaction with the local magnetization. Together they permit reasonable quantitative predictions of a number of types of behavior that have been observed.

KEY WORDS

magnetism, magnetic materials, permanent magnets

INFORMATION PREPARED FOR _____

_____

A MODEL FOR THE FIELD DEPENDENCE OF MAGNETIZATION DISCONTINUITIES IN HIGH-ANISOTROPY MATERIALS

J. J. Becker

INTRODUCTION

Many of the cobalt-rare-earths show a marked dependence of intrinsic coercive force H_c on previous magnetizing field H_m. Any model that describes permanent magnet behavior in terms of the reversal of defect-free particles predicts but one coercive force per particle. A dependence of H_c on H_m in an assembly of particles would then require a distribution of individual particle properties.[1] However, individual cobalt-rare-earth particles can show a number of magnetization jumps at fields H_n whose values are quantized and depend on the magnetizing field H_m.[2] This type of behavior has also been observed in individual particles of other high-anisotropy materials (Refs. 3, 4). These H_n in general are small compared to the anisotropy field $2K/M_s$ and are associated with the appearance and motion of visible domain walls. Thus a single particle contains a number of defects that facilitate reversal by domain boundary motion. Which of these defects are active in a given situation depends in some way on the previous magnetic history of the particle.

The purpose of this report is to show how on a simple physical model numerical predictions can be made that in many instances correspond well with available measurements.

TYPES OF REVERSAL NUCLEI

It has been pointed out before[5] that many types of defects can be envisaged, including various geometrical, chemical, and lattice irregularities, that modify the local magnetic properties. These defects then dominate the magnetic behavior of the entire particle, by providing sites at which the nucleation of magnetization reversal is facilitated. A nucleus is here taken to mean any small region from which magnetization reversal propagates a finite amount at a definite constant internal field which is less than $2K/M_s$ but greater than the coercive force of a freely moving wall.

Whatever their structural source, all nuclei as defined above can be classified by their magnetic behavior into one of two basic types:

Type 1: A small region of reverse magnetization enclosed by a locally pinned domain boundary is counted as a nucleus on the above definition. Once the local pinning field is exceeded, the wall will expand and move rapidly, giving rise to a magnetization discontinuity. Bulk wall pinning, in the sense of interference with the motion of a wall of essentially

constant area by a dispersion of many inhomogeneities, is not considered here but included in the wall coercive force. Local pinning may be due to one or a very few defects. A moving wall can leave behind fragments at local pinning sites, which are likely to be primarily near the surface. Such a fragment is a nucleus of the first type. It will move out of its local energy minimum in either direction in a field large enough to dislodge it, in one case reversing the magnetization again, in the other case disappearing completely. In what follows, the magnitude of this local field is taken to be the same for either direction of motion. This represents the simplest physical situation and leads to quite reasonable quantitative predictions in many cases.

Type 2: A defect can produce a magnetization reversal nucleus by its interaction with the local magnetization. For example, the large local demagnetizing fields that can be present at a corner[6] or pit[7] or nonmagnetic inclusion[8] can aid the formation of a small reversed region. Inhomogeneities with different K or M can do the same. Again, local lattice misorientation may give rise to a partial domain wall. In any case, a large saturating field may remove a region of this type while the field is applied, but at some time during its removal and reversal the region will form again, and at some definite field will break loose and initiate the reversal of the magnetization. When the magnetization has been reversed the nucleus is present once again but with the opposite magnetization. The essential difference between this and a type 1 nucleus is that the type 2 cannot be deactivated. It "fires" at its own definite H_n which is completely independent of any previous H_m. Its behavior is "symmetrical," in that it is present for either sense of magnetization with the same magnitude of H_n. If several such defects are present in one particle, the one that fires the most easily will fix the ultimate H_n that can ever be reached in that particle no matter how large an H_m is applied.

MAGNETIC BEHAVIOR OF PARTICLES WITH DEFECTS

On the basis of these two types of defects, we now develop the relationship between domain wall motion and magnetization behavior, as follows:

If a freely movable wall is present, the curve of magnetization M vs applied field H_{app} is taken to be as shown in Fig. 1. H_d is the demagnetizing field at saturation due to the shape of the particle, and wall motion is infinitely easy, the sloping line corresponding to zero internal field, H_{int}, on the wall. In practice such loops show some deviation from these idealizations, being slightly curved and having a small but nonzero width.

As the wall moves, it leaves fragments behind at regions of high defect concentration, primarily
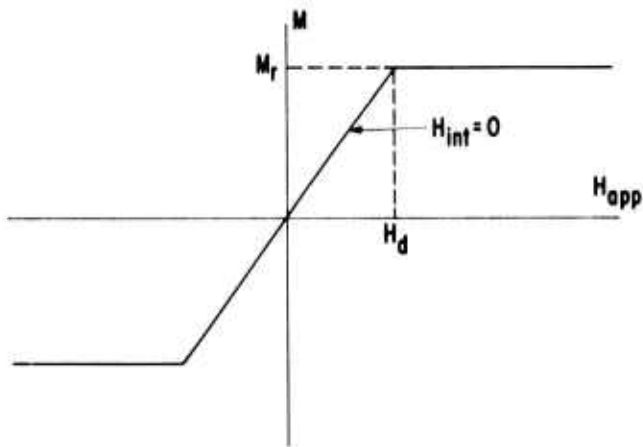

Fig. 1 Behavior of magnetization M as a function of applied field H_{app} for a particle containing a freely moving wall.

near the surface. This is shown in a schematic way in Fig. 2. The fragments left by the wall moving in one direction are necessarily different from those resulting from its motion in the opposite sense. All such fragments are the first type of nucleus discussed above. The configurations A and E in the figure correspond to $\pm M_r$ except for the very small magnetization due to the fragments themselves. Further increases of applied field would drive out the fragments one by one. On the other hand, if the applied field were reduced, the least deeply trapped wall fragment would expand to reverse the magnetization. As it moved it would annihilate the remaining fragments of the same size and leave behind a new set of the opposite sign.
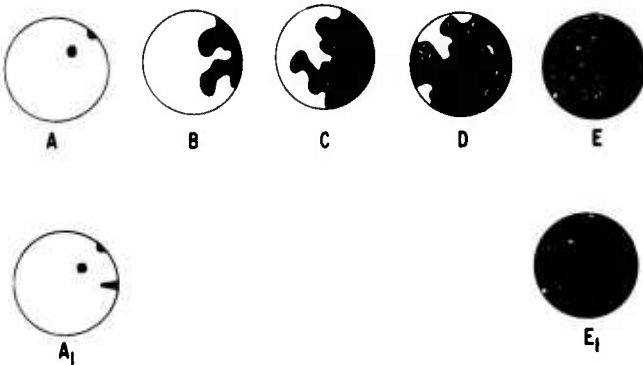

Fig. 2 Schematic representation of domain configuration as M is reversed from one direction in A to the opposite in E, leaving wall fragments. A type 2 nucleus is shown in addition in A_1 and E_1 (spike-shaped nucleus at the right).

Type 2 nuclei, on the other hand, are present in the same place for either sign of the local magnetization. One such is indicated in A_1 and E_1.

The behavior due to type 1 nuclei is described with the aid of Fig. 3. A wall moving across the sample in increasing H_{app} will stop moving at H_d, leaving a trapped fragment. This fragment is characterized by the local field H_1 for motion in either direction. If the applied field is further increased, the wall will be freed at $H_d + H_1$ and will leave the sample. The slight corresponding increase in M_r is omitted for simplicity. The trap has been deactivated and is no longer a reversal nucleus. On the other hand, if the maximum field H_m had been decreased from a value between H_d and $H_d + H_1$, the wall would break loose at $(H_n)_1 = H_d - H_1$ and quickly move until $M = M_1$, at which point it would stop because the local field on it is zero. Further changes in H_{app} would move the wall along the $H_{int} = 0$ line. If the field were returned to an H_m between H_d and $H_d + H_1$, then decreased, the jump would occur once again at $(H_n)_1$. For $H_m > H_d + H_1$ trap 1 is deactivated. Suppose another trap 2 with characteristic local field H_2, had been filled along with 1 by the moving wall. Then for H_m between $H_d + H_1$ and $H_d + H_2$, trap 2 would fire at $(H_n)_2 = H_d - H_2$, causing a magnetization jump from M_r to M_2.
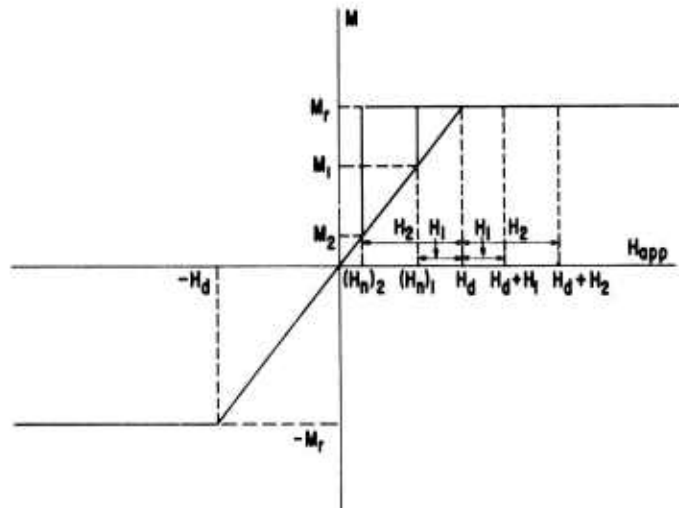

Fig. 3 Behavior of magnetization with applied field due to type 1 nuclei.

The same considerations would apply to the series of different trapped fragments left by the wall moving in the other direction until $M = -M_r$ at $H_{app} = -H_d$.

It is then possible to work out the magnetic behavior due to a series of traps of varying strengths. This is shown in Figs. 4 and 5 for a sample with four traps of each sense. It can be seen in Fig. 5 that the plot of H_n vs H_m due to these traps has an offset of H_d on both axes and a slope of -1. At some point

there is a sudden drop to a constant H_n corresponding to the firing of the most active type 2 nucleus present. Figures 4 and 5 also illustrate three different types of limiting behavior from type 2 nuclei. Three such possible nuclei are shown, having characteristic fields $H_d - H_x$, $H_d - H_y$, and $H_d - H_z$. In each case such a nucleus sets a limit on H_n. Jumps cannot occur outside the loop defined by it. For nucleus x, these limiting jumps occur for $H_m > H_d + H_4$ on the right and $-H_m < - (H_d + H_8)$ on the left. For y, they occur for $H_m > H_d + H_y$ on the right and $-H_m < -(H_d + H_8)$ on the left. For z, they occur whenever H_m is equal to or greater than the jump field. These three nuclei, of course, illustrate three separate limiting possibilities. If all three of them were simultaneously present in one particle, only the loop due to nucleus x would ever appear. If it were removed, as by an etching process, the limiting H_n would suddenly become H_y, a type of behavior that has been observed. [9]

Fig. 5 Nucleating field H_n as a function of magnetizing field H_m for the nuclei shown in Fig. 4. A positive H_n means that H_n was in the same direction as H_m. Solid lines represent reversals taking place for positive H_m, dashed lines for negative H_m.
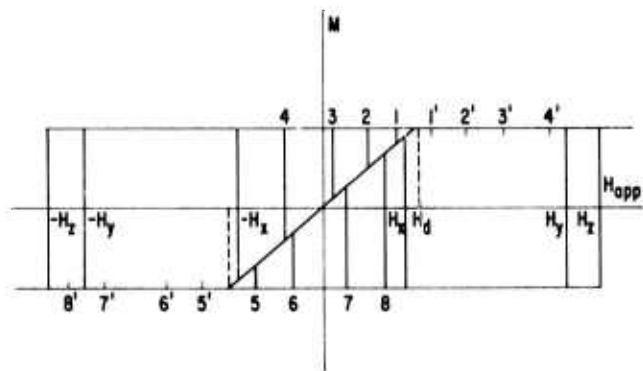

Fig. 4 Hysteresis loops for a sample containing eight type 1 nuclei, four of each sense. The fields are denoted as follows: 1' represents $H_d + H_1$, 1 represents $H_d - H_1$, etc. Also shown are three jumps from type 2 nuclei at fields H_x, H_y, and H_z.

Figure 5 shows the behavior for alternating H_m of gradually increasing magnitude. Thus if z were the only type 2 nucleus present, there would be no jumps for H_m between H_8 and H_z after the first cycle.

COMPARISON WITH EXPERIMENT

This description fits in well with many features of single particle behavior that have been observed. The square loop behavior of a chemically polished Co_5Y single particle has been described previously. [9] It reversed at H_n of 3800 Oc for all $H_m > 4200$ Oe. It was possible to get inside this loop by quickly reducing the field to zero as the reversal began. When this was done, H_n as a function of H_m appeared as in Fig. 6. It can be seen that the predicted slope of -1 fits the unsymmetrical H_n well, until H_n drops to 3800 Oe, precisely the same in both directions for all measured H_m from 4.2 to 30 kOe.
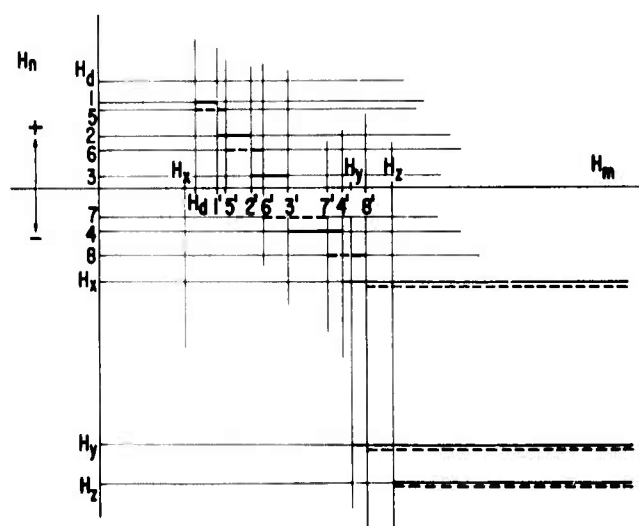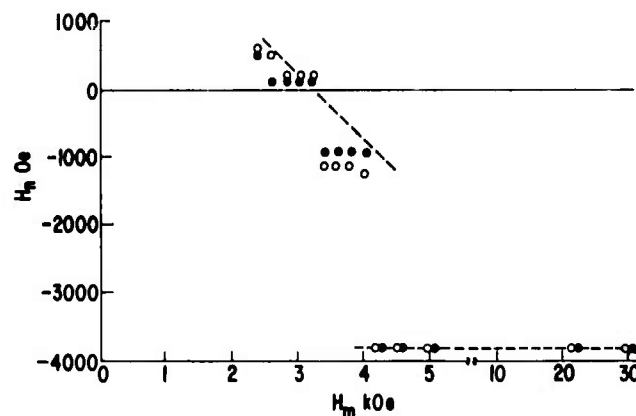

Fig. 6 Behavior of H_n with H_m for a chemically polished Co_5Y single particle. Open and filled circles represent opposite directions of H_m.

The H_d from magnetization curves was about 900 Oe, somewhat less than the offset indicated in Fig. 6. Thus the jump at -1150 Oe corresponds to an internal field of -2050 Oe. The corresponding type 1 trap would have a deactivating field of 2950 Oe, less than H_n for the final jump, which would occur for all $H_m > H_n$, exactly as observed.

If the final jump field is very much larger than the largest deactivating field for type 1 nuclei, the initial magnetization curve, as from a thermally demagnetized state, may be followed by a coercive

force much larger than the initial saturating field, as observed in orthoferrites[10] and MnBi.[11] More often, the final jump occurs in a field not large enough to deactivate all type 1 nuclei. It may even be less than H_d, as in Fig. 3 of Ref. 12. The limiting H_n may then first appear at different H_m on the two sides of the loop, as indeed happened in this case. Another consequence of the final H_n not deactivating all type 1's is the following: If an H_m is applied large enough to deactivate all type 1's, then removed, nothing will happen when a field is applied in the other direction until the final H_n is reached. As soon as this jump has occurred, domain wall is available and, if the field is reduced, the unsymmetrical behavior associated with type 1 nuclei can then be observed. If, however, the initial large H_m had been in the opposite direction, the same configuration would exist after the subsequent H_n but with all the magnetizations reversed. Then the same unsymmetrical behavior as before would be observed but the entire M vs H plot would be reflected through the origin. This type of behavior has been observed many times. The small-field and minor-loop behavior, even when many type 1 nuclei appear to be present, is reproducible in the most minute detail for either sense of M, depending on how the sample was previously "set." This cannot be done with type 1 nuclei alone.

Measurements of the nucleating fields of a $SrO \cdot 4Fe_2O_3 \cdot 2Al_2O_3$ single crystal as a function of saturating field[4] show a slope of -1 and an offset of H_d, exactly as this theory predicts. Materials of this type and orthoferrites, for which bulk rotation plays no part in the magnetization process, should be expected to behave in accordance with this model. Indeed, the plot of starting field as a function of magnetizing field shown by Shur and Khrabrov[3] for their orthoferrite sample after annealing to remove the effects of mechanical polishing also shows this behavior. They also observed symmetrical behavior in high fields and asymmetrical in low, and discussed their observations qualitatively in terms of two types of nuclei.

Measurements of coercive force as a function of magnetizing field should also correspond to this picture. The coercive force, that is, negative values of H_n in Fig. 5, should remain zero until $H_m = 2H_d$ and then rise with a slope of 1, if H_c is plotted as a positive quantity as it usually is, until it reaches a saturation level. This behavior is strikingly shown in MnBi powders[11] in which H_c remains zero until H_m = about 2500 Oe, a reasonable value for $2H_d$ for powders of this material, then rises with a slope of one until it saturates.

The coercivity of an yttrium orthoferrite crystal measured by Craik and McIntyre[13] and shown in their Fig. 1 is fitted very well in this way, estimating H_d as about 35 Oe.

The way in which Craik and McIntyre's Fig. 2, reproduced here as Fig. 7(a), can be described on this picture is even more remarkable. They state that this sample showed H_c of 30 Oe for all H_m

greater than 60 Oe, and hysteresis loops as in the figure for H_m between 45 and 60 Oe. From the figure, H_d can be taken as 37 Oe, from the H_{int} = 0 line. Then if the sample contained one type 1 nucleus with a characteristic field of 39 Oe and a type 2 with 74 Oe, symmetrical loops with H_c of 37 Oe would appear for all H_c > 76 Oe, and a single jump at 2 Oe would appear for H_m between 37 and 76 Oe, and single jump at 2 Oe would appear for H_m between 37 and 76 Oe, exactly the kind of behavior described. The predicted loop for H_m between 37 and 76 Oe is shown in Fig. 7(b).
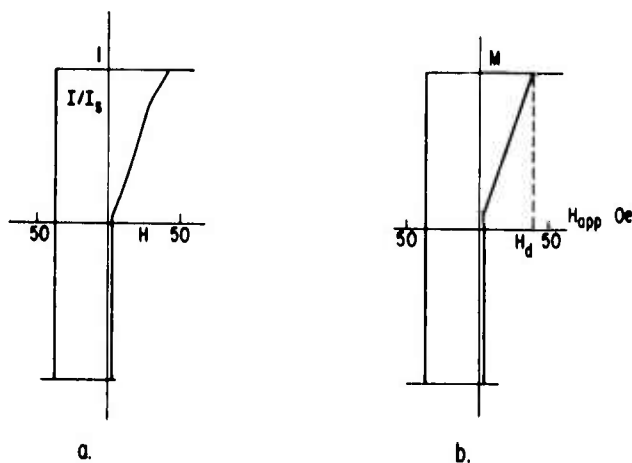

a.   b.

Fig. 7 (a) Hysteresis loop of $YFeO_3$ crystal, from Ref. 13. (b) Hysteresis loop calculated from two-nucleus model.

CONCLUSION

A simple model involving two types of nuclei, neither with any unusual or unsymmetrical properties, can describe a large variety of phenomena related to the field dependence of coercive force in powders and nucleating fields in single particles of high-anisotropy materials, including orthoferrites and hexagonal oxides as well as cobalt-rare-earths.

REFERENCES

1. J.J. Becker, "Angular Variation of Coercive Force in Permanent Magnet Materials," J. Appl. Phys. 38, 1015-1017 (March 1967).

2. J.J. Becker, "Observations of Magnetization Reversal in Cobalt-Rare-Earth Particles," IEEE Trans. Magn. MAG-5, 211-214 (Sept. 1969).

3. Ya. S. Shur and V. I. Khrabrov, "Magnetization Proeesses and Domain Structure in Orthoferrite Monoerystals with Weak Ferromagnetism," Soviet Phys. JETP 30, 1027-1031 (June 1970).

4. M. Rosenberg, C. Tanasoiu, and V. Floreseu, "Magnetization Reversal in Ferrimagnetic Oxides with High Anisotropy Field," Phys. Letters 23, 540-541 (Nov. 1966).

5. J. J. Becker, "Angular Dependenee of Nucleating Fields in Co-Rare Earth Particles," AIP Conf. Proc. No. 5, Part 2, 1067-1071 (1972).

6. S. Shtrikman and D. Treves, "On the Resolution of Brown's Paradox," J. Appl. Phys. 31, 72S-73S (May 1960).

7. H. Zijlstra, "The Coercivity of Permanent Magnets," Z. angew. Phys. 21, 6-13 (June 1966).

8. R. Carey and B. W. J. Thomas, "The Effect of Inclusion Energy on Domain Nucleation at Inclusions in Uniaxial Materials," J. Phys. D: Appl. Phys. 5, 200-202 (Jan. 1972).

9. J. J. Becker, "Magnetization Discontinuities in Cobalt-Rare Earth Particles," J. Appl. Phys. 42, 1537-1538 (March 1971).

10. R. C. Sherwood, J. P. Remeika, and H. J. Williams, "Domain Behavior in Some Transparent Magnetic Oxides," J. Appl. Phys. 30, 217-225 (Feb. 1959).

11. Ya. S. Shur, E. V. Shtol'ts and G. S. Kandaurova, "Charaeteristics of Technical Magnetization in Grain-oriented Fine Powder Specimens," Bull. Acad. Sci. USSR, Phys. Series, 21; English ed., pp. 1205-1209 (1957).

12. J. J. Becker, "Interpretation of Hysteresis Loops of Cobalt-Rare-Earth Single Particles," IEEE Trans. Magn. MAG-7, 644-647 (Sept. 1971).

13. D. J. Craik and D. A. McIntyre, "Critical Fields for Magnetization Reversal in Yttrium Orthoferrite," Phys. Letters 21, 288-289 (May 1966).

71-C-295

M. G. Benz and D. L. Martin

SINTERING OF COBALT-RARE EARTH PERMANENT MAGNETS

60<

AUTHOR Benz, MG Martin, DL	SUBJECT sintering; permanent magnets	NO 71-C-295
		DATE October 1971
TITLE Sintering of Cobalt-Rare Earth Permanent Magnets		GE CLASS 1
		NO. PAGES 3
ORIGINATING COMPONENT Metallurgy and Ceramics Laboratory		CORPORATE RESEARCH AND DEVELOPMENT SCHENECTADY, N.Y.

SUMMARY The process sequence used to fabricate high performance cobalt-rare earth permanent magnets is a powder metallurgy type of process with sintering as a key step. The objective of such an approach is to form a dense, fine-grained, polycrystalline body within which the individual grains are oriented with their crystal axes in the same direction.

Precise control of the composition of the sintered magnet is essential if high magnetic performance is to be achieved. In this study we compare results from two approaches: (1) direct control of composition at the melting stage, and (2) control of composition by blending together powders of different compositions at a stage prior to alignment and densification. Although high performance magnets can be produced by either approach, one of the factors which lead to continued usage of the blending approach is the ability to optimize properties by making small shifts in composition at the powder stage.

KEY WORDS

sintering, permanent magnets,
Co-rare earths

SINTERING OF COBALT-RARE EARTH PERMANENT MAGNETS

M. G. Benz and D. L. Martin

INTRODUCTION

Several combinations of one or more of the rare earths have been used to fabricate sintered cobalt-rare earth permanent magnets.[1-10] These combinations generally include one or more of the rare earth elements La, Ce, Pr, Nd, and Sm. In an effort to simplify this discussion, work considered in this report will be limited to the Co_5Sm system. Since the rare earths are a close-knit family of elements, Co_5Sm serves well as a model for what is observed in the other systems.

PROCESS

The process sequence used to fabricate high performance cobalt-rare earth permanent magnets usually consists of: (1) alloy preparation by melting and casting, (2) comminution of the cast alloy to a fine powder (particle size approximately 10 μM. At this stage each powder grain is essentially a single crystal), (3) magnetic alignment of the powder grains (c-axis parallel to the direction of the applied field), (4) densification by application of pressure followed by high temperature diffusion type sintering, (5) post sintering thermal treatment to optimize coercivity, and (6) magnetization.

OXYGEN

Oxygen is a factor in this process, as it is in most powder metallurgy type processes. The oxygen content of the magnets fabricated for this study varied between 0.3 and 0.7 wt %, as determined by vacuum fusion analysis. These are large values for metallic systems, and hence the source and location of the oxygen must be carefully considered.

During melting, vacuum melting practices are used to reduce the dissolved oxygen level in the cobalt prior to addition of the rare earth metal. The rare earth metal is added to the deoxidized cobalt under an inert atmosphere, and a further reduction in the dissolved oxygen level occurs by oxidation of a very small portion of the rare earth. This rare earth oxide forms a slag which is left behind in the crucible during the casting process. Little is known about the solubility of oxygen in bulk castings. They are too difficult to sample directly without introduction of additional oxygen by the sampling process itself. One can estimate, however, that the oxygen content of the casting is much less than 0.01 wt %.

Next the casting is crushed. At -20 mesh, analytical samples can be readily taken and show 0.03 to 0.05 wt % oxygen for a Co + 34 wt % Sm alloy. This increase in oxygen level is considered to result from the increased surface area and hence the volume of surface oxide.

As the crushed alloys are pulverized and finally milled to smaller diameters, the surface area increases and the surface oxide layer formed on these fresh surfaces represent a greater fraction of the total. At the 10 μM particle size for powder milled in nitrogen but subsequently handled in air, one measures 0.3 to 0.7 wt % oxygen. This is a tenfold increase over the oxygen content for the -20 mesh sample, and indicates that most of the oxygen in the system at this stage exists as a oxide layer coating the surface of each powder grain.

During magnetic alignment no change is noted in the oxygen level.

During the first stage of densification by pressing, no change in the oxygen level is observed. A surface oxide layer is still considered to exist on each crystal grain in the pressed compact.

During the final stage of densification by sintering, again _no_ change in the total oxygen level is observed, _but_ a significant change in the _location_ of this oxygen does occur. After sintering, the oxide layers no longer coat each grain. Furthermore, small oxide particles (diameter <<1 μM) are not left behind at the grain boundaries. At least they have not been observed along the grain boundaries using electron microscopy of replicas of fractured surfaces. What is observed, however, are large crystals (size approximately 1 μM) located in the pores which exist at multigrain corners. These are clearly observed using scanning electron microscopy to view a fractured surface. Use of an x-ray scan of such an area shows a change in the Sm peak to Co peak ratio from 0.85 for the bulk grain to 3.0 for the pore area. This strongly suggests that the pore area is rich in samarium, and we postulate that this is due to the presence of samarium oxide in the pore.

COMPOSITION

On the basis of the above, the sintered alloy will be considered to exist as a mixture of one or more Co-Sm metal phases with an oxide phase. The oxide phase will be considered to be Sm_2O_3. Furthermore, it will be assumed that the oxygen solubility in the Co-Sm metal phases is so small that for a first approximation all of the oxygen measured for a particular sintered sample will be assumed to be present as part of the oxide phase. Hence the composition of the Co-Sm metal phases must be adjusted to take into account the Sm that went to make up the Sm_2O_3. For example, a sample containing 62.1 wt % Co, 37.5 wt % Sm, and 0.4 wt % oxygen would be assumed to consist of 2.77 wt % oxide phase and 97.23 wt % Co-Sm metal phases. Hence, the Co-Sm metal phases would have an average

composition of 64.1 wt % Co and 35.9 wt % Sm instead of 62.1 wt % Co and 37.5 wt % Sm that exist for the total system.

COMPOSITION AND SINTERING

In order to determine what influence composition might have on sintering and magnetic properties, a series of four alloys was prepared with nominal compositions varying from Co + 34 wt % Sm to Co + 37 wt % Sm. Powders with an average particle size of 5.4 µM were prepared from these alloys. Samples were prepared from each powder by magnetic alignment at 60 kOe, hydrostatic pressing with 200 kpsi to a density of 6.88 g/cm^3 (relative density = 0.8), sintering at 1120°C for 1 hour, age cooling at a rate of approximately 1°C/min to 900°C, and chamber cooling to room temperature. At this point, shrinkage $\Delta V/V_0$ was calculated from the measured change in density and the intrinsic coercive force was measured after magnetization at 60 kOe. These results are listed in Table I:

TABLE I

Powder Lot:	D	C	B	A
Nominal Composition				
Sm, wt %	34	35	36	37
Co, wt %	66	65	64	63
After Sintering				
$\Delta V/V_0$	0.069	0.086	0.090	0.167
H_{ci}, kOe	-6.0	-4.1	-2.4	-17.5
Analytical Composition				
Sm, wt %			35.6	36.8
Co, wt %			63.4	62.5
O, wt %			0.64	0.56
Phases				
Sm$_2$O$_3$, wt %			4.4	3.9
Co-Sm, wt %			95.6	96.1
In Co-Sm Phases				
Sm, wt %			32.9	34.5
Sm, at %			16.1	17.1
δ_{Sm}, at % Sm			-0.5	+0.5

Remarkable increases in $\Delta V/V_0$ and H_{ci} are noted for the sample from powder lot A as compared to the samples from powder lots B through D. Analysis of lots A and B for Co, Sm and oxygen, and adjustment of the compositions of the metal Co-Sm phases as outlined in the preceding section, showed that lot A has an adjusted composition of 34.5 wt % Sm and lot B has an adjusted composition of 32.9 wt % Sm. On an atomic % basis, precise stoichiometry for Co$_5$Sm occurs at 16.66 at % Sm. Deviations from this composition will be noted by the symbol δ_{Sm}. When δ_{Sm} is positive, the alloy will be referred to as

hyperstoichiometric. When δ_{Sm} is negative, the alloy will be referred to as substoichiometric. As noted in Table I, samples from lots A and B have adjusted compositions in the Co-Sm metal phases which bracket the stoichiometric composition of 16.6 atom % Sm. Furthermore, the remarkable increase in shrinkage and the dramatic increase in intrinsic coercive force occur as the composition goes from substoichiometric to hyperstoichiometric.

BLENDING

From the preceding section it would appear that the final composition of the sintered alloy must be hyperstoichiometric with regard to the Co-Sm metal phases. In order to achieve this, one must control not only the Sm content of the alloy but also the oxygen content of the powder. Rather than attempt to control this delicate balance at the melt stage, we have used blending of powders of different compositions to achieve the desired final composition. In this way the Co, Sm, and O content of each powder is established by the original melt compositions and the state of surface oxidation of the powder. This in turn is determined by the particle size and shape. By blending two such powders, one is able to achieve a hyperstoichiometric Co-Sm metal phase in the sintered alloy. As noted in Tables II and III, the same remarkable increases in shrinkage and H_{ci} are noted for the blend cases at a nominal 36 to 37 wt % Sm final composition. These studies were done without precise analysis, but as the oxygen levels will be somewhat similar to the direct melt study discussed in the previous section, one can again draw the conclusion that hyperstoichmetric compositions after adjustment for oxygen are essential in order to achieve rapid shrinkage and a high intrinsic coercive force.

TABLE II

Shrinkage $\Delta V/V_0$

		Wt %, Sm (Nominal)							
						Blend			
Base	Add	32	35	35.5	36	36.5	37	37.5	38
25	60	0.097							0.135
32	43					0.116	0.162	0.167	0.172
34	41		0.039	0.059	0.143	0.143			
34	50			0.067	0.121	0.154	0.146		
34	60			0.073	0.112	0.144	0.154		
36	37				0.089	0.158	0.167		

SUMMARY

Using Co$_5$Sm as a model cobalt-rare earth permanent magnet system, this report includes a discussion of: (1) the process sequence used to fabricate high performance cobalt-rare earth permanent magnets, (2) the role of oxygen in this process, (3) the

TABLE III

Intrinsic Coercive Force, H_{ci} kOe

		Wt %, Sm (Nominal) Blend							
Base	Add	32	35	35.5	36	36.5	37	37.5	38
25	60	-1.8							-45.4 *
32	43					-9.7	-14.3	-13.0	-11.1
34	41		-3.5	-2.6	-15.8	-13.7			
34	50			-2.1	-9.9	-12.4	-11.1		
34	60			-2.0	-9.9	-11.3	-9.9		
36	37				-2.4	-19.2	-17.5		

*Sample not aligned.

adjustment of composition necessary to account for the oxide present, (4) observations relating shrinkage during sintering and intrinsic coercive force to deviations from stoichiometry, and (5) the use of blending for composition control.

For: (1) observations of time and temperature effects during sintering, (2) a model to explain the shrinkage observations, and (3) several reasons that might explain why a high intrinsic coercive force is observed for hyperstoichiometric compositions, the reader is referred to Ref. 11.

ACKNOWLEDGMENTS

REFERENCES

1. D.K. Das, IEEE Trans. Magnetics MAG-5, 214 (1969).

2. M.G. Benz and D.L. Martin, Appl. Phys. Letters, 17, 176 (1970).

3. R.E. Cech, J. Appl. Phys. 41, 5247 (1970).

4. D.K. Das, IEEE Trans. Magnetics MAG-7 (Sept. 1971).

5. D.L. Martin and M.G. Benz, Cobalt No. 50, 11 (1971).

6. J. Tsui and K. Strnat, Appl. Phys. Letters 18, 107 (1971).

7. J. Tsui, K. Strnat, and R. Harmer, J. Appl. Phys. 42, 1539 (1971).

8. M.G. Benz and D.L. Martin, ibid., p. 2786.

9. D.L. Martin and M.G. Benz, IEEE Trans. Magnetics MAG-7, 291 (1971).

10. R.J. Charles, D.L. Martin, L. Valentine, and R.E. Cech, 17th Ann. Conf. on Magnetism and Magnetic Materials, Chicago, Nov. 1971. To be published AIP Conf. Proceedings.

11. M.G. Benz and D.L. Martin, "On The Mechanism of Sintering in Cobalt-Rare Earth Permanent Magnets Alloys." Submitted for publication in J. Appl. Phys.

M. G. Benz and D. L. Martin

ANISOTROPY PARAMETERS AND COERCIVITY FOR SINTERED
Co_5Sm PERMANENT MAGNET ALLOYS

65<

TECHNICAL INFORMATION SERIES

AUTHOR Benz, MG Martin, DL	SUBJECT cobalt-rare earth permanent magnets	NO 72CRD104
		DATE April 1972
TITLE Anisotropy Parameters and Coercivity for Sintered Co$_5$Sm Permanent Magnet Alloys		GE CLASS 1
		NO. PAGES 12
ORIGINATING COMPONENT Metallurgy and Ceramics Laboratory		CORPORATE RESEARCH AND DEVELOPMENT SCHENECTADY, N.Y.

SUMMARY

Saturation magnetization, intrinsic coercive force, anisotropy field, and anisotropy constants were determined for a sample of sintered Co$_5$Sm at 4.2, 77, 300, and 500°K. The relationship between the temperature dependence of the coercivity and the anisotropy parameters is discussed.

KEY WORDS

permanent magnets, cobalt-rare earths, magnetic anisotropy

INFORMATION PREPARED FOR _____

ANISOTROPY PARAMETERS AND COERCIVITY
FOR SINTERED Co$_5$Sm PERMANENT MAGNET ALLOYS

M.G. Benz and D.L. Martin
General Electric Company
Corporate Research and Development
Schenectady, New York 12301

INTRODUCTION

Previous efforts to understand the irreversible losses observed for cobalt-rare earth permanent magnets demonstrated that these losses are best understood by measurement of a series of demagnetization curves at the temperatures of interest.[1] The dominant feature of such a family of curves is the very large temperature dependence of intrinsic coercive force H_{ci}. Examination of a variety of cobalt samarium samples with large differences in H_{ci} (-12 kOe to -33 kOe at 300°K) showed them to have a common response of relative coercivity to temperature, as given in Fig. 1.[2]

In this study; saturation magnetization $4\pi J_S$, intrinsic coercive force H_{ci}, anisotropy field H_A, anisotropy constants K_1, K_2 and domain wall energy γ were determined for a single sample of sintered Co$_5$Sm at temperatures between 4.2°K and 500°K, in order to see if the temperature dependence of relative coercivity could be related to the temperature dependence of the anisotropy parameters and wall energy.

SAMPLE PREPARATION

A highly aligned polycrystalline sample of Co$_5$Sm was prepared by the multiphase sintering approach outlined previously.[3] From this cylindrical sample (7.5 mm diameter × 2.5 cm long); a cube, 3.2 mm on edge, was cut such that one principle axis of the cube was parallel to the alignment direction

of the original cylinder and hence parallel to the hexagonal axes of the Co_5Sm grains. This principle axis of the sample will be referred to as the c-axis. From density measurements and chemical analysis, this sample was estimated to consist of 8 volume % voids, 3.2 volume % Sm_2O_3 (2.8 wt %), and 88.8 volume % Co_5Sm with an average composition of 16.7 at % Sm. The Co_5Sm contained a trace amount of Co_7Sm_2 as indicated by metallography and x-ray measurement of the lattice parameter. The lattice parameters c = 3.970 ± 0.001Å and a = 5.002 ± 0.001Å were similar to those previously observed for Co_5Sm in equilibrium with the Co_7Sm_2 phase.[4] The grain size for the sintered grains was between 5 and 10 μm. At room temperature this sample had a magnetiz ion at 100 kOe of 9.35 kGauss; a remanent magnetization of 8.93 kGauss, an open circuit magnetization of 8.16 kGauss at a field of -1.99 kOe; and an intri..sic coercive force of -30.5 kOe. The magnetic alignment factor, estimated by dividing the remanent magnetization by the magnetization at 100 kOe, was 0.96. The shape dependent demagnetizing field, opposing the applied field for these measurements, was estimated by means of the polar radiation model[5] to be 0.244 × 4πJ.

SAMPLE MEASUREMENT

The magnetization of the sample was measured parallel and perpendicular to the c-axis by the ballistic method for small samples outlined previously.[1]

The applied field was provided by a superconducting solenoid. The 4.2°K and 77°K measurements were made at the boiling points of liquid helium and liquid nitrogen, respectively. The 500°K measurement was made with the sample heated by a small electric furnace which fitted inside the superconducting solenoid system.

The sequence used for the measurements at each temperature was as follows: 1) Magnetize the sample parallel to the c-axis at 300°K. 2) Measure the magnetization of the sample parallel to the c-axis at the temperature T (T = 4.2 , 77 , 300 , or 500°K). 3) Re-magnetize the sample parallel to the c-axis at 300°K. 4) Measure the magnetization of the sample perpendicular to the c-axis at the temperature T as a function of increasing field.

RESULTS

With the magnetizing field parallel to the c-axis, the magnetization of the sample was measured in the direction of the c-axis in order to determine $4\pi J_S$. The values for $4\pi J_S$ were taken as the values for $4\pi J$ measured at 100 kOe at 4.2, 77 , and 300°K; and the value measured at 60 kOe at 500°K. These values are listed in Table I.

With the demagnetizing field parallel to the c-axis, the magnetization of the sample was measured in the direction of the c-axis in order to determine H_{ci}. These values are also listed in Table I.

With the magnetizing field perpendicular to the c-axis, the magnetization of the sample was measured in the direction of the magnetizing field as a function of increasing field. These data are shown in Fig.2. The 4.2°K data are plotted separately to show the low field nonlinear portion of the curve. This effect is unexplained, but shows the necessity of fields approaching 100 kOe and above for this type of measurement.

As discussed by Sucksmith and Thompson,[6] when the magnetizing field is perpendicular to the c-axis, the saturation magnetic moment per unit

volume J measured in the direction of the magnetizing field is given by the expression:

$$J_S H = 2K_1 \left(\frac{J}{J_S}\right) + 4 K_2 \left(\frac{J}{J_S}\right)^3 \tag{1}$$

Here K_1, K_2 are the anisotropy constants, J_S is the saturation magnetic moment per unit volume, and H is the effective magnetizing field perpendicular to the c-axis. By rearrangement:

$$\frac{H}{J} = \frac{2K_1}{J_S^2} + \frac{4K_2}{J_S^4} J^2 \tag{2}$$

Hence, a plot of H/J vs J^2, as given in Fig. 3, can be used to determine $2K_1/J_S^2$ from the intercept and $4K_2/J_S^4$ from the slope. Values for $2K_1/J_S^2$ taken from this figure are listed in Table I. The slope $4K_2/J_S^4$ was considered to be equal to zero for these plots.

Using the above data, values for the anisotropy field H_A, the anisotropy constant K_1 and the domain wall energy γ were calculated by use of the expressions:

$$H_A = \left(\frac{4\pi J_S}{4\pi}\right) \left(\frac{2K_1}{J_S^2}\right) \tag{3}$$

$$K_1 = \frac{1}{2} \left(\frac{4\pi J_S}{4\pi}\right)^2 \left(\frac{2K_1}{J_S^2}\right) \tag{4}$$

$$\gamma = (2k \, T_c \, K_1/d)^{1/2} \tag{5}$$

Here k is Boltzmann's constant, T_c is the Curie temperature (984°K from Ref. 7), and d is the distance between magnetic atoms[8] (taken as equal to one half of the a lattice parameter). These values were also listed in Table I.

The upper half of Table I is calculated on the basis of the total sample; 8 volume % voids, 3.2 volume % Sm_2O_3 and 88.8 volume % Co_5Sm. The

4

lower half of the table is calculated on the basis of 100 volume % Co_5Sm.

DISCUSSION

The values for $4\pi J_s$ and H_{ci} measured for this sample are in agreement with previous values presented by the authors. [2, 9]

The values for anisotropy field H_A and the anisotropy constant K_1 at 300°K are in good agreement with data for single crystals presented by Strnat, [10] Buschow, [11] and Tatsumoto et al. [7] A much different temperature dependence is observed, however. This may be due to the polycrystalline nature of the sample used for this study, differences in composition, or the higher fields used for these measurements.

Accepting the temperature dependence of anisotropy field, anisotropy constant, and domain wall energy presented here; the most striking aspect of the results presented in Table I is the similarity between the temperature dependence of these anisotropy parameters and the temperature dependence of H_{ci}. As indicated in Figs. 4-6, these data support models for relating coercivity directly to the anisotropy constant [Fig. 4]; or models relating coercivity to the anisotropy field as advanced by McCurrie [12] [Fig. 5]; or models relating coercivity to the domain wall energy (γ/J_s actually) as advanced by Zijlstra [8] and Westendorp [13, 14] [Fig. 6]. This later model is only supported by the data if the model is modified to include the concept that H_{ci} drops to zero at some finite value of γ/J_s (viz. 0.0275 erg/G·cm²). Which of these models truly describes the case at hand is yet to be firmly established.

An attempt was also made to relate the above to the classical temperature dependence of magnetic anisotropy presented by Zener.[15] As illustrated in Fig. 7, it was found that the relationship had to be modified in a manner similar to the work of Carr for hexagonal cobalt[16] in order to fit the data.

ACKNOWLEDGMENTS

References

1. D.L. Martin and M.G. Benz, "Magnetization Changes for Cobalt-Rare Earth Permanent Magnet Alloys When Heated Up to 650°C," IEEE Trans. Magn. MAG-8, 35 (1972).

2. D.L. Martin and M.G. Benz, "Temperature Dependence of Coercivity for Co-Sm Permanent Magnet Alloys," Proc. International Magnetics Conference, Kyoto, Japan, April 10-13, 1972, IEEE Trans. Magn. MAG-8, Sept. (1972).

3. M.G. Benz and D.L. Martin, "Cobalt-Samarium Permanent Magnets Prepared by Liquid Phase Sintering," Appl. Phys. Letters 17, 176 (1970).

4. M.G. Benz and D.L Martin, unpublished.

5. R.J. Parker and R.J. Studders, Permanent Magnets and Their Application, John Wiley and Sons, Inc., New York, pp 163-168 (1962).

6. W. Sucksmith and J.E. Thompson, "The Magnetic Anisotropy of Cobalt," Proc. R. Soc. 225, 362 (1954).

7. E. Tatsumoto, T. Okamoto, H. Fujii, and C. Inoue, "Saturation Magnetic Moment and Crystalline Anisotropy of Single Crystals of Light Rare Earth Cobalt Compounds RCo_5," Supplement J. de Physique 32, C1-550 (1971).

8. J. Zijlstra, "Domain-Wall Processes in $SmCo_5$ Powders," J. Appl. Physics 41, 4881 (1970).

9. S. Foner, E.J. McNiff, Jr., D.L. Martin, and M.G. Benz, "Magnetic Properties of Cobalt-Samarium with a 24 MGOe Engergy Product," General Electric Company TIS Report 72-CRD-073, submitted to Appl. Phys. Letters.

10. K. Strnat, "The Recent Development of Permanent Magnet Materials Containing Rare Earth Metals," IEEE Trans. Mag. MAG-6, 182 (1970).

11. K.H.J. Buschow and W.A.J.J. Velge, "Permanent Magnetic Materials of Rare Earth Cobalt Compounds," Z. angew. Phys. 26, 157 (1969).

12. R.A. McCurrie, "Determination of Intrinsic Coercivity Distributions in Aligned Assemblies of Uniaxial $SmCo_5$ and $LaCo_5$," Phil. Mag. 22, 1013 (1970).

13. F.F. Westendorp, "Domain-Wall Energy and Coercive Force of Cobalt Rare-Earth Permanent Magnet Materials," J. Appl. Phys. 42, 5727 (1971).

14. F.F. Westendorp, "Domains in $SmCo_5$ at Low Temperature," to be published - Applied Physics Letters.

15. C. Zener, "Classical Theory of Temperature Dependence of Magnetic Anisotropy Energy," Phys. Rev. 96, 1335 (1954).

16. W.J. Carr, Jr., "Temperature Dependence of Ferromagnetic Anisotropy," Phys. Rev. 109, 1971 (1958).

TABLE I

Magnetization and Anisotropy Data for Sintered Co_5Sm

Basis†	T $^\circ K$	$4\pi J_S$ kG	H_{ci} kOe	$2K_1/J_S^2$ Oe/G	H_A kOe	K_1^* 10^7 erg/cm³	γ erg/cm²
	4.2	10.0	-52.0	530			
Sample	77	9.88	-52.7	570			
	300	9.35	-30.5	385			
	500	8.53	-16.7	250			
Co_5Sm	4.2	11.2	-52.0	472	421	18.9	45.3
	77	11.1	-52.7	507	448	19.8	46.4
	300	10.5	-30.5	343	286	11.9	35.9
	500	9.58	-16.7	223	170	6.47	26.5

†The values listed on a sample basis are those actually measured
for the sample as a whole. The values listed on a Co_5Sm basis
are those the sample would have if it were 100 volume % Co_5Sm
instead of 88.8 volume % Co_5Sm.

*1 G·Oe = 1 erg/cm³.
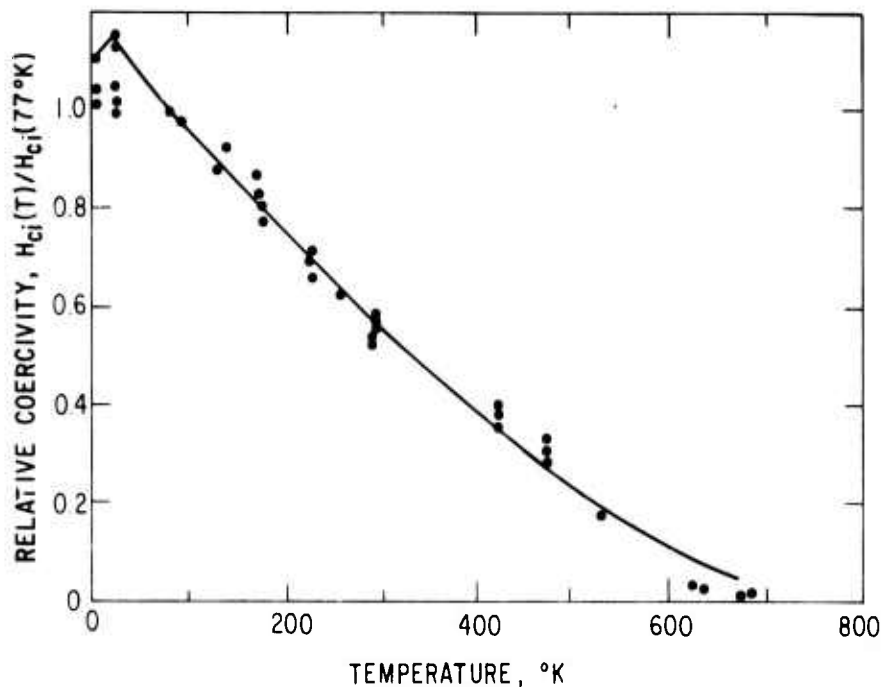
Fig. 1 Relative coercivity vs temperature. The data were normalized so
that the relative coercivity at 77° K was equal to 1.

Fig. 3 H/J vs J². The intercept is equal to $2K_1/J_s^2$.

Fig. 2 Magnetization of the sample measured perpendicular to the c-axis as a function of field applied perpendicular to the c-axis.

Fig. 5 H_{ci} vs the anisotropy field H_A.

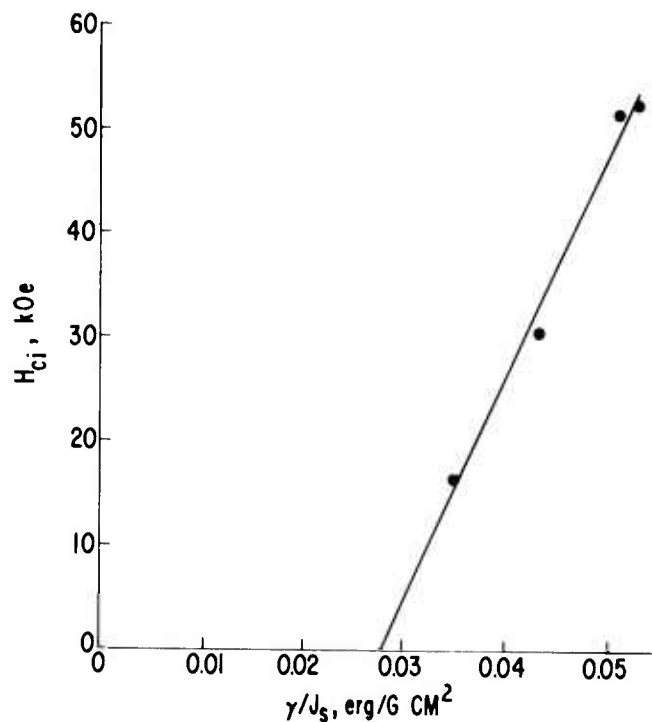Fig. 4 H_{ci} vs the anisotropy constant K_1.

Fig. 6 H_{ci} vs the domain wall energy γ divided by the saturation magnetic moment per unit volume J_S.
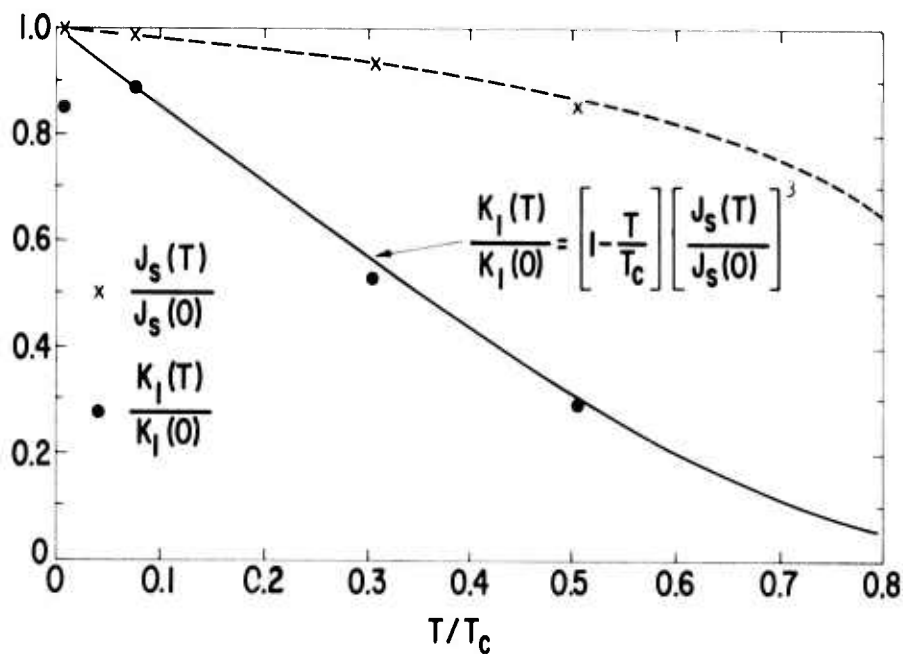
Fig. 7 $J_S(T)/J_S(0)$ and $K_1(T)/K_1(0)$ as a function of T/T_c. $J_S(0)$ was taken as the value for J_S at 4.2° K. $K_1(0)$ was taken as $K_1(77^{\circ}$K$)/0.889$, the value 0.889 being $[1-T/T_c][J_S(T)/J_S(0)]^3$ at $T = 77^{\circ}$ K. The solid curve was calculated by placing the empirically determined Carr[16] type factor $(1-T/T_c)$ into the Zener[15] equation. T_c was taken as 984° K. [7]

12

79<

GENERAL ⊛ ELECTRIC

General Electric Company
Corporate Research and Development
Schenectady, New York

TECHNICAL INFORMATION SERIES

AUTHOR Charles, RJ et al.	SUBJECT permanent magnetic materials	NO 71-C-281
		DATE October 1971
TITLE A 10,000 Oe B-Coercive Force Magnet		GE CLASS 1
		NO PAGES 6
ORIGINATING COMPONENT Metallurgy and Ceramics Laboratory		CORPORATE RESEARCH AND DEVELOPMENT SCHENECTADY, N.Y.

SUMMARY

The current study outlines the importance of controlling composition and sintering temperature in optimizing the magnetic properties of Co-Pr-Sm alloys. A series of alloys was made from a $Co_5Pr_{0.76}Sm_{0.24}$ base metal powder and an additive powder. For a final nominal composition of 62.9 w/o Co, 21.3 w/o Pr and 15.8 w/o Sm, the following properties have been attained: B-coercive force 1.01 [10.1 kOe] and a $(BH)_{max}$ value of 207 kJ/m^3 [26 MGOe]. In view of the usual difficulty of attaining high coercivity in this class of alloys the above BH_c value is particularly noteworthy.

KEY WORDS

permanent magnetic materials

INFORMATION PREPARED FOR _____

Additional Hard Copies Available From

Microfiche Copies Available From

RD-54 (10/70)

Corporate Research & Development Distribution
P.O. Box 43 Bldg. 5, Schenectady, N.Y., 12301

Technical Information Exchange
P.O. Box 43 Bldg. 5, Schenectady, N.Y., 12301

A 10,000 Oe B-COERCIVE FORCE MAGNET*

R. J. Charles, D. L. Martin, L. Valentine and R. E. Cech[†]

INTRODUCTION

Many previous researches[1-7] have illustrated that the production of high-energy, fine particle permanent magnets from transition metal-rare earth compounds depends sensitively on the degree to which control can be exercised on interdependent processing parameters. The present work describes a series of high performance cobalt-rare earth magnets in which sintering practice, composition, and heat treatment have been systematically adjusted to attain an optimum remanent magnetization with near theoretical B-coercive force.

EXPERIMENTAL PROCEDURES

Composition: Within the class of cobalt-rare earth compounds, Co_5R, with a single axis of magnetization the Co_5Pr phase exhibits the highest saturation value (≈ 1.2 tesla [12 kGauss]) and thus the highest potential energy product ($BH_{max} \approx 286$ kJ/m^3 [36 MGOe]). [†]

Utilizing liquid phase sintering, Tsui and Strnat[7] have described an off-stoichiometry cobalt praseodymium magnet (61.8 w/o Co, balance Pr) yielding an energy product of 127 kJ/m^3 [16 MGOe] or about 45% of the theoretical maximum for this composition. The B-coercive force, $\mu_0 H_c [H_c]$ of 0.5 tesla [5 kOe] was about 59% of that theoretically attainable for the particular magnet described (i.e., $0.59 B_r$). Martin and Benz[6] had previously shown that the substitution of half of the praseodymium by samarium yielded higher coercivities and consequently higher magnet properties even though the saturation magnetization suffered by the samarium substitution. The particular specimen showing the highest energy product, 183 kJ/m^3 [23 MGOe], and remanent magnetization, 0.996 tesla [9.96 kGauss], was of the nominal composition 63 w/o Co, 13.6 w/o Pr, and 23.4 w/o Sm. It gave a B-coercive force ($\mu_0 H_c$) of 0.68 tesla or 69% of that attainable for this particular magnet. In the same study of Co-Pr-Sm alloys the maximum B-coercive force achieved was 0.88 tesla [8.8 kOe] or 99% of the limiting value set by the remanence, J_r.

Because of the higher coercivities presently attainable with Co-Pr-Sm alloys, additional experimentation has been made on this system. In the current work the Pr/Sm weight ratio was increased to about 1.3 while the cobalt content was maintained at about 63 w/o. Alloy powders were prepared by blending a base powder containing the praseodymium with a 60% Sm - 40% Co additive. The additive was used to promote densification by a liquid phase sintering process.[4] The base material, containing about 67% Co, was prepared by direct reduction of praseodymium and samarium oxides in the presence of cobalt by calcium.[8] Following the high-temperature reduction reaction, soluble products were removed by washing and the cobalt intermetallic compounds (primarily Co_5R) were dried and stored. In order to assure that the resultant alloy powder consisted of individual grains of a sufficiently small size for magnet fabrication ($\approx 10\mu$), the alloy was processed through a fluid energy mill.[9] Measurements of the J-coercive force of the alloy base powder gave the relatively low value of $\mu_0 H_c$ of about 0.15 tesla [1.5 kOe].

Magnet fabrication: The importance of maintaining high coercivity in a magnet structure has been previously indicated. Our experience indicates that it is often difficult to maintain high, reproducible coercivity in samples sintered to full density. In general, a small amount of porosity obtained by slightly "under sintering" is usually preferable. Such "under sintering" prevents a compact from undergoing exaggerated grain growth which may tend to diminish coercivity. Systematic study of temperatures and times

of sintering is necessary, therefore, to delineate optimum conditions for a given composition. This is particularly so in view of the fact that excessive porosity is deleterious to magnetization.

Successful sintering of near 5-1 compounds of cobalt-rare earths has been generally shown to require off-stoichiometry compositions (rare earth excess) of the final magnets.[4,5,10] Such off-stoichiometry will, to a first approximation, reduce the saturation magnetizations from stoichiometric values in direct proportion to the reduced cobalt contents of the final alloys. Such reductions must presently be tolerated, for only in this manner is it possible to achieve high coercivity simultaneous with high sintered density.

Test samples in this work were aligned and pressed to a packing density of about 80% by methods previously described.[4,6,9] After sintering all samples exhibited a packing fraction (p) greater than 0.9 of that for full density (8.5 g/cc) and an alignment factor $(A=J_r/J_s)$ greater than 0.95.

RESULTS

Figure 1 shows data, typical for each of a number of blended Co-Pr-Sm compositions, from which an optimum sintering temperature can be determined for a given composition. The sintering times were fixed at one hour. The results shown include the sample of nominal composition 62.87% Co which exhibited the highest properties obtained in this investigation. Similar results were obtained for near neighbor compositions and indicate that satisfactory magnet properties can be achieved by sintering for one hour at a temperature between 1105° and 1120°C. Outside of this temperature-time range the properties decrease markedly. Figure 2 shows the demagnetization results for the sample of 62.87% Co which showed
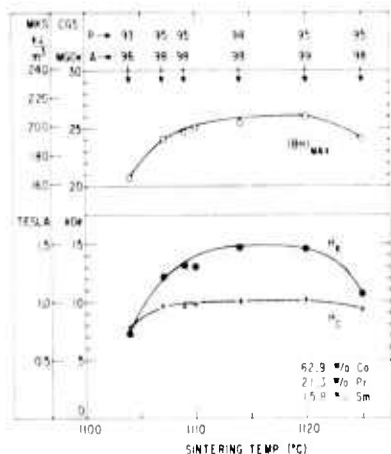
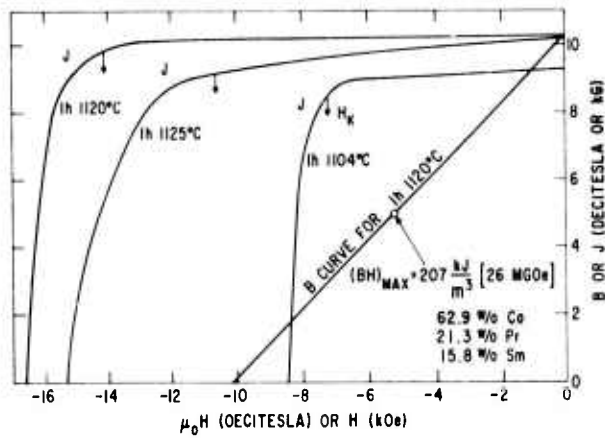Fig. 1 Variation of magnetic properties, packing (p), and alignment (A) with sintering temperature.

Fig. 2 Changes in the J-demagnetization curve with sintering temperature. The B-demagnetization curve for the 1120°C sample is also given.

Fig. 3 Variation of magnetic properties, packing (p), and alignment (A) with composition for a series of Co-Pr-Sm alloys sintered in the range 1105° to 1125°C. The peak value for each composition is listed.
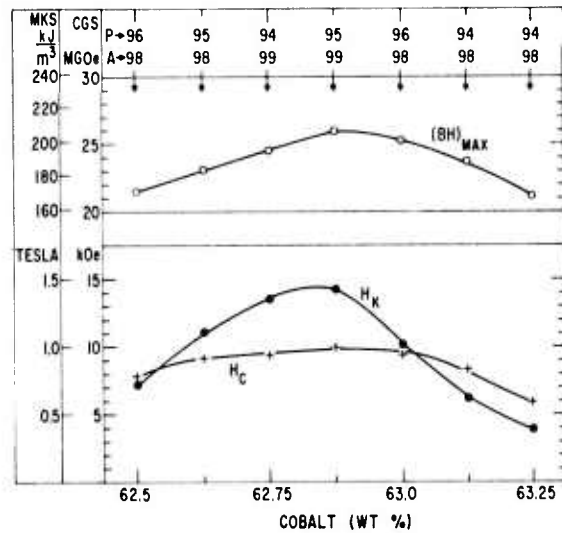
the highest magnet properties. The energy product is high (207 kJ/m^3 [26 MGOe]), but attention should be drawn to the fact that the B-coercive force exceeds 0.1 tesla [10 KOe] and that this value is about 99% of the limit set by the remanent magnetization.

Figure 3 illustrates the effect of composition on properties. In this case the points plotted correspond to the results obtained at an optimum sintering temperature for each composition. These optimum temperatures varied over the full range of sintering temperatures shown in Fig. 1 with the highest optimum sintering temperatures occurring for those compositions near 63 w/o Co.

It is important to note that the most desirable composition ranges shown in Fig. 3 are those in which H_k exceeds the B-coercive

force. * In such a case the demagnetization curve exhibits nearly ideal behavior and the low load line irreversible losses encountered at elevated temperature operation will, in general, tend to be minimized. The effect of sintering temperature on H_k is further illustrated in Fig. 2 in which the J curves for various sintering temperatures are given. The temperature of 1120°C was the optimum temperature resulting in a sufficiently high H_k to allow a coercive force of 99% of that possible. At sintering temperatures above and below 1120°C the properties decrease substantially. With reference to the numerical sample data given in Figs. 1 and 3, it is clear that the exceptional properties of the sample in Fig. 2 result from a high alignment factor (A), an adequate packing fraction (P), and a sufficiently high H_k to allow nearly ideal B-coercive force.

SUMMARY

By optimization of composition and sintering heat treatment, the following properties of a Co-Pr-Sm permanent magnet have been achieved:

$$J_r = 1.026 \text{ tesla } [10.26 \text{ kG}]$$
$$\mu_0 H_c = 1.013 \text{ tesla } [10.13 \text{ kOe}]$$
$$(BH)_{max} = 206.9 \text{ kJ/m}^3 \ [26.0 \text{ MGOe}]$$

It has also been shown that the magnetic properties of such magnets are highly sensitive to variations in composition and sintering temperature.

ACKNOWLEDGMENTS

REFERENCES

1. K. H. Buschow, W. Luiten, P. A. Naastepad, and F. F. Westendorp, Philips Tech. Rev. 29, 336 (1968).

2. D. K. Das, IEEE Trans. Magnetics MAG-5, 214 (1969).

---

* H_k is defined as that demagnetizing field at which
$J = 0.9 \ J_r [4\pi J = 0.9 B_r]$.

3. K. H. J. Bushow, P. A. Naastepad, and F. F. Westendorp, J. Appl. Phys. 40, 4029 (1969).

4. M. G. Benz and D. L. Martin, Appl. Phys. Letters 17, 176 (1970).

5. R. E. Cech, J. Appl. Phys. 41, 5247 (1970).

6. D. L. Martin and M. G. Benz, COBALT, No. 50, 11 (1971).

7. J. Tsui and K. Strnat, Appl. Phys. Letters 18, 107 (1971).

8. R. E. Cech, unpublished.

9. M. G. Benz et al., Tech. Rept., AFML-TR-71-142, Air Force Materials Lab., Wright-Patterson Air Force Base.

10. D. K. Das, IEEE Intermag. Conf., Denver, April 1971, unpublished.

87<

GENERAL ⊛ ELECTRIC

General Electric Company
Corporate Research and Development
Schenectady, New York

TECHNICAL INFORMATION SERIES

AUTHOR Doser, M. Smeggil, JG	SUBJECT cobalt-samarium	NO 73CRD126
		DATE May 1973

TITLE Some Observations of the Magnetic Properties of Fluid-Quenched Co$_5$Sm Magnets	GE CLASS 1
	NO. PAGES 5

ORIGINATING COMPONENT Metallurgy and Ceramics Laboratory	CORPORATE RESEARCH AND DEVELOPMENT SCHENECTADY, N.Y.

SUMMARY

The purpose of this work was to study the effect of different quenching rates from 900°C on the magnetic properties of liquid phase sintered Co$_5$Sm magnets. Various fluids with different thermal conductivities were used to achieve different cooling rates. Interpretations of this behavior were warranted in terms of the microstructures and chemical compositions of the samples examined. The results of this work indicate that the magnetic properties of Co$_5$Sm magnets are strongly dependent on the particular cooling rate used to come from 900°C to room temperature.

KEY WORDS

cobalt-samarium, magnetism, magnetic properties

INFORMATION PREPARED FOR _____

Additional Hard Copies Available From

Microfiche Copies Available From

68<

RD-54 (10/70)

SOME OBSERVATIONS OF THE MAGNETIC PROPERTIES OF FLUID-QUENCHED Co$_5$Sm MAGNETS

M. Doser and J. G. Smeggil

INTRODUCTION

Several authors[1-3] have shown that both post-sintering heat treatments and quench treatments from $900°C$ improve the magnetic properties of cobalt-rare earth magnets. The degree of improvement is closely related to the particular starting post-sintering heat treatment temperature. Jones, Lehman, and Smeggil[4] have reported the effects of water-quenching on second quadrant properties for various starting heat treatment temperatures. Their work resulted in the production of severe kinks in second quadrant demagnetization curves even though substantial H_{ci} values were obtained from cobalt-samarium material water quenched from $900°C$. The purpose of this work was: (1) to obtain faster quenching rates than those attained by chamber cooling yet slower than those obtained from water quenching; (2) to study the effect of these different rates on the magnetic properties of liquid phase sintered Co$_5$Sm magnets having had a post-sintering aging treatment at $900°C$; and finally (3) to determine any observable metallurgical effects of these treatments on the samples by x-ray and optical metallography.

PROCEDURE

Test rod samples were prepared by aligning appropriately blended jet-milled powders in a 60 kOe superconducting field and pressing in a hydropress at 150 kpsi. The resulting magnets, approximately 0.70 cm in diameter and 2 cm long, were sintered at $1116°C$ for one hour in an argon atmosphere. Densities of 95% to 97% theoretical were achieved. The nominal starting composition of the powder was 63.6% Co, 35.9% Sm, with a residual oxygen content of $\approx 0.4\%$. Each rod was reheated to $1100°C$ in argon, cooled to $900°C$ at $3°$ per minute, pulled from the furnace and quenched into various fluids with substantially different thermal conductivities in order to achieve different cooling rates. The magnetic properties of the sintered materials were determined using a 60 kOe pulsed field for magnetization and a 30 kOe hysteresisograph for tracing second quadrant curves. Selected samples were subsequently examined by optical metallography, scanning electron microscopy, and x-ray diffraction (FeKα radiation). In addition chemical analyses were determined on chosen samples for Co, Sm, Al, and Ni.

RESULTS AND DISCUSSION

Figure 1 indicates the squareness H_k (the value of the demagnetizing field required to reduce magnetization to a value equal to 0.9 B_r) for Co$_5$Sm plotted against the reported conductivities[5] for the fluids used in this work. The second quadrant demagnetization curves for reheated samples quenched in these fluids are presented in Fig. 2. The data show that the fluid quenched samples all exhibit higher H_{ci} values than are exhibited by the chamber cooled samples (rate of chamber cooling is approximately $18°C/min$). The remanence, B_r, for chamber-cooled samples was 9900 gauss. Fluid-quenched samples exhibited a slight kink in the demagnetization
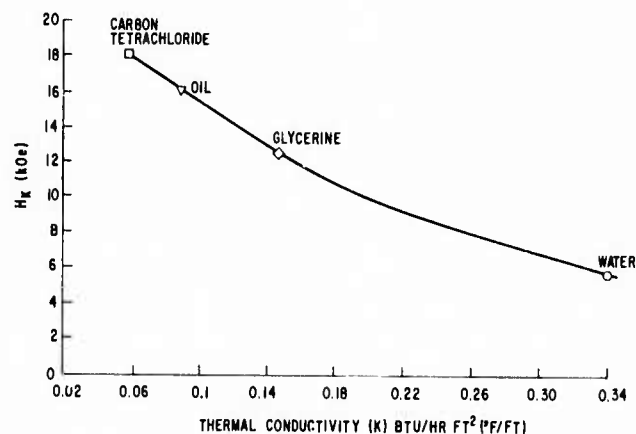

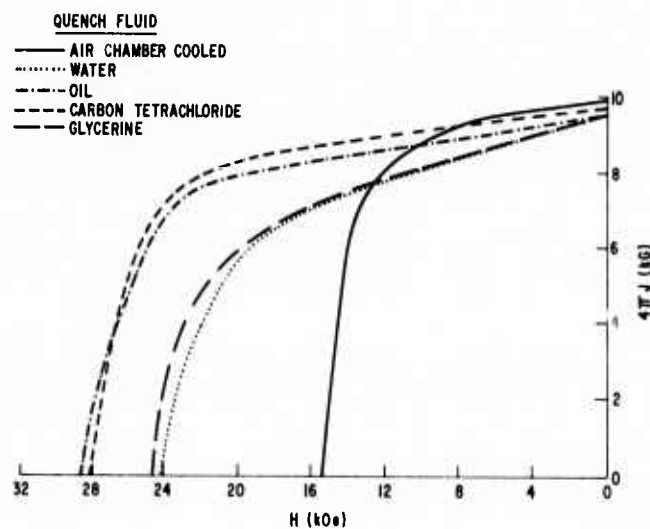Fig. 1 Dependence of H_k for Co$_5$Sm on thermal conductivity of quenching fluid.

Fig. 2 Demagnetization properties of fluid-quenched Co$_5$Sm.

curve occurring around 800 Oe resulting in a lowering of the value of the magnetic induction by 200 gauss. The squareness, H_k, steadily increased as the thermal conductivity of the fluid quenching medium decreased (Fig. 1).

The chemical compositions of all of the above samples were essentially identical and found to be 63.7 wt % Co, 35.2 wt % Sm, 0.035 wt % Ni, and 0.025 wt % Al. The experimental errors in these values were ± 0.2 wt % for Co and Sm and ± 10% for Ni and Al.

Water-quenched samples of the chemical composition examined here did not produce the severe kinks in the demagnetization curves as previously
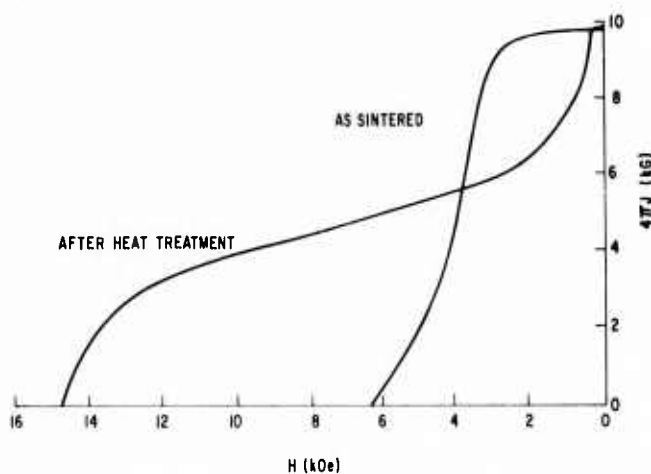

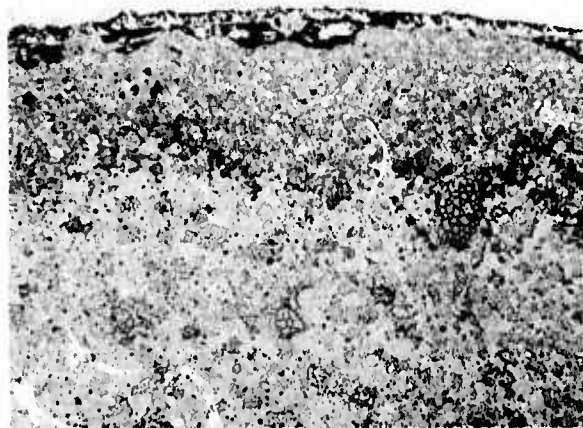Fig. 3 Demagnetization properties of a sintered Co_5Sm magnet exhibiting a "kink."

Fig. 4 Oil quenched sample, D, indicating reversed domain layer.   75X

reported.[4] However, samples from another powder lot which had essentially the same wet chemistry as the above material produced severe kinking even when oil quenched (Fig. 3). Examination of this specimen by optical metallography using the Kerr magnetic effect indicated the presence of an annular layer ($\approx 300\mu$ thick) of continuous reversed domains extending into the sample. No other specimens observed indicated this reversed domain layer (Fig. 4).

In an effort to further determine the cause for the severe kinks in sintered samples from one lot of powder and not in the others, oxygen determinations were attempted by a vacuum fusion technique. The results, however, on the fluid-quenched samples were too high when compared to a chamber-cooled sample of the same composition. We suspect that some residual material on the surface of the magnet (left over from the fluid quenching operation) affected the vacuum fusion results.

To circumvent this problem, x-ray studies of lattice parameters were made with selected samples and are shown in Table 1. Samples D and E represent materials which produced severe kinks in the demagnetization curve when quenched in the listed fluids.

TABLE I

Summary of X-ray Lattice Parameters

Sample	Quenching Fluid	$A(Å)$	$C(Å)$	C/a	At. % Sm[6]
A	Water	4.999 (±1)	3.971 (±1)	0.7944	16.7
B	Oil	5.000	3.970	0.7940	16.75
C	CCl_4	5.000	3.970	0.7940	16.75
D	Oil	4.996	3.973	0.7952	16.55
E	Oil	4.995	3.973	0.7954	16.52

The x-ray lattice parameter values although not greatly different in samples A and D may be significant in view of Martin, Benz, and Rockwood's results[6] in comparing the variation of lattice parameters of Co_5Sm with available Sm content in the magnetic alloys. By comparing our x-ray data with this work, there is some indication that samples D and E might have low Sm contents (possibly due to oxidation of the powder) which would make the material hypo-stoichiometric (<16.66 at % Sm).[7] None of the samples richer than 16.66 at % Sm produced severe kinks in the second quadrant demagnetization curve.

To further study the effects of cooling rate on the magnetic properties of Co_5Sm, two samples were centerless ground and their magnetic properties were measured as material was removed from the diameter. When 0.13mm was removed from the surface of a chamber-cooled specimen (Fig. 5), the value of B_r increased (probably due to the removal of a layer of samarium oxides(s), cobalt oxides(s) and cobalt metal). Although B_r remained constant after the initial removal of material, the squareness, H_k, of the intrinsic curve steadily declined as material was
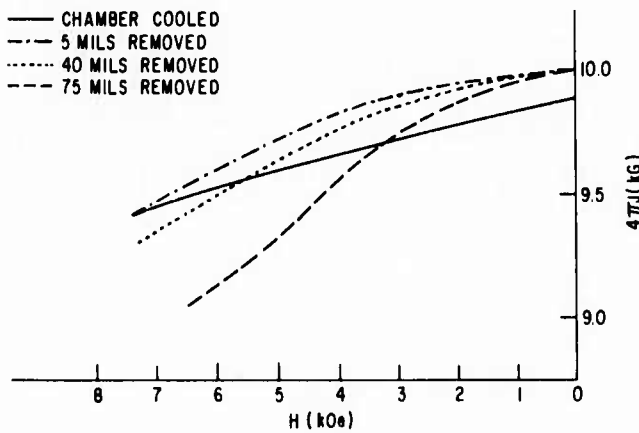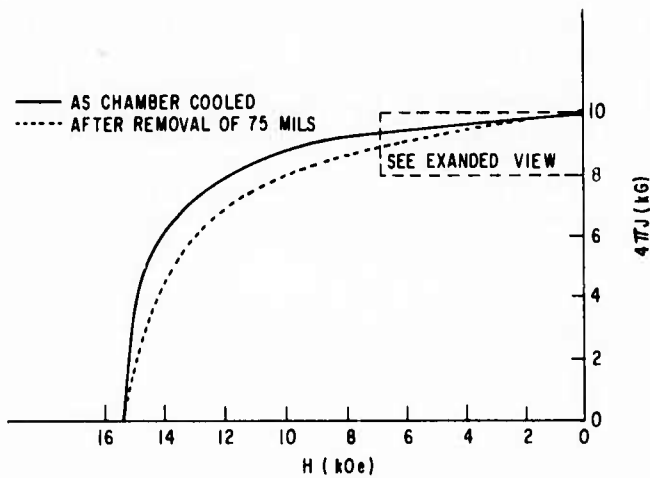
Fig. 5 Magnetic properties of chamber-cooled
sample after removal of varying amounts of ma-
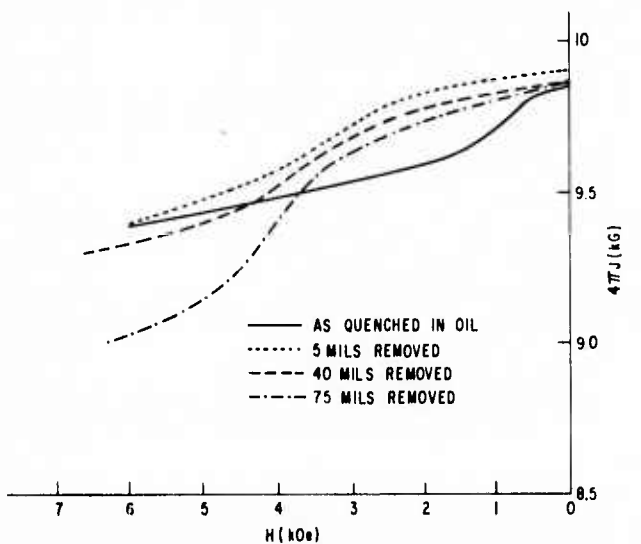terial from the sample rod radius.

Fig. 6 Magnetic properties of oil quenched sample
after removal of varying amounts of material from
the sample rod radius.

Fig. 7 Sample A showing intergranular fracture.
500X

removed from the surface. H_{ci} values for these
ground samples remained essentially constant within
experimental error. Similarly, the H_k value of an
oil-quenched sample (Fig. 6) decreased as material
was removed. It might be expected that the slight
dip in the demagnetization curve was a surface effect
due to a surface chemical inhomogeneity. However,
the kink for the oil-quenched sample remained even
after removal of 1.87 mm from the surface. There-
fore, the dip in the observed $4\pi J$ curve for the above
ground specimen, although not fully understood at
this time, is clearly not a surface effect. Metal-
lography examination of this sample failed to detect
an annular ring of reversed domain material as ob-
served in sample D.

During the preparation of the samples for metal-
lographic observation, sample A (water quenched)
crumbled while being cut. Other samples quenched
from fluids having lower thermal conductivities did
not break during this preparation. When the naturally
occurring fracture of sample A was examined under
a scanning electron microscope, the fracture was
observed to be intergranular (Fig. 7). Subsequently,
other samples including A were purposely fractured
and again examined by scanning electron microscopy.
The resultant surfaces (Fig. 8) indicated both inter-
and intragranular fractures. Accordingly, exami-
nation of the intergranularly cracked sample A would
indicate that the cooling rate is too severe causing
highly stressed regions.

Fig. 8 Sample B showing intergranular and intra-
granular fracture. 500X

SUMMARY

Our work shows that good magnetic character-
istics can be obtained for liquid phase sintered Co_5Sm
material by fluid quenching from $900°C$. The cooling
rate from $900°C$ to room temperature appears to be
critical in optimizing H_{ci} and obtaining maximum
squareness, H_k, of the second quadrant demagne-
tization curve. The data imply that there may be a
quenching rate superior to oil quenching lying be-
tween those obtained for oil and chamber cooling.

In general, too slow a cooling rate reduces H_{ci}
and squareness, H_k (possibly either due to precipi-
tation or eutectoid decomposition). Recent evidence
indicates that around $700°C$, Co_5Sm may decompose
into $Co_{17}Sm_2$ and Co_7Sm_2, thereby producing nuclei
for easy magnetization reversal.[8-10] Too fast a
cooling rate also reduces these values as is evident
by our water and glycerine quench results. The
deterioration mechanism is less understood for fast
cooling but may be due to internal stresses or mag-
netostrictive forces.

Fractography of water quenched samples indicates
highly strained regions causing breakage along grain
boundaries. All samples artifically fractured exhib-
ited both inter- and intragranular breakage.

Indications are that the entire quenching tech-
nique including the fluid used and possibly even the
starting quench temperature may have to be altered
as the Co_5Sm magnet samples vary in size and
shape. Thus Co_5Sm magnets may behave in a manner
very similar to some of the alnicos, resulting in the
need to accept property trade-offs with very large
sizes and shapes.

All fluid-quenched samples showed some slight
degree of kinking in the demagnetization curve.
Samples from some lots of powder, however, ex-
hibited severe kinks in the demagnetization curve.
Samples possessing these severely kinked character-
istics showed annular rings on reverse domains ex-
tending to a depth of $\approx300\mu$. X-ray lattice parameter
studies indicate that there is a possibility that these
samples may be deficient in Sm resulting in a hypo-
stoichiometric alloy. No severe kinks were obtained
in samarium-rich compositions.

ACKNOWLEDGMENTS

REFERENCES

1. M. G. Benz and D. L. Martin, "Cobalt-Misch-
   metal-Samarium Permanent Magnet Alloys;
   Process and Properties," J. Appl. Phys. 42,
   2786 (June 1971).

2. D. L. Martin and M. G. Benz, "Magnetization
   Changes for Cobalt-Rare Earth Permanent
   Magnet Alloys When Heated Up To $650°C$,"
   IEEE Trans. Magn. (March 1971).

3. K. Bachmann and A. Menth, "Magnetic Phase
   Analysis of $RECo_5$ Permanent Magnetic
   Materials," 18th Ann. Conf. on Magnetism and
   Magnetic Materials, Denver, Colo. (1972).

4. F. G. Jones, H. E. Lehman, and J. G. Smeggil,
   "Quenching Experiments on Cobalt-Samarium
   Magnets," IEEE Trans. (Sept. 1972).

5. Handbook of Chemistry and Physics, 41st ed.,
   Chemical Rubber Publishing Co , Cleveland,
   Ohio (1960), p. 2438.

6. D. L. Martin, M. G. Benz, and A. C. Rockwood,
   "Cobalt-Samarium Permanent Magnet Alloys;
   Variation of Lattice Parameters with Composition
   and Temperature," 18th Ann. Conf. on Magne-
   tism and magnetic Materials, Denver, Colo. (1972).

7. M. G. Benz and D. L. Martin, "Mechanisms of
   Sintering in Cobalt Rare Earth Permanent Mag-
   net Alloys," J. Appl. Phys. 43, 3165-3170
   (July 1971).

8. S. Foner, E. J. McNiff, Jr., D. L. Martin, and
    M. G. Benz, "Magnetic Properties of Cobalt-
    Samarium with a 24 M. G. O. Energy Product,"
    General Electric TIS Report 72CRD073
    (March 1972).

9. K. H. J. Buschow, J. Less-Common Metals 29,
    283 (1972).

10. J. D. Livingston, "Present Understanding of
    Coercivity in Cobalt-Rare Earths," 18th Ann.
    Conf. on Magnetism and Magnetic Materials,
    Denver, Colo. (1972).

72CRD073

S. Foner, E.J. McNiff, Jr., D.L. Martin, and M.G. Benz

MAGNETIC PROPERTIES OF COBALT-SAMARIUM
WITH A 24 MGOe ENERGY PRODUCT

94<

GENERAL ⊛ ELECTRIC

General Electric Company
Corporate Research and Development
Schenectady, New York

TECHNICAL INFORMATION SERIES

AUTHOR Foner, S., * McNiff, EJ, Jr, * Martin, DL, and Benz, MG	NO 72CRD073
	DATE March 1972
TITLE Magnetic Properties of Cobalt-Samarium with a 24 MGOe Energy Product	GE CLASS 1
	NO. PAGES 4

| ORIGINATING COMPONENT Metallurgy and Ceramics Laboratory | CORPORATE RESEARCH AND DEVELOPMENT SCHENECTADY, N.Y. |

SUMMARY The magnetic moment and hysteresis properties of a high-density, nearly completely oriented, Co_5Sm magnet alloy have been measured from 300° to 4.2°K and in applied fields up to 140 kOe. A saturation moment per gram of 98 G-cm^3/g is measured at 300°K and shows a slight increase as temperature is decreased. After adjustment for voids and oxide the saturation moment per gram of the Co-Sm alloy is 102 G-cm^3/g, or equivalent to 11,000 gauss for the saturation magnetization, $4\pi J_s$. An energy product of approximately 24 MGOe is attained at 300°K.

*Francis Bitter National Magnet Lab.,
MIT, Cambridge, Mass.

SUBJECT: permanent magnets

KEY WORDS: permanent magnets, magnetic measurements

INFORMATION PREPARED FOR _____

MAGNETIC PROPERTIES OF COBALT-SAMARIUM WITH A 24 MGOe ENERGY-PRODUCT

S. Foner,* E.J. McNiff, Jr.,* D. L. Martin,† and M. G. Benz†

High energy-product permanent magnet materials have been developed with rare earth-cobalt alloys (Refs. 1-6), particularly with Sm-Co. In this report we describe properties of a Sm-Co alloy with an energy-product of 24 MGOe, the largest reported to date for this material. By optimizing parameters of fabrication, nearly complete alignment of the magnetic particles was achieved with a relative density which is 95% of the theoretical maximum (calculated from x-ray data). Because of the exceptional alignment, saturation of the magnetic moment could be achieved in this highly anisotropic material at an applied field well below the maximum of 140 kOe used for these experiments. Thus, in addition to the large energy-product, we observe a saturation moment ~10% or more above that reported in earlier literature. [7-13]

The sample was prepared by a liquid-phase sintering process which has been used successfully to make high-energy cobalt-samarium permanent magnets. [4-5] A Co_5Sm base metal powder and a 60 wt % Sm - 40 wt % Co additive powder were blended to a nominal composition of 36 wt % Sm. The blended powder was made into a test bar by aligning the powder in a rubber tube in a 60 kOe magnetic field. The aligned powder was compressed slightly while still in the field to stabilize the particle alignment. Subsequently the bar was hydropressed at 200 kpsi to a relative density of about 80%. The bar was ground into a cylinder, and sintered in an argon atmosphere at 1135°C for 1 hour.

The sample was given a post-sintering treatment of 20 minutes at 1100°C, slow cooled to 850°C, held for 1 hour at that temperature, and cooled rapidly to room temperature.

The sample had a relative density of 94.6% of 8.6 g/cm³, and was 0.256 inch (0.65 cm) diameter by 1.06 inches (2.69 cm) long. Magnetic measurements at fields up to 60 kOe were made on the sintered bar prior to cutting it into shorter pieces for x-ray lattice parameter measurements, oxygen determination, and additional magnetic measurements at higher fields.

During the processing the oxygen content of the alloy increased. In the sintered sample the oxygen was determined by vacuum fusion analysis to be 0.46 ±0.2 wt %. Assuming all the oxygen reacts with some of the Sm to form Sm_2O_3, the composition of the magnet material, based on chemical analyses, was 63.7 wt % Co, 32.6 wt % Sm, and 3.3 wt % Sm_2O_3. The sample also contains 0.26 wt % Ni and 0.07 wt % Al. The Sm content of the metallic phase is calculated to be 16.7 at. %.

The hexagonal lattice constants for the Co_5Sm phase measured on powder from the sintered bar were: a = 5.002 ± 0.002Å, c = 3.963Å ± 0.001Å, and cell volume = 85.94(Å)³. The calculated density of the Co_5Sm phase was 8.60 g/cm³.

Magnetic measurements were made on the heat-treated bar by ballistic methods[14] in a superconducting solenoid with a peak field of 60 kOe, and on a disk cut from the center of the same bar, in water-cooled Bitter solenoids with a maximum field of 140 kOe.

Since the sample contains an appreciable volume of voids and Sm_2O_3, we report the saturation value for the ideal magnetic Co-Sm alloy as well as the measured values for the sample. The saturation moment per unit mass of the alloy, σ_s (alloy), is related to the saturation moment per unit mass of the sample, σ_s, by the following:

$$\sigma_s(\text{alloy}) = \sigma_s/X_w, \tag{1}$$

where X_w is the weight fraction of the alloy in the sample (0.978 for the sample used in this study). Similarly, the magnetization or magnetic moment per unit volume of the alloy, $4\pi J_s$(alloy) is related to that the sample, $4\pi J_s$, by the relation:

$$4\pi J_s(\text{alloy}) = 4\pi J_s/X_v \tag{2}$$

where X_v is the volume fraction of the alloy in the sample (0.929 for sample studied). The volume fraction is related to the weight fraction by the relation:

$$X_v = \frac{\rho(\text{sample})}{\rho(\text{alloy})} X_w. \tag{3}$$

The magnetic moment measurements on the thin disk were made with a low-frequency vibrating sample magnetometer. [15] The field was furnished by water-cooled Bitter solenoids with a maximum
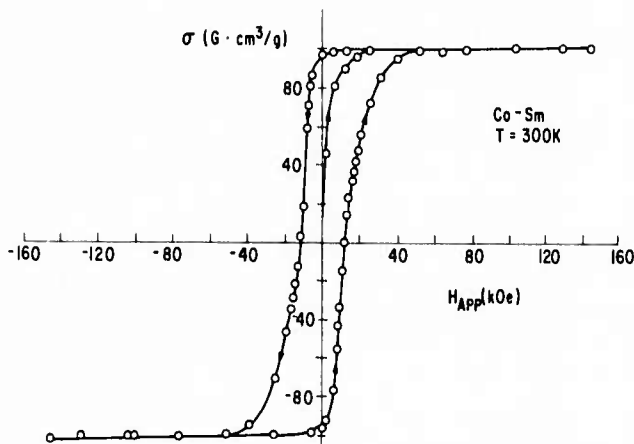
Fig. 1 Magnetic moment, σ, vs applied field H_{APP}, for a small disk of Co-Sm magnet. The high degree of alignment is evidenced by saturation above 80 kOe.

TABLE I

Properties of a 63.7 Wt % Co, 32.6 Wt % Sm, 3.3 Wt % Sm_2O_3 Magnet Material as a Function of Temperature

Temperature (°K)	300	300	77	4.2
Magnetizing field (kOe)	60	100	100	100
Sample length/diameter	4.12	0.635	0.635	0.635
Demagnetizing factor	~0.027[a]	~0.4[b]	~0.4[b]	~0.4[b]
Density ρ (sample)(g/cm^3)	8.17	8.17	8.17	8.17
Density ρ (alloy)(g/cm^3)	8.6	8.6	8.6	8.6
Weight fraction (alloy), X_w	0.967	0.967	0.967	0.967
Volume fraction (alloy), X_v	0.918	0.918	0.918	0.918
σ_s (G-cm^3/g)	97.4	98.4	102.5	103.0
σ_s (alloy)(G-cm^3/g)	100.7	101.8	106.0	106.5
$4\pi J_s$ (kG)	10.0	10.1	10.5	10.6
$4\pi J_s$ (alloy)(kG)	10.9	11.0	11.4	11.5
σ_r (G-cm^3/g)	95	95.5	101	102
$4\pi J_r$ (kG)	9.7	9.8	10.4	10.5
H_c (kOe)	-9.5	-8.7	-10.3	-10.1
H_k (kOe)	-10.0	-8.5±1	-14.7±1	-16.3±1
H_{ci} (kOe)	-13.2	-12	-19.0	-20.6
$(BH)_{max}$ (MGOe)	23.4	24.0±0.5	28±1	27±1
Alignment factor A	0.97	0.97	0.98	0.99

Notes for Table I:

(a) - Ballastic demagnetization factor, N_b (Ref. 16).

(b) - Magnetometric demagnetization factor, $\dot{N}_m$ (Ref. 16).

σ_s - Saturation moment per unit mass of sample. $\sigma_s \simeq \sigma$ measured at H_m.

σ_s(alloy) - Saturation moment per unit mass of the Co-Sm alloy in the sample σ_s(alloy) = σ_s/X_w.

$4\pi J_s$ - Saturation moment per unit of sample volume $4\pi J_s = 4\pi\sigma_s\rho$(sample).

$4\pi J_s$(alloy) - Saturation moment per unit of alloy volume in the sample.
$$4\pi J_s(\text{alloy}) = 4\pi\sigma(\text{alloy})\rho(\text{alloy}) = 4\pi J_s/X_v.$$

σ_r - Remanent moment per unit of sample mass at H = 0.

$4\pi J_r$ - Magnetic moment per unit of sample volume at H = 0. $4\pi J_r = 4\pi\sigma_r\rho$(sample)

A - Alignment factor = $\sigma_r/\sigma_s = 4\pi J_r/4\pi J_s$.

H_k - Demagnetizing field for which $4\pi J = (0.9)4\pi J_r$.

H_c - Demagnetizing field for B = 0.

H_{ci} - Demagnetizing field for $4\pi J = 0$.

field of 140 kOe. The sample and detection coils were surrounded by suitable Dewars in order to maintain constant temperatures and measurements were made at 300°, 77°, and 4.2°K. The accuracy of the magnetic moment measurements is well within 2% and the applied field is known to at least 1%.

The magnetic moment per unit mass σ vs the applied field H_{APP} is shown in Fig. 1 for the Co-Sm alloy at room temperature. (We will present measured quantities throughout the text and tabulate derived quantities when indicated.) The sample is a right circular cylinder with its axis parallel to H_{APP}. The dimensions of the sample were 0.192 inch in diameter and 0.122 inch in length. Several features are noteworthy: (1) saturation is achieved for an applied field of about 80 kOe; and (2) above this field, σ is almost constant--the susceptibility $\Delta\sigma/\Delta H_{APP}$ is less than 2×10^{-5} G-cm^3/g-Oe above saturation for $4.2 \le T \le 300$ K. Assuming that this small effect may be due to misaligned crystallites we estimate that less than 2% of the material is misaligned (assuming an anisotropy field of ~ 250 kOe); (3) the value of $\sigma = \sigma_s$ at 300 K is 10% larger than that reported recently for single-crystal Co$_5$Sm;[12] and also higher than reported on aligned powder or sintered samples. [5, 7-13]

The general features of Fig. 1 are maintained as the temperature is reduced; the area of the hysteresis loop increases somewhat and the value of σ_s increases slightly. Several properties of this Co$_5$Sm material are tabulated in Table I. The values of σ_s at each temperature are larger than reported earlier[8, 12] and the temperature dependence of σ_s is somewhat smaller than reported earlier. [8, 12] The reasons for these differences are not clear. However, one possible source of error in the earlier data may be that the measurements were made at fields below that needed for saturation. A second possibility may involve differences in alloy composition or the presence of substantial amounts of oxide.

To correct the data in Fig. 1 to the conventional B-H plots we require a measure of the demagnetization or depolarizing factor as well as the actual density of the material. Measurements of the density yields $\rho = 8.17$ g/cm^3; close to the x-ray density ρ(alloy) $= 8.6$ g/cm^3. Estimates of the depolarizing factor were obtained from Joseph's tabulation[16] from which we obtain $N_m = 0.4$. Using these data, the derived quantities involving the magnetization (per unit volume) were calculated. These quantities are tabulated in Table I along with the maximum energy-products obtained from B versus H plots. The results for 77° and 4.2°K are included for comparison. It is apparent that a small variation in the (BH)$_{max}$ occurs as a function of temperature. Because N_m is not exactly known for our geometry, the values of N_m were varied from 0.35 to 0.45, but essentially no change in the calculated (BH)$_{max}$ was observed.

Other quantities in Table I include A (the alignment factor $= \sigma_r/\sigma_s$), the alloy saturation moment,
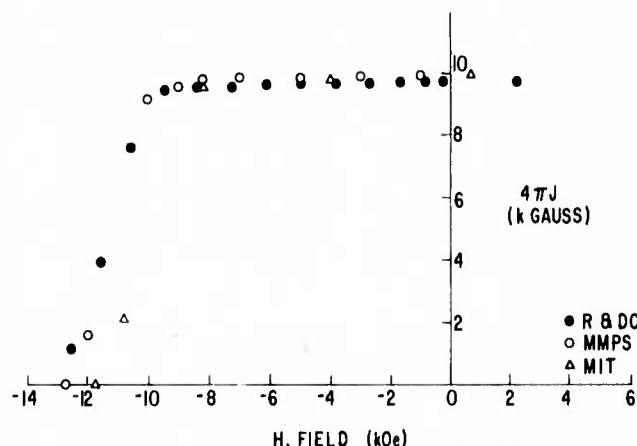

Fig. 2 Comparison of test results obtained on a long sintered bar as measured at the GE Magnetic Materials Product Section, Edmore, Mich., and CR&D with results measured on a disk at MIT.

and H_k which gives a measure of the shape of the hysteresis loop. Data for the long sintered bar at 300 K are also listed for comparison with the thin disk results, and plotted in Fig. 2 together with test results measured on the sintered bar at the General Electric Magnetic Materials Product Section, Edmore, Mich. The agreement is good considering that the bar was only magnetized at 60 kOe. The differences in the coercive force measurements are within experimental error.

The appreciable increase in (BH)$_{max}$ over previous Co$_5$Sm permanent magnet materials[1-5] is clearly due to the very nearly complete alignment of the compacted small magnetic particles together with a high relative density. This increase also is reflected in the larger value of σ_s(alloy) which is a basic property of the compound. Based on these results it is expected that appreciable gains in (BH)$_{max}$ and σ_s will be realized when other Co rare-earth permanent magnet materials are fabricated under optimum conditions for complete alignment. Such experiments are now in progress.

ACKNOWLEDGMENTS

REFERENCES

1. K. H. J. Buschow, W. Luiten, P. A. Naastepad, and F. F. Westendorp, Philips Tech. Rev. 29, 336 (1968).

2. K. H. J. Buschow, W. Luiten, and F. F. Westendorp, J. Appl. Phys. 40, 1309 (1969).

3. D. K. Das, IEEE Trans. Magnetics MAG-5, 214 (1969).

4. M. G. Benz and D. L. Martin, Appl. Phys. Letters 17, 176 (1970).

5. D. L. Martin and M. G. Benz, Cobalt, No. 50, 11 (1971).

6. J. Tsui and K. Strnat, Appl. Phys. Letters 18, 107 (1971).

7. K. Nassau, L. V. Cherry, and W. E. Wallace, J. Phys. Chem. Solids 16, 123 (1960).

8. E. A. Nesbitt, H. J. Williams, J. H. Wernick, and R. C. Sherwood, J. Appl. Phys. 32, 342S (1961).

9. K. Strnat, G. Hoffer, J. Olson, W. Ostertag, and J. J. Becker, J. Appl. Phys. 38, 1001 (1967).

10. W. A. J. J. Velge and K. H. J. Buschow, J. Appl. Phys. 39, 1717 (1968); also Z. angew. Phys. 26, 157 (1969).

11. K. H. J. Buschow, W. Luiten, and F. F. Westendorp, J. Appl. Phys. 40, 1309 (1969).

12. E. Tatsumoto, T. Okamoto, H. Fujii, and C. Inoue, J. Physique 32, C1-550 (1971).

13. H. Umebayashi and Y. Fujimura, Japan. J. Appl. Phys. 10, 1585 (1971).

14. M. G. Benz and D. L. Martin, IEEE Trans. Magnetics MAG-7, 285 (1971).

15. S. Foner and E. J. McNiff, Jr., Rev. Sci. Instr. 39, 171 (1968).

16. R. I. Joseph, J. Appl. Phys. 37, 4639 (1966).

TECHNICAL INFORMATION SERIES

AUTHOR Livingston, JD	SUBJECT permanent magnet materials	NO 72CRD152
		DATE May 1972
TITLE Magnetic Domains in $Co_{17}R_2$, $(Co, Fe)_{17}R_2$, and Co_7R_2 Compounds		GE CLASS 1
		NO. PAGES 7
ORIGINATING COMPONENT Metallurgy and Ceramics Laboratory		CORPORATE RESEARCH AND DEVELOPMENT SCHENECTADY, N.Y.

SUMMARY

We have examined magnetic domain structures in several $Co_{17}R_2$, $(Co, Fe)_{17}R_2$, and Co_7R_2 phases using polarized light. Characteristic easy-axis domain patterns were seen in $Co_{17}Sm_2$, $Co_{17}Gd_2$, and $(Co, Fe)_{17}R_2$, and Co_7R_2 phases. Domains were not seen in $Co_{17}Pr_2$, $Co_{17}Ce_2$, $Co_{17}Y_2$, and $Co_{17}Nd_2$, all of which are believed to have easy-plane rather than easy-axis magnetic symmetry.

KEY WORDS

permanent magnets, cobalt-rare earths

MAGNETIC DOMAINS IN $Co_{17}R_2$, $(Co, Fe)_{17}R_2$, AND Co_7R_2 COMPOUNDS

J. D. Livingston

INTRODUCTION

The excellent permanent magnet properties of Co_5R^* compounds[1-3] are based on a high, positive, uniaxial magnetocrystalline anisotropy. This "easy-axis" magnetic symmetry produces magnetic domain patterns[4-8] of a type well characterized by earlier work on other easy-axis materials.[9-12]

The Co-R alloy system contains $Co_{17}R_2$ and Co_7R_2 phases with crystal structures closely related to that of the Co_5R compounds.[13] The $Co_{17}R_2$ phases, of potential interest as permanent magnet materials, are generally of easy-plane, rather than easy-axis, magnetic symmetry. However, Ray and Strnat[14] have recently reported that partial substitution of iron for cobalt in some cases transforms the symmetry to easy-axis. The Co_7R_2 phases are not of direct interest as permanent magnet materials, but are of indirect interest because optimum Co_5R magnets are hyperstoichiometric and contain several percent of Co_7R_2.[3, 15]

We have studied magnetic symmetries in several $Co_{17}R_2$, $(Co, Fe)_{17}R_2$, and Co_7R_2 phases by means of magnetic domain observations.

EXPERIMENTAL

Compounds were arc-cast from high-purity materials and studied metallographically either in the as-cast condition or after annealing overnight about 100° to 200°C below their respective melting points. Domains were observed in polarized light on a Bausch and Lomb metallograph, using an elliptical compensator[16] to optimize the contrast.

RESULTS

As shown earlier by Becker,[1] an as-cast sample of $Co_{17}Sm_2$ contains classic easy-axis domain structures (Fig. 1). Magnetic domain walls in such materials lie nearly parallel to the magnetization direction. Therefore, in grains in which this easy-axis has a substantial component in the surface plane, the domain patterns are elongated in this direction. However, in grains with the easy-axis nearly normal to the surface, "rosette" patterns are seen, as in the grain at the right in Fig. 1. These patterns result from a surface refinement of the domain structure that occurs to reduce magnetostatic energy.[6, 9-12] Domain walls become corrugated in the surface region, domains are split by reverse "spike" domains, and the resulting rosette patterns

are sufficiently characteristic that their observation can be taken as evidence of easy-axis magnetic symmetry. For example, Fig. 2(a) shows domains in a casting of composition $(Co_{0.75} Fe_{0.25})_{17}Sm_2$. This confirms results of Ray and Strnat[14] that easy-axis symmetry is retained in this system.

In contrast, we were unable to detect any magnetic domain structures in as-cast or annealed samples of $Co_{17}Pr_2$, $Co_{17}Y_2$, or $Co_{17}Nd_2$. An as-cast sample of $Co_{17}Ce_2$ contained two phases and faint lamellar domains, but an annealed sample was single phase and showed no domains. These results are consistent with earlier results that these four compounds have easy-plane rather than easy-axis symmetry.[1, 2, 14] Presumably the magnetization in each domain can rotate freely in the easy plane and, to decrease magnetostatic energy, will lie parallel to the surface. The Kerr-effect contrast in Co-R compounds arises primarily from the component of magnetization normal to the surface, and thus domains are not seen in these easy-plane materials. Substitution of iron for cobalt in $Co_{17}Pr_2$, $Co_{17}Y_2$, and $Co_{17}Ce_2$ transforms the magnetic symmetry to easy-axis,[14] as confirmed by the domain patterns in Figs. 2(b), (c), and (d).

Mechanically polished surfaces of $Co_{17}Gd_2$ reveal a fine and complex domain structure (Fig. 3). This structure appears to be related to surface strain introduced by polishing, an effect well known in soft magnetic materials.[17] If a strain-free surface is prepared by electropolishing in phosphoric acid, a fine but very faint rosette domain pattern can be seen. (On $Co_{17}Sm_2$ and other compounds tested, domains on mechanically polished and electropolished surfaces appeared the same.) We conclude that $Co_{17}Gd_2$ is of easy-axis symmetry, but probably has a rather low crystal anisotropy. If 30 percent of the cobalt is replaced by iron, coarser easy-axis patterns of much stronger contrast are seen [Fig. 2(e)].

Prior to this work, no information was available on the magnetic symmetry of Co_7R_2 compounds. As seen in Fig. 4, easy-axis patterns are seen in annealed samples of Co_7Sm_2, Co_7Pr_2, Co_7Y_2, and Co_7Nd_2. Domains were similar in Co_7La_2, but optical contrast was very low. Patterns were also easy-axis in as-cast samples, but were more complex because grain structure was fine and complex.

An interesting special case is Co_7Gd_2. Because the Gd and Co moments are antiparallel, this compound has a very low net moment,[18] which leads us to expect very large domains.[9-12] The domain size was in fact found to be comparable to the grain size, and domains were most easily recognized by comparing the same area before and after moving the domains with a magnet (Fig. 5). Our
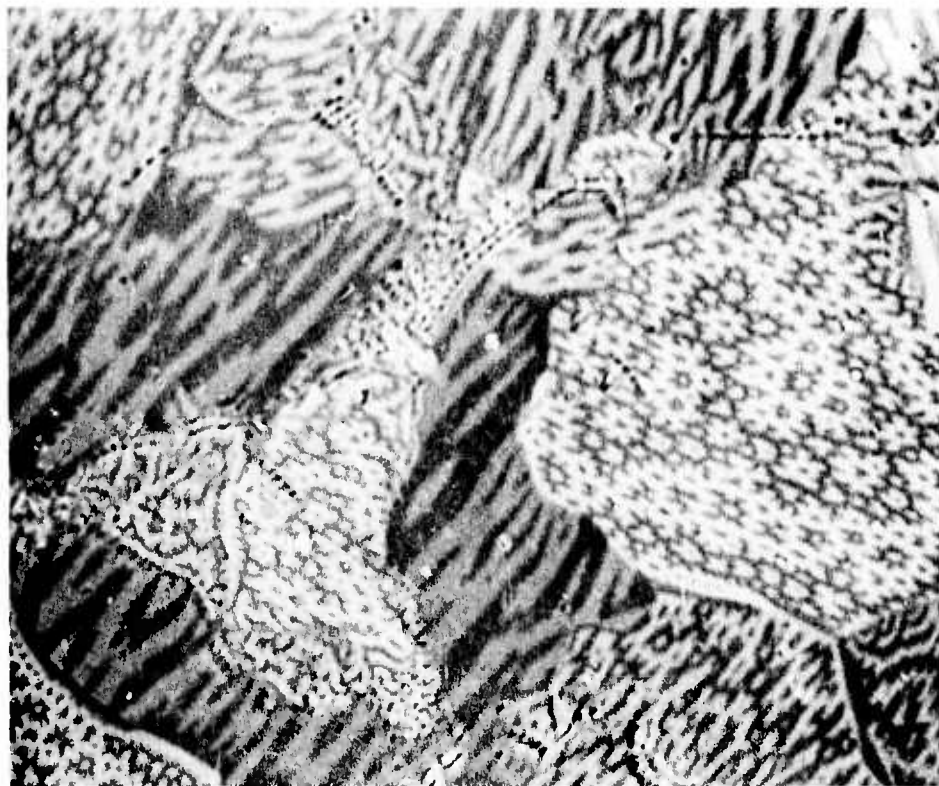
---

*R = rare earth, La, or Y.

Fig. 1 Magnetic domains in $Co_{17}Sm_2$. Rosette structure in grain at right is characteristic of easy-axis magnetic symmetry (photograph from J. J. Becker). 530X
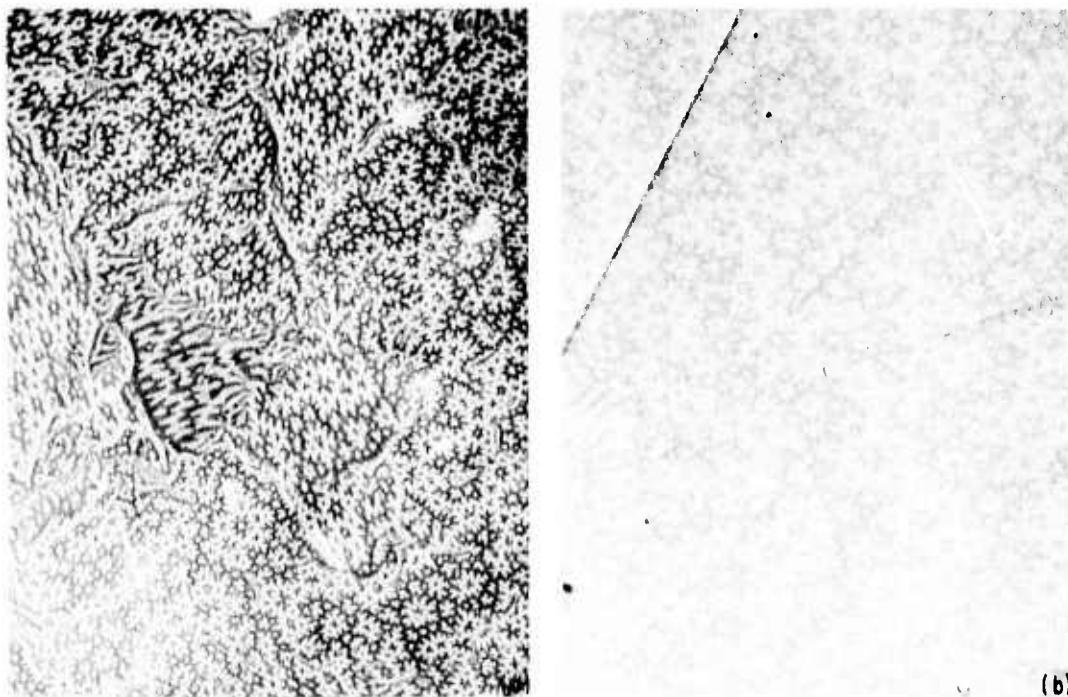

(b)

Fig. 2 Easy-axis domain patterns in (a) $(Co_{0.75}Fe_{0.25})_{17}Sm_2$. (b) $(Co_{0.6}Fe_{0.4})_{17}Pr_2$. 550X
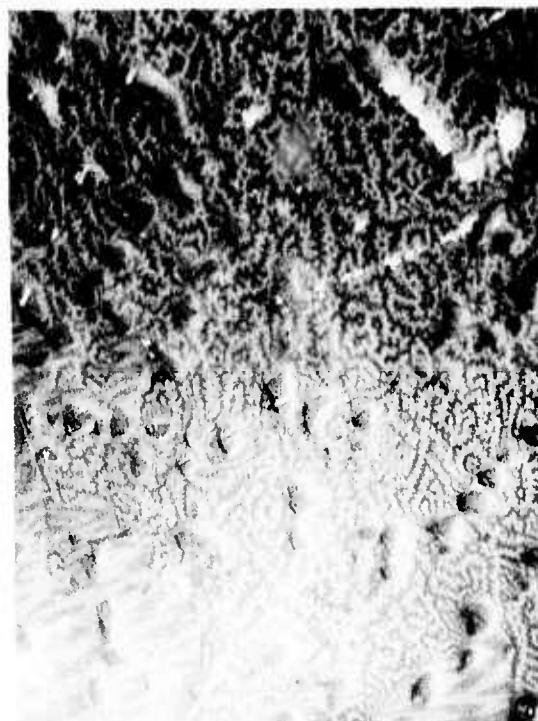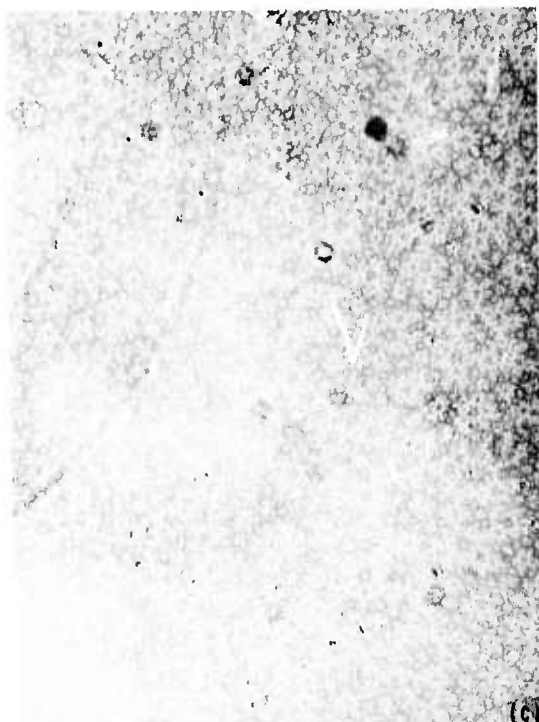
Fig. 2 (Contd) (c) $(Co_{0.7}Fe_{0.3})_{17}Y_2$, (d) $(Co_{0.75}Fe_{0.25})_{17}Ce_2$. 570X

Fig. 2 (Concluded) (e) $(Co_{0.7}Fe_{0.3})Gd_2$. 620X

observations on this sample were consistent with earlier observations on easy-axis materials with low moment.[9-12]

SUMMARY AND DISCUSSION

Characteristic easy-axis domain patterns were seen in $Co_{17}Sm_2$, $Co_{17}Gd_2$, and several $(Co, Fe)_{17}R_2$ and Co_7R_2 compounds. Domains were not seen in $Co_{17}Pr_2$, $Co_{17}Y_2$, $Co_{17}Nd_2$, or $Co_{17}Ce_2$.

In a recent study of domain widths and domain-wall energies in Co_5R compounds,[19] it was suggested that the wavelength of surface domain corrugations on bulk samples may be a rough measure of the fineness of grain size necessary to produce good coercive forces in sintered magnets. For example, this dimension was about 6μ in Co_5Sm, 3μ in Co_5Pr, and 30μ in Co_5Gd. Applying this criterion to the domain patterns reported above, we estimate this dimension to be $1u$ to 2μ in $Co_{17}Gd_2$ and the various $(Co, Fe)_{17}R_2$ compounds, 2μ to 3μ for $Co_{17}Sm_2$ and most of the Co_7R_2 compounds, $5u$ for Co_7Sm_2, and very large but undetermined for Co_7Gd_2. In combination with saturation magnetization values, these dimensions may also be used to estimate domain-wall energies.[19]

ACKNOWLEDGMENTS

Fig. 3 Domain patterns in mechanically polished $Co_{17}Gd_2$. These maze patterns are believed to be caused by surface strains. 690X
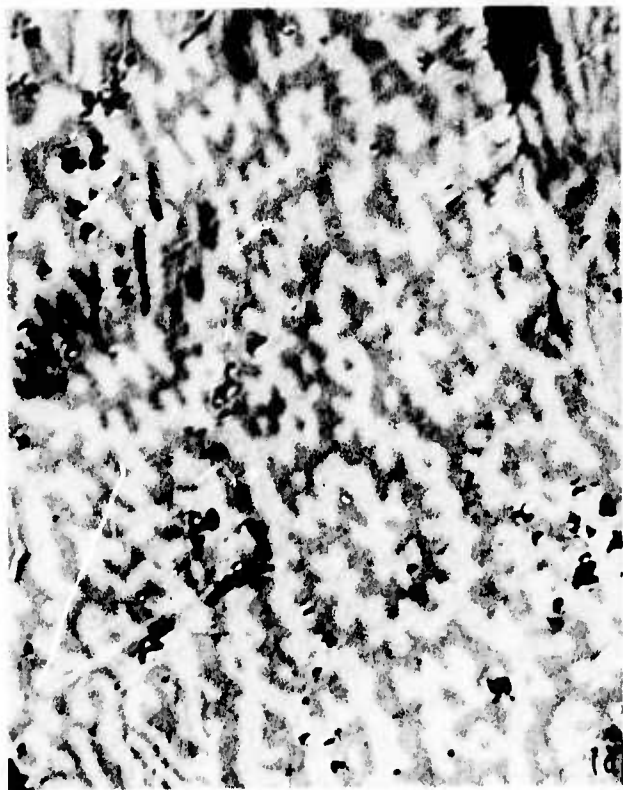
Fig. 4 Easy-axis domain patterns in (a) Co_7Sm_2, (b) Co_7Pr_2. 660X
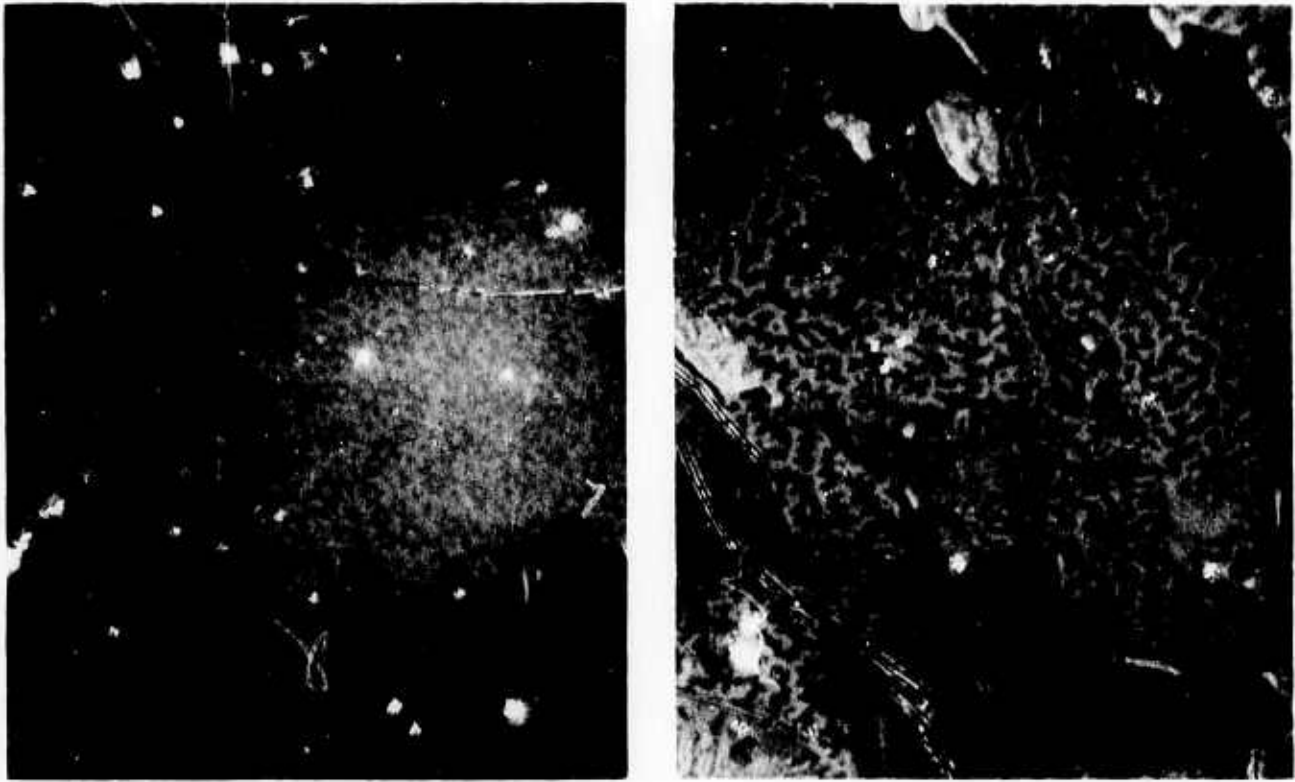
Fig. 4 (Concluded) Easy-axis domain patterns in (c) Co_7Y_2, and (d) Co_7Nd_2. 670X

Fig. 5 Magnetic domains in Co_7Gd_2 (a) before and (b) after touching sample with a magnet. Note downward motion of domain wall at right center and disappearance of dark domain at lower left. Domains are large because of low magnetic moment.

469X

REFERENCES

1. J. J. Becker, J. Appl. Phys. **41**, 1055 (1970).

2. K. J. Strnat and A. E. Ray, Z. Metallk. **61**, 461 (1970); K. Strnat, IEEE Trans. Mag. **6**, 182 (1970).

3. D. L. Martin and M. G. Benz, Proc. 1971 Conf. on Magnetism and Magnetic Materials, Am. Inst. Physics Conf. Proc. No. 5, p. 970 (1972).

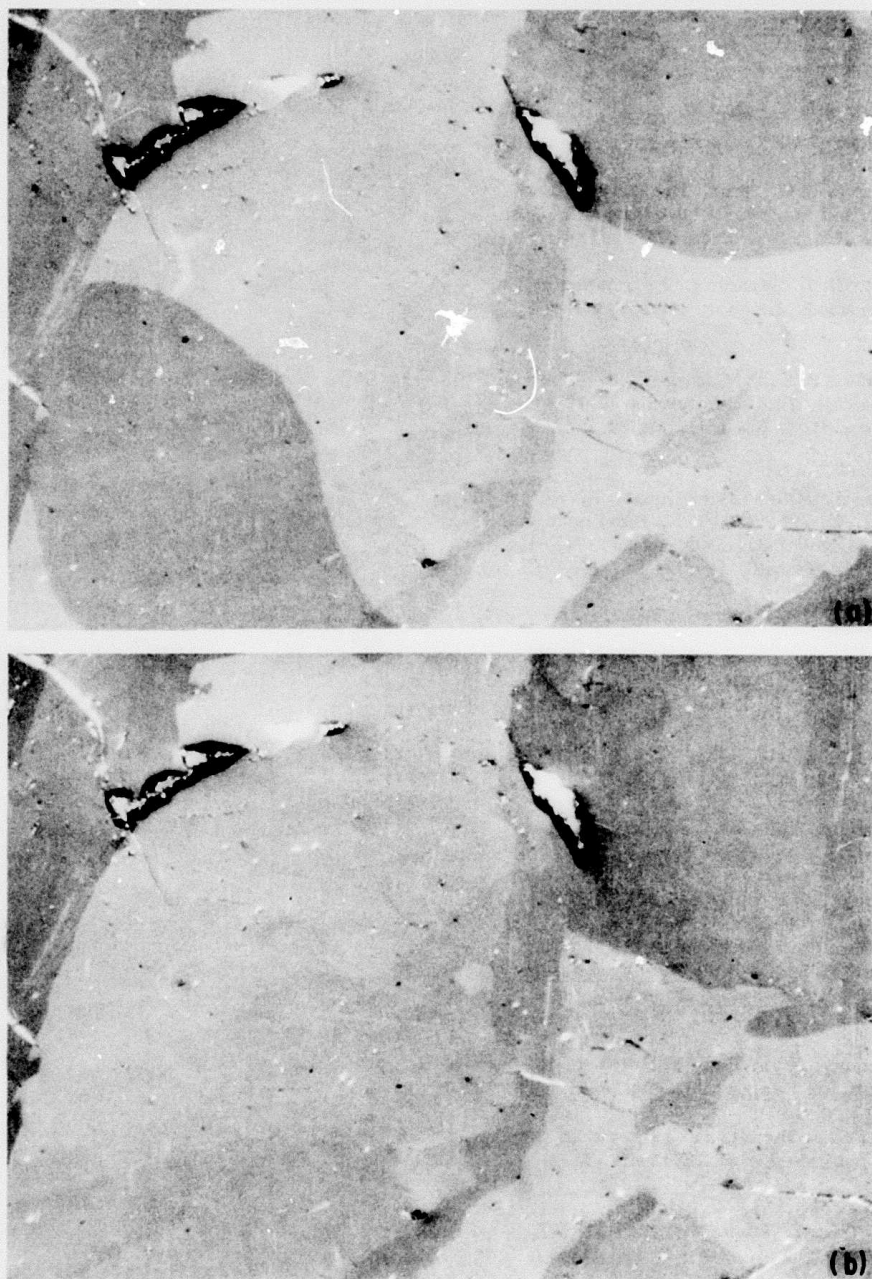4. E. A. Nesbitt, H. J. Williams, J. H. Wernick, and R. C. Sherwood, J. Appl. Phys. **33**. 1674 (1962).

5. R. A. McCurrie and G. P. Carswell, J. Mater. Sci. **5**, 825 (1970); R. A. McCurrie, G. P. Carswell, and J. B. O'Neill, J. Mater. Sci. **6**, 164 (1970).

6. K. Bachmann, A. Bischofberger, and F. Hofer, J. Mater. Sci. **6**, 169 (1971); K. Bachmann and F. Hofer, Z. Angew. Physik **32**, 41 (1971); K. Bachmann, IEEE Trans. Mag. **7**, 647 (1971).

7. R. G. Wells and D. V. Ratnam, IEEE Trans. Mag. **7**, 651 (1971).

8. F. F. Westendorp, J. Appl. Phys. **42**, 5727 (1971).

9. J. Kaczer, IEEE Trans. Mag. **6**, 442 (1970); Soviet Phys. -JETP **19**, 1204 (1964).

10. M. Rosenberg, C. Tanasoiu, and V. Florescu, J. Appl. Phys. **37**, 3826 (1966).

11. A. Hubert, Phys. Stat. Sol. **24**, 669 (1967).

12. D. J. Craik, Contemp. Phys. **11**, 65 (1970); D. J. Craik and R. S. Tebble, Ferromagnetism and Ferromagnetic Domains, John Wiley and Sons, Inc., New York (1965).

13. K. H. J. Buschow, Phys. Stat. Sol. (a) **7**, 199 (1971); Philips Res. Repts. **26**, 49 (1971).

14. A. E. Ray and K. J. Strnat, 1972 Intermag. Conf., Kyoto, to be published in IEEE Trans. Mag. **8** (1972).

15. R. E. Cech, J. Appl. Phys. **41**, 5247 (1970); D. K. Das, IEEE Trans. Mag. **7**, 432 (1971).

16. A. F. Turner, J. R. Benford, and W. J. McLean, Economic Geol. **40**, 18 (1945).

17. S. Chikazumi and K. Suzuki, J. Phys. Soc. Japan **10**, 523 (1955).

18. R. Lemaire, Cobalt **33**, 201 (1966).

19. J. D. Livingston, submitted to J. Appl. Phys.

109<

GENERAL ✦ ELECTRIC

General Electric Company
Corporate Research and Development
Schenectady, New York

TECHNICAL INFORMATION SERIES

AUTHOR Livingston, J D McConnell, MD	SUBJECT permanent magnet materials	NO: 72CRD166
		DATE May 1972
TITLE Domain-Wall Energy in Cobalt-Rare Earth Compounds		GE CLASS 1
		NO. PAGES 11

ORIGINATING COMPONENT Metallurgy and Ceramics Laboratory, Materials Science and Engineering — CORPORATE RESEARCH AND DEVELOPMENT SCHENECTADY, N.Y.

SUMMARY We have used polarized light metallography to study magnetic domain configurations in Co_5Sm, Co_5Y, Co_5Ce, and Co_5Pr as a function of crystal thickness. From measurements of equilibrium domain widths on thin crystals, we estimate the domain wall energy in these compounds to be 85, 35, 25, and 40 $ergs/cm^2$, respectively. From surface domain observations on bulk crystals, we have also made crude estimates of wall energy for Co_5Nd, Co_5La, and Co_5Gd.

From these wall energies and published anisotropy constants, we have calculated exchange constants, domain-wall thicknesses, and critical single-domain particle sizes. We find this critical particle size to be larger for Co_5Sm and Co_5Gd than for the other compounds, and suggest that this may partly explain why high coercive forces are more easily attained in powders of these two compounds.

KEY WORDS

permanent magnets, coercive force, magnetic domain, cobalt-rare earths

INFORMATION PREPARED FOR _____

DOMAIN-WALL ENERGY IN COBALT-RARE EARTH COMPOUNDS

J. D. Livingston and M. D. McConnell

INTRODUCTION

The cobalt-rare earth compounds, especially Co_5Sm, provide the basis for a new class of permanent magnet materials with coercive forces and energy products significantly higher than those of previous magnet materials. [1-3] These compounds possess a large magnetocrystalline anisotropy of uniaxial symmetry. Coercive force appears to be controlled by the nucleation and pinning of magnetic domain walls. [1, 4]

Such mechanisms depend on the energy per unit area of a domain wall, and observations by Westendorp[5] indicate that this quantity may be larger for Co_5Sm than for other Co_5R compounds (R = rare earth, La, or Y). He suggested that this may explain why high coercive forces are easily attained in Co_5Sm, but not in most of the other compounds.

There has been considerable study of the domain structures of uniaxial ferromagnetic materials. [6-8] Of particular interest are the domain structures in thin plates in which the magnetic easy axis is normal to the face of the plate. Theory for these structures is well developed, and allows determination of domain-wall energies by measurements of domain widths. Although several observations of domain patterns in Co_5R compounds have been reported in the literature (Ref. 5, 9-12), no domain-wall energy measurements have been made. We report below the results of such measurements.

EXPERIMENTAL

The compounds were prepared by arc-casting from high-purity materials and annealed for 24 hours at 1100°C (or, for Co_5La, at 1000°C) for homogenization and grain growth.

Samples were initially mounted in epoxy resin and vacuum impregnated. After curing, the mounted sample was ground and polished on one face. This face was examined under polarized light to locate a suitable grain of satisfactory size and orientation. We used a Bausch and Lomb metallograph with an elliptical compensator to optimize the optical contrast. [13] After mapping the location of the grain, the polished face was cemented with clear epoxy to a cleaned glass petrographic slide. The mounted sample was placed in a vacuum chuck and most of the sample was removed with a precision saw. With a special petrographic slide holder, the sample was ground to a thickness of about 75μ on a rotating lap. Sample thickness was monitored by micrometer, allowing for the thickness of the glass slide and epoxy cement.

Micrographs were then taken in polarized light

of the original polished surface of the chosen grain. Thinning of the sample was continued by hand polishing on bond paper with 6μ diamond paste or, in the later stages, 3μ diamond paste. At suitable intervals the thickness was monitored and the grain photographed. Average width of magnetic domains was measured from micrographs at 500X magnification. When the sample was approximately 10μ thick, the sample and glass slide were mounted on edge in epoxy. They were ground until the grain was intercepted and an accurate measurement of the sample thickness could be made on the metallographic microscope. This allowed calibration of the thicknesses measured by micrometer.

OBSERVATIONS

The qualitative observations were consistent with earlier observations on Co_5R[5, 9-12] and other easy-axis materials. [6-8] In most grains, the easy-axis had a substantial component within the surface plane, and domain patterns were elongated in this direction. For our measurements, however, we were interested in grains with the easy-axis nearly normal to the surface, which are recognizable by characteristic patterns such as seen in Co_5Sm in Fig. 1(a).

To reduce magnetostatic energy, the simple maze domain structures that are present in the interior of the crystal are refined in the vicinity of the surface. This surface domain refinement has two distinct features: extreme corrugations and the introduction of reverse "spike" domains visible as small spots in Fig. 1(a). When the crystal is thinned sufficiently, such surface refinement can no longer occur, and the simple maze structure extends throughout the thickness. Thus, the domain patterns observed gradually simplify as thickness is reduced, as seen in Figs. 1(b) through (f). Qualitative observations for Co_5Y, Co_5Ce, and Co_5Pr are similar, as shown in Figs. 2 through 4.

To see how well the domain structures approach equilibrium, domains were occasionally removed by saturating the magnetization with a field of 20,000 Oe normal to the surface and then removing the field to allow re-nucleation of the domains. Domain patterns were photographed before and after this process, and examples of the changes produced are seen by comparing Figs. 1(c) and 1(d), 1(e) and 1(f), 2(e) and 2(f), and 3(c) and 3(d).

We also found characteristic easy-axis domain patterns in samples of Co_5Nd, Co_5La, and Co_5Gd (Fig. 5). The optical contrast was rather faint in Co_5Nd and Co_5La, and domain motion and nucleation were found to be very restricted in Co_5Gd. [The domains in Fig. 5(c) showed no change after slight
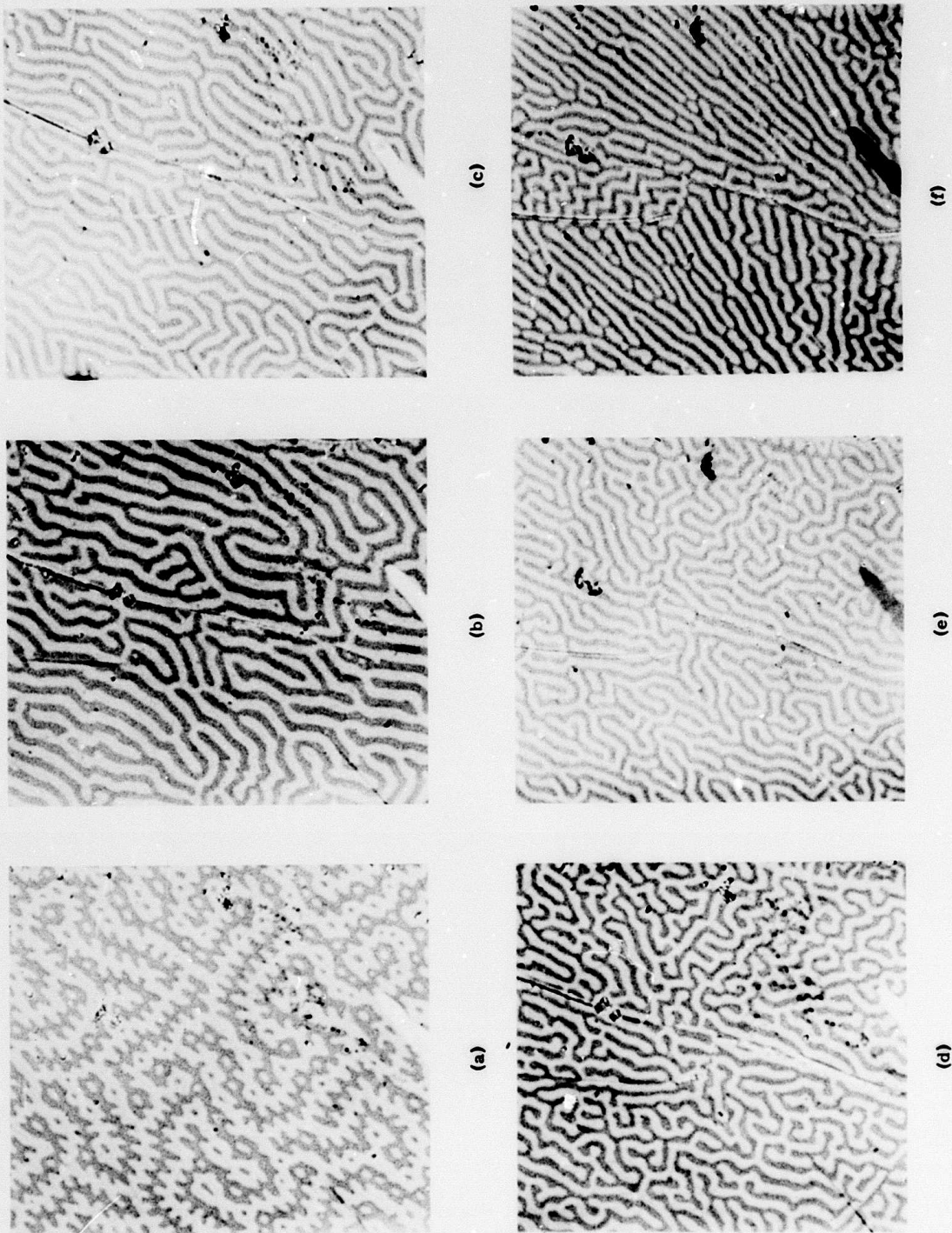
Fig. 1 Magnetic domain patterns in a thin Co$_5$Sm crystal after polishing to thicknesses of (a) 74μ, (b) 24μ, (c) 16μ, (d) 16μ, after application of normal magnetic field; and (e) 13μ, after field. (f) 13μ, after field. Magnetic easy-axis normal to surface. 375X
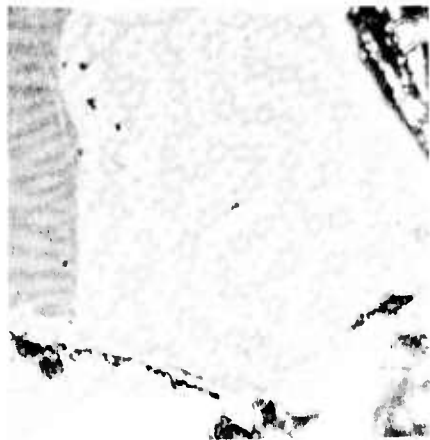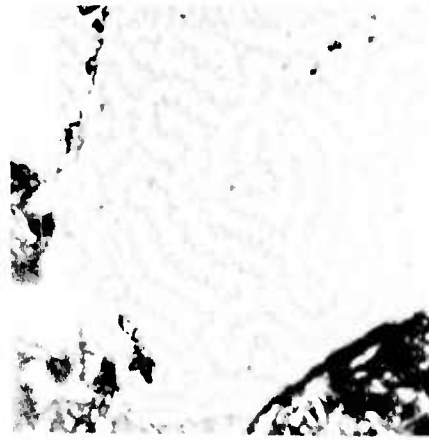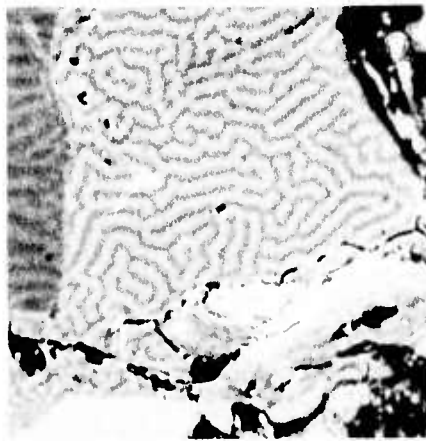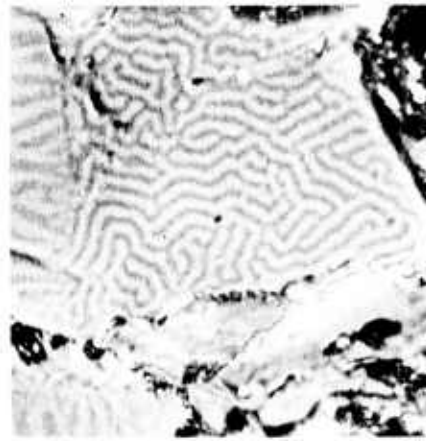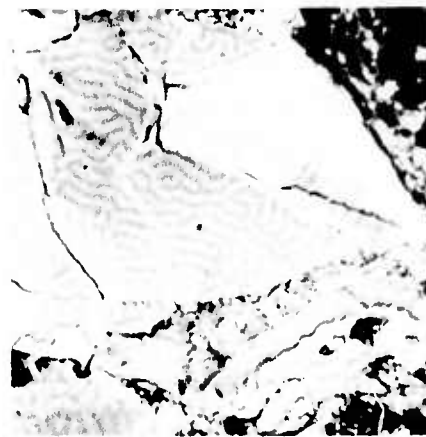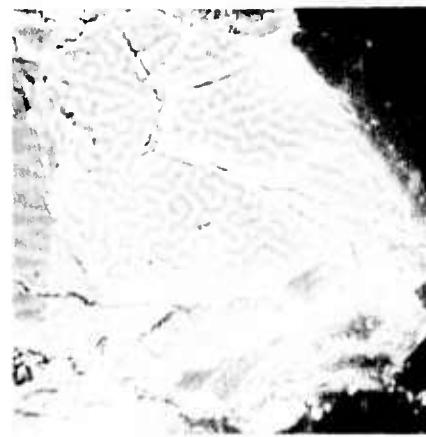
Fig. 2 Magnetic domains in Co_5Y at thicknesses of (a) 63u, (b) 30u, (c) 18u, (d) 15u, (e) 10u, and (f) 10u, after field. 500X
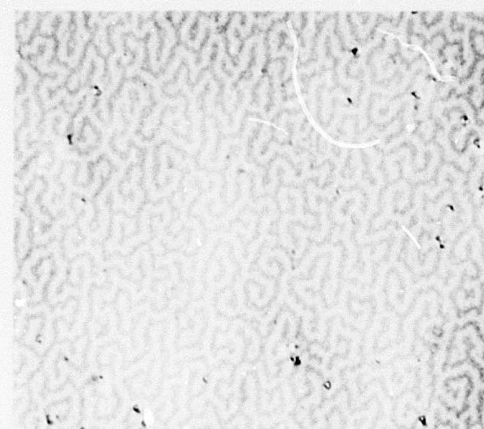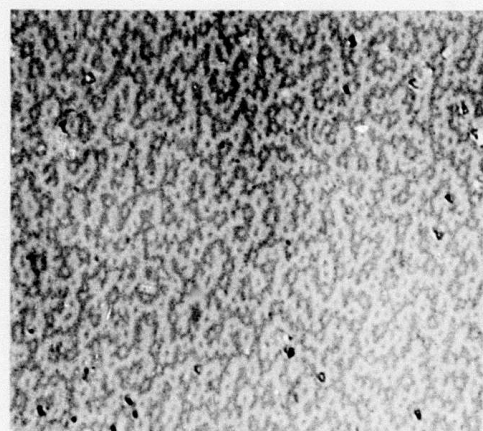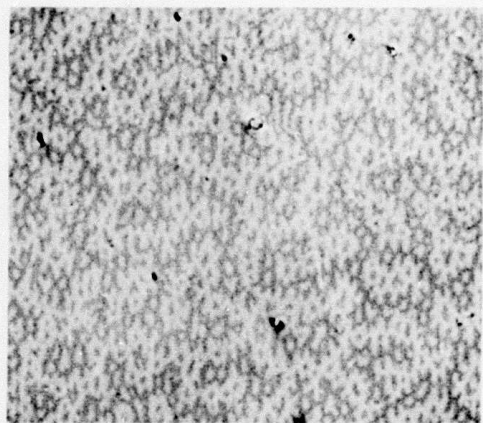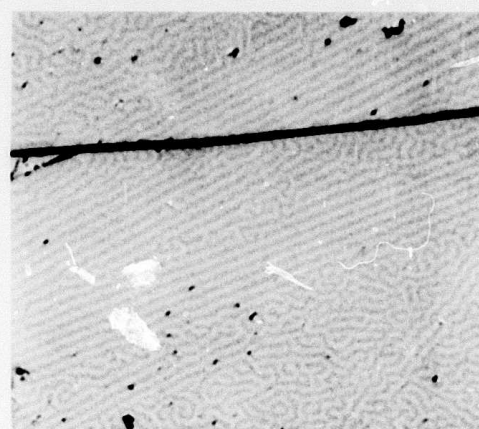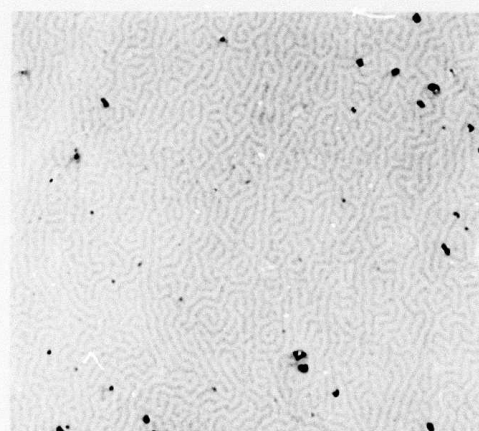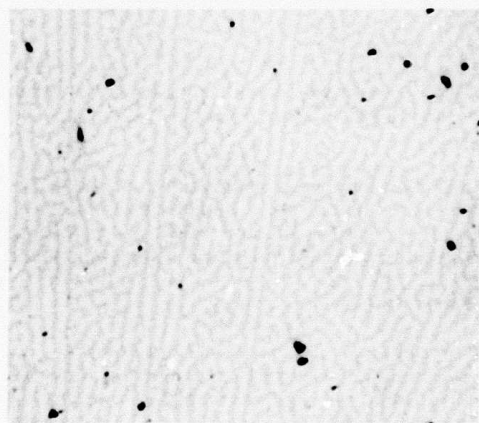
Fig. 3 Magnetic domains in Co_5Ce at thicknesses of (a) 96μ, (b) 38μ, (c) 18μ, (d) 18μ, after field; and (e) 10μ, (f) 10μ, different area. 375X

(a)

(b)

(c)

(d)
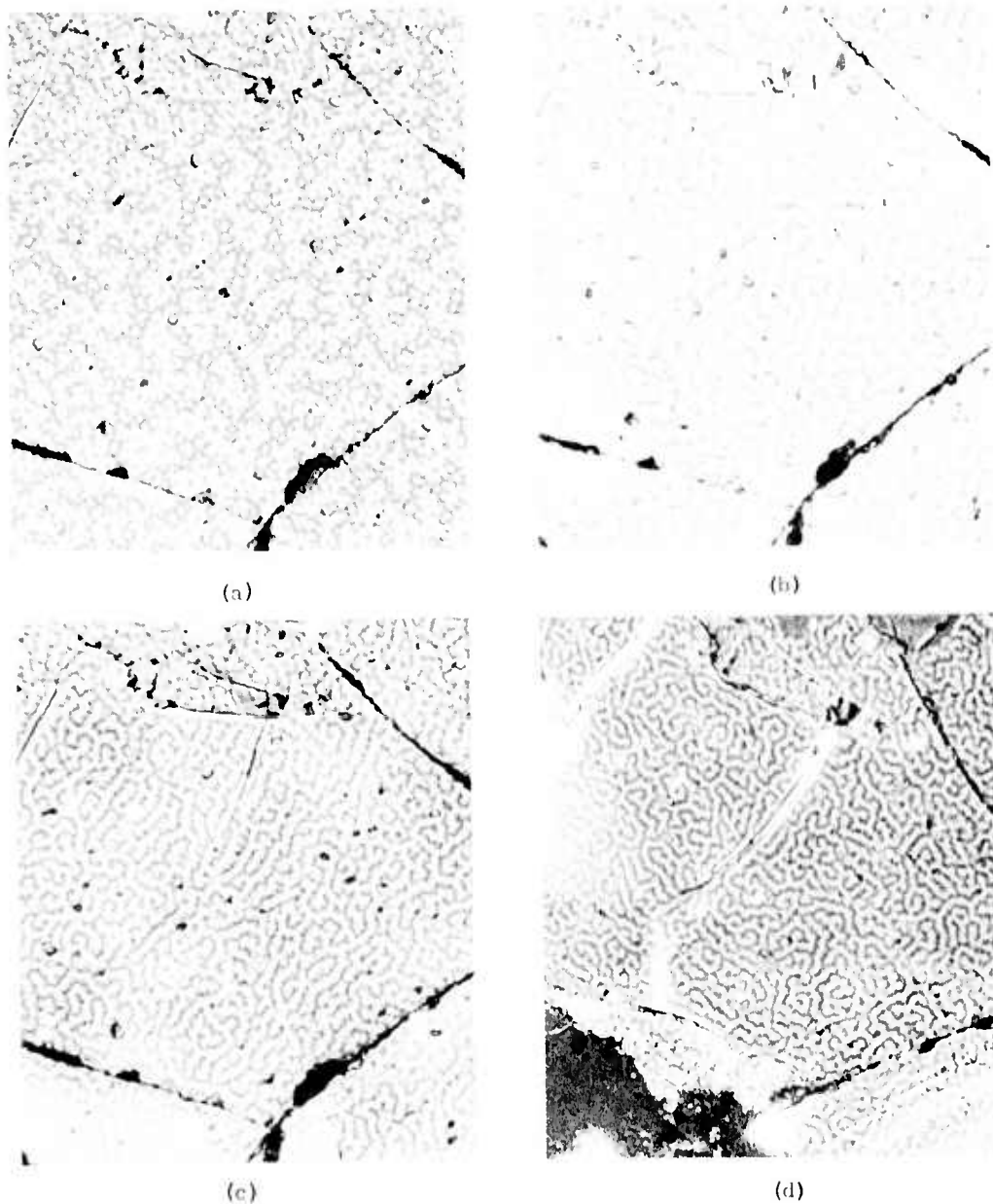
Fig. 4 Magnetic domains in Co_5Pr at thicknesses of (a) 84μ, (b) 33μ, (c) 23μ, after field; and (d) 13μ, after field. 375X

thinning, and when they were removed by magnetizing in 20,000 Oe, domains did not re-nucleate on returning to zero field.] We therefore decided not to initiate the tedious thinning process for these three compounds.

WALL ENERGY DETERMINATION

Kittel[14] considered the equilibrium domain structure of a high-anisotropy ferromagnetic plate of thickness T with the easy-axis normal to the plate. The total energy per unit area of an array of parallel plate domains of width W is the sum of the magneto-static energy, $1.7 M_S^2 W$, and the domain-wall energy,

$\gamma T/W$. (Here M_S is the magnetic moment per unit volume and γ is the domain-wall energy per unit area of wall.) The equilibrium domain width is obtained by minimizing this total energy, which yields

$$W = (\gamma T/1.7M_S^2)^{1/2} \qquad (1)$$

Hence if M_S is known, γ can be determined by measuring W at a given T.

Several questions arise concerning the application of Eq. (1) and Kittel's simple model to our results. First, although regions of parallel plates are
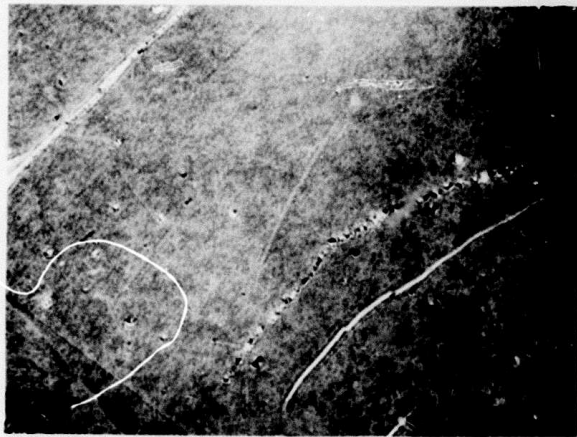
(a)
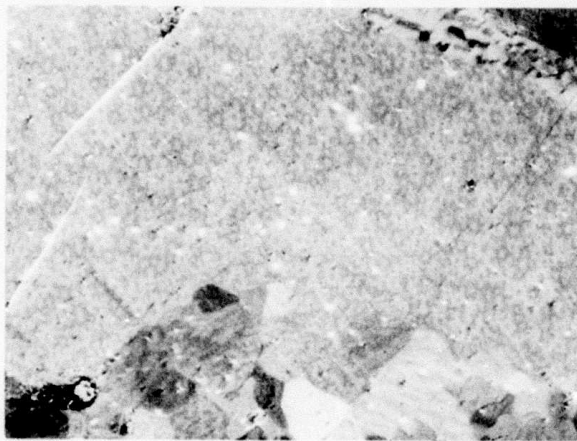
(b)
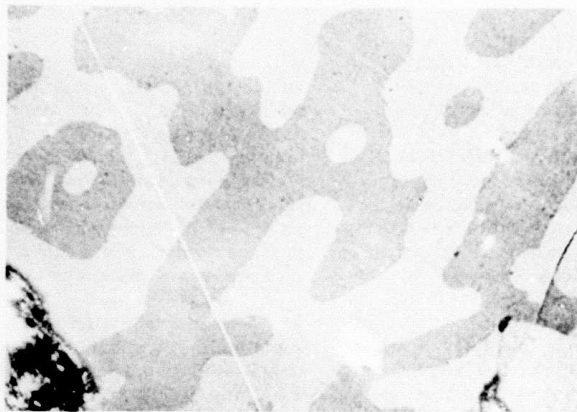
(c)

Fig. 5 Domain patterns in bulk samples of (a) Co_5Nd (750X),   (b) Co_5La (375X), and (c) Co_5Gd (375X).

TABLE I

Equilibrium Domain Widths and Domain-Wall Energies of Co_5R Compounds

Material	Saturation Magnetization[3] M_S (emu)	Thickness T (μ)	Average Domain Width W (μ)	Domain-Wall Energy γ (ergs/cm^2)	
Co_5Sm	855				
Grain A		6	2.1	90	
		6	2.0*	83	
		14	3.3	92	
Grain B		13	3.0	86	
		13	2.8*	74	} 85
		16	3.2	79	
		16	3.2*	79	
		19	3.5	79	
		24	4.0	83	
Co_5Y	848	10	1.7	35	
		10	1.7*	35	} 35
		15	2.0	33	
		18	2.2	33	
Co_5Ce	615	10	1.9	23	
		10	1.9*	23	} 25
		18	2.8*	28	
Co_5Pr	960	13	1.9	44	
		13	1.8*	40	} 40
		23	2.4*	39	
Co_5Nd	983	--		($\approx$20)	
Co_5La	725	--		($\approx$30)	
Co_5Gd	287	--		($\approx$30?)	

* After application of field.

sometimes seen [Fig. 3(f)], we commonly observe maze structures. Fortunately, maze and parallel plate structures of the same width have nearly the same energy, so this difference is unimportant. [6] Second is the question of how closely equilibrium is achieved. Since the removal and re-nucleation of domains by the application and removal of a field usually resulted in a demagnetized sample with nearly the same average domain width, it is felt that equilibrium is closely approached in these materials (with the exception of Co_5Gd).

Several theoretical limitations to Eq. (1) have been discussed by Kaczer. [6] Deviation of the magnetization direction from the easy-axis direction, the so-called μ* effect, is important in some materials but is negligible in these high-anisotropy materials. Below a thickness of about $T_1 = \gamma/2M_S^2$, the magnetostatic interaction between top and bottom surfaces becomes important, and the equilibrium W goes through a minimum and begins to increase with decreasing T. This limitation is not important in our experiments because we always have $T \gg T_1$. More important to

our experiments is the upper thickness limit for the validity of Eq. (1), which Kaczer[6] gives approximately as $T_2 = 32\gamma/M_S^2$. This marks the thickness at which surface refinement of the domain structure begins to appear, usually by the appearance of corrugations and spike domains. For $T > T_2$, the equilibrium internal domain width now increases more rapidly, as $T^{2/3}$.[6,15] However, theory predicts an average surface domain width that eventually becomes independent of thickness and proportional to γ/M_S^2.[15]

We have tabulated in Table I our data for equilibrium domain width W for thicknesses where spike domains and corrugations had essentially disappeared, i.e., for $T < T_2$. Each value of W is the average of at least 20 measurements. Since Eq. (1) is valid in this regime, we have calculated from each W a value of domain-wall energy γ, and averaged these for each compound. In view of the inaccuracies in our measurements of W and T, and possible slight departure from equilibrium in some cases, we estimate the values of γ listed in Table I to be accurate to $\pm 15\%$.
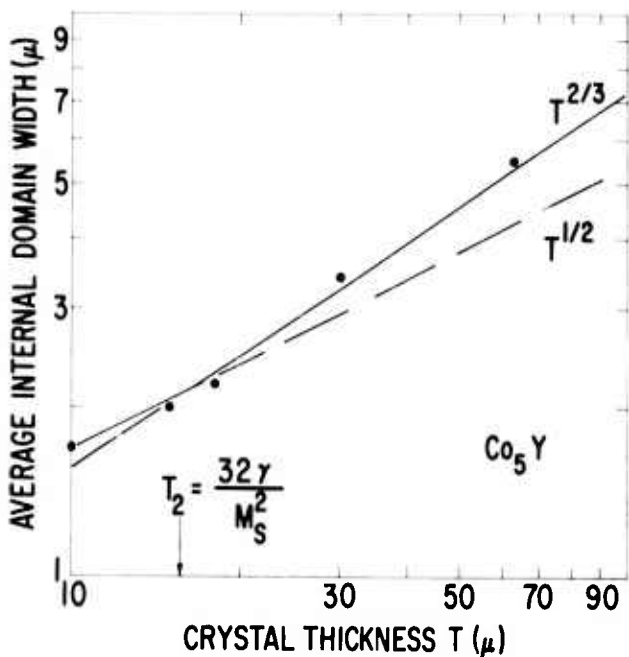
Fig. 6 Average internal domain width W vs thickness T for Co₅Y. Theory predicts a shift from $T^{1/2}$ to $T^{2/3}$ dependence at $T_2 = 32\gamma/M_s^2$. Calculated T_2 marked with arrow on abcissa.

For thicknesses $T > T_2$, the internal domain width can be measured from surface domain patterns by ignoring corrugations and spike domains. Data for Co₅Y, shown in Fig. 6, demonstrate the shift from $T^{1/2}$ to $T^{2/3}$ dependence predicted by theory. By Kaczer's formula, this dependence should change at $T_2 = 16\mu$, in reasonable agreement with Fig. 6.

According to theory, [15] the surface domain width at large thicknesses is constant and could also be used as a measure of γ. Surface domain patterns are more complex than considered by theory, and it is not clear just what should be measured. However, for semiquantitative estimates of γ, it may be satisfactory to measure some characteristic distance, such as average wavelength λ of corrugations. On thick samples of Co₅Gd, Co₅Sm, Co₅Ce, Co₅Y, Co₅La, Co₅Pr, and Co₅Nd, we measured $\lambda = 30\mu$, 6μ, 4μ, 3.5μ, 3.5μ, 3μ, and 1.5μ, respectively. Use of comparative λM_s^2 values as a rough measure of comparative γ values led to the estimates for Co₅Nd, Co₅La, and Co₅Gd listed in Table 1. The estimate for Co₅Gd should be considered as particularly questionable because of the evidence discussed earlier of nonequilibrium domain behavior in this material.

DISCUSSION

The wall energies listed in Table 1 are the highest yet measured for any material. [For comparison, $\gamma = 1 - 5$ erg/cm² for various ferrites[6, 8] and

$\gamma = 11$ ergs/cm² for cobalt. [6]] This was expected, because the wall energy depends on the magnetocrystalline anisotropy constant K, which is extremely high for these compounds. The standard continuum model of a domain wall yields the formula:[7]

$$\gamma = 4(AK)^{1/2} \qquad (2)$$

where A is the exchange constant.

We have listed in Table 11 our measured values of γ and values of K from single-crystal measurements by Tatsumoto et al. [16] The qualitative correlation is good. From these values and Eq. (2), we have calculated values for A and listed them in Table 11. [For comparison, $A = 3 \times 10^{-6}$ ergs/cm for hexagonal cobalt. [17, 18]] The exchange constant A for Co₅Sm appears to be significantly higher than for the other compounds. However, for reasons discussed in the next two paragraphs, the validity of Eq. (2) for these materials is questionable.

The exchange constant A is sometimes[19] approximated by $kT_C/8d$, where k is Boltzmann's constant, T_C is the Curie temperature, and d is the nearest neighbor distance between spins in a direction normal to the domain wall. Both A and d have ambiguity for a structure such as that of Co₅R compounds, in which there are two moment-bearing elements and two nonequivalent sites for cobalt atoms. However, a logical choice for d appears to be $a/2$. Using these distances, we have included in Table 11 values of Ad/kT_C. The values vary, and differ significantly from 0.125. Although some of the variation may be associated with experimental error, we feel the discrepancies are large enough to indicate that this common approximation for A is somewhat inaccurate for these materials.

The standard continuum model of a domain wall also leads to the following equation for the thickness of a domain wall:[7]

$$\delta = \pi(A/K)^{1/2} = \pi\gamma/4K \qquad (3)$$

We have included in Table 11 values of δ calculated from measured values of γ and K. These values indicate that the domain walls in these compounds are so thin that the continuum model may not be a satisfactory approximation, and discrete models considering detailed atomic positions[21, 22] may be necessary.

Our measurements of γ have confirmed the suggestion of Westendorp[5] that the domain-wall energy of Co₅Sm is higher than that of most other Co₅R compounds. However, he estimated that it may be as much as five times as great, whereas it is only two or three times as great according to our results. His estimates were made from observations on small grains of unknown shape and thickness, and this may account for the quantitative difference in our results.

TABLE II

Some Fundamental Magnetic Properties of Co$_5$R Compounds*

Material	Domain-Wall Energy γ (ergs/cm^2)	Anisotropy Constant K[16] (ergs/cm^3)	Exchange Constant A (ergs/cm)	Curie Point[3] T_C (°K)	Interatomic[20] Distance d (Å)	Ad $\frac{A}{kT_C}$	Domain-Wall Thickness δ (Å)	Single-Domain Particle Size D_C (μ)
Co$_5$Sm	85	$13 \cdot 10^7$	$3.5 \cdot 10^{-6}$	1000	2.50	0.63	51	1.6
Co$_5$Y	35	5	1.5	920	2.47	0.29	55	0.68
Co$_5$Ce	25	3	1.3	650	2.46	0.36	65	0.92
Co$_5$Pr	40	9	1.1	890	2.51	0.22	35	0.61

*The measurements of W(T) and Eq. (1) directly yield γ/M_s^2. From this and Eq. (4), D_C is calculated. Values of M_s from Ref. 3 are used to calculate γ. Values of K from Ref. 16 and Eqs. (2) and (3) are used to calculate A and δ.

Westendorp also speculates that the higher domain-wall energy of Co$_5$Sm may explain why high coercive forces are more easily obtained with ground powders of this compound than of the other compounds. This is possible, because theories based on domain wall nucleation or pinning are likely to predict a coercive force proportional to γ, as does the pinning model of Zijlstra.[4] However, the differences in coercive forces obtained with similar processing of the various compounds are much greater than the differences in wall energy we have measured. High coercive forces are also very easily obtained with ground powders of Co$_5$Gd.[23,24] Although this is undoubtedly related in some way to the low magnetization of Co$_5$Gd, we suggest that the quantity of most direct relevance is the particle size for single-domain behavior. The diameter of a sphere below which a single-domain structure is of lower energy than a multidomain structure is approximately[19]

$$D_C = 1.4 \ \gamma/M_s^2 . \qquad (4)$$

We have included D_C values in Table II. Using our estimated γ values from Table I, we also estimate D_C to be 0.29μ, 0.80μ, and 5.1μ for Co$_5$Nd, Co$_5$La, and Co$_5$Gd, respectively.

It is known, of course, that high coercive forces can be obtained with particles considerably larger than D_C. Commercial sintered Co$_5$Sm magnets contain grains averaging 5μ to 10μ in diameter and, in a thermally demagnetized state, contain several domains per grain.[25] However, it is likely that the fundamental domain behavior of a particle of diameter D scales with D/D_C or, equivalently, with DM_s^2/γ. [The fundamental domain behavior of thin plates, discussed above, scales with TM_s^2/γ,[6] as is evident from the equations for T_1 and T_2.] Therefore, it seems likely that the optimum properties of various Co$_5$R and Co$_{17}$R$_2$ compounds with smaller D_C than that of Co$_5$Sm would be achieved at smaller particle sizes than for Co$_5$Sm. For example, 2μ to 4μ diameter for Co$_5$Y is equivalent to 5μ to 10μ for Co$_5$Sm. Difficulties,

however, will be expected from the greater mechanical strains and increased oxidation associated with finer particles. This may explain why it has been found much more difficult to produce high coercive forces with most of the compounds than with Co$_5$Sm and Co$_5$Gd, which have a large D_C.

We note that the equilibrium surface domain width on bulk specimens, discussed earlier, also scales with γ/M_s^2. Specifically, the wavelength λ of domain corrugations for Co$_5$Sm was 6μ, of the order of the grain size used in commercial magnets. Thus such measurements may be useful as a crude but easy means of estimating the relative particle refinement necessary to achieve high coercive forces in sintered magnets of various materials. We have recently applied this criterion to domain patterns observed on several Co$_{17}$R$_2$, (Co, Fe)$_{17}$R$_2$, and Co$_7$R$_2$ compounds.[26]

Finally, we should recall that the coercive force in these compounds is controlled by the nucleation and/or pinning of domain walls, and therefore is sensitive not only to fundamental magnetic properties such as K, γ, M_s, and D_C, but also to detailed defects in the metallurgical structure, such as surface irregularities, precipitates, cracks, dislocations, etc. Some of the differences in properties attained with different materials may of course be associated with differences in metallurgical defects rather than with differences in fundamental magnetic properties.

SUMMARY

1. We have studied domain patterns in single-crystal plates of Co$_5$R compounds with the easy magnetic axis normal to the plate. As thickness is decreased, the surface domain structure of corrugations and spike domains disappears and simple maze patterns are produced.

2. The variation of internal domain width with thickness T changes from $T^{2/3}$ to $T^{1/2}$ at a thickness roughly equivalent to that predicted by theory.

3. From measurements of equilibrium domain width in the $T^{1/2}$ region we have determined domain-wall energies for several compounds, and from surface domain observations on bulk specimens we have estimated it for several others.

4. These measured values of wall energy correlate qualitatively with anisotropy constants measured by Tatsumoto et al.

5. From wall energies and anisotropy constants we have calculated exchange constants and domain-wall thicknesses. Domain-walls are so thin in these compounds, however, that the standard continuum model for a domain-wall may not be adequate.

6. Our measurements have confirmed Westendorp's suggestion that the wall energy of Co_5Sm is larger than that of other Co_5R compounds, but our results differ quantitatively from his estimates.

7. We have calculated the critical single-domain particle size D_C for various Co_5R compounds. It is higher for Co_5Sm and Co_5Gd than for the other compounds, and we suggest that this may partly explain why high coercive forces are more easily obtained in Co_5Sm and Co_5Gd than in the other compounds.

8. We suggest that measurements of surface domain width on bulk samples may be useful to estimate D_C and the optimum particle size for commercial sintered magnets.

ACKNOWLEDGMENTS

NOTE ADDED IN PROOF:

Two recent theoretical estimates of domain-wall energy for Co_5Sm are 36 ergs/cm^2[27] and 154 ergs/cm^2. [28] The large difference between these two estimates results mostly from the uncertainty in the approximate equations used to relate γ to T_C, K, and other known parameters. Considering these uncertainties, the result that both theoretical estimates are within about a factor of two of our experimental value of 85 ergs/cm^2 should be considered reasonable agreement.

REFERENCES

1. J. J. Becker, J. Appl. Phys. 41, 1055 (1970).

2. K. J. Strnat and A. E. Ray, Z. Metallk. 61, 461 (1970); K. Strnat, IEEE Trans. Mag. 6, 182 (1970).

3. D. L. Martin and M. G. Benz, Proc. 1971 Conf. on Magnetism and Magnetic Materials, A. I. P. Conf. Proc. No. 5, Part 2, 970 (1972).

4. H. Zijlstra, J. Appl. Phys. 41, 4881 (1970); J. Appl. Phys. 42, 1510 (1971).

5. F. F. Westendorp, J. Appl. Phys. 42, 5727 (1971).

6. J. Kaczer, IEEE Trans. Mag. 6, 442 (1970); Sov. Phys. JETP 19, 1204 (1964).

7. D. J. Craik, Contemp. Phys. 11, 65 (1970); D. J. Craik and R. S. Tebble, Ferromagnetism and Ferromagnetic Domains, J. Wiley and Sons, Inc., New York (1965).

8. M. Rosenberg, C. Tanasoiu, and V. Florescu, J. Appl. Phys. 37, 3826 (1966).

9. E. A. Nesbitt, H. J. Williams, J. H. Wernick, and R. C. Sherwood, J. Appl. Phys. 33, 1674 (1962).

10. R. A. McCurrie and G. P. Carswell, J. Mater. Sci. 5, 825 (1970); R. A. McCurrie, G. P. Carswell, and J. B. O'Neill, J. Mater. Sci. 6, 164 (1970).

11. K. Bachmann, A. Bischofberger, and F. Hofer, J. Mater. Sci. 6, 169 (1971); K. Bachmann and F. Hofer, Z. angew. Phys. 32, 41 (1971); K. Bachmann, IEEE Trans. Mag. 7, 647 (1971).

12. R. G. Wells and D. V. Ratnam, IEEE Trans. Mag. 7, 651 (1971).

13. A. F. Turner, J. R. Benford, and W. J. McLean, Economic Geology 40, 18 (1945).

14. C. Kittel, Phys. Rev. 70, 965 (1946).

15. A. Hubert, Phys. Stat. Sol. 24, 669 (1967).

16. E. Tatsumoto, T. Okamoto, H. Fujii, and C. Inoue, Suppl. J. Physique 32, C1-550 (1971).

17. R. Gemperle and A. Gemperle, Phys. Stat. Sol. 26, 207 (1968).

18. H. A. Alperin, O. Steinsvoll, G. Shirane, and R. Nathans, J. Appl. Phys. 37, 1052 (1966).

19. J. Smit and H. P. J. Wijn, Ferrites, John Wiley and Sons, Inc., New York (1959).

20. W. A. J. J. Velge and K. H. J. Buschow, J. Appl. Phys. 39, 1717 (1968).

21. T. Egami and C. D. Graham, Jr., J. Appl. Phys. 42, 1299 (1971).

22. J. J. van den Broek and H. Zijlstra, IEEE Trans. Mag. 7, 226 (1971).

23. W. M. Hubbard, E. Adams, and J. V. Gilfrich, J. Appl. Phys. 31, 368S (1960).

24. K. H. J. Buschow and A. S. van der Goot, J. Less Common Metals 17, 249 (1969).

25. J. D. Livingston, to be published.

26. J. D. Livingston, submitted to J. Mater.Sci.

27. M. G. Benz and D. L. Martin, J. Appl. Phys. to be published.

28. R. A. McCurrie and G. P. Carswell, Phil. Mag. 23, 333 (1971).

72CRD316

J. D. Livingston

PRESENT UNDERSTANDING OF COERCIVITY IN COBALT-RARE EARTHS

TECHNICAL INFORMATION SERIES

AUTHOR Livingston, JD	SUBJECT permanent magnets	NO 72CRD316
		DATE November 1972
TITLE Present Understanding of Coercivity in Cobalt-Rare Earths		GE CLASS 1
		NO. PAGES 9
ORIGINATING COMPONENT Metallurgy and Ceramics Laboratory		CORPORATE RESEARCH AND DEVELOPMENT SCHENECTADY, N.Y.

SUMMARY
   Theory and experiments relating to coercivity in cobalt-rare earth compounds are reviewed. Coercivity is predominantly limited by the nucleation of reverse domains by defects. Domain-wall pinning also influences coercivity in some cases. The specific defects responsible for domain nucleation have not been conclusively identified, but may be cobalt-rich regions and deformation-induced dislocations and stacking faults. This review was prepared for a symposium-workshop at the 1972 Conference on Magnetism and Magnetic Materials.

KEY WORDS
   permanent magnets, coercivity, cobalt-rare earth compounds

PRESENT UNDERSTANDING OF COERCIVITY IN COBALT-RARE EARTHS

J. D. Livingston

INTRODUCTION

Co_5Sm and Co_5Sm-based ternary compounds have recently been developed into permanent magnets with energy products and coercivities substantially greater than was possible with previous materials.[1-3] However, in other Co_5R, $Co_{17}R_2$, and $(Co, Fe)_{17}R_2$ compounds with the potential for higher energy products and/or lower material costs than Co_5Sm, high coercivities have not yet been achieved. Even in Co_5Sm, coercivities remain almost an order of magnitude below those theoretically possible. Thus there remains considerable technological potential in improved understanding of the factors determining coercivity in these materials.

The Co_5R compounds are of hexagonal symmetry, and the basis for large coercivities is the large, easy-axis, magnetocrystalline anisotropy which has been measured on single crystals[4-6] and aligned powders[5,7] We will review first the theory of magnetization reversal in easy-axis materials, and then the experiments relating to coercivity in the cobalt-rare earths. We will deal exclusively with the intrinsic coercivity H_{ci}, the reverse field in which half of the specimen magnetization is reversed. Unless otherwise specified, we will be considering the case in which magnetic field is applied parallel to the easy axis.

THEORY

Critical Particle Sizes

There are three different size parameters of significance to single-domain behavior.[8] These are $D_c = 1.4\gamma/M_s^2$, $b_c = 2A^{\frac{1}{2}}/M_s$, and $\delta = \pi(A/K)^{\frac{1}{2}}$, where M_s is saturation magnetization, K is magnetocrystalline anisotropy, A is the exchange constant and $\gamma = 4(AK)^{\frac{1}{2}}$ is the domain-wall energy per unit area.

The first parameter, D_c, is the diameter of a sphere below which a single-domain structure is of lower energy at zero field than a multidomain structure. The dimension b_c is the cylinder diameter below which magnetization reversal by coherent rotation is favored over the incoherent curling process. The third parameter, δ, is the width of a domain wall.

The three parameters are related through $b_c \approx \frac{1}{2}(D_c \delta)^{\frac{1}{2}}$. The ratio $D_c/\delta \approx K/M_s^2$ is a measure of the relative importance of crystal and shape anisotropies. In most Co_5R compounds, crystal anisotropy dominates, i.e., $K \gg M_s^2$. The various size parameters for these compounds are typically $D_c \approx 1\mu$, $b_c \approx 400\text{Å}$, and $\delta \approx 60\text{Å}$. In contrast, in pure cobalt, all three size parameter are of the same order of magnitude, about 150Å to 300Å. In iron and nickel, $D_c < \delta$.

We consider first the equilibrium or lowest-energy magnetization states of a uniaxial particle temporarily ignoring the accessibility of those states. The equilibrium magnetization curves for spherical particles with $D \leq D_c$, $D \gtrsim D_c$, and $D \gg D_c$ are shown in the top half of Fig. 1. For $D \leq D_c$, the particle is always fully saturated, i.e., single domain, in its lowest-energy state. For a bulk sphere ($D \gg D_c$), a multidomain state with zero internal field is of lowest energy for applied fields below the saturating field of $4\pi M_s/3$. For intermediate particle sizes, the field range over which the multidomain state is favored decreases with decreasing diameter, with the fractional decrease in saturating field varying approximately as $(D_c/D).^{\frac{1}{2}}$[9] Thus the transition from multidomain behavior to single-domain behavior is gradual, and does not occur abruptly at $D = D_c$.
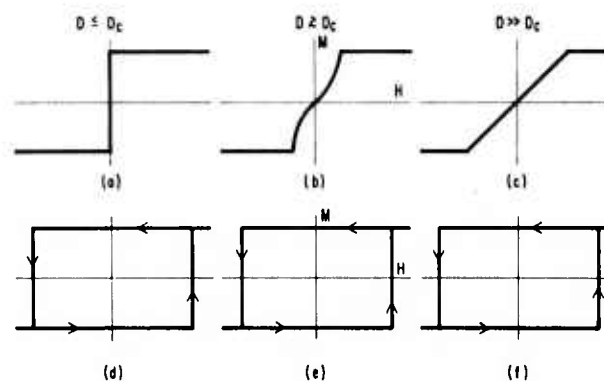
Fig. 1 (a)-(c): Equilibrium magnetization curves for spheres of various diameters. (d)-(f): Ideal hysteresis curves for same particles, assuming $D \gg b_c$. Coercivity is $(2K/M_s) - N_1 M_s$.

These equilibrium curves correspond to lowest-energy states, and it is the energy barriers between these states that lead to hysteresis and coercive force. In particular, micromagnetic theory[10] indicates that a fully saturated magnetization state is very stable. For a saturated, defect-free ellipsoid of rotation with $D < b_c$, the second size parameter, this theory predicts that magnetization reversal cannot be nucleated until the application of a reverse field $-H_n = 2K/M_s + (N_2 - N_1)M_s$, where N_1 and N_2 are the longitudinal and transverse demagnetizing factors. This field corresponds to the coercivity for coherent rotation, i.e., Stoner-Wohlfarth[11] behavior. For $D > b_c$, nucleation can occur via the curling mode at a lower field, which approaches $2K/M_s - N_1 M_s$ for $D \gg b_c$. For materials for which $K \gg M_s^2$, such as Co_5Sm, this decreases in nucleating field provided by curling is minor. The magnetization curves predicted by micromagnetic theory for defect-free particles are shown in the bottom half of Fig. 1. For $D \gg b_c$, the predicted coercivity is size-independent (Brown's paradox).

For any real particle, the magnetization curve for each size range must fall between the two limiting curves at the top and bottom of Fig. 1, i.e., between equilibrium and ideally hysteretic behavior. Defects play two contrary roles in determining where the real particle's magnetization curve will fall. On the one hand, they can provide sites for heterogeneous nucleation of magnetization reversal, and thereby aid the approach to equilibrium. On the other hand, they can inhibit the motion of domain walls, and thereby oppose the approach to equilibrium. Through these two effects--nucleation and pinning--defects can therefore either decrease or increase coercivity.

Heterogeneous Domain Nucleation

The maximum room-temperature H_{ci} produced to date with Co_5Sm is 43 kOe,[12] about one-seventh of $2K/M_s$, the ultimate coercivity predicted by theory $(N_1 \to 0)$. Most magnets and powders have coercivities considerably smaller. Since coherent rotation and curling are impossible at such low fields, it appears likely that reverse domains are being nucleated at defects.

One possible cause for nucleation is high local demagnetizing fields at surface irregularities (sharp corners or pits)[13-15] or inclusions.[16] Although the demagnetizing field at a mathematically sharp corner is infinite,[13] Aharoni noted that a radius less than atomic dimensions is unrealistic, and for realistic dimensions the maximum local demagnetizing field possible is about $18M_s$.[17] When $K \gg M_s^2$, these maximum demagnetizing fields are much smaller than $2K/M_s$, and therefore cannot directly explain the low coercivities observed. However, these sites will require magnetizing fields above 18 M_s, e.g., about 15 kOe for Co_5Sm, to remove residual reverse domains and produce initial saturation.

Another possible nucleation site is a local region in which K is appreciably lowered. In Co-R magnets, this could correspond to a cobalt-rich region produced, for example, by preferential oxidation of the rare earth. Local elastic strains, e.g., around a dislocation, could also decrease K, although magnetostrictive constants would have to be unusually high to reduce K to near zero in a high-anisotropy material such as Co_5Sm. Abraham and Aharoni[18] calculated the reduction in nucleation field produced by a cylinder or slab of material with $K = 0$ lying parallel to the field. The reduction is substantial once the cylinder diameter or slab thickness becomes larger than δ, the domain-wall width. For defects smaller than δ, exchange forces are sufficient to resist reversal by this mechanism.

Another possible nucleation site in ordered magnetic crystals is a stacking fault. Magnetic coupling in some structures can be greatly altered across a fault, and may even be antiferromagnetic.[15, 19] Such a fault may be an easy nucleation source for a $180°$ domain wall.

Even after a small reverse domain has been formed at a defect, the domain-wall surface energy γ can resist its expansion.[20, 21] For example, calculations for plane domains in spherical particles[22] and cylindrical domains in plates[9] show an energy barrier opposing domain growth until the domain reaches a critical breakaway size. The calculated size decreases with increasing field, and perhaps breakaway can first occur when this size equals the size of the defect. For the case of a cylindrical domain in a plate of thickness T, a domain nucleated at a defect of size Δ would then break away at a field of $-H_n = (\gamma/2M_s\Delta) + (32M_s\Delta/T) - 4\pi M_s$. The first term represents the resistance to breakaway provided by wall energy. For Co_5Sm and $\Delta = 500Å$, this term is about 10 kOe.

The likelihood of a particle containing a defect capable of nucleating a reverse domain is expected to decrease with decreasing particle size. Thus when nucleation controls coercivity, coercivity increases as particle size decreases. Attempts to explain the experimentally observed variations of coercivity with size have been made from domain models using arbitrary assumptions about the size or height of energy barriers that can be overcome[22] or models based on the statistical probability of effective nucei in particles of a given size.[10]

Domain-Wall Pinning

Local variations in magnetic properties can produce local variations in domain-wall energy and thereby produce forces that resist wall motion. Nonmagnetic inclusions, for example, produce an attractive force because of a reduction in both wall energy and demagnetizing energy. The former is more important for inclusions smaller than D_c in diameter. If the pinning centers are few and widely spaced, the wall is presumed to bow between pins, and theory predicts an intrinsic coercivity proportional to $v/M_s\lambda$, where λ is the spacing between pins.[23] If the density of pinning centers becomes high, the problem becomes much more complex, and coercivity is no longer proportional to v.[24]

Zijlstra[23] and Westendorp[25] suggested a model in which pinning centers do not exist throughout a particle, but only within a surface layer. Possible pinning centers include inclusions, dislocations, stacking faults, and surface irregularities. If nucleation sites for reverse domains also exist within this layer, then these pinning centers, although only local can limit the expansion of the reverse domains and thereby influence coercivity. If these pinning centers are limited only to the immediate vicinity of the nucleation site, this model becomes difficult to distinguish from a nucleation model. A local region of closely spaced pinning sites or a stacking fault[26] could also serve to retain a residual reverse domain to high magnetizing fields, and thereby create a subsequent nucleation site.

It has recently been suggested that in some materials with large values of the ratio K/A the domain wall may be thinner than predicted by the standard expression for δ.[27] These narrow walls may produce an intrinsic lattice resistance to domain wall motion analogous to the Peierls force that resist conlocation motion. This will probably provide little wall coercivity at room temperature, but the narrow-wall structure may alter γ and its dependence on K and A.

Particle Interaction

When an assembly of particles is aligned and sintered into a dense compact, it is no longer reasonable to consider the particles as fully independent. At the very least, each grain will have strong magnetostatic interaction with neighboring grains. The reversal of neighbors along the field direction will produce extra fields tending to reverse a grain's magnetization, whereas the reversal of neighbors in the direction transverse to the field will produce the opposite effect. The most extreme case will be the field on a transverse plane of unreversed particles if the entire remainder of the sample is reversed. This will produce a field of $8\pi M_S$ tending to reverse the magnetization of that plane. If a single spherical grain remains unreversed, the reversing field will be $8\pi M_S/3$. Unaligned grains will have more complex effects.

If sintering produces actual exchange contact between spins in neighboring grains, magnetization reversal can proceed directly from grain to grain by wall motion unless the boundaries provide sufficient pinning sites. Possible pinning sites are dislocations, voids, and oxide particles. It is also possible that exchange contact between the grains is blocked by a thin layer, perhaps of oxide, or greatly weakened because of atomic disorder in the boundary. Then each grain can be viewed as requiring a separate nucleation event to produce reversal. The results of Craik[28] suggest the existence of an effective gap between grains in oriented barium ferrite.

EXPERIMENT

Precipitation Alloys

Nesbitt et al.[29] have studied the magnetic behavior of a single crystal of Co-Fe-Cu-Ce alloy heat treated to produce a dispersion of very fine precipitates within a Co_5Ce-rich matrix. In a thermally demagnetized specimen, they found little magnetization change at fields below the coercive field, and a very abrupt increase to near saturation at the coercive field. Since such a specimen contained many domains, this behavior is characteristic not of nucleation, but of general wall pinning. Other evidence indicating general wall pinning was a lack of dependence of coercivity on magnetizing field, and the ability to achieve high coercivity in a bulk crystal. Magnetic viscosity has also been reported.[79, 80]

Single Particles

The magnetic behavior of predominantly single-phase Co_5R materials is contrary to that for the pre-

phase Co_5R materials is contrary to that for the precipitation alloys. A thermally demagnetized sample can be magnetized to near saturation in low fields, coercivity generally increases with increasing magnetizing field, and high coercivities are attained only in fine particles or sintered assemblies of particles (Refs. 3, 25, 30, 31). These characteristics indicate that general wall pinning is low and suggest that coercivity is dominated by domain nucleation. Direct magnetization studies of single particles of other uniaxial hard magnetic materials, such as orthoferrites (Refs. 32-34), MnBi,[35] and MnGa,[36] show that nucleation determines coercivity in these materials. However, the results of similar studies on single fine particles of Co_5R compounds are more complex. While confirming the importance of domain nucleation, they indicate that local wall pinning can influence coercivity in some cases.

Consider the experimental magnetization curves in Figs. 2 through 5. The particle in Fig. 2 shows simple rectangular-loop behavior, similar to the bottom of Fig. 1, but with a much smaller coercivity (Ref. 37). In this particle, once the reverse domain was nucleated, it swept through and completely reversed the particle magnetization. The nucleation field and coercivity were identical. In Fig. 3, a domain nucleated and moved abruptly to a near-equilibrium position.[38] It then moved to maintain zero internal field, approximating the equilibrium behavior of Fig. 1(c), but modified by a slight wall coercivity.

However, the behavior of the particles in Figs. 4 and 5 is not so clearcut. The first shows two distinct magnetization discontinuities separated by a region of gradual change. Becker[38] interpreted this as the sum of two magnetization loops, one similar to Fig. 2 and one similar to Fig. 3 (but with nucleation at a negative applied field). He suggested that a small-angle boundary divided the particle into two magnetically independent regions. The particle in Fig. 5 shows an extensive region of gradual magnetization change, presumably corresponding to gradual wall motion, before the occurrence of a jump. Zijlstra[23, 26] interpreted this as wall motion limited by pinning in parts of the crystal, but not in other parts. The minor loops shown for demagnetized particles confirm that wall motion is easy over large portions of the particle.

In Figs. 2 and 3, the nucleation of one reverse domain was sufficient to reverse the particle magnetization or reach approximately equilibrium behavior. In Figs. 4 and 5, however, the nucleation of one reverse domain was insufficient, and a single barrier to wall motion or a region of pinning strongly influenced magnetization reversal.

The relative importance of domain nucleation and local wall-pinning varies greatly from particle to particle, and the properties of various powders and sintered magnets may be influenced by both. Pragmatically, the goal is to increase coercivity. A nucleation-dominated model suggests we want to decrease defect density, whereas a pinning-dominated
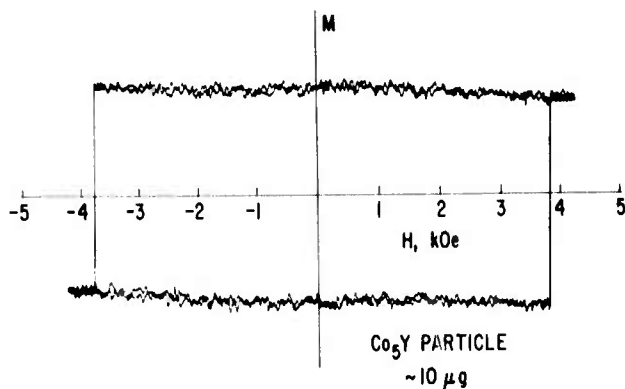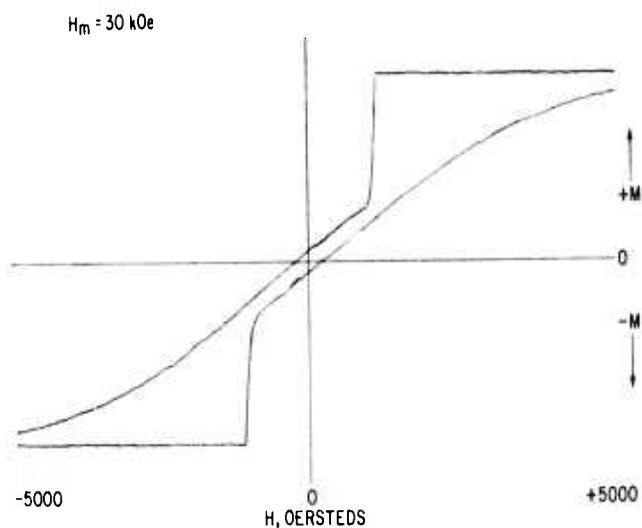
Fig. 2 Hysteresis loop of Co_5Y particle [from Becker[37]].

Fig. 3 Hysteresis loop of 200μ Co_5Sm particle [from Becker[38]].

Fig. 4 Hysteresis loop of 50μ Co_5Sm particle [from Becker[38]].

Fig. 5 Hysteresis loop of $5\mu Co_5Sm$ particle [from Zijlstra[23]].

model suggests we want to increase defect density. Most evidence points to the former alternative. However, incomplete evidence of the nature of the important defects and their connection with processing variables sometimes makes interpretation ambiguous.

Single-particle experiments have shown that increasing magnetizing field increases the reverse field necessary for domain nucleation in a stepwise way (Ref. 39). This suggests that residual domains, maintained by local demagnetizing fields or local pinning, are serving as reversal nuclei, and require specific magnetizing fields to remove them. Similar observations have been made on orthoferrite crystals.[32-34] Because of their low magnetization, orthoferrites have a very large D_c, and single-domains behavior is approached with dimensions of several mm. This allows direct optical observation of domain throughout the hysteresis loops. Nucleation of domains is seen to occur at specific locations in the crystal, sometimes identifiable as the location of a residual domain. When the magnetizing field is sufficiently
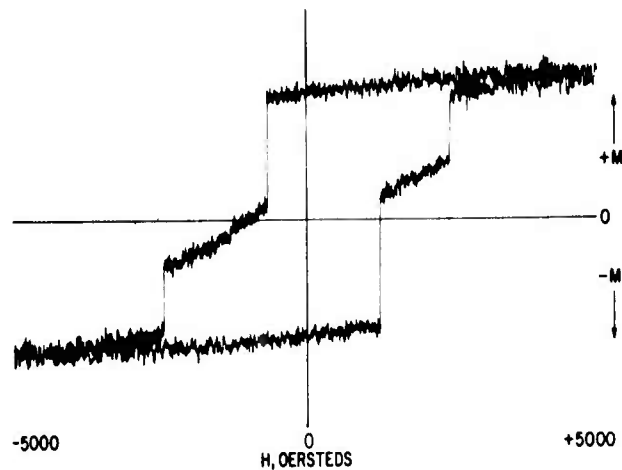
large to remove the residual domain, nucleation occurs at another location at a larger field. It was found that mechanical polishing made nucleation easier and annealing made it more difficult, suggesting dislocations as favored sites for magnetization reversals.[34, 40]

If individual magnetization discontinuities in a single particle can be associated with individual defects, the dependence of the nucleation fields on variables such as temperature or field orientation may shed light on the nature of the defects. Becker has reported that two such fields in one particle had different temperature dependences.[41] The $1/\cos\theta$ dependence of coercivity expected for $180°$ domain-wall motion[42] was found displaced from $\theta=0$ in some particles, suggesting a misoriented region as the defect site.[43]

Powders

Coercivity of Co_5R powders first increases and then decreases with increasing grinding time, i.e., with decreasing particle size.[3, 5, 7, 30, 81] The decrease for fine sizes is usually ascribed to the plastic deformation produce by grinding. Consistent with this interpretation are the higher coercivities obtained by grinding at liquid nitrogen temperature (Refs. 7, 44, 45, 82).

McCurrie et al.[46] have observed a difference in mechanical hardness behavior between Co_5La and Co_5Sm. They conclude that plastic deformation will occur less easily in Co_5Sm, and suggest that may explain why higher coercivities are attained in that compound. A difficulty with this explanation is that Co_5Ce has similar hardness properties to Co_5Sm, but has low coercivities in ground powder, like Co_5La (Ref. 47).

Etching ground particles in various chemical reagents usually increases the coercivity, sometimes as much as twenty-fold.[3, 37, 48, 83] This may be caused by the removal of mechanically damaged surface layers, in which dislocations and stacking faults had been serving as nucleation sites. However, etching has also been observed to decrease coercive force in some cases, which was explained by the removal of a surface pinning layer.[23]

With long holding times at room temperature or slightly elevated temperatures, the coercivity of powders gradually drops,[30, 48, 80] an effect that depends on contact with oxygen[49] and can be avoided or slowed by appropriately coating the particle.[48, 50, 82, 83] This aging phenomenon may be caused by the creation of low-K cobalt-rich surface regions by preferential oxidation of the rare earth.

As mentioned earlier, thermally demagnetized Co_5R powders can be magnetized to near saturation in low fields, indicating that general wall pinning is low. Coercivity is sensitive to magnetizing field, indicating that nucleation from residual domains is controlling coercivity. Becker studied the angular dependence of the dependence of coercivity on magnetizing field, and found it consistent with a model based on the motion of 180° domain walls and particular assumed distributions of individual particle coercivities[51] McCurrie[52, 53] has used demagnetizing remanence curves as a means of estimating coercivity distributions, a technique that depends on questionable assumptions about the shape of the magnetization curves of individual particles.

Zijlstra[23] measured minor loops at various positions along the reversal portion of the major hysteresis loop, and noted a nonzero susceptibility χ which seemed likely to be caused by reversible displacements of domain walls. He then noted that χ and coercivity H_{ci} varied with heat treatment of the powders such that χH_{ci}^2 remained constant. He explained this correlation with a wall-pinning model. This interesting result calls for further investigation.

Annealing at temperatures near $1000^\circ C$ can increase coercivity, perhaps because of the annealing of defects produced by grinding. However, annealing of Co_5Sm in the vicinity of $700^\circ C$ can substantially reduce coercivity, an effect that can be reversed by a subsequent anneal at $1000^\circ C$ (Fig. 6). Recent evidence indicates that the deleterious effect of intermediate-temperature heat treatments may be caused by a eutectoidal decomposition of Co_5Sm into $Co_{17}Sm_2$ and Co_7Sm_2, thereby producing nuclei for easy magnetization reversal.[54, 55]

Westendorp noted a similar dependence of coercivity on heat treatment for Co_5Pr, but noted that coercivity always remained about five times smaller than for Co_5Sm (Fig. 6).[56] From domain-width observations, he concluded that the domain-wall energy for Co_5Sm was larger than for other Co_5R compounds, and suggested that the resulting increased wall-pinning forces might explain the higher coercivities of Co_5Sm. More detailed measurements have recently confirmed that the wall energy of Co_5Sm is higher than for the other compounds.[57] It was noted that this also leads to higher values of D_c, so that to grind the other compounds to an equivalent D/D_c requires finer particle sizes and therefore more mechanical damage and oxidation. This was suggested
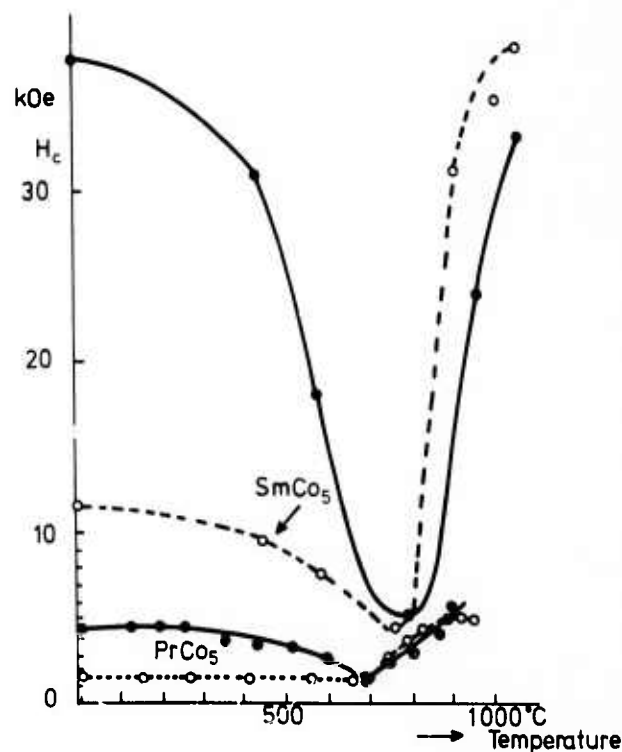

Fig. 6 Coercivity vs annealing temperature for Co_5Sm and Co_5Pr. Dashed lines for as-ground specimens. Solid lines after initial anneal near $1000^\circ C$ [from Westendorp[56]].

as another possible reason for the superior properties of Co_5Sm. Domain measurements were also used to estimate D_C for various 17-2 and 7-2 compounds, and it was found that only Co_5Gd and Co_7Gd_2 had larger D_C values than Co_5Sm.[57, 58] In both of these compounds, high coercivities are easily attained in ground powders.[59]

Sintered Magnets

Domain studies on sintered Co_5Sm magnets[60] show that each grain contains several domains in the thermally demagnetized condition, and that these domains move about easily throughout most of the material. Hence, general wall pinning remains low. Once the magnet is magnetized, however, most grains apparently reverse abruptly in a "single-domain" process, and only a minority of grains show an internal domain structure. Individual grains can resist reversal to high fields despite the early reversal of neighboring grains, indicating either strong pinning at the grain boundary or no exchange contact between grains.

The coercivity of sintered Co_5Sm-based magnets depends sensitively on composition, sintering temperature and time, and post-sintering heat treatment (Refs. 1, 25, 61-66). Maximum coercivity occurs when the Co_5Sm phase reaches the Sm-rich limit of its composition range.[67, 68] (Total Sm content would be well into the two-phase range, but account is taken of the Sm tied up in the form of Sm_2O_3.) It is not yet clear how much of this composition sensitivity is caused by a dependence of K on deviations from stoichiometry, and how much is caused by a change in defect distribution. Benz and Martin[67] have suggested that cobalt vacancies present in hyperstoichiometric alloys not only accelerate sintering, but also aid coercivity. The deleterious effect of heat treatments near 700°C is probably caused by eutectoid decomposition, as mentioned above. The beneficial effect of heat treatment near 900°C may result from the dissolution of cobalt-rich regions associated with residual composition inhomogeneities[69] or formed by eutectoid decomposition during prior cooling.

Several investigators have produced good properties in sintered magnets by blending together powders of two different compositions, one of which is rare-earth-rich and liquid at the sintering temperature.[1, 70] This and other observations led Schweizer et al.[71] to suggest a modification of Zijlstra's surface-pinning theory in which each Co_5Sm grain is presumed enclosed by an epitaxial Co_7Sm_2 shell, which contains pinning sites. However, there has been no direct evidence of the existence of such a shell, and experience indicates that high coercivities can also be obtained without the use of a liquid-phase sintering additive.

Martin and Benz[72] recently measured the temperature dependence of coercivity in a number of sintered magnets of varying coercivity, and found that the results could all be normalized to a single curve

representing the increase of relative coercivity with decreasing temperature (Fig. 7). They also measured the temperature dependence of the anisotropy constant K for one of these magnets, and found it identical to the temperature dependence of coercivity (Fig. 8).[73] This suggests that thermal activation plays no major role in producing the temperature dependence of coercivity. This is in contrast to the view of other workers[52, 74, 75] who had noted that coercivity was much more temperature-dependent than the anisotropy
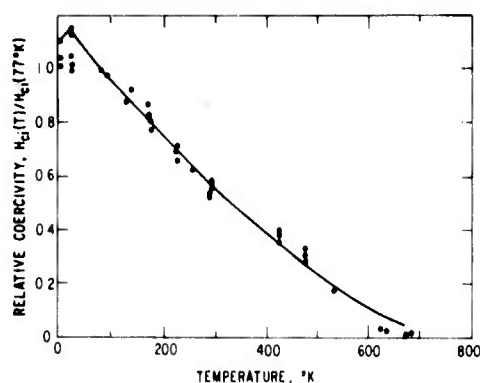

Fig. 7 Relative coercivity vs temperature for a series of Co_5Sm sintered magnets [from Martin and Benz[72]].
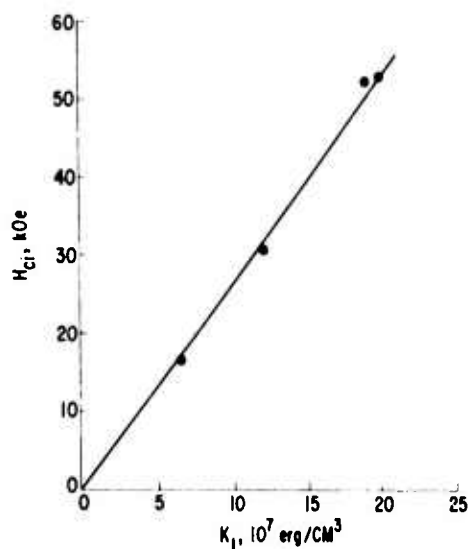
Fig. 8 Coercivity vs anisotropy constant (measured at various temperatures) for a Co_5Sm sintered magnet [from Benz and Martin[73]].

constants reported by Tatsumoto et al.[6] However since the anisotropy measurements of Benz and Martin were obtained with much larger measuring fields, they are probably more reliable. Because of the likely variation of K with deviations from stoichiometry, it is also highly desirable to measure coercivity and K on the same samples, as did Benz and Martin. Nesbitt et al.[29] measured coercivity and K on a single crystal of a Co-Fe-Cu-Ce alloy, in which

coercivity is controlled by general wall pinning. Most of the temperature dependence of coercivity could be explained by the temperature dependence of K in this case as well.

Domain studies of sintered magnets water-quenched from high temperatures have shown the existence of a surface layer of low-coercivity grains about 200μ thick.[76] This layer accounts for the kinked magnetization curves previously reported.[77] Further studies indicate that this layer is caused by thermal stresses produced from the temperature gradients during quenching.[76]

CONCLUSIONS

Since coercivities so far attained are far below $2K/M_S$, it is clear that coherent rotation or incoherent rotation processes such as curling do not operate. Except in the copper-bearing precipitation alloys, general wall pinning is low. Domain nucleation and local wall pinning both influence coercivity, and are even interrelated in some models. However, since most experiments suggest that defects decrease coercivity, coercivity appears to be limited primarily by domain nucleation.

The specific defects responsible for nucleation, or for local pinning, have not been conclusively identified. The effects of low-temperature aging of powders, and of composition and heat treatment on sintered magnets, suggest that low-K cobalt-rich regions may serve as defects for domain nucleation. The effects of grinding on powders and of thermal stresses on sintered magnets suggest that plastic deformation may produce nucleation sites, presumably either dislocations or stacking faults.

The superiority of Co_5Sm to other cobalt-rare earth compounds is attributable in part to the higher K, which results in a higher γ and a higher H_c. Another possible factor is less sensitivity of K to composition, particularly increases in cobalt concentration. (This can be inferred from the observation that $Co_{17}Sm_2$ remains easy-axis while most of the other $Co_{17}R_2$ compounds are easy-plane, i.e., they have negative K.)[3]

More information is needed on the dependence of K on deviations from stoichiometry. Measurements of magnetostriction coefficients are necessary to assess the importance of dislocations. [Some data already exist for Co-Gd compounds.[78]] Experimental and theoretical study of various stacking faults possible in these systems would help assess their importance. More metallurgical work focused on the grain boundaries in sintered magnets would help us understand how neighboring grains remain so magnetically independent.

ACKNOWLEDGMENTS

REFERENCES

1. D.L. Martin and M.G. Benz, Proc. 1971 Conf. on Magnetism and Magnetic Materials, A.I.P. Conf. Proc. 5, 970 (1970).

2. K.J. Strnat, ibid., p. 1047.

3. J.J. Becker, J. Appl. Phys. 41, 1055 (1970).

4. G. Hoffer and K Strnat, IEEE Trans. Mag. 2, 487 (1966).

5. K.H. Buschow and W.A.J.J. Velge, Z. angew. Phys. 26, 157 (1969).

6. E. Tatsumoto, J. Okamoto, H. Fujii, and C. Inoue, Suppl. J. Physique 32, C1-550 (1971).

7. K. Strnat, G. Hoffer, J. Olson, W. Ostertag, and J.J. Becker, J. Appl. Phys. 38, 1001 (1967).

8. D.J. Craik and R.S. Tebble, Ferromagnetism and Ferromagnetic Domains, John Wiley and Sons, Inc., New York (1965), p. 47.

9. C. Kooy and U. Enz, Philips Res. Repts. 15, 7 (1960).

10. W.F. Brown, Jr., Micromagnetics, Interscience, New York (1963).

11. E.C. Stoner and E.P. Wohlfarth, Phil. Trans. Roy. Soc. London A240 599 (1948).

12. K.H.J. Buschow, P.A. Naastepad, and F.F. Westendorp, IEEE Trans. Mag. 6, 301 (1970).

13. S. Shtrikman and D. Treves, J. Appl. Phys. Suppl. 31, 72S (1960).

14. U. Dehlinger and A. Holz, Z. Metallk. 59, 822 (1968); A. Holz, Phys. Stat. Sol. 25, 567 (1968); J. Appl. Phys. 41, 1095 (1970).

15. H. Zijlstra, Z. angew. Phys. 21, 6 (1966); IEEE Trans. Mag. 6, 179 (1070).

16. R. Carey and B.W.J. Thomas, J. Phys. D: Appl. Phys. 5, 200 (1972).

17. A. Aharoni, Rev. Mod Phys. 34, 227 (1962); Phys. Stat. Sol. 16, 3 (1966).

18. C. Abraham and A. Aharoni, Phys. Rev. 128, 2496 (1962).

19. H. Zijlstra and H. B. Haanstra, J. Appl. Phys. 37, 2853 (1966).

20. R. Becker and W. Döring, Ferromagnetismus, Springer, Berlin (1939), p. 192.

21. L. J. Dijkstra, in Thermodynamics in Physical Metallurgy, American Society for Metals, Cleveland (1950), p. 271.

22. R. Carey, J. E. Coleman, and I. V. F. Viney, Proc. Roy. Soc. London A328, 143 (1972).

23. H. Zijlstra, J. Appl. Phys. 41, 4881 (1970).

24. P. Haasen, Mater. Sci. Eng. 9, 191 (1972).

25. F. F. Westendorp, Sol. State Commun. 8, 139 (1970).

26. H. Zijlstra, J. Appl. Phys. 42 1510 (1971).

27. J. J. van den Broek and H. Zijlstra, IEEE Trans. Mag. 7, 226 (1970).

28. D. J. Craik, Proc. Internat. Conf. on Magnetism, Nottingham, Inst. of Physics and Physical Soc., London (1964), p. 693.

29. E. A. Nesbitt, G. Y. Chin, G. W. Hull, R. C. Sherwood, M. L. Green and J. H. Wernick, Proc. 1972 Conf. on Magnetism and Magnet Materials, A. I. P. Conf. Proc. 10, (1973).

30. J. J. Becker, IEEE Trans. Mag. 4, 239 (1968).

31. J. J. Becker, J. Appl. Phys. 39, 1270 (1968).

32. D. J. Craik and D. A. McIntyre, Phys. Letters 21, 288 (1966).

33. M. Rosenberg, C. Tanasoiu, and V. Florescu, Phys. Letters 23, 540 (1966).

34. Ya. S. Shur and V. I. Khrabrov, Sov. Phys. -JETP 30, 1027 (1970).

35. Ya. S. Shur, E. V. Shtol'ts, and V. L. Margolina, Sov. Phys. -JETP 11, 33 (1960).

36. Ya. S. Shur, A. V. Deryagin, T. V. Sysolina, and G. S. Kandaurova, Phys. Met. Metallog. 30, 12 (1970).

37. J. J. Becker, J. Appl. Phys. 42, 1537 (1971).

38. J. J. Becker, IEEE Trans. Mag. 7, 644 (1971).

39. J. J. Becker, IEEE Trans. Mag. 5, 211 (1969).

40. R. C. Sherwood, J. P. Remeika, and H. J. Williams, J. Appl. Phys. 30, 217 (1959).

41. J. J. Becker, IEEE Trans. Mag. 8 (1972).

42. S. Reich, S. Shtrikman, and D. Treves, J. Appl. Phys. 36, 140 (1965).

43. J. J. Becker, Proc. 1971 Conf. on Magnetism and Magnetic Materials, A. I. P. Conf. Proc. 5, 1067 (1972).

44. K. J. Strnat, J. C. Olson, and G. Hoffer, Proc. 6th Rare Earth Res. Conf., Gatlinburg, Tenn., 603 (1967).

45. K. J. Strnat, J. C. Olson, and G. Hoffer, J. Appl. Phys. 39, 1263 (1968).

46. R. A. McCurrie, G. P. Carswell, and J. B. O'Neill, J. Mater. Sci 6, 164 (1970).

47. R. A. McCurrie and G. P. Carswell, J. Mater. Sci. 5, 825 (1970).

48. K. H. J. Buschow, P. A. Naastepad, and F. F. Westendorp, J. Appl. Phys. 40, 4029 (1969).

49. F. F. Westendorp, IEEE Trans. Mag. 6, 472 (1970).

50. J. J. Becker and R. E. Cech, U. S. Patent No. 3, 615, 914, filed 1968, patented 1971.

51. J. J. Becker, J. Appl. Phys. 38, 1015 (1967).

52. R. A. McCurrie, Phil. Mag. 22, 1013 (1970).

53. R. A. McCurrie and G. P. Carswell, Phil. Mag. 2, 333 (1971).

54. F. A. J. den Broeder and K. H. J. Buschow, J. Less-Common Metals 29, 65 (1972).

55. K. H. J. Buschow, ibid., p. 283.

56. F. F. Westendorp, J. Appl. Phys. 42, 5727 (1971).

57. J. D. Livingston, J. Appl. Phys., 43, 4756 (1972).

58. J. D. Livingston, J. Mater. Sci., to be published.

59. K. H. J. Buschow and A. S. van der Goot, J. Less-Common Metals 17, 249 (1969).

60. J. D. Livingston, unpublished research.

61. D. L. Martin and M. G. Benz, Cobalt 50, 11 (1971).

62. M. G. Benz and D. L. Martin, J. Appl. Phys. 42, 2786 (1971).

63. M. G. Benz and D. L. Martin, Proc. 1971 Conf. on Magnetism and Magnetic Materials, A. I. P. Conf. Proc. 5, 1082 (1972).

64. R.J. Charles, D.L. Martin, L. Valentine, and R.E. Cech, _ibid._, p. 1072.

65. R.E. Cech, J. Appl. Phys. **41,** 5247 (1970).

66. D.K. Das, IEEE Trans. Mag. **7,** 432 (1971).

67. M.G. Benz and D.L. Martin, J. Appl. Phys. **43,** 3165 (1972).

68. M.G. Benz, D.L. Martin, and A.C. Rockwood, Proc. 1972 Conf. on Magnetism and Magnetic Materials, A.I.P. Conf. Proc. **10,** (1973).

69. A. Menth, Proc. 1972 Conf. on Magnetism and Magnetic Materials, A.I.P. Conf. Proc. **10,** (1973).

70. M.G. Benz and D.L. Martin, Appl. Phys. Letters **17,** 176 (1970).

71. J. Schweizer, K.J. Strnat, and J.B.Y. Tsui, IEEE Trans. Mag. **7,** 429 (1971).

72. D.L. Martin and M.G. Benz, IEEE Trans. Mag. **8,** (1972).

73. M.G. Benz and D.L. Martin, J. Appl. Phys., to be published.

74. R.A. McCurrie, Proc, 1972 Conf. on Magnetism Magnetic Materials, A.I.P. Conf. Proc. **10,** (1973).

75. P. Gaunt, J. Appl. Phys. 43, 637 (1972).

76. F.G. Jones, J.D. Livingston, and J.G. Smeggil, unpublished research.

77. F.G. Jones, H.E. Lehman, and J.G. Smeggil, IEEE Trans. Mag. **8,** (1972).

78. O.A.W. Strydom and L. Alberts, J. Less-Common Metals **22,** 503 (1970).

79. A.E. Ray, H. Mildrum, K. Strnat, and R. Harmer, Suppl. J. de Physique **32,** C1-554 (1971).

80. H. Mildrum, A.E. Ray, and K. Strnat. Proc. 8th Rare Earth Res. Conf. Vol. 1, 21 (1970).

81. K. Strnat, Cobalt **36,** 133 (1967).

82. K. Strnat, A.E. Ray, and C. Herget, Suppl. J. de Physique **32,** C1-552 (1971).

83. K. Strnat and J. Tsui, Proc. 8th Rare Earth Res. Conf., Vol. 1, 3 (1970).

73CRD135

J. D. Livingston

DOMAINS IN SINTERED Co_5Sm MAGNETS

TECHNICAL INFORMATION SERIES

AUTHOR Livingston, JD	SUBJECT permanent magnet materials	NO. 73CRD135
		DATE April 1973
TITLE Domains in Sintered Co$_5$Sm Magnets		GE CLASS 1
		NO. PAGES 8
ORIGINATING COMPONENT Metallurgy and Ceramics Laboratory		CORPORATE RESEARCH AND DEVELOPMENT SCHENECTADY, N.Y.

SUMMARY

Magnetic domains in high-coercivity sintered Co$_5$Sm magnets have been studied using polarized light. Grain boundaries block the propagation of magnetic reversal from grain to grain. General domain-wall pinning is low, and oversized grains show low-coercivity, multidomain behavior. In most grains, however, once domain walls are removed, large reverse fields are required to nucleate magnetization reversal.

KEY WORDS   permanent magnets, coercive force, magnetic domain, cobalt-rare earths

DOMAINS IN SINTERED Co$_5$Sm MAGNETS

J. D. Livingston

I. INTRODUCTION

There have been several previous studies of magnetic domains in cobalt-rare earth compounds (Refs. 1-11). However, these studies have been limited to large crystals or small isolated particles, whereas commercial magnets are sintered assemblies of small particles. We report here polarized-light studies of domain structures and magnetization processes in high-coercivity sintered Co-Sm and Co-Pr-Sm magnets.

II. EXPERIMENTAL TECHNIQUE

Details of the manufacturing methods used to produce Co$_5$Sm-based magnets have been published (Refs. 12, 13). Briefly, castings are ground to fine powder, blended with a Sm-rich powder (to aid sintering), aligned in a large magnetic field, pressed, sintered to high density, and heat treated to increase coercivity. Most of the grains in the resulting magnet are aligned with their easy magnetic axis, i.e., the hexagonal axis, parallel to the magnet axis. Table I characterizes the magnets which appear in the subsequent figures.

Magnetic domains were observed with polarized light in normal incidence using either a Zeiss or Bausch and Lomb metallograph. Domain contrast is produced by the polar Kerr effect, which depends on the component of magnetization normal to the surface.[17] Therefore, metallographic sections were usually prepared transverse to the magnet axis, in order to optimize domain contrast. (The magnetocrystalline anisotropy of Co$_5$Sm is so high that we can assume that the magnetization always remains parallel to the hexagonal axis.)

Contrast with polarized light can also result from crystallographic effects, but on a transverse section of an aligned sample such contrast can occur only from misaligned grains or other phases. Crystallographic contrast reverses sign when the sample is rotated by 90°, whereas magnetic contrast does

not, since such a rotation does not change the normal component of magnetization. Such a rotation, coupled with observation of the changes produced by magnetic fields, was used to distinguish magnetically reversed grains from misaligned grains. Fields up to 3000 Oe could be applied to the specimen while mounted on the metallograph, employing a special specimen holder containing a large movable permanent magnet. To study the effects of larger fields, samples were removed from the metallograph. Fields were applied to the samples in an electromagnet, reduced to zero, and then the sample was returned to the metallograph for observation of the domain structure.

Domain studies were usually made on freshly polished, unetched surfaces, but etches were necessary to bring out various microstructural features. An etch in 1% nital followed by a rinse in 5% hydrol revealed interphase boundaries (Figs. 1a through c), and an etch consisting of 10 CH$_3$COOH, 10 H$_2$O, 10 HNO$_3$, and 40 HCl was used to reveal grain boundaries in the Co$_5$Sm phase (Fig. 1d).

III. MICROSTRUCTURE

Detailed phase analysis of sintered Co$_5$Sm magnets has been reported elsewhere.[18] The most prominent features in most micrographs are the large voids resulting from incomplete sintering. These voids are generally associated with Sm$_2$O$_3$, and appear dark on bright-field micrographs (Fig. 1a through c). Also visible are many micron-sized features, which are often small voids and/or Sm$_2$O$_3$ particles, but may in some cases be metallic phases. Hyper-stoichiometric (excess Sm) magnets contain appreciable amounts of Co$_7$Sm$_2$ (Fig. 1a), while hypostoichiometric magnets contain much Co$_{17}$Sm$_2$, largely along grain boundaries (Fig. 1b). Also commonly observed is a darker, not-yet-identified, Sm-rich phase (Fig. 1c).[18] Optimum magnetic properties are attained at a slightly hyperstoichiometric composition (Ref. 14). At this composition, several percent of Co$_7$Sm$_2$ and about one percent of the Sm-rich phase are usually present. The grain structure in the Co$_5$Sm phase is seen in Fig. 1d (and in Ref. 19). The average grain size in the magnets studied was about 10μ.

IV. MAGNETIC DOMAINS

The initial domain structure of a thermally demagnetized magnet in zero external field is shown in Fig. 2a. The light and dark regions are domains of opposite magnetization, i.e., magnetization directed out of or into the surface. The very bright regions are voids. Comparisons of domain structures with grain structures reveal that most grains contain domain walls in the thermally demagnetized condition, and that domain walls are usually continuous from grain to grain.

TABLE I

Characterization of Magnets

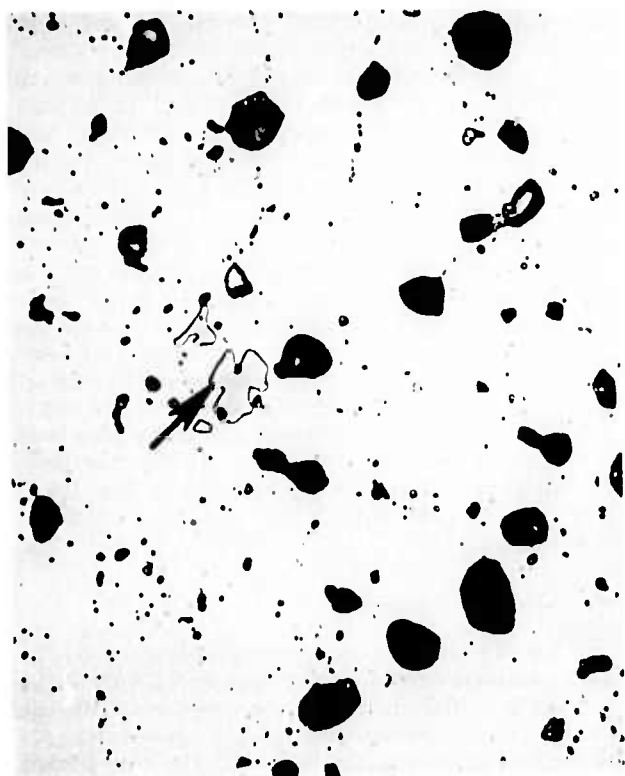| Figure	Composition (at. % Sm)*	Intrinsic Coercivity (Oe)	Length/Diam.	Remarks
1a	17.8	8,700	--	Sample L, Ref. 14
1b	16.2	2,700	--	A, Ref. 14
1c	16.8	16,800	--	F, Ref. 14
1d	18.8	16,800	--	
2	17.1	17,500	0.2	A, Ref. 15
3	17.1	17,500	5	
4	7.8 Sm, 9.6 Pr (unadj.)	12,800	5	--
5	17.1	22,500	4	900°C, Ref. 16
6a	14	Low	--	
6b	17.6	8,700	--	L, Ref. 14

*Adjusted by subtracting Sm tied up in Sm$_2$O$_3$.

Fig. 1 Microstructure of sintered Co_5Sm magnets: (a) hyperstoichiometric, showing Co_7Sm_2: (b) Hypo-stoichiometric, showing $Co_{17}Sm_2$: (c) near-stoichiometric, showing Sm-rich phase; and (d) near-stoichiometric, etched to reveal Co_5Sm grain boundaries, photographed using Nomarski contrast.   1000X

(a)
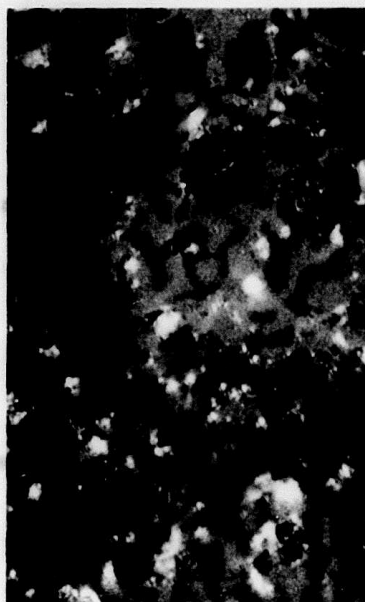
Fig. 2 Domain-wall motion in thermally demagnetized magnet: (a) initial domain structure, (b) field applied, and (c) field removed. 1000X. Bright spots in this and subsequent figures are voids.


(b)

Fig. 2 (Continued)

(c)

Fig. 2 (Continued)

Gradual application of a magnetic field normal to the surface caused a gradual growth of the lighter domains at the expense of the darker domains (Fig. 2b). On the scale of observation, the domain walls moved smoothly. Although the external field applied to this thin, disk-shaped sample was about 3000 Oe, because of the large demagnetizing field the internal field was at most a few hundred Oe. Removal of the applied field resulted in a re-expansion of the darker domains until at zero field (Fig. 2c) the domains had returned to nearly their initial positions. Thus domain walls, once present in the grains of a sintered magnet, move nearly reversibly at low internal fields.

A long cylindrical magnet of low demagnetizing factor was used in a study of zero-field domain structures after the application of large magnetic fields. The magnet was magnetized in a field of 21,000 Oe, the applied field was removed, and the magnet was returned to the metallograph. Contrast was set so that magnetically reversed regions appeared light. For example, region A in Fig. 3a shows a domain structure and therefore has partially reversed. Most of the other grains remain fully magnetized and appear dark. [The other light regions in Fig. 3a (B and C) are misaligned grains, as can be seen by the reversal of their contrast in Fig. 3b, which was taken with the sample in a position rotated 90° from that of Fig. 3a. Similarly, the light hexagonal grain D near the center of Figs. 3b through e is a misaligned grain.]
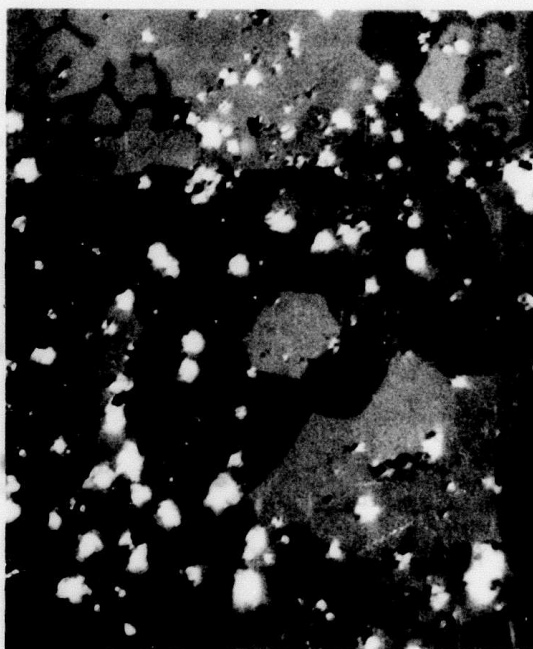
(a)
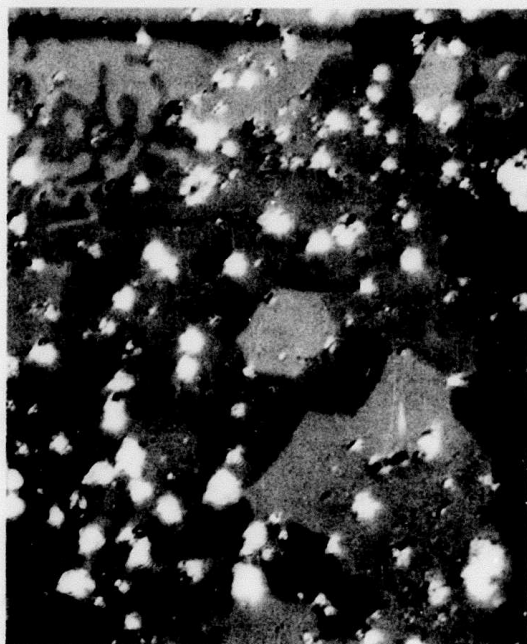
(c)

(b)

(d)

Fig. 3 Progressive reversal of initially magnetized magnet, showing effectiveness of grain boundaries as a magnetic barrier. Zero-field structures after (a) magnetization at 21,000 Oe, and subsequent exposure to reversing fields of (b) 4,800 Oe, (c) 10,000 Oe, (d) 17,500 Oe, and (e) 19,000 Oe. 1000X. Plane of polarization for (a) was at 90° to that for (b) through (e).

(e)

Fig. 3 (Continued)

Various reverse fields were then applied and
removed, and the magnetization changes resulting
are seen in Figs. 3b through e. Increasing magnetic
reversal appears as increasing proportions of light-
contrast areas. A reverse field of 4800 Oe produced
very little change, but 10,000 Oe produced substantial
reversal. Regions E and F, unreversed after expo-
sure to 10,000 Oe, were reversed after exposure to
17,500 Oe. An increase to 19,000 Oe reversed re-
gion G and eliminated the domain walls in region H.
[A multidomain region such as H in Fig. 3d was un-
doubtedly nearly saturated by the reverse field of
17,500 Oe. However, some residual domains mag-
netized in the initial direction were presumably still
present, and expanded on return to zero field to pro-
duce the domain structure shown. Apparently these
residual domains were eliminated by a reverse field
of 19,000 Oe, allowing region H to remain reversed
on return to zero field (Fig. 3e).]

As is clear from Figs. 2 and 3, the domain
structures of Co-Sm magnets are very sensitive to
magnetic history. Although most grains contain
domain walls in the thermally demagnetized state
(Fig. 2), most are single-domain, i.e., fully mag-
netized in one direction or the other, while traversing
a hysteresis loop after magnetization in a high field
(Fig. 3). However, it is observed that oversized
grains commonly show multidomain structures re-
gardless of magnetic history, e.g., grain A in Fig. 4a
and grains B and C in Fig. 4b. (The net magnetiza-
tions of grains B and C are nonzero and opposite in

sign, presumably because of differing local fields.)
An unusual exception is grain D in Fig. 4b, which,
despite its large size, has retained its initial direc-
tion of magnetization even after exposure to a reverse
field of 11,000 Oe.

Despite microscopic variations, the magnetization
reversal of sintered Co₅Sm magnets is usually macro-
scopically homogeneous. However, magnets quenched
in water after a high-temperature heat treatment
sometimes show thick surface layers that reverse at
much lower fields than the bulk of the magnet (Fig. 5).
This observation provides an explanation for the
severe low-field kinks observed in the magnetization
curves of these specimens. [16] The cause of the low-
coercivity surface layer has not yet been conclusively
established, but may be deformation from thermal
stresses during the quench.
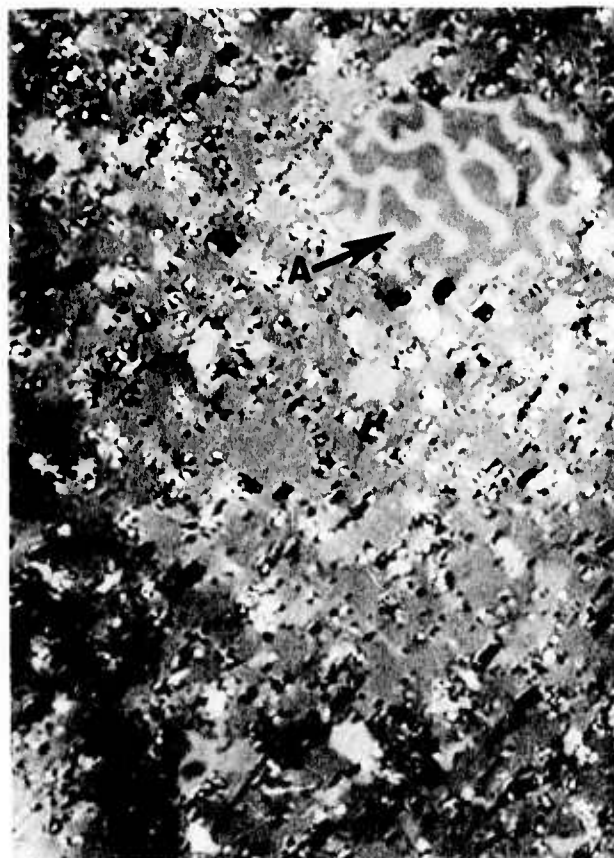
(a)

Fig. 4 Multidomain structures in oversized grains.
Zero-field structures after (a) magnetization at
21,000 Oe and (b) different area after exposure
to reversing field of 11,000 Oe.   1000X
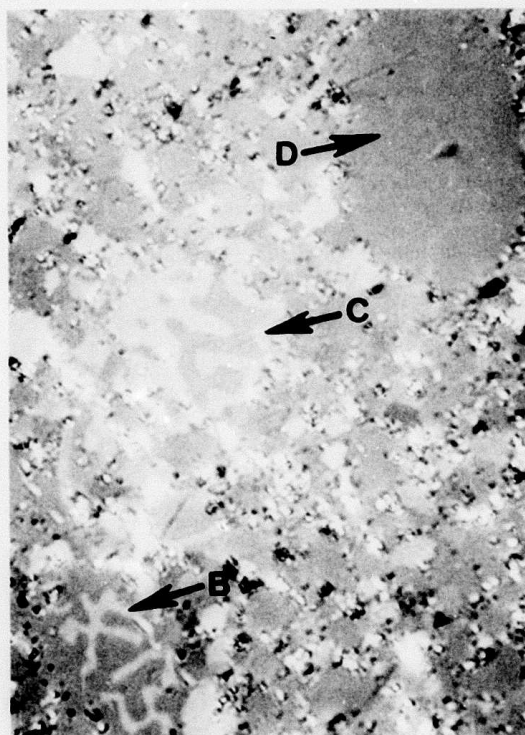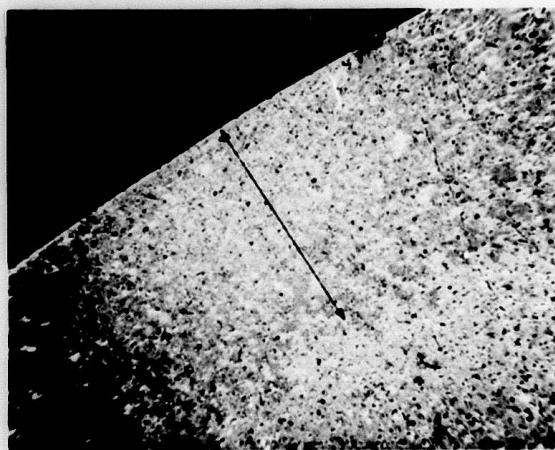
(b)

Fig. 4 (Continued)

Fig. 5 Low-coercivity surface layer on water-quenched magnet. Sample demagnetizing field has reversed magnetization of surface layer, which appears dark compared to bulk. 102X

Domain observations can also provide a simple technique for distinguishing $Co_{17}Sm_2$ grains from Co_5Sm grains in Co-rich magnets (Fig. 6a) because of the characteristically finer domain patterns in $Co_{17}Sm_2$.[11] On the other hand, domains in Co_7Sm_2 grains are of similar spacing to those in Co_5Sm,[11] and may even be continuous with the domain structure in surrounding Co_5Sm grains (Fig. 6b). No domain structure has been observed within the Sm-rich particles (Fig. 1c).

V. DISCUSSION

Despite the complex microstructure of sintered Co_5Sm magnets, the above observations indicate that the magnetic behavior of the individual grains is in many ways similar to that of isolated Co_5Sm particles, as discussed in a recent review.[20] Large grains usually act as multidomain particles with a low coercive force, regardless of magnetic field history (Fig. 4). Smaller grains, when in a thermally demagnetized state, also contain domain walls and are easily magnetizable in low fields (Fig. 2). Such behavior is characteristic of materials in which general domain-wall pinning is low.

When domain walls are driven out by magnetization in a high field, the magnetic behavior of most grains is very different (Fig. 3). Grains retain their initial direction of magnetization to large reverse fields because of the difficulty of nucleating reverse domains. Once reversal is nucleated, some grains reverse completely and thereby show "square loop" behavior, i.e., their zero-field state is fully magnetized in one direction or the other. In others, residual domains of the original direction of magnetization are retained, leading to demagnetized multidomain regions on return to zero field (e.g., H in Fig. 3d). However, larger reverse fields apparently remove these residual domains and produce "square loop" behavior (H in Fig. 3e). These various observations are characteristic of materials in which magnetization reversal is controlled by the nucleation of reverse domains, and are similar to earlier observations on isolated particles of Co_5Sm.[21-23]

This similarity results from the ability of boundaries between sintered grains to serve as barriers to the propagation of magnetization reversal. In Fig. 3e, for example, a closed loop of grain boundaries separates a group of unreversed grains from the surrounding reversed region. Although domain walls which already cross grain boundaries can move easily in a direction along the grain boundary (Fig. 2), a domain wall cannot easily move across a grain boundary, i.e., propagate magnetization reversal from one grain to another.

It is this barrier property of grain boundaries that makes possible the high coercivities and energy products attainable in sintered magnets. It is not known, however, whether the barrier property results
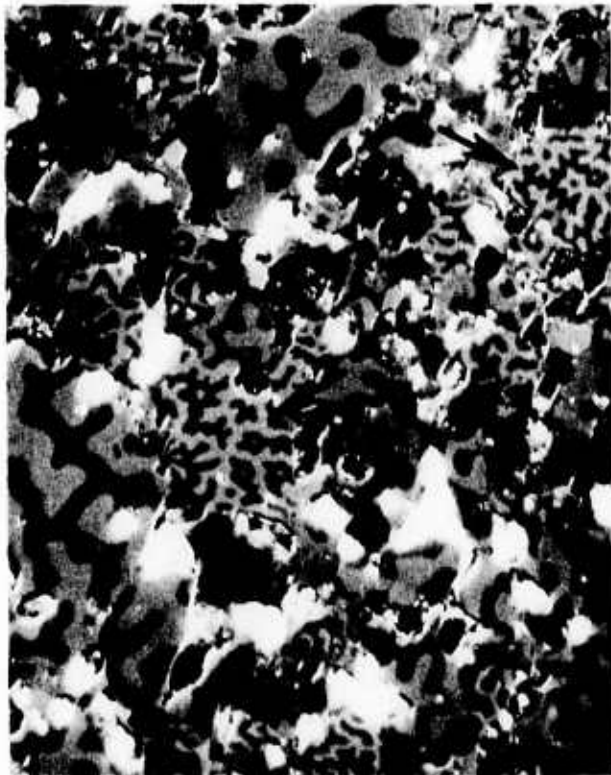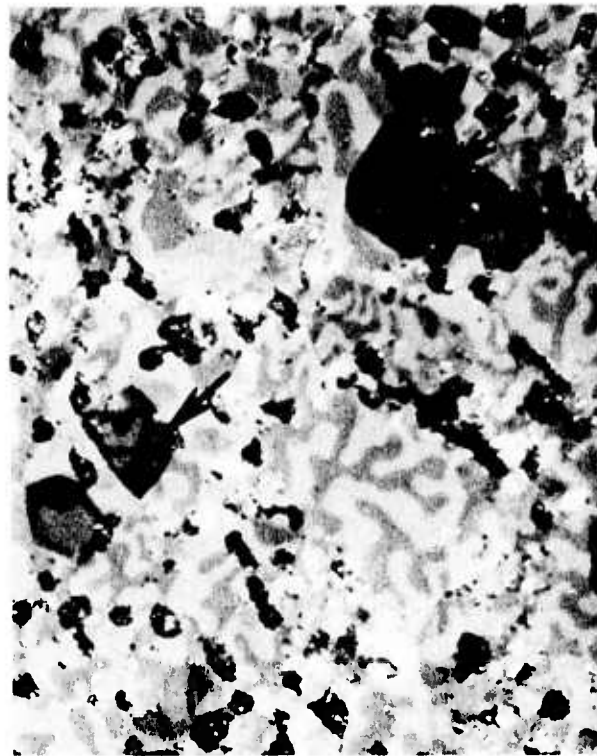
<div align="center">(a)   (b)</div>

Fig. 6 Domains in neighboring phases: (a) large $Co_{17}Sm_2$ regions show finer domain structure than Co_5Sm, and (b) dark Co_7Sm_2 regions show domains continuous with surrounding Co_5Sm.   1000X

from the inherent grain boundary structure or from chemical inhomogenities in the boundary. It is possible that some of the known effects of processing variables (sintering time and temperature, composition, heat treatment) on coercivity are caused by chemical and physical changes in the grain boundary that affect its ability to serve as a magnetic barrier.

It is known that, in hypostoichiometric magnets, $Co_{17}Sm_2$ precipitates along the grain boundaries (Fig. 1b). Such precipitates probably provide easy nuclei for magnetization reversal in each grain, and may explain the low coercivities observed in this composition range.[14] In contrast, the Co_7Sm_2 and Sm-rich inclusions (Figs. 1a and c, respectively) appear in only a small fraction of the grains and apparently are less deleterious to coercivity. [However, even in hyperstoichiometric magnets a $750^\circ C$ anneal drastically reduces coercivity, perhaps because of a grain boundary precipitation of fine $Co_{17}Sm_2$ particles.[24]]

The low-coercivity, multidomain behavior usually observed in oversized grains (Fig. 4) suggests that removal of oversized grains from the ground powders would improve magnet properties.

VI. SUMMARY

The boundaries between sintered grains act as a barrier to the propagation of magnetic reversal. As a result, the magnetic behavior of grains in sintered Co_5Sm magnets is similar to that of isolated Co_5Sm particles.

Domain walls in thermally demagnetized magnets move easily, indicating general wall pinning is low. Oversized grains show low-coercivity, multidomain behavior regardless of magnetic history. However, in most grains, once domain walls are removed by magnetizing in a high field, large reverse fields are required to nucleate magnetization reversal. If the reversing field is large enough to remove residual domains, reversed grains remain fully reversed on return to zero field.

Kerr effect domain contrast was also useful in identifying second-phase grains and in locating gross magnetic inhomogeneities, such as a low-coercivity surface layer on water-quenched magnets.

ACKNOWLEDGMENTS

REFERENCES

1. R. A. McCurrie and G. P. Carswell, J. Mater. Sci. **5**, 825 (1970).

2. R. A. McCurrie, G. P. Carswell, and J. B. O'Neill, J. Mater. Sci. **6**, 164 (1970).

3. K. Bachmann, A. Bischofberger, and F. Hofer, J. Mater. Sci. **6**, 169 (1971).

4. K. Bachmann and F. Hofer, Z. angew. Phys. **32**, 41 (1971).

5. K. Bachmann, IEEE Trans. Mag. **7**, 647 (1971).

6. R. G. Wells and D. V. Ratnam, IEEE Trans. Mag. **7**, 651 (1971).

7. D. V. Ratnam and R. G. Wells, Proc. 1972 Conf. on Magnetism and Magnetic Materials, AIP Conf. Proc. **10** (1973).

8. F. F. Westendorp, J. Appl. Phys **42**, 5727 (1971).

9. F. F. Westendorp, Appl. Phys. Letters **20**, 441 (1972).

10. J. D. Livingston and M. D. McConnell, J. Appl. Phys. **43**, 4756 (1972).

11. J. D. Livingston, J. Mater. Sci. **7**, 1472 (1972).

12. M. G. Benz and D. L. Martin, Appl. Phys. Letters **17**, 176 (1970).

13. D. L. Martin and M. G. Benz, Proc. 1971 Conf. on Magnetism and Magnetic Materials, AIP Conf. Proc. **5**, 970 (1970).

14. D. L. Martin, M. G. Benz, and A. C. Rockwood, Proc. 1972 Conf. on Magnetism and Magnetic Materials, AIP Conf. Proc. **10**, (1973).

15. M. G. Benz and D. L. Martin, Proc. 1971 Conf. on Magnetism and Magnetic Materials, AIP Conf. Proc. **5**, 1082 (1972).

16. F. G. Jones, H. E. Lehman, and J. G. Smeggil, IEEE Trans. Mag. **8**, 555 (1972).

17. R. Carey and E. D. Isaac, Magnetic Domains and Techniques for Their Observation, Academic Press, New York (1966), p. 67.

18. J. G. Smeggil, 1972 Intermag. Conf., Washington, D. C., April 1972.

19. M. G. Benz and D. L. Martin, J. Appl. Phys. **43**, 3165 (1972).

20. J. D. Livingston, Proc. 1972 Conf. on Magnetism and Magnetic Materials, AIP Conf. Proc. **10** (1973).

21. J. J. Becker, IEEE Trans. Mag. **5**, 211 (1969).

22. J. J. Becker, J. Appl. Phys. **42**, 1537 (1971).

23. J. J. Becker, IEEE Trans. Mag. **7**, 644 (1971).

24. F. A. J. den Broeder and K. H. J. Buschow, J. Less-Common Metals **29**, 65 (1972).

72CRD078

D. L. Martin and M. G. Benz

TEMPERATURE VARIATION OF COERCIVITY
FOR Co-Sm PERMANENT MAGNET ALLOYS

143<

TECHNICAL INFORMATION SERIES

AUTHOR Martin, DL Benz, MG	SUBJECT permanent magnets	NO 72CRD078
		DATE March 1972
TITLE Temperature Variation of Coercivity For Co-Sm Permanent Magnet Alloys		GE CLASS 1
		NO. PAGES 3

ORIGINATING COMPONENT
Metallurgy and Ceramics Laboratory

CORPORATE RESEARCH AND DEVELOPMENT SCHENECTADY, N.Y.

SUMMARY The demagnetization properties of a series of sintered Co-Sm magnets have been measured over the range 0° to 750°K. The intrinsic coercive force of the samples varied from 19 to 65 kOe at 27°K, but decreased with increasing temperature to zero at about 700°K. The relative change of coercivity with temperature was the same for all the samples. Thus, it appears that the factors which influence the magnitude of coercivity do not influence the temperature dependence.

KEY WORDS

permanent magnets, temperature-dependent coercivity, cobalt-rare earths

INFORMATION PREPARED FOR _____

144<

TEMPERATURE VARIATION OF COERCIVITY FOR Co-Sm PERMANENT MAGNET ALLOYS*

D. L. Martin and M. G. Benz

INTRODUCTION

Changes in the magnetic properties of Co_5R permanent magnet alloys with temperature are of interest for two reasons:

1. The usefulness of a particular alloy will depend upon how much the magnetization of that alloy changes with temperature over the operating range of the device.

2. An understanding of how and why the changes in magnetization occur with changes in temperature might contribute to our overall understanding of the basic factors which govern coercivity. This property currently limits the performance of many Co_5R alloys.

A strong temperature dependence of intrinsic coercivity has been noted for Co_5La[1,2] and Co_5Sm (Refs. 2, 3) powder samples. The intrinsic coercive force, H_{ci}, for each alloy was observed to increase by a factor of two as the temperature decreased from 300° to 80°K. This change of coercivity with temperature continues with increasing temperatures above room temperature, decreasing as the temperature increases, and relates to the irreversible losses which occur when Co-Sm magnets are heated.[4]

Westendorp[5] has explained the increase of coercivity with decreasing temperature on the basis of an increase of domain-wall energy with decreasing temperature. He cited an increase of domain spacing by a factor of 1.5 between 300° and 90°K to explain the factor of two increase of coercive force over the same temperature range.

McCurrie[3] and Gaunt[6] have proposed that the observed temperature effect can be accounted for by a thermal activation process in which magnetization reversal is assisted by thermal energy. The simple model proposed is domain wall pinning by inhomogeneities.[6]

In this report we describe a study in which the magnetic measurements on sintered magnets have been extended to cover a wider temperature range 4.2° to 750°K, and have included samples with a wide variation of coercivity values due to variations in composition and processing.

EXPERIMENTAL

The sintered test bars were about 0.75 cm in diameter by 2.5 cm long. The magnetization was measured by a point-by-point ballistic method described previously.[7] The applied field was provided by either a 5 kOe copper solenoid or a 100 kOe superconducting solenoid. The sample and pickup coils were surrounded by suitable dewars. Below 80°K, measurements were made at the boiling points of helium, neon, and nitrogen. Between 80° and 300°K the system was first cooled with liquid nitrogen, and measurements were made as the sample heated slowly. Above 300°K the sample was heated by a small electric furnace. Sufficient data were obtained to plot the demagnetization curves at all the test temperatures, except above 500°K where only the H_{ci} value was determined. The usual procedure was to magnetize the sample in a 60 kOe field at room temperature before heating or cooling to the test temperature.

RESULTS

In Fig. 1 the demagnetization vs temperature results are plotted for a sintered Co-Sm magnet with the following room-temperature properties: $4\pi J$ (at 60 kOe) = 10 kG, B_r = 9.4 kG, H_c = -9.2 kOe, H_{ci} = -20 kOe, and $(BH)_{max}$ = 21.4 MGOe. The remanent magnetization $4\pi J_r$ and intrinsic coercive force H_{ci} increase significantly with decreasing temperature, except at very low temperatures. At 4.2°K the H_{ci} value was slightly lower than that measured at 27.1°K. After testing at high or low temperatures the properties at room temperature were recoverable by remagnetization.

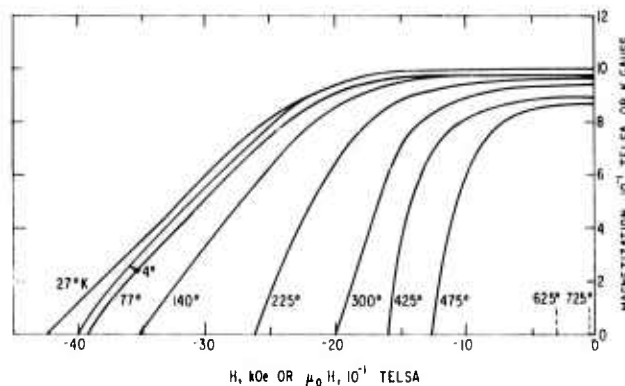A summary of the test results for a series of sintered magnets is presented in Fig. 2. The coercivity

Fig. 1 Variation of demagnetization characteristics of a Co-Sm magnet with measurement temperature.
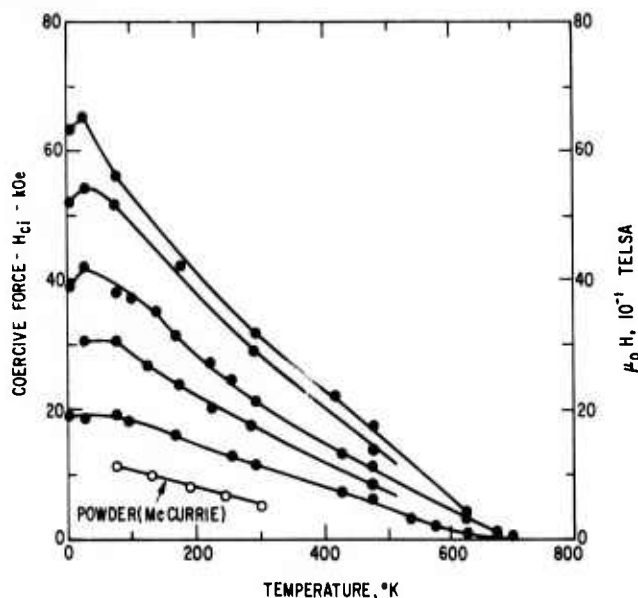
Fig. 2 Change of intrinsic coercive force with temperature for a series of Co-Sm magnet samples. The data for the powder are from McCurrie.[2]

Fig. 3 Relative coercivity vs temperature. The data in Fig. 2 have been normalized so that the relative coercivity at 77°K is 1.

was altered by varying the samarium composition slightly or by use of different post-sintering heat treatments.[8] Results by McCurrie[2] for Co_5Sm powder (particle size less than 20μ) are included for comparison. Several features stand out:

1. The highest value of H_{ci} measured was 65 kOe. This value is a substantial fraction of the anisotropy field [estimated to be about 200 kOe at 0°K from data given by Tatsumoto et al.[9]]; however, as pointed out by McCurrie,[2] at the H_{ci} point where the net magnetization is zero, only half the volume of the sample has been reversed. Still higher fields are required to reverse the magnetization of all the particles; therefore, many particles in the sample had H_{ci} values >> 65 kOe.

2. The coercivity for all the samples drops to zero at about 700°K.

3. Below 100°K the coercivity of some of the samples peaks near 27°K and then drops slightly; and in others only small changes occur with temperature.

It is interesting to note that when these data are normalized to the H_{ci} measured at 77°K, the points for all the samples fall on the same curve as shown in Fig. 3. From this we conclude:

1. Factors which influence the magnitude of H_{ci} at any temperature do not influence the relative change of coercivity with temperature.

2. Structural factors giving rise to a high intrinsic coercive force are most effective at low temperatures and least effective at high temperatures.
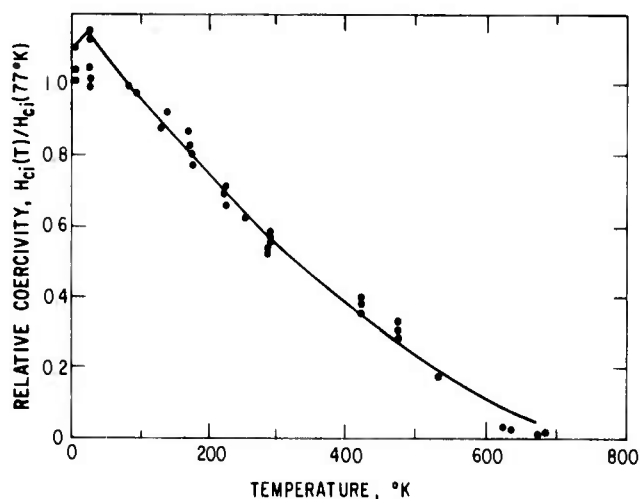
The temperature dependence of coercivity for Co-Sm magnets appears to correlate best with observations by Westendorp[4] regarding the change in domain wall energy with temperature.

ACKNOWLEDGMENTS

REFERENCES

1. W. A. J. J. Velge and K. H. J. Buschow, "Permanent Magnetic Properties of Rare Earth Cobalt Compounds (RCo_5)," Proc. IEE Conf. on Magnetic Materials and Their Applications, London, Sept. 1967, pp. 44-50.

2. R. A. McCurrie, "Determination of Intrinsic Coercivity Distributions in Aligned Assemblies of Uniaxial $SmCo_5$ and $LaCo_5$ Particles," Phil. Mag. 22, No. 179, 1013-1023 (1970).

3. R. A. McCurrie and G. P. Carswell, "Magnetic Hardness of the Intermetallic Compound $SmCo_5$ as a Function of Particle Size," Phil. Mag. 23, 333 (1971).

4. D. L. Martin and M. G. Benz, "Magnetization Changes for Cobalt-Rare Earth Permanent Magnet Alloys When Heated up to 650°C," IEEE Trans., MAG-8, 35 (March 1972).

5. F. F. Westendorp, "Domains in $SmCo_5$ at Low Temperature," Conference on Magnetism and Magnetic Materials, Chicago, Paper 3F-2 (Nov. 1971).

6. P. Gaunt, "Domain Wall Pinning as a Source of
    Magnetic Hardening in Alloys," J. Appl. Phys.
    43, 637 (1972).

7. M. G. Benz and D. L. Martin, "Measurement of
    Magnetic Properties of Cobalt-Rare Earth
    Permanent Magnets," IEEE Trans., MAG-7,
    285-291 (1971).

8. M. G. Benz and D. L. Martin, "Cobalt-
    Mischmetal-Samarium Permanent Magnet
    Alloys: Process and Properties," J. Appl. Phys.,
    42, 2786-2789 (1971).

9. E. Tatsumoto, T. Okamoto, H. Fujii, and C.
    Inoue, "Saturation Magnetic Moment and
    Crystalline Anisotropy of Single Crystals of
    Light Rare Earth Cobalt Compounds RCo_5,"
    J. Physique 32, C1, 550-551 (1971).

D.L. Martin, M.G. Benz, and A.C. Rockwood

COBALT-SAMARIUM PERMANENT MAGNET ALLOYS:
VARIATION OF LATTICE PARAMETERS
WITH COMPOSITION AND TEMPERATURE

TECHNICAL INFORMATION SERIES

AUTHOR Martin, DL Benz, MG Rockwood, AC	SUBJECT permanent magnets	NO. 72CRD310
		DATE November 1972
TITLE Cobalt-Samarium Permanent Magnet Alloys: Variation of Lattice Parameters with Composition and Temperature		GE CLASS 1
		NO. PAGES 4
ORIGINATING COMPONENT Metallurgy and Ceramics Laboratory		CORPORATE RESEARCH AND DEVELOPMENT SCHENECTADY, N.Y.

SUMMARY   Previous studies have shown that the magnetic prop-
erties of Co_5Sm permanent magnets are greatly improved
when the composition after sintering is hyperstoichiometric
(Sm rich).

In this study, x-ray lattice parameters, chemical
composition, phase identification by metallography and
magnetic properties have been measured for a series of
closely spaced composition, in order to determine conclu-
sively the phases present at the optimum composition.
From these observations, one can conclude that the peak
magnetic properties do indeed occur when the composition
is hyperstoichiometric; i.e., close to the $Co_5Sm-Co_7Sm_2$
phase boundary as determined by x-ray measurements,
16.85 at.% Sm as determined by measurements of the
chemical composition.

In addition, changes in lattice parameter with temper-
ture over the range 77° to $300^\circ K$ are reported.

KEY WORDS

permanent magnets, cobalt-samarium, lattice parameters

INFORMATION PREPARED FOR _____

COBALT-SAMARIUM PERMANENT MAGNET ALLOYS:
VARIATION OF LATTICE PARAMETERS WITH COMPOSITION AND TEMPERATURE

P. L. Martin, M. G. Benz, and A. C. Rockwood

INTRODUCTION

The peak magnetic properties for Co_5Sm-type magnets are obtained in alloys with samarium in excess of the stoichiometric composition, that is, about 37 wt% Sm vs 33.8 wt% Sm in Co_5Sm. [1-3] The samarium in the magnet sample may be present as cobalt-samarium alloy phases or as samarium oxide. Oxygen is unavoidable in these alloys because of the high reactivity of powders containing samarium. A sintered magnet might contain as much as 0.4 wt% oxygen. This amount of oxygen would combine with 2.5 wt% Sm to form 2.9 wt% Sm_2O_3. Therefore, it is important to adjust for Sm_2O_3 in determining the amount of samarium available to combine with the cobalt.

In a recent study, [4] we showed that the peak intrinsic coercive force, H_{ci}, occurred at an adjusted composition of 17.3 at.% samarium compared to 16.7 at.% samarium for stoichiometric Co_5Sm. A correlation was observed also between sintering shrinkage and coercive force. The alloys showing the greatest shrinkage also possessed the highest coercive force. A model for the mechanism of sintering was postulated where the slow step was the diffusion of samarium atoms in the grain-boundary regions via a samarium-atom-cobalt-vacancy cluster exchange mechanism. Central to the considerations advanced for the sintering model are the point defect structures which lead to a broad Co_5Sm, homogeneity region extending beyond the stoichiometric composition to higher samarium alloys. Such a region has been reported to exist above 800°C and, at 1200° to 1300°C to extend from 14.5 at.% Sm to the hyperstoichiometric composition of 17.0 at.% Sm. [5]

EXPERIMENTAL

The samples were prepared by careful blending of two powders using different ratios to vary the composition. The chemical compositions (wt%) of the base metal and additive powder were as follows:

	Co	Sm	O_2	Ni	Al
Base	65.4	33.9	0.24	0.05	0.05
Additive	39.4	59.6	0.76	0.19	<0.01

These powders were blended into 12 closely spaced mixes covering the range 16.25 to 17.5 at.% Sm after adjusting for Sm_2O_3. The blended powders were aligned, pressed, and sintered for 1 hour 1120°C in argon. The samples were cooled slowly from the sintering temperature to 900°C, and then rapidly in a cooling chamber. The chemical composition of Sample F was determined by analytical means as a check on the calculated compositions. Its composition was found to be: 64.0 wt% Co, 35.2% Sm, 0.05% Ni, 0.05% Al, and 0.33% O_2. This corresponds to an adjusted alloy

composition of 16.85 at.% Sm as compared to the value of 16.84 at.% Sm calculated from the analyses for the base metal and additive powders. This agreement is better than is to be expected in view of an experimental error of ±0.2 wt% for Co and Sm analysis; nevertheless, it does give credence to the accuracy of the blending procedure.

RESULTS AND DISCUSSION

X-ray Parameter Data.

The lattice parameters were determined from the powder diffraction x-ray data (Co-K_α and Fe-K_α radiation) by well-known methods. [6,7] The a_0 and c_0 results are plotted in Fig. 1 together with the density

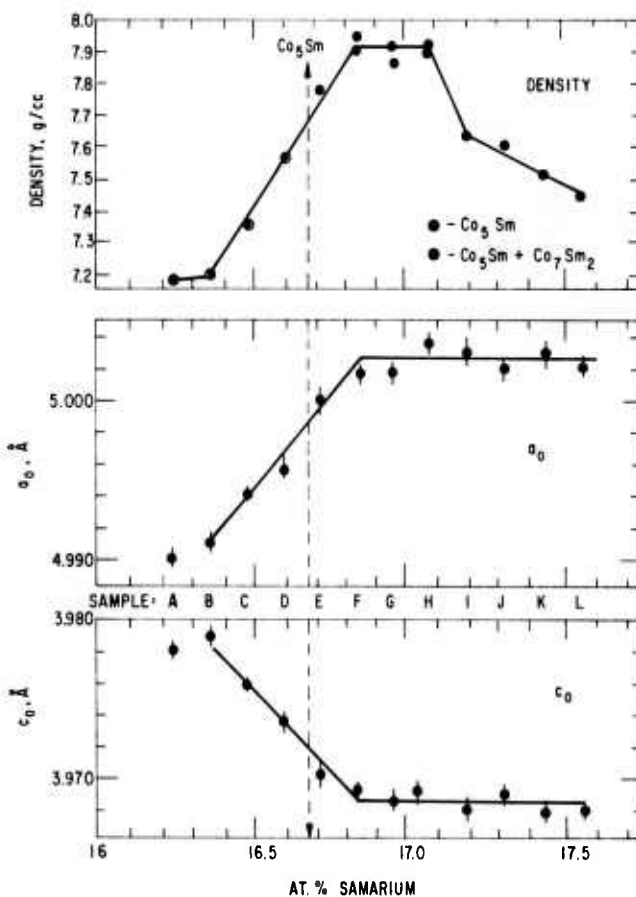Fig. 1 Change of Co_5Sm lattice parameters and density with adjusted samarium content.

The x-ray parameter values for Co_5Sm become constant for alloys containing more than 16.85 at.% Sm. The constant level of the x-ray parameters signifies a two-phase field, and the inflection point indicates the end of the Co_5Sm phase field and the beginning of the $Co_5Sm + Co_7Sm_2$ two-phase field. X-ray

diffraction methods are generally insensitive to small volume fractions of a second phase so that the presence of the Co_7Sm_2 phase was detected first by x-ray means in Sample 1 (17.2 at.% Sm). Microscopic examination is a more sensitive method and it showed small, isolated Co_7Sm_2 particles in Sample E (16.72 at.% Sm).

The change in the a_0 and c_0 lattice parameters with composition below 16.8 at.% Sm is evidence for the existence of a broad homogeneity range as already reported.[5, 8] While our results indicate that this homogeneity range extends slightly beyond the Co_5Sm stoichiometric composition to higher samarium alloys, the chemical analysis error is such that it is difficult to determine the absolute position of the stoichiometric composition.

The lattice parameter data are in good agreement with those published by others if one takes into consideration the measurement error. In Table 1, published x-ray data for Co_5Sm samples located near the Co_5Sm-Co_7Sm_2 boundary are compared with our data.

Density and Metallographic Results

Note in Fig. 1 that the density peaks near the Co_5Sm-Co_7Sm_2 boundary and falls rapidly a short distance on either side of the boundary.

The Co_7Sm_2 phase was detected by metallographic examination in Samples E to L. This would place the Co_5Sm-Co_7Sm_2 boundary at about 17.7 at.% Sm compared to a value of 17.85 at.% Sm as indicated by the break in the a_0 or c_0 curves.

Magnetic Measurements

The change of magnetic properties with composition is shown in Fig. 2. A summary of pertinent magnetic data and other information is listed in Table II. The highest values of coercive force and $(BH)_{max}$ are obtained in the same region where the

density peaks, and the lattice parameter values become constant. The magnetic properties, in particular the H_{ci} and H_c values, drop rapidly on either side of the boundary, although the drop is more severe on the cobalt-rich side than on the samarium-rich side. However, it should be noted that Samples C and D (16.48 and 16.60 at.% Sm), which do not
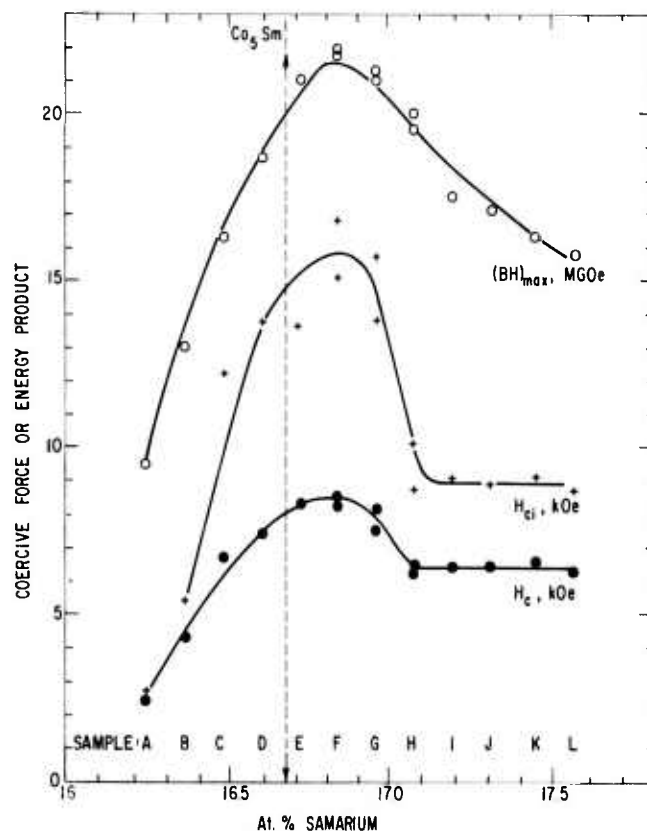
Fig. 2 Magnetic properties after sintering and aging as a function of the adjusted samarium content of the Co-Sm alloy phase or phases.

TABLE 1

X-ray Data for Co_5Sm Near the Co_5Sm-Co_7Sm_2 Boundary

Reference	Exptl Error (Å)	a (Å)	c (Å)	c/a	Vol. (Å³)
Umebayashi and Fujimura[8]	±0.002	5.004	3.969	0.793	86.17
Austin and Miller[9]	±0.002	5.002	3.969	0.793	86.10
Buschow and Van der Goot[5]	±0.005	4.995	3.965	0.794	85.74
Velge and Buschow[10]	±0.005	5.004	3.969	0.793	86.14
Haszko[11]	±0.005	5.004	3.971	0.794	86.18
This study--Sample E	±0.001	5.000	3.972	0.794	86.08
This study--Sample F	±0.001	5.0015	3.9692	0.794	86.08
This study--Sample G	±0.001	5.0017	3.9686	0.793	86.08
Average		5.002	3.969	0.793	86.07

Table II

Summary of Data for a Co-Sm Alloy Series

Sample	At. % Sm*	Co_7Sm_2	$4\pi J_s$ (kG)	B_r (kG)	H_c (kOe)	jHc kOe	$(BH)_{max}$ (MGOe)	Density (g/cc)
A	16.24	No	10.4	8.4	2.4	2.7	9.5	7.18
B	16.36	No	10.4	8.6	4.3	5.4	13.0	7.20
C	16.48	No	10.3	8.7	6.7	12.2	16.3	7.36
D	16.60	No	10.4	9.0	7.4	13.7	18.7	7.57
E	16.72	Yes	10.4	9.3	8.3	13.6	21.0	7.78
F	16.84	Yes	10.4	9.5	8.5	16.8	21.9	7.94
F-2	16.84	Yes	10.4	9.4	8.2	15.1	21.8	7.91
G	16.96	Yes	10.3	9.3	8.1	15.7	21.3	7.92
G-2	16.96	Yes	10.3	9.3	7.5	13.8	21.0	7.87
H	17.08	Yes	10.1	9.1	6.5	10.1	19.5	7.90
H-2	17.08	Yes	10.3	9.2	6.2	8.7	20.0	7.93
I	17.20	Yes †	9.9	8.6	6.4	9.1	17.5	7.64
J	17.32	Yes †	9.8	8.5	6.4	8.9	17.1	7.61
K	17.45	Yes †	9.6	8.3	6.6	9.1	16.3	7.53
L	17.56	Yes †	9.6	8.2	6.3	8.7	15.8	7.45

* Calculated on assumption that oxygen forms Sm_2O_3.
† Detected by x-ray as well as by metallographic examination.

contain Co_7Sm_2, have relatively high values of coercive force. Beyond 17.1 at. % Sm, the coercive force (H_{ci} and H_c) level out with increasing samarium.

The high $(BH)_{max}$ values for the samples E, F, and G reflect the higher density of those samples (Fig. 1 or Table II). The coercive force generally follows the density trend, the exception being Sample H (17.08 at. % Sm) where the coercive force dropped and the density remained at a high level. At substantially higher sintering temperatures, a high H_{ci} will not occur, even though higher densities will be achieved.

Lattice Parameters vs Temperature

The change of lattice parameters over the temperature range 77° to 300°K are plotted in Fig. 3. The a_0 and c_0 parameters increase with increasing temperature but the c/a ratio decreases with increasing temperature. The thermal expansion coefficients calculated from these data for the temperature range -20° to +24°C are:

$$\alpha_{a_0} = 12.24 \times 10^{-6} \ /^\circ C$$

$$\alpha_{c_0} = 4.00 \times 10^{-6} \ /^\circ C$$

$$\alpha_{vol.} = 28.94 \times 10^{-6} \ /^\circ C$$

SUMMARY

We conclude that the peak coercive force and energy product values occur when the alloy composition is close to the Co_5Sm-Co_7Sm_2 boundary (16.8 at. % Sm after adjustment for the formation of Sm_2O_3).

The highest magnetic properties have been achieved for samples with a small amount of Co_7Sm_2. Samples located in the single phase, Co_5Sm region or with more than a few volume percent of Co_7Sm_2 have lower density when sintered under similar conditions and lower magnetic properties. Previously we observed a similar correlation and postulated that the high coercive force and rapid sintering observed in the hyperstoichiometric alloys may be due to the presence of cobalt-vacancy-clusters in the grain-boundary region.[4]

The change of the x-ray lattice parameters over the range 77° to 300°K was measured, and thermal expansion coefficients were calculated. The a-axis thermal expansion being about three times that of the c-axis.
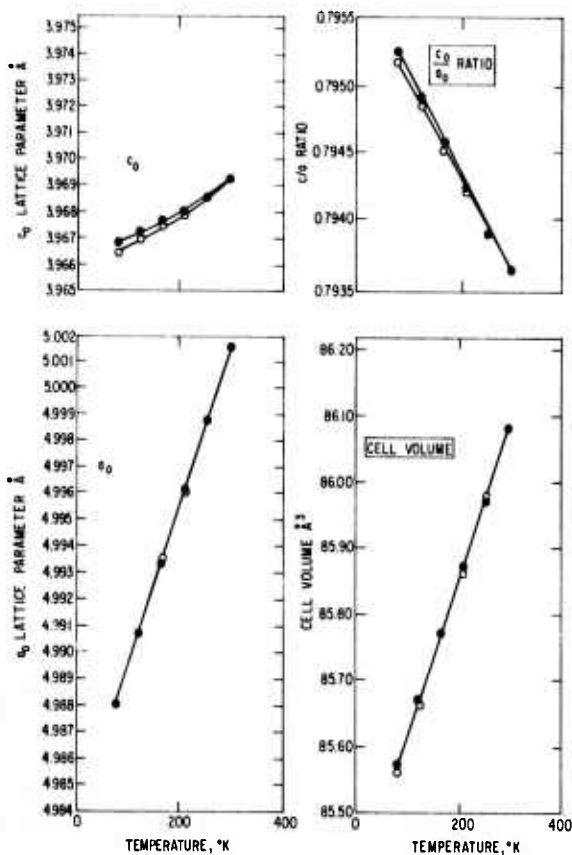
Fig. 3 Change of x-ray parameters with temperature
for two Co-Sm samples. The o points are for a
16.8 at. % Sm sample, and the ● points are for a
16.7 at. % Sm sample.

REFERENCES

1. M. G. Benz and D. L. Martin, Appl. Phys. Let-
ters 17, 176 (1970).

2. R. E. Cech, J. Appl. Phys. 41, 5247 (1970).

3. J. K. Das, IEEE Trans. Magnetics MAG-7 482
(1971).

4. M. G. Benz and D. L. Martin, J. Appl. Phys. 43,
3165 (1971).

5. K. H. J. Buschow and A. S. Van Der Goot, J. Less-
Common Metals 14, 323 (1968).

6. M. U. Cohen, Rev. Sci. Instr. 6, 68 (1935); Rev.
Sci. Instr. 7, 155 (1936); Z. Krist. (A), 94,
288 (1936).

7. E. R. Jette and F. Foote, J. Chem. Phys. 3,
605 (1935).

8. H. Umbayashi and V. Fujimura, Jap. J. Appl.
Phys. 10, 1585 (1971).

9. A. E. Austin and J. F. Miller, Tech. Rept. AFML-
TR-72-132, July 1972, Air Force Materials Lab.,
Wright-Patterson Air Force Base, Ohio.

10. W. A. J. J. Velge and K. H. J. Buschow, J. Appl.
Phys. 39, 1717 (1968).

11. S. E. Haszko, Trans. AIME 218, 763 (Aug. 1960).

73CRD140

D. L. Martin, R. P. Laforce, and M. G. Benz

POST-SINTERING HEAT TREATMENT OF COBALT-
SAMARIUM MAGNET ALLOYS

154<

GENERAL ⊕ ELECTRIC

General Electric Company
Corporate Research and Development
Schenectady, New York

TECHNICAL INFORMATION SERIES

AUTHOR Martin, DL Laforce, RP Benz, MG	SUBJECT permanent magnets	NO. 73CRD140
		DATE April 1973
TITLE Post-Sintering Heat Treatment of Cobalt-Samarium Magnet Alloys		GE CLASS 1
		NO. PAGES 8
ORIGINATING COMPONENT Metallurgy and Ceramics Laboratory		CORPORATE RESEARCH AND DEVELOPMENT SCHENECTAOY, N.Y.

SUMMARY

The results of a study to determine the effect of heat treatment on the permanent magnet properties of sintered Co-Sm alloys are presented. The degree of squareness of the demagnetization curve and the intrinsic coercive force are influenced very markedly by heat treatment, the former varying as much as three and the latter by as much as ten depending upon the composition. The best combination of demagnetization characteristics was obtained by cooling slowly the magnet sample from $1100°$ to about $900° C$, aging at that temperature, and then cooling rapidly to room temperature.

KEY WORDS

permanent magnets, rare earth magnets, cobalt-samarium

INFORMATION PREPARED FOR _____

POST-SINTERING HEAT TREATMENT OF COBALT-SAMARIUM MAGNET ALLOYS*

D. L. Martin, R. P. Laforce, and M. G. Benz

INTRODUCTION

A high value of induction coercive force, H_c, is the most difficult of the permanent magnet properties to achieve in the cobalt-rare earth magnet alloys. It is very structure sensitive and almost every processing step has an influence. Since the upper limit of H_c is the remanent magnetization B_r, any factor such as saturation, relative density, or alignment which influences B_r, also affects the coercive force H_c as well. In addition, there are numerous processing variables, such as composition, particle size, sintering time, and temperature which influence coercivity.

A necessary condition for H_c to equal B_r is that the $4\pi J$ demagnetization curve be horizontal to the H-axis out to a demagnetizing field much greater than H_c. That is, the knee of the $4\pi J$ curve, as well as the intrinsic coercive force, should be at a field much greater than H_c.

It was shown previously that the intrinsic coercivity of sintered Co-MM-Sm magnets could be increased tenfold by a post-sintering heat treatment several hundred degrees below the sintering temperature. [1] One advantage of such a treatment is that the coercivity sometimes "lost" during high-temperature sintering can be regained, thus combining both high density and high coercivity.

Westendorp has shown that the intrinsic coercivity of unsintered $Co_5 Sm$ powder could be increased manyfold by heating to $1080^\circ C$, but that the treatment at higher or lower temperatures resulted in a sharp decrease of coercivity. [2] The explanation offered was that at high temperatures $Co_5 Sm$ is single phase (low $_jH_c$), that near $1080^\circ C$ precipitation occurs (high $_jH_c$), while at lower temperatures the precipitation coarsens (low $_jH_c$).

Den Broeder and Buschow observed that samples richer in samarium, within the two-phase region $Co_5 Sm-Co_7 Sm_2$, also exhibited a decrease of coercivity on annealing at a low temperature. [3] They proposed, on the basis of microstructural observations, that the $Co_5 Sm$ phase is unstable in the $750^\circ C$ range and decomposes on annealing by an eutectoid reaction into $Co_{17} Sm_2$ and $Co_7 Sm_2$; and that "the behavior of the coercive force of powder compacts of $SmCo_5$ and $GdCo_5$ when subjected to different annealing temperatures between $700^\circ C$ and $1000^\circ C$ can be related to the phase transformation of RCo_5 into $R_2 Co_7$ and $R_2 Co_{17}$ and vice versa."

We have made a detailed study of the effect of post-sintering heat treatment on the magnetic properties of Co-Sm permanent magnetic materials in order to find the conditions for optimum properties. The highest properties were obtained by cooling to a temperature in the $900^\circ C$ range from a temperature near the sintering temperature rather than heating to $900^\circ C$ from room temperature. Details of our study are given in the following sections.

EXPERIMENTAL

1. Sample Preparation and Magnetic Measurements

Test bars were prepared by a liquid-phase sintering process which has been used successfully to make high-performance cobalt-samarium magnets (Refs. 4, 5). A $Co_5 Sm$ base metal powder and a cobalt-rare earth additive powder richer in rare earth content than the base powder were blended to a nominal composition of about 17 at. % Sm after adjustment for samarium combined with oxygen as Sm_2O_3. The blended powder was made into a test bar by aligning the powder in a magnetic field, compressing slightly while in the field, then hydropressing without a field to a relative density of about 80%. The bar was ground into a cylinder and sintered in the range 1120° to $1130^\circ C$ depending upon the composition. The samples were magnetized in a field of 60 kOe and the demagnetization properties measured by the ballistic method previously described. [6]

2. Co-Sm Compositions Studied

Three different sample series were used in the study. Chemical analyses, as determined by wet chemistry and vacuum-fusion analysis, are listed in Table I together with some lattice parameter data. We have considered the sample to consist of a Co-Sm alloy phase or phases with the nickel or aluminum in solid solution, and an oxide phase consisting of Sm_2O_3. In Table I, the adjusted samarium content of the alloys are listed. This is the samarium available to alloy with the cobalt after subtracting that combined with oxygen as Sm_2O_3.

Fifteen test bars of Alloy P were made from the same batch of blended powder and used for determination of the optimum post-sintering heat treatment.

The effects of samarium content and post-sintering treatment were studied with the L-series alloys. The six alloy samples were prepared by blending of the base and additive powders to cover the range 16.5 to 17.8 at. %.

The third alloy (G) used in the study was one with a nominal composition of 17 at. % Sm. The chemical analysis was not determined, but the x-ray parameter

TABLE I

Chemical Analyses of the Alloys Studied

Alloy	Chemical Analysis, (wt%)					Adjusted Sm (at. %)	Sm Oxide (wt %)	X-ray (Å)	
	Co	Ni	Al	O	Sm			a_0	c_0
P	63.11	0.24	0.06	0.48	36.11	17.6	3.49	5.003	3.969
L-Base	63.89	0.25	0.07	0.45	35.34	16.5	3.27	--	--
LA*	--	--	--	--	--	16.8	--	4.997	3.973
LB*	--	--	--	--	--	17.1	--	--	--
LC*	--	--	--	--	--	17.3	--	--	--
LD*	--	--	--	--	--	17.5	--	--	--
LE*	--	--	--	--	--	17.8	--	--	--
L-Add	39.43	0.15	0.05	0.79	59.57	35.1	5.74	--	--
G	--	--	--	--	--	17	--	5.001	3.969

*Composition was calculated from the weight of L-Base and L-Additive used to make the blend.

values are of the magnitude expected for an alloy of about 17 at. % Sm; for example, compare with Alloy P in Table I or data in Ref. 7. The eleven samples in this series had a higher density and better alignment than the P and L alloy samples so that the B_r and energy product values are significantly higher.

3. Heat Treatment

The sintered samples were heat treated in a variety of ways to study the effect of heating, cooling, temperature, time, etc. During these treatments, the samples were protected against oxidation by wrapping with tantalum and zirconium foils.

One series of treatments, called heating-aging, involved heating a sintered sample to $600°$C for 1/2 hour, cooling to room temperature, and measuring the magnetic properties; then, reheating to increasingly higher temperature to determine the effect of temperature on the properties. This was similar to the treatment used by Westendorp in his study of powder compacts.[2]

A second series of treatments, called step-cooling, involved slowly cooling the sample from the sintering temperature, or slightly below the sintering temperature (e.g., $1100°$C) if the sample had previously been sintered, to a temperature in the range $1050°$ to $700°$C before cooling rapidly to room temperature. To achieve a controlled cooling rate from the high temperature, the furnace was cooled in $50°$ steps for 30, 60, or 120 minutes. For example, a sample step-cooled to $1000°$C would have had 30 minutes cooling from $1100°$ to $1050°$C, and 30 minutes from $1050°$ to $1000°$C.

There is a degree of reversibility to the results in that a good sample can be retreated to have low properties and vice versa. To restore the best properties, a short treatment at about $1100°$C, followed by cooling to the $900°$C range, works very well. In our studies, we reused some samples several times by reheating to $1100°$C to "erase" the past thermal history of the sample, followed by the desired treatment.

1. Heating vs Cooling

The intrinsic coercive force undergoes the greatest change with the post-sintering treatments. In Fig. 1, the change of $_jH_c$ with heating-aging and cooling-aging treatments are compared. The heating curve is similar in shape to that observed by Westendorp[2] on powder compacts with a minimum near $700°$C and a maximum near $1000°$C.
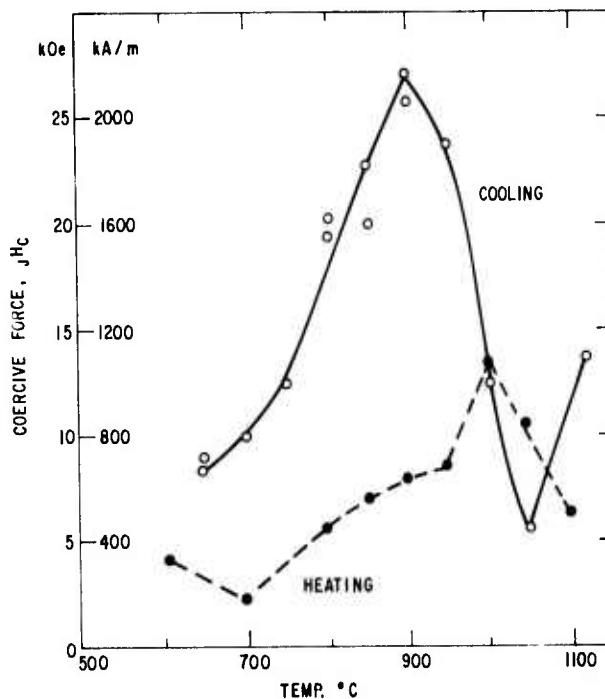

Fig. 1 Change of room-temperature intrinsic coercive force with heat treatment (Alloy P).

The change for the cooling-aging treatment is quite different. A minimum was obtained at $1050°$C, a maximum at $900°$C, followed by a sharp decrease below $900°$C. The maximum $_jH_c$ value for cooling was double that obtained during heating.

The use of the intrinsic coercive force, $_jH_c$, as in Fig. 1 is somewhat misleading as one can judge by examining the demagnetization curves in Figs. 2 and 3. Note in Fig. 2 that, while the $1000°$ and $1050°$C treatments resulted in relatively high $_jH_c$ values, the $850°$C heating treatment yields the best combination of demagnetization properties. The kinks in the curves near B_r and the long tails in the $1000°$ and $1050°$C curves indicate a mixed structure containing phases or grains with different demagnetization characteristics.

The intrinsic demagnetization curves for the Alloy P samples, after various step-cooling treatments, are given in Fig. 3. The squareness and the intrinsic coercive force change the most drastically.
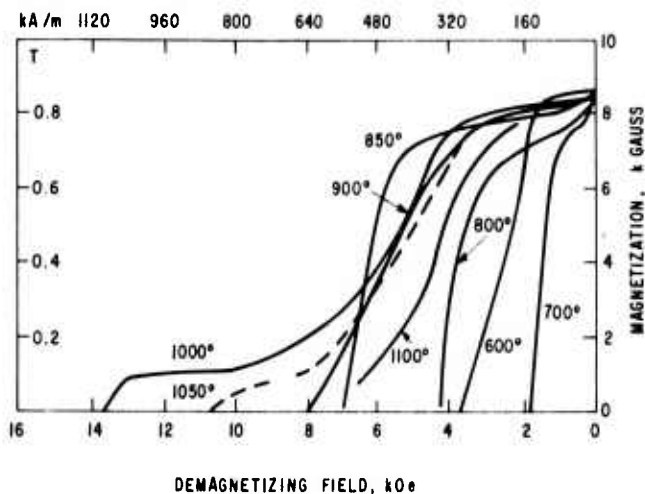
157

Fig. 2 Demagnetization curves (20° C) for a sample heated progressively to the temperature indicated and held 1/2 hour before cooling to room temperature.
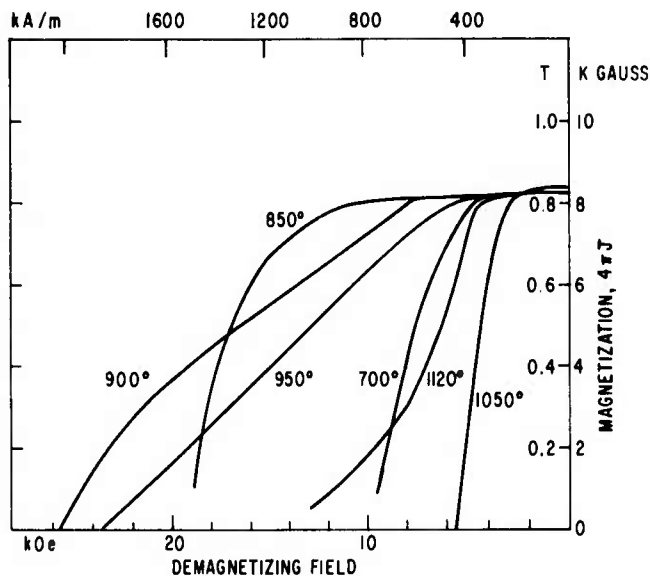

Fig. 3 Intrinsic demagnetization curves for sintered Co-Sm magnets after step-cooling treatment to temperature indicated from 1100° C (Alloy P).

The B_r changes very slightly. Note that the 850° C treatment results in a high degree of squareness and that the knee of the curve is at a higher demagnetizing field than for any other treatment. This is of value when it is desirable to reduce the irreversible temperature loss, for it has been shown that a high H_k (the demagnetizing field resulting in a 10% drop of magnetization below the B_r value) is associated with a low irreversible loss. [8]

The squareness of the sample cooled to 700° C and absence of any discontinuities or kinks is a surprise in view of the evidence offered by den Broeder

and Buschow[3] that $Co_5 Sm$ is unstable and decomposes into two phases. A structure consisting of a mixture of $Co_{17} Sm_2$ and $Co_7 Sm_2$ seems unlikely to have a square demagnetization curve with a B_r value unchanged from that for $Co_5 Sm$, but rather to show a break in the demagnetization curve due to the different magnetic properties of the two phases. It appears that the relatively short time involved in the thermal aging treatment is sufficient time to damage the coercive force due to its structure sensitivity but insufficient time to permit extensive eutectoid transformation to take place.

The results in Fig. 3 should be compared to those in Fig. 2 for the heating-aging treatments. The kink in the curves for the heating-aging samples near B_r is missing in the cooling-aging curves as is the long tail for the 1050° C sample. It is surprising that in each instance the sample with the 850° C treatment had the demagnetization curve with the best combination of demagnetization characteristics; however, the properties of the 850° C cooling-aging properties are significantly better by a factor of two to three times.

The effect of step-cooling (30 minutes per step) on the H_c and $(BH)_{max}$ values is shown in Fig. 4. The changes are significant and of practical value, but not as pronounced as for $_jH_c$.
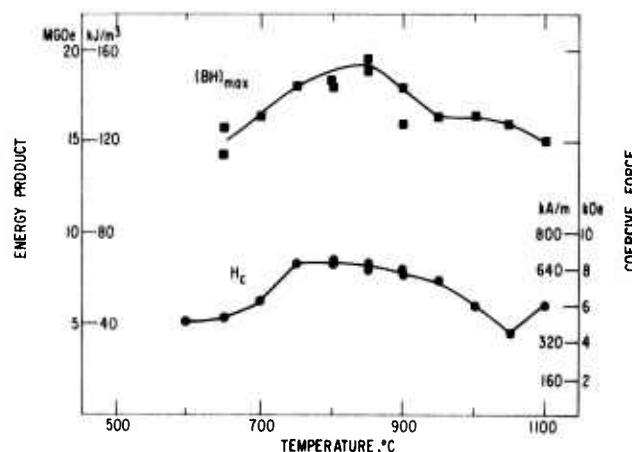

Fig. 4 The effect of step-cooling treatment on the coercive force and energy product (Alloy P).

Isothermal heating resulted in improved properties with increasing time, but the results after 50 hours at 850° C are inferior to those obtained by a 3-hour, step-cooling treatment to the same temperature. This is shown in Fig. 5.

A comparison of the results obtained for different cooling rates is given in Fig. 6. The scatter is large, but there appears to be no advantage for cooling at a rate slower than 1.6° C/min from the high temperature to the aging temperature. A slightly faster cooling rate of about 3° C/min has been found to be acceptable.
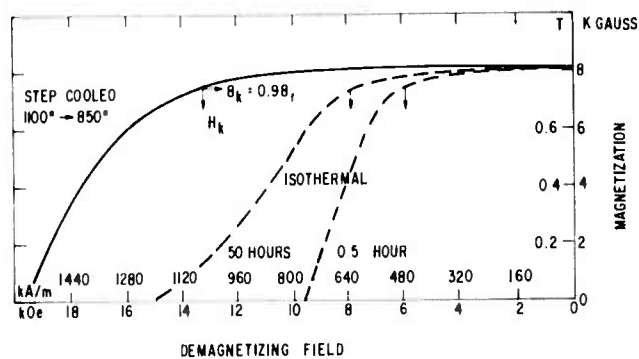
Fig. 5 Comparison of intrinsic demagnetization curves for a step-cooled magnet with samples isothermally aged at 850° C (Alloy P). The H_k values are indicated with an arrow.
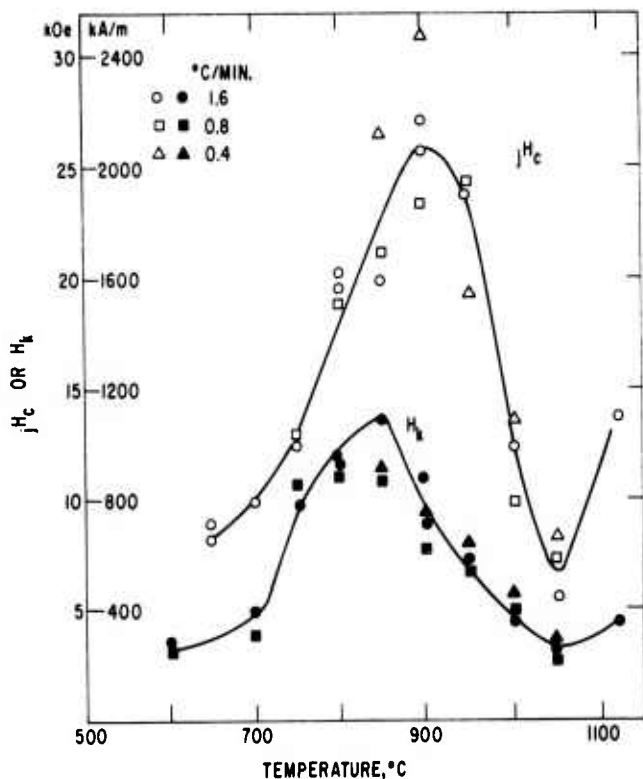

Fig. 6 Effect of step-cooling rate from 1100° C and aging temperature on the intrinsic coercive force and H_k (Alloy P).

The minimum of coercivity observed for a 1050° C cooling-aging treatment in Fig. 1 is reflected also in Figs. 3, 4, and 6. The demagnetization curve (Fig. 3) shows a significant drop of coercivity between the 1120° and 1050° C samples, and the tail in the 1120° C curve has disappeared after the 1050° C treatment.

The cooling rate from the aging temperature is critical.[8,9] It should be fast enough to avoid the sharp drop of coercivity that can occur in the 600° to 750° C range (Fig. 1), but not too fast to cause cracking

or magnetically damaging effects.[9,10] In this work we cooled the samples in a room-temperature cooling chamber with a flow of argon gas.

2. Effect of Samarium Variation

Samples of six Co-Sm alloys (L-series) with a composition variation from 16.5 to 17.8 at. % samarium were given cooling-aging treatments from 1100° to 925°, 900°, and 850° C. Some of the magnetic results obtained are plotted in Figs. 7 and 8. There are a number of interesting points to be made in regard to these results:
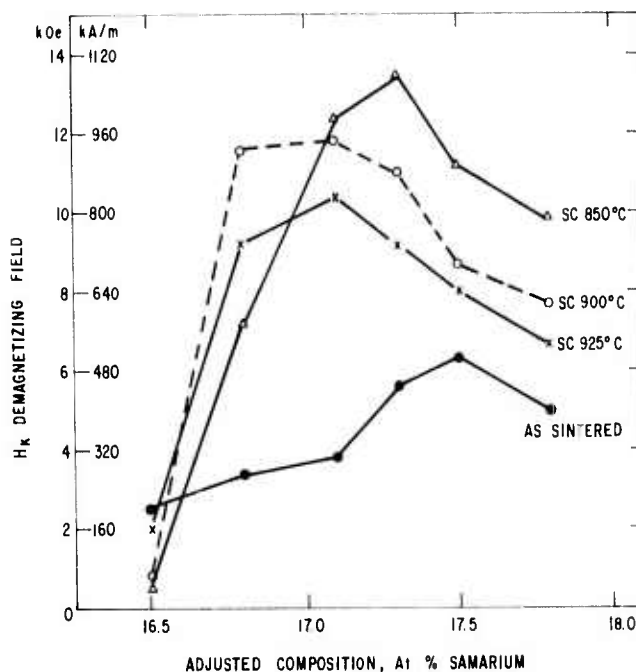

Fig. 7 Variation of the demagnetizing field H_k with samarium content and step-cooling-aging treatment (L-series). "SC" refers to step-cooling.

(a). The cooling-aging treatment improved markedly the coercive force and energy product of the sintered magnets except for the 16.5 at. % Sm alloy. In the case of that alloy, which we judge to be in the homogeneous Co_5Sm range based on previous results (Ref. 7), step-cooling to 900° or 850° C resulted in a drop from the as-sintered properties.

(b). Over a narrow composition range of 0.3 at. % Sm, the cooling-aging treatment becomes very effective in increasing the properties. In this same region, the Co_5Sm homogeneity field ends and the two-phase $Co_5Sm-Co_7Sm_2$ field begins.[7]

(c). The cooling-aging treatment was most effective for improving the properties of the 16.8 to 17.1 at. % Sm alloys. The H_k value of these sintered magnets increased by a factor of three to four compared to a factor of two for the higher samarium alloys (Fig. 7).
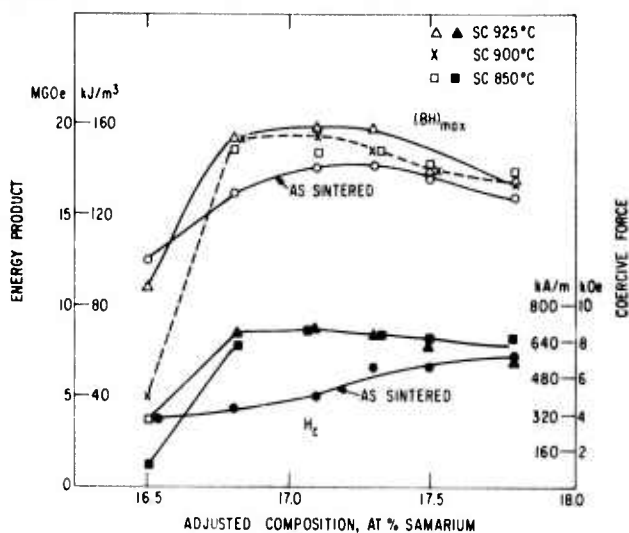
Fig. 8 Variation of coercive force and energy product with step-cooling-aging treatment and samarium content of the alloys (L-series).

(d). The optimum composition range, based on H_c, H_k, and $(BH)_{max}$, is 16.8 to 17.3 at. % Sm.

3. Sintering Temperature

The objective of the sintering process is to increase the relative density of the sample in order to impart greater thermal stability by closing off pores to oxidation, and improve its magnetic properties by increasing the remanent magnetization. It has been shown that sintering of Co-Sm magnets above $1110°$ C results in high density, but that the coercive force usually drops sharply with increasing temperature (Refs. 11, 12). Thus, there is only a narrow temperature range suitable for sintering in order to optimize both coercivity and density. In the case of the Co-MM-Sm alloys, the coercivity of an over-sintered bar could be markedly increased by a post-sintering heat treatment.[1] Similarly, the Co-Sm sample, sintered at $1130°$ to $1140°$ C, followed by a cooling-aging treatment in the $875°$ to $900°$ C range, did not suffer a severe drop of coercivity (shown in Fig. 9 for Alloy G samples). Note the minimum H_k values are in the 14 to 15 kOe range, which compares very favorably with the results in Fig. 2 for samples of another alloy sintered at $1120°$ C and aged at $850°$ C. However, the coercivity after sintering at $1110°$ C was higher than after sintering at higher temperatures. Note also in Fig. 7 that the step-cooling treatment with a 15-hour holding period at $875°$ C yielded higher properties than the $900°$ C treatment.

The magnetic properties of an Alloy G sample sintered 2 hours at $1125°$ C, reheated to $1100°$ C for 1 hour, followed by cooling at a rate of about $3°$ C/min to $875°$ C, holding for 16 hours, and cooling rapidly to room temperature are as follows: B_s, 10.25 kG; B_r, 9.78 kG; H_c, 9.68 kOe; H_k, 23.6 kOe; $_jH_c$, 31.1 kOe; and $(BH)_{max}$, 23.6 MGOe. These excellent
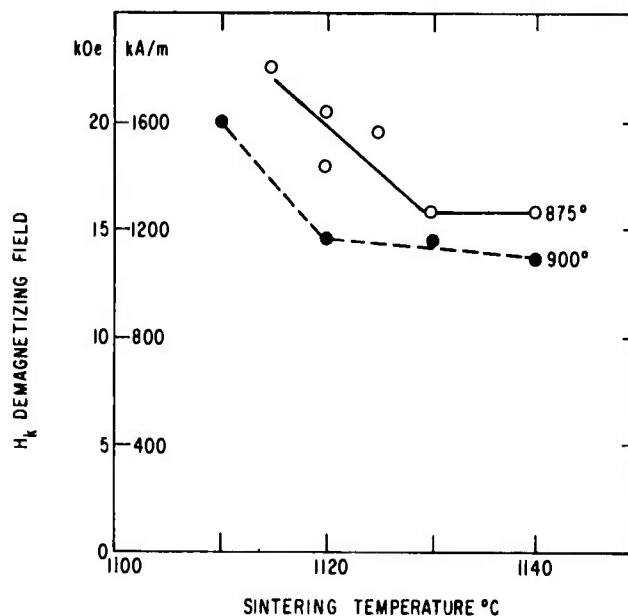

Fig. 9 Effect of sintering temperature on the demagnetizing field H_k of Alloy G samples cooled to $875°$ and $900°$ C.
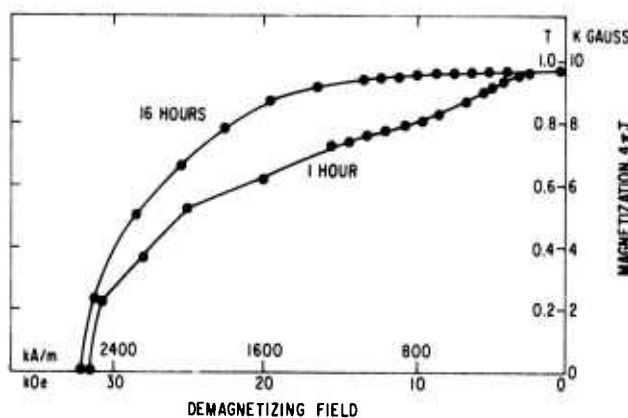

Fig. 10 Effect of holding time on the intrinsic demagnetization curve for Alloy G samples cooled from the $1100°$ C range to $875°$ C and held for the time indicated before fast cooling to room temperature.

properties can be attributed to the combination of a high density (8.26 g/cc), a high degree of alignment ($B_r/4\pi J_{so}$, 0.99), and a high resistance to demagnetization.

4. Effect of Thermal Aging Time

The time that the sample is held at the end of the cooling treatment is important for some samples. The data for Alloy P and series L samples (Figs. 1 through 8) were obtained on samples held only 1/2 hour at the final aging temperature before cooling to room temperature. A comparison of the intrinsic demagnetization curve of a sample, held 1 hour at $875°$ C after cooling from $1100°$ C, with the curve for

a sample held 16 hours, is given in Fig. 10. The longer aging resulted in a "squarer" curve and a much higher H_k value without appreciably changing the $_jH_c$ value. Holding for a period longer than 15 hours has been found to effect further improvement but not enough to justify aging more than one day in a commercial process.

SUMMARY

1. The effect of a post-sintering, thermal treatment on the magnetic properties of Co-Sm magnet samples has been studied. The intrinsic coercive force shows the most pronounced change with heat treatment, varying by a factor of ten. The changes in $(BH)_{max}$ and H_c are less pronounced but are still of practical value.

2. A large difference in the room temperature properties has been observed between sintered samples heated from room temperature and those cooled from near the sintering temperature to an intermediate temperature of about 900° C before cooling to room temperature.

3. For a heating-aging treatment, the intrinsic coercivity decreases initially to a minimum at 700° C, followed by a sharp increase to a maximum at about 1000° C.

4. The cooling-aging treatments from 1100° C over the same temperature range show a coercivity minimum at 1050° C, a sharp increase to a maximum at about 900° C, followed by a sharp decrease to a low value in the 700° C range.

5. The best combination of demagnetization characteristics; that is, squareness and intrinsic coercive force, was obtained by an aging treatment in the 850° to 900° C range depending upon the composition. This was observed to be the case whether the sample was given a heating-aging or a cooling-aging treatment. However, the magnitude of coercivity was two to three times higher for the cooling-aging treatment.

6. The cooling rate from the high temperature to the aging temperature for the cooling-aging treatment was varied from 0.4 to 3° C/min, and was found to be not critical. A rate of 1° to 3° C/min appeared to be a practical rate to use.

7. The holding time at the final aging temperature was observed to be important. In particular, a 15-hour hold at 875° C improved the "squareness" of the demagnetization curve.

8. The cooling-aging treatment was effective in increasing the coercivity of oversintered samples, thus obtaining the combination of high density and high coercivity.

9. Alloys with a samarium content above 16.8 at. % responded to the cooling-aging, thermal treatment

whereas the properties of a 16.5 at. % Sm sample did not improve when given the same treatments.

10. There is a degree of reversibility to the results in that a poor sample could be retreated to have good properties and vice versa.

DISCUSSION

The wide variation of magnetic properties resulting from variations of heat treatment are reflected mainly in the shape of the $4\pi J$ demagnetization curve and the magnitude of the intrinsic coercive force. The residual induction, B_r, changes at most 5% to 10%, whereas the intrinsic coercive force, $_jH_c$, can vary by a factor of ten.

The demagnetization curve in the second and third quadrant of the hysteresis loop can be considered a transformation curve from the magnetization state represented by B_r to that of the saturated condition in the third quadrant. The $_jH_c$ point represents 50% transformation or reversal of the magnetization of half of the sample volume. The H_k point represents approximately the 5% transformation level.

It also is useful to consider the concept of a distribution of coercivities of the grains, as discussed by McCurrie.[13] Thus, a "square" demagnetization curve is one for which the magnetization of all the grains reverse at the same field. This is the ideal demagnetization curve and has been observed for small single particles.[14] A measure of squareness is the ratio of H_k to the intrinsic coercive force, $_jH_c$. In this study, the squareness ratio $H_k/_jH_c$ varied from 0.26 for the sample heated to 1000° C (Fig. 2) to 0.88 for a sample step-cooled from 1100° to 750° C at a rate of 50° C per hour. A high-performance magnet (e.g., the 15-hour sample in Fig. 10) would be expected to have a ratio of 0.6 to 0.7.

A high squareness ratio signifies that the distribution of coercivities is concentrated over a narrow reverse field range. That is, the intrinsic coercive force of all the grains in the specimen is about the same. Likewise, it can be stated that a treatment which results in a high squareness ratio (>0.5) is one which is influencing most of the grains in a similar manner. This is the case for samples step-cooled to 1050°, 850°, and 700° C (Fig. 3).

Squareness and intrinsic coercive force are not related. This is clear by examination of Figs. 2, 3, 5, and 10. The treatments ending in the temperature range 650° to 850° C give a high degree of squareness whereas treatments in the range 900° to 1000° C resulted in a low degree of squareness. However, the intrinsic coercive force varies by a factor of five, depending upon whether the sample was given a cooling-aging treatment or a heating-aging treatment. The best combination of squareness and intrinsic coercive force were obtained by cooling from about 1100° C to a temperature of 850° to 900° C and holding for about 15 hours.

The difference between heating and cooling may be explained by assuming that the intrinsic coercive force of any sample heated in the range 600° to 700° C will be lowered, and that a temperature in excess of 1000° C is needed to erase the damage. On the other hand, a sample heated to 1100° C must be cooled below 850° C before the coercivity is greatly reduced (Fig. 1).

There are two major phenomena that need explaining: (1) what causes the drop of coercivity in the 700° C range, and (2) what causes the high level of coercivity in the 850° to 900° C range after cooling from a higher temperature? A third effect, of lesser importance, is the minimum of coercivity for the cooling samples at 1050° C (Fig. 1).

The damaging effect of a 600° to 750° C treatment may be due to the eutectoid decomposition of Co_5Sm into $Co_{17}Sm_2$ and Co_7Sm_2 as proposed by den Broeder and Busehow.[3] However, additional verification of that decomposition is needed since they were unable to detect Co_7Sm_2 by x-ray diffraction techniques in samples that had an eutectoid-type microstructure. The presence of even a small amount of the $Co_{17}Sm_2$ phase is undesirable whether it is from a eutectoid decomposition or a precipitation reaction,[15] whereas a few percent of Co_7Sm_2 particles need not be harmful.[7]

The sharp increase of coercivity observed for samples given a cooling-aging treatment to a temperature 850° to 925° C, depending upon the composition, is not readily explained. Neither the microstructure nor x-ray diffraction studies have revealed any basis for an explanation. The alloys which respond to heat treatment are hyperstoichiometric Co_5Sm compositions near the Co_5Sm-Co_7Sm_2 phase boundary.[7] Therefore, precipitation of Co_7Sm_2 is a possible explanation if one believes in the local-pinning model (Ref. 16). Or, if coercivity is limited by the nucleation of reverse domains, then one must postulate that the cooling and aging treatment results in a Co_5Sm structure with fewer defects. More information is needed and, in particular, the identification of defects which influence reverse domain nucleation, or local pinning is needed before an explanation of the heat-treating effects can be forthcoming.

The cause of the drop of coercivity at 1050° C for samples step-cooled from 1100° C (Figs. 1 and 6) is not understood. X-ray diffraction results on powder samples do not reveal any significant difference in the lattice parameters of the Co_5Sm phase between 1050°, 850°, or 650° C step-cooled samples. The phase diagram does not offer the basis of any explanation as was the case for the Co-Pr alloys where a coercive force peak was related to the formation of a Co_7Pr_2 shell.[17]

ACKNOWLEDGMENTS

REFERENCES

1. M. G. Benz and D. L. Martin, "Cobalt-Misch-metal-Samarium Permanent Magnet Alloys: Process and Properties," J. Appl. Phys. 42, 2786-2789 (1971).

2. W. F. Westendorp, "On the Coercivity of $SmCo_5$," Solid State Commun. 8, 139-141 (1970).

3. F. J. A. den Broeder and K. H. J. Busehow, "Coercive Force and Stability of $SmCo_5$ and $GdCo_5$," J. Less-Common Metals 29, 65-71 (1972).

4. M. G. Benz and D. L. Martin, "Cobalt-Samarium Magnets Prepared by Liquid-Phase Sintering," Appl. Phys. Letters 17, 176-177 (1970).

5. D. L. Martin and M. G. Benz, "Cobalt-Rare Earth Permanent Magnet Alloys," Cobalt, No. 50, 11-15 (March 1971).

6. M. G. Benz and D. L. Martin, "Measurement of Magnetic Properties of Cobalt-Rare Earth Permanent Magnets," IEEE Trans. Magnetics MAG-7, 285 (1971).

7. D. L. Martin, M. G. Benz, and A. C. Rockwood, "Cobalt-Samarium Permanent Magnet Alloys: Variation of Lattice Parameters with Composition and Temperature," AIP Conf. Proc. No. 10, New York, Am. Inst. Phy. (1973).

8. D. L. Martin and M. G. Benz, "Magnetization Changes for Cobalt-Rare Earth Permanent Magnet Alloys When Heated Up to 650° C," IEEE Trans. Magnetics MAG-8, 35-41 (1972).

9. M. Doser and J. Smeggil, "Some Observations of the Magnetic Properties of Fluid-Quenched Co_5Sm Magnets," Intermag. Conf. Paper, Washington, D. C. (April 1973).

10. F. G. Jones, H. E. Lehman, and J. G. Smeggil, "Quenching Experiments on Cobalt-Samarium Magnets," IEEE Trans. Magnetics MAG-8, 555-557 (1972).

11. D. K. Das, "Influence of Sintering Temperature on Magnetic Properties of Samarium-Cobalt Magnets," IEEE Trans. Magnetics MAG-7, 432-435 (1971).

12. D. L. Martin and M. G. Benz, "Review of Cobalt-Rare Earth Permanent Magnet Alloys," AIP Conf. Proc. No. 5, Magnetism and Magnetic Materials, Am. Inst. Phy., New York (1972), pp. 970-990.

13. R. A. McCurrie, "Determination of Intrinsic Coercivity Distributions in Aligned Assemblies of Uniaxial $SmCo_5$ and $LaCo_5$ Particles," Phil. Mag. 22, No. 179, 1013-1023 (1970).

14. J. J. Becker, "Magnetization Discontinuities in Cobalt-Rare-Earth Particles," J. Appl Phys. 42, 1537-1538 (1971).

15. A. Menth and K. Bachmann, "Magnetic Phase Analysis of $RECo_5$ Permanent Magnet Materials," 18th Conf. Mag. Mag. Mater., Denver (Nov. 1972).

16. J. D. Livingston, "Present Understanding of Coercivity in Cobalt-Rare Earths," AIP Conf. Proc. No. 10, N. Y., Am. Inst. Phys. (1973).

17. J. Schweizer, K. J. Strnat, and J. B. Tsui, "Coercivity of Heat Treated Pr-Co Powder Compacts," IEEE Trans. Magnetics MAG-7, 429-431 (1971).

73CRD120

P. Rao, J.G. Smeggil, and E.F. Koch

PHASE TRANSFORMATIONS $\therefore$ Co$_5$Sm

GENERAL ⊛ ELECTRIC

General Electric Company
Corporate Research and Development
Schenectady, New York

TECHNICAL INFORMATION SERIES

AUTHOR Rao, P Smeggil, JG * Koch, EF	SUBJECT cobalt-samarium	NO 73CRD120
		DATE April 1973
TITLE Phase Transformations In Co_5Sm		GE CLASS 1
		NO. PAGES 2
ORIGINATING COMPONENT Materials Characterization Operation Materials Science and Engineering		CORPORATE RESEARCH AND DEVELOPMENT SCHENECTADY, N Y

SUMMARY

Transmission electron microscopy studies of high-quality Co_5Sm crystals annealed at 750°C indicate that there is a partial breakdown of hexagonal Co_5Sm into rhombohedral $Co_{17}Sm_2$ and a disordered Co_7Sm_2-type faulted structure in the Co_5Sm matrix. Orientation relationships between the phases are presented.

*Metallurgy and Ceramics Laboratory

KEY WORDS

cobalt-samarium, magnetic materials
transmission electron microscopy

PD-54 (10/70)

PHASE TRANSFORMATIONS IN Co_5Sm*

P. Rao, J. G. Smeggil, and E. F. Koch

Much higher magnetic coercivities than were previously available have been attained with the compound Co_5Sm. However, coercivity is very sensitive to heat treatment; in particular, annealing near $750^\circ C$ substantially reduces coercivity. This has been attributed to a possible eutectoidal decomposition of Co_5Sm into $Co_{17}Sm_2$ and Co_7Sm_2 on the basis of optical metallography.[1] This possibility makes it necessary to obtain basic electron microstructural information from Co_5Sm heat treated in this temperature range.

High-quality Co_5Sm crystals were annealed in sealed Mo bombs at $750^\circ C$ for 10 days. Electron transparent specimens were prepared by ion thinning in a commercial ion milling apparatus. Typical bright field and dark field images are shown in Figs. 1, 2, and 3. The first observation is the existence of interfaces identified as basal stacking faults (Fig. 1) on the basis of their characteristic dynamical image contrast.[2] Some of the features, such as A in Fig. 1, consist of several closely spaced faults. It is of interest to note that the Co_7Sm_2 structure can be produced from hexagonal Co_5Sm by a series of basal stacking faults. Some of the extra diffraction spots arising from heavily faulted areas can be indexed in terms of hexagonal Co_7Sm_2 [similar to the wurtzite-to-sphalerite transformation[2]].

The second observation is the existence of a lath-shaped precipitate phase shown in bright field and dark field images in Fig. 2a, and 2b and 2c, respectively. This phase appears as regions with considerable internal microstructure in the form of closely spaced antiphase boundaries (APB's) (marked B in Fig. 2c). The phase is identified as rhombohedral $Co_{17}Sm_2$,[3] and the co-existence of Co_5Sm and $Co_{17}Sm_2$ is shown in the selected area diffraction pattern (Fig. 2d). Dark field images from $Co_5Sm + Co_{17}Sm_2$ diffraction spots (Fig. 2b) show that the matrix as well as the precipitates light up, while using only a $Co_{17}Sm_2$ spot (Fig. 2c), alternated areas of the precipitate phase, separated by APB's, show strong contrast. The $Co_{17}Sm_2$ laths grow such that their common interface is given by $\{11\bar{2}1\}$ $(Co_5Sm) \parallel \{1\bar{1}03\}$ $(Co_{17}Sm_2)$. The coexistence of basal stacking faults and $Co_{17}Sm_2$ is shown in Fig. 3. The faults in Co_5Sm appear to propagate into $Co_{17}Sm_2$ as APB's along their common basal planes.

The results indicate that under the present heat-treatment conditions, there is a partial breakdown of hexagonal Co_5Sm to rhombohedral $Co_{17}Sm_2$ and a disorder Co_7Sm_2-type faulted structure in the Co_5Sm matrix.

REFERENCES AND FOOTNOTE

1. F. J. A. Den Broeder and K. H. J. Buschow, J. Less Common Metals 29, 65 (1972).

Fig. 1 Bright (a and c) and dark field (b) images of Co_5Sm showing the existence of basal stacking faults.

Fig. 2 Bright (a) and dark field (b and c) images of the lath-shaped $Co_{17}Sm_2$ phase in matrix Co_5Sm.

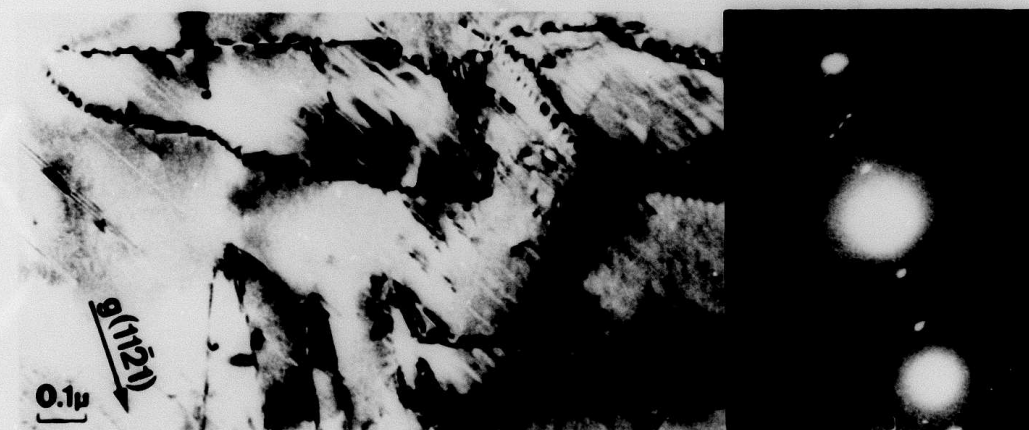
Fig. 3 Coexistence of basal stacking faults and lath-shaped $Co_{17}Sm_2$ showing the partial breakdown of Co_5Sm_2 to $Co_{17}Sm_2$ and a disordered Co_7Sm_2-type faulted structure in the Co_5Sm matrix.

2. H. Blank, P. Delavignette, R. Gevers, and
   S. Amelinckx, Phys. Stat. Sol. 7, 747 (1964).

3. Rhombohedral structure indexed in terms of
   hexagonal axes.

73CRD102

J. G. Smeggil

PHASE ANALYSIS OF LIQUID PHASE SINTERED
Co_5Sm MAGNET COMPACTS

168<

TECHNICAL INFORMATION SERIES

AUTHOR	SUBJECT	NO. 73CRD102
Smeggil, JG	cobalt-samarium	DATE March 1973
TITLE Phase Analysis of Liquid Phase Sintered Co5Sm Magnet Compacts		GE CLASS 1
		NO PAGES 3
ORIGINATING COMPONENT Metallurgy and Ceramics Laboratory		CORPORATE RESEARCH AND DEVELOPMENT SCHENECTADY, N.Y

SUMMARY

The purpose of this work is to determine the phases present in liquid phase sintered Co_5Sm magnets. Specimens sintered at $1100^\circ C$ and given subsequent thermal treatments were examined by optical metallography, electron microprobe, and x-ray diffraction techniques. The results of this work suggest that these materials do not exhibit an equilibrium configuration of phases.

KEY WORDS

cobalt-samarium, magnets, cobalt-rare earth alloys

PHASE ANALYSIS OF LIQUID PHASE SINTERED Co_5Sm MAGNET COMPACTS

J. G. Smeggil

INTRODUCTION

Sintering techniques are reported to be extensively used to fabricate cobalt-rare earth magnets.[1] Once formed, these magnets and their measured physical properties are generally discussed in terms of a supposed equilibrium phase configuration. The purpose of this work, then, is to examine this suggested situation by determining the phases present in liquid phase sintered Co_5Sm magnets.

PROCEDURE

Rod magnets, approximately 2.5 cm in length and 0.7 cm in diameter, were prepared with nominal compositions of 63.5 ± 0.2 wt % Co, 36.2 ± 0.2 wt % Sm, as discussed elsewhere.[1,2] In addition, these materials are known to exhibit oxygen concentrations at levels of 0.3 to 0.5 wt %. Individual magnets were sintered at $1100°C$ to a relative density of 95%, reheated for 1 hour at either $750°$ or $900°C$, and finally either chamber-cooled or water-quenched.[1,2]

Selected samples were then subsequently polished for examination by the electron and optical metallography techniques.

Solutions of 1% nital or acetic acid-HNO_3-HCl (10:10:10) were used for etching. No significant differences in microstructure were observed between samples etched with these two different solutions. Subsequent to etching, 5% hydrol solution was used to wash the samples. X-ray diffraction was done both on the bulk samples and on residues obtained from the electrolytic dissolution of the bulk material in HCl-methanol solutions.

RESULTS

Electron Microprobe

A Cameca electron microprobe indicated the presence of Co_5Sm (calc.: 33.8 wt % Sm, 66.2 wt % Co; obs.: 34 wt % Sm and 66 wt % Co) and Co_7Sm_2 (calc.: 42.2 wt % Sm, 57.8 wt % Co; obs.: 44 wt % Sm, 56 wt % Co). In addition, regions containing only Sm and O were detected and assumed to be a form of Sm_2O_3 (cal.: 86.2 wt % Sm, 13.8 wt % O; obs.: 85 wt % Sm, 15 wt % O). Small amounts of Al were detected, concentrated largely in pore areas. Whenever Al was detected in a pore area, a sizable oxygen peak was simultaneously registered. The amount of Al in the bulk of the sample was measured at no more than the background level. Accordingly, this Al resulted from either the incomplete removal of grit in the polishing process or from eroded pieces of the Al_2O_3 crucible used to make the bulk alloy. The overall Al concentration in these magnets as determined by analytical chemistry is known to be generally less than 0.1 wt %. Ni, known to be present at levels of about 0.05 wt % from analytical chemistry, was looked for using an x-ray imaging technique. No localized concentrations of this element were observed in any of the samples examined. Additionally, Cu and Fe, two likely trace contaminants in a metallurgical process, were not observed at levels above background.

Regions rich in Sm, containing about 75 wt % Sm with the remainder Co, were detected. No oxygen, aluminum, or nickel above background levels was detected in these regions. In addition, no diffusion zones were detectable between these Sm-rich regions and adjacent grains of either Co_5Sm or Co_7Sm_2.

Once these four regions (Co_5Sm, Co_7Sm_2, Sm_2O_3, and Sm-rich grains) were distinguished by the microprobe, they could be visually differentiated from each other on the basis of slight differences in color in the etched, magnetically aligned samples.

Optical Metallography

Quantitative metallographic examination of sintered Co_5Sm magnets annealed at $750°$ or $900°C$ was undertaken to determine if any substantial variations could be observed in either grain size or distribution of the various phases. Table 1 lists the results of the observations based on 500 random points on the surface of each magnet. The differences in the listed values for the two samples are considered negligible except that possibly more Sm-rich regions may be present in the sample annealed at $750°C$.

TABLE 1

Volume % Various Phases Observed By Optical Metallography In Co_5Sm Sintered Compacts Annealed At $750°$ and $900°C$

Annealing Temp (°C)	Volume %			
	Co_5Sm	Co_7Sm_2	Sm-rich Regions	Oxides & Voids
900	78.6	5.4	0.2	15.8
750	74.7	4.0	2.4	18.8

Optical examination of samples annealed at either $750°$ or $900°C$ indicated no observable differences at 1000X in phases corresponding to Co_5Sm, Co_7Sm_2, or Sm_2O_3 in samples examined in either the as-polished or etched states.

When Sm-rich regions were etched, some surface topology was observable and could be interpreted as either growth planes and/or grain boundaries. When these regions were examined for magnetic Kerr effects, no domain patterns were observed, whereas domains were observed in regions thought to be Co_5Sm and Co_7Sm_2. In addition, samples known to be $Co_{17}Sm_2$ have been observed to exhibit domain patterns under appropriate examination.

X-ray Diffraction

The a and c lattice parameters of the Co_5Sm phase in samples quenched from temperatures ranging from 750° to 1100°C were found to be virtually invariant. These values ranged from a = 5.000 (±1)Å and c = 3.972 (±1)Å at 750°C to a = 4.998 (±1)Å and c = 3.971 (±1)Å at 1100°C.

Residues from Co_5Sm magnets subjected to slow electrolytic dissolution in solutions of 7 vol % HCl-methanol were examined by x-ray diffraction. The following phases were detected in these residues: $B-Sm_2O_3$;[3] $C-Sm_2O_3$;[4,5] a-quartz, SiO_2;[6] pryophyllite, $Al_2Si_4O_{10}$ $(OH)_2$;[7] griffithite, $Ca_{0.5}Na_{0.1}$ $(Mg_{1.9}Fe_{0.9}Al_{0.04})$ $(Al_{0.8}Si_{3.2})$ $(OH)_2O_{10}$;[8] and an as-yet-unidentified phase. The strong lines exhibited by this phase can be indexed on the unit cell exhibited by the complex oxides with the stoichiometry M_7O_{12}, e.g., $AO_3 \cdot 3Sm_2O_3$, A=U.[9-11] Examination of this material by the solid-state detector attached to a scanning electron microscope failed to indicate the presence of any metal atoms, other than Sm, at levels higher than 0.1 wt %. The three Sm-oxide phases were observed in approximately equal amounts in the magnets examined.

DISCUSSION

The results of this work suggest than an equilibrium situation is not found in liquid phase sintered Co_5Sm magnets fabricated as described earlier.

The presence of the Sm-rich regions is not readily reconcilable with phases predicted by the equilibrium phase diagram for the Co-Sm system[12] for alloys with about 36 wt % Sm. Two explanations can be suggested to account for the presence of these regions. Either they are the result of some kind of precipitation reaction or else they are the remnant liquid phase additive used as a sintering aid. However, examination of Co_5Sm magnets prepared without the use of a sintering aid has failed to indicate the presence of the Sm-rich regions. Consequently, the first explanation seemingly is incorrect. Moreover, the composition of the Sm-rich regions is approximately that expected at 750° to 900°C for the liquidus of the Co-Sm additive (60 wt % Sm) used to adjust the stoichiometry of the base-metal alloy powder. This explanation, however, suggests that these regions, if they do represent part of the alloy powder used as a liquid phase sintering aid, during some part of the sintering process apparently have supplied Co and not Sm to the base-metal alloy. No

$Co_{17}Sm_2$ phase was detected during the examination of the magnets reported here. The work reported here does not support the results of either Jorgensen and Bartlett[13] or Bachmann and Menth,[14] suggesting the presence of $Co_{17}Sm_2$ in these materials.

The x-ray diffraction results independently lend additional support to the presence of a nonequilibrium situation in these materials; namely, the lattice parameters measured for Co_5Sm quenched at temperatures from 750° to 1100°C are essentially constant. Some support is also given by the fact that $C-Sm_2O_3$ is observed at temperatures above which it is reported to convert to the B-form (860°C) although Gschneidner[15] states the transformation is "sluggish."

The role of the residual (or contaminant) phases in influencing the magnetic properties of the sintered Co_5Sm magnets will not be discussed here. However, the magnetic properties of these phases should be considered in a proper understanding of the magnetic properties of the Co_5Sm magnet materials. Too, these phases must be properly accounted for in any analytical chemistry scheme used to define the composition of the magnets to a high degree of precision and accuracy. The exact nature of these phases can be expected to vary substantially, depending upon the exact metallurgical practices used to fabricate the magnets. The presence of the Sm-rich regions can cause further difficulty in interpreting the results of the chemical analysis of these materials. The interpretation of the relative amounts of Co_5Sm and Co_7Sm_2, based on equilibrium phase diagram considerations and values of Sm and Co reported from chemical analyses, is somewhat clouded by the presence of the Sm-rich regions even if the oxygen present is taken into consideration as Sm_2O_3.

REFERENCES

1. M.G. Benz and D.L. Martin, "Mechanism of Sintering in Cobalt-Rare Earth Permanent Magnet Alloys," J. Appl. Phys. 43, 3165 (1972).

2. F.G. Jones, H.E. Lehman, and J.G. Smeggil, "Quenching Experiments on Cobalt-Samarium Magnets," IEEE Trans. MAG-8, 555 (1972).

3. D.T. Cromer, "The Crystal Structure of Mono-clinic Sm_2O_3," J. Phys. Chem. **61**, 753 (1957).

4. G. Brauer and H. Grodinger, "Uber heterotypen Mischphasen bei Seltencroxyden. 1." Z. anorg. allg. Chem. **276**, 209 (1954).

5. C.E. Curtis and J.R. Johnson, "Ceramic Properties of Samarium Oxide and Gadolinium Oxide; X-ray Studies of Other Rare Earth Oxides and Some Compounds," J. Am. Ceram. Soc. **40**, 15 (1957).

6. Swanson and Fuyat, U.S. Dept. of Commerce, NBS Circ. 539, **III**, 24 (1954).

7. J.W. Gruner, "The Crystal Structure of Talc and Pyrophyllite," Z. Krist. **88**, 415 (1934).

8. ASTM Powder Diffraction File, pub. by Joint Committee on Powder Diffraction Standards, Card No. 13-305, Philadelphia, Pa. (1972).

9. E.A. Aitken, S.F. Bartram, and E.F. Juenke, "Crystal Chemistry of the Rhombohedral $MO_3 \cdot 3R_2O_3$ Compounds," Inorg. Chem. **3**, 949 (1972).

10. M.R. Thornber, D.J.M. Bevan, and J. Graham, "Mixed Oxides of the Type MO_2 (Fluorite)-M_2O_3. III. Crystal Structure of the Intermediate Phases $Zr_5Sc_2O_{13}$ and $Zr_3Sc_4O_{12}$," Acta. Cryst. **B24**, 1183 (1968).

11. M.R. Thornber, D.J. Bevan, and E. Summerville, "Mixed Oxides of the Type MO_2(Fluorite)-M_2O_3. V. Phase Studies in the Systems ZrO_2-M_2O_3 (M=Sc, Yb, Er, Dy)," J. Solid State Chem. **1**, 545 (1970).

12. K.H.J. Buschow and A.S. Van Der Goot, "Intermetallic Compounds in the System Samarium-Cobalt," J. Less-Common Metals **14**, 323 (1968).

13. P.J. Jorgensen and R.W. Bartlett, Technical Report AFML-TR-71-142, Wright-Patterson Air Force Base, 1972.

14. K. Bachmann and A. Menth, "Magnetic Phase Analysis of $RECo_5$ Permanent Magnet Materials," 18th Ann. Conf. on Magnetism and Magnetic Materials, Denver, Colo. (1972).

15. K. Gschneidner, *Rare Earth Alloys*, Princeton; D. Van Nostrand (1951), pp. 239-255.

J.G. Smeggil, P. Rao, J.D. Livingston, and E.F. Koch

MICROSTRUCTURAL IMPLICATIONS CONCERNING
THE MAGNETIC BEHAVIOR OF Co_5Sm

Conference on Magnetism and Magnetic Materials 1973

173<

MICROSTRUCTURAL IMPLICATIONS CONCERNING THE
MACNETIC BEHAVIOR OF Co_5Sm

J. G. SMEGGIL, P. RAO, J.D. LIVINGSTON AND E.F. KOCH
General Electric Corporate Research & Development
Center, Schenectady, New York 12301

Extreme variations are observed in the coercivity
of Co_5Sm as a function of prior heat treatment. One
argument has suggested this behavior to result from
a eutectoid decomposition of Co_5Sm into $Co_{17}Sm_2$ and
Co_7Sm_2. To further examine this hypothesis, basic
microstructural information concerning the transfor-
mation was obtained from samples of Co_5Sm annealed
at 750°C using transmission electron microscopy
techniques. The results of this work indicated the
presence of Co_5Sm, lath-shaped precipitates and
basal stacking faults. The lath-shaped precipitates
exhibited electron diffraction patterns which could
be indexed as rhombohedral $Co_{17}Sm_2$. On the other
hand, electron diffraction patterns resulting from
regions containing basal stacking faults could be
interpreted as originating from disordered Co_7Sm_2.
The inter-relationships between the crystal struc-
tures involved and possible effects of this trans-
formation on the magnetic properties of the Co_5Sm
phase will be discussed.